Towards a fundamental understanding of the polyethylene and polyethylene terephthalate degradation in *Streptomyces* sp.

Thesis submitted to the University of Nottingham for the degree of Doctor of Philosophy

Pierre Reitzer

30/09/2022

Abstract

Plastic is essential to modern society, driven primarily by its incredible versatility as a material coupled with its low production costs. However, this utility has come at a significant environmental cost, given 8.3 billion tonnes of plastic waste have been generated globally since the 1950s. A third of all plastics end up in the environment with 165 million tons/year ending up in the oceans, creating vast accumulations of life-choking rubbish. As recently highlighted in Blue Planet, plastic accumulation in the oceans has devastating consequences for marine life, with nearly 700 different species affected by plastics every year. Oil-based plastics are being produced at a rate exceeding 330 million tons per annum. Plastics were originally developed for performance, with little consideration given to the environmental impact. However, the enormity of the multi-tiered (behavioural, lack of recycling etc.) plastic problem is now very apparent and a sustainable solution to the plastic problem is urgently required. The crux of the problem lies with the molecular nature of the materials, which makes them difficult to degrade. Although some plastics can be recycled this is a finite process, with many eventually ending up in landfill.

Several studies have already identified several microorganisms that can utilize plastics as "food." Although these studies have addressed some aspects of how the bacteria degrade the plastic there are still several unknowns which need to be addressed. Recent research has started to address how bacteria degrade plastics but in-depth knowledge on pathways and enzymes is still missing for most plastics. Furthermore, previous reports have described the degradation of chemical additives, without detailing the specific degradation of the polymer. This thesis aimed to provide a comprehensive understanding of the metabolic and enzymatic degradation of virgin polyethylene terephthalate (PET) and polyethylene (PE) by *Streptomyces* sp. F. A novel Streptomyces sp. isolated from soil and previously shown to degrade commercial PET and PE. Growth was confirmed on both PET and PE utilising a combination of colony forming units, metabolomics and transcriptomic analysis. Significant differences were

seen in the both the metabolite and transcriptomic profile when the cells were grown on both PET and PE. Finally, the genome was sequenced enabling bioinformatics analysis of predicted pathways for both PE and PET degradation. This research has identified a strain which can grow on two different plastics, the first time this has been reported and is a first step towards understanding the degradation process for PE and PET in a Streptomyces.

Acknowledgements

I would like to firstly thank my supervisors Dr Samantha Bryan and Professor Alex Conradie. My PhD projects were not an easy ride and I had a lot of failures along the way. Throughout this Sam supported me and never stopped believing in me even when I was down. I owe her more than this PhD.

I am also grateful for the different people who supported me during my PhD. I would like to thank Denise Mclean for her training on the SEM, Alex Busnel for her training in fermentation technic, Laudina Amugi and Dong-hyun Kim for their help on the LC-MS analysis and Edward Spence for his support on this project. I want to especially thank Sean Craig, for his support, his knowledge and his laugh.

To the BBSRC DTP for funding this work.

I want to thank all my colleagues for making long shifts in the lab an almost pleasant time.

To my tribe, too many to be all named, you kept me going when there was no reason to.

I would like to thank Samantha Paterson, for her continuous support throughout my PhD, for her encouragement and her calm in the storm.

Finally, I would like to thank my parents, my sisters, my grandmother and the rest of my family. Some support with words, others with a silent trust.

Table of Contents

1 Introduction 21
1.1 Plastics: a modern material which has led to a global crisis 21
1.1.1 A history of Plastic 21
1.1.2 Recycling, is it a viable solution to the plastic problem? 24
1.1.3 Plastic degradation in the environment: Biotic vs abiotic degradation. 28
1.1.4 The impact of plastic on the environment 30
1.2 . Biodegradation of plastic 33
1.2.1 The technical limitations with assessing the biotic degradation of plastic 33
1.2.2 Polyethylene terephthalate biodegradation 39
1.2.3 Polyethylene biodegradation 47
1.2.4 Bioplastics 51
1.3 Streptomyces sp. 52
1.3.1 Streptomyces as potential plastic degraders 52
1.3.2 Streptomyces Life cycle and Morphology 55
1.4 Project aim and objectives 57
2 Materials and Methods 59
2.1 Media 59
2.1.1 Minimal medium 59
2.1.2 Rich medium 60
2.1.3 General chemicals 60
2.2 Biological manipulation 61
2.2.1 List of organisms used in this study 61
2.2.2 Culture growth 61
2.2.3 Bacterial storage 61
2.3 Molecular procedures 61

2.3.1 Extraction and purification of chromosomal DNA 61

2.3.2 List of primer used 62

2.3.3 Dreamtaq-polymerase colony PCR (cPCR) for sequencing 62

2.3.4 DNA analysis via agarose gel electrophoresis 63

2.3.5 Extraction and purification of DNA from agarose gel 64

2.3.6 Quantification of nucleic acids 64

2.4 SEM picture 64
2.5 Fermentation on plastic 65
2.5.1 Fermentation conditions 65

2.5.2 LC-MS analysis 65

2.6 Genome data mining 66
2.6.1 Extraction and purification of chromosomal DNA 66

2.6.2 Genome sequencing 66

2.6.3 Transcriptomic analysis 66

2.6.4 ANTISMASH analysis 67

2.6.5 BLAST analysis 67

2.6.6 Modelling of PETase 67

2.6.7 Modelling of MHETase 68

3 Chapter 3 Characterisation of the biodegradation of PE and PET 69
3.1 Introduction 69
3.2 Phylogenetic Identification of the Streptomyces isolate 71
3.3 Evaluation of the growth of *Streptomyces* sp. F on virgin PET and PE. of plastic degradation 75
3.3.1 Evaluation of growth of *Streptomyces* sp. F on PET and PE ... 75

3.3.2 SEM Analysis of the plastic film from PET and PE 77

3.4 Characterisation of the growth of *Streptomyces F* on PET and PE plastic in Fermentation 79
3.4.1 Evaluation of *Streptomyces* sp. F on glucose 79

3.4.2 Fermentation Characterisation of the growth of *Streptomyces* sp. F on polyethylene terephthalate 83

3.4.3 Characterisation of the growth of *Streptomyces* sp. F on PE ... 87

3.5 Metabolomics analysis of the supernatant and cell pellet of *Streptomyces* sp. F on PET and PE 90
3.5.1 Metabolomic analysis: PET vs glucose 91

3.5.2 Metabolomics analysis: PE vs glucose 101

3.5.3 Metabolomics analysis: PE vs PET 111

3.6 Characterisation of the growth of *Streptomyces* sp. F on the monomeric breakdown products of PET 119
3.6.1 Characterisation of the growth of *Streptomyces* sp. F on TPA and EG 119

3.7 Transcriptomic analysis of *Streptomyces* sp. F on PET and PE. .. 120
3.7.1 Transcriptomic analysis of *Streptomyces* sp. F on PET 121

3.7.2 Transcriptomic comparison of growth on PE vs Glucose 125

3.7.3 Transcriptomic comparison between growth on PET vs PE ... 127

3.8 Discussion 130
3.8.1 Degradation of PET by *Streptomyces* sp. F 130

3.8.2 Degradation of PE by Streptomyces sp. F 132

4 Chapter 4 Genomic Sequencing and Bioinformatic Analysis to Identify key Enzymes and Metabolic Pathways for the Degradation of PET and PE in *Streptomyces* sp. F 135
4.1 Introduction 135
4.2 Genome Sequencing of *Streptomyces* sp. F 137
4.2.1 Analysis of the secondary metabolite clusters in the genome of *Streptomyces* sp. F utilising ANTISMASH 140

4.3 Detection of the degradation pathways involved in the degradation of PE and PET 141
4.3.1 Characterisation of the degradation pathways of aromatic compounds 143

4.3.2 Characterisation of the degradation pathway for ethylene glycol (EG) 147

4.3.3 Bioinformatic analysis of potential PE degradation pathways 150

4.3.4 Bioinformatic characterisation of the PETase homologous found in the genome of *Streptomyces sp. F* 152

4.3.5 Characterisation of the MHETase homologous found in the *Streptomyces sp. F* 158

4.3.6 Bioinformatic analysis of the enzymes responsible for the degradation of PE 163

4.4 Discussion 168
5 The sequencing of the genome of *Streptomyces* sp. F enabled several potential PET and PE candidate enzymes and pathways to be uncovered. Validating the TPA and ethylene glycol growth data presented in Chapter 3. It would be interesting to re-evaluate the expression data from Chapter 3 pathways on both PET and PE against the fully sequenced genomes, given the size differences between the two to further identify potential gene candidates. Discussion 170
5.1 Future Work 172
6 References 173

List of figures

Figure 1-1: Estimated global plastic production in 2020, with estimated production of each plastic and their molecular structure. Note that the chemical structure of polyurethane is shown using a representative example and is not the only possible structure to represent this diverse polymer group (Lear et al., 2022). The category “other plastic” regroups several plastic polymers from the thermoset family such as silicone, phenolic resins, acrylic resins etc… The category “other thermoplastic”, regroups several thermoplastic polymers such as polyamides, polycarbonate, poly methyl methacrylate etc… This figure is adapted from EuropePlastics, 2020 and Lear et al., 2022. 22

Figure 1-2: Structural formula of polyethylene (A), structure of High-Density PE (PE-HD) (B), structure of Low-Density PE (PE-LD) (C)..... 23

Figure 1-3 : Categorisation of the plastic particles and their main effects on organisms. This figure is adapted from Essel et al., 2015..... 31

Figure 1-4 : Skeletal structure of polyethylene terephthalate (PET)..... 39

Figure 1-5 : PETase catalyses the depolymerization of PET to terephthalic acid (TPA), bis(2-hydroxyethyl)- TPA (BHET) and mono(2-hydroxyethyl)-TPA (MHET). MHETase converts MHET to terephthalic acid and ethylene glycol (EG) 41

Figure 1-6 : (A) Crystal structure of a PET hydrolase R103G/S131A mutant in complex with HEMT from *Ideonella sakaiensis*, PDB: 5XH3 (Han *et al.*, 2017), (B) Crystal structure of the MHETase from *Ideonella sakaiensis* in complex with BHET, lid domain in dark grey, PDB: 6JTT (Sagong *et al.*, 2020), (C) Secondary structure of a PET hydrolase R103G/S131A mutant in complex with HEMT from *Ideonella sakaiensis*, in yellow the β-strands and in red the α-helices PDB: 5XH3 (Han *et al.*, 2017), (D) Secondary structure of the MHETase from Ideonella sakaiensis in complex with BHET, lid domain in dark grey, in yellow the β-strands and in red the α-helices, PDB: 6JTT (Sagong *et al.*, 2020) 42

Figure 1-7 :Predicted mutations from MutCompute algorithm stabilize FAST-PETase (I–VI). Structural comparison between (I, III, V) WT PETase (tan-coloured cartoon model, PDB code 5XJH) and (II, IV, VI) FAST-PETase (blue-coloured cartoon model, PDB code 7SH6) near the predicted mutation sites (S121E, R224Q, N233K, respectively). Hydrogen-bonding and salt bridge interactions are shown and highlighted as yellow dotted lines. The figure is taken from Lu et al., 2022. 45

Figure 8: diagram highlighting the difference between the conventional plastics and the different types of “bioplastics”. The figure is taken from European Bioplastics, 2018 52

Figure 1-9 : Schematic representation of the life cycle of Streptomyces. This figure is taken from Barka et al., 2016 55

Figure 3-1 : Chemical structure of PET (A) and PEF (B) 70

Figure 3-2 : Picture of the electrophoresis gel of the 16S PCR of *Streptomyces* sp. F (Well 1 and 2), with a ladder (1 kb fragment marked with red arrow) and a positive control (+) 72

Figure 3-3 : Alignment of the 16S region of *Streptomyces* sp. F and *Streptomyces fulvissimus* DSM 40593..... 73

Figure 3-4: Phylogenetic tree of 16S..... 74

Figure 3-5 : Picture of the electrophoresis gel of the PCR of *trpB, recA, atpD* and *rpoB* (in triplicate), with a ladder (1 kb fragment marked with red arrow) 74

Figure 3-6 :Phylogenetic tree for different genes: *recA* (A), *atpD* (B), *tprB* (C) and *rpoB* (D) 75

Figure 3-7 : Graph to show CFU counts from *Streptomyces* sp. F on media only, PET, PE and glucose. Grown in flaks, in SMMmod media at 30℃, ... 77

Figure 3-8: SEM picture showing virgin PE film: media only control (A) and film from the “PE” condition, grown in SMMmod media at 30℃, with 0.1% glucose and 1 % PE film (B). White arrows depict the holes. 78

Figure 3-9: SEM images of virgin PET film: control (A) and film from the "PET" condition, grown in SMMmod at 30℃, with 0.1% glucose and 1 % PET film (B). White arrows depict the holes. 78

Figure 3-10: Differences between the colour of the fermentation with *Streptomyces* sp. F on SMMmodFm at 30℃, with 1% glucose after 24 hours (A) and after 216 hours (B) 80

Figure 3-11: Graph to show growth of *Streptomyces* sp. F in SMMmodFm at 30℃, with 1% glucose. 81

Figure 3-12: Fermentation of *Streptomyces* sp. F on on SMMmodFm at 30℃, with 1% glucose and 1 % PET powder after 72 h (A), microscopic observation of mycelia embedded in the PET particles after 72 h (B)..... 84

Figure 3-13: Fermentation of *Streptomyces* sp. F on SMMmodFm at 30℃, with 1% glucose and 1 % PET powder after 48 h (A) and after 312 hours (B) 85

Figure 3-14: Graph to show growth of *Streptomyces* sp. F in SMMmodFm at 30℃, with 1% glucose and 1 % PET powder. 86

Figure 3-15: Fermentation of *Streptomyces* sp. F on SMMmodFm at 30℃, with 1% glucose and 1 % PE powder after 48 h (A) and after 384 h (B)..... 88

Figure 3-16: Graph to show CFU count from the fermentations of *Streptomyces* sp. F in SMMmodFm at 30℃, with .1% glucose and 1 % PE powder. 89

Figure 3-17 : Bar chart to show peak area of the glucose present in the supernatant during both the fermentation of *Streptomyces* sp. F on glucose and PET 92

Figure 3-18: OPLS-DA analysis showing the differences between the glucose (light blue) and PET (dark blue) supernatant throughout the fermentation, each point corresponds to the overall metabolite profile of one sample(A), volcano plot of glucose Vs PET showing significant increases and decreases in extracellular metabolites during the fermentation, in green metabolites with

higher concentration on PET, in red metabolites with higher concentration on glucose, each point corresponds to a metabolite (B) 94

Figure 3-19: Heat map of the nine metabolites which had either increased or decreased concentrations on both PET and glucose in the supernatant. In blue the highest peak area measured, in red the lowest. 96

Figure 3-20: OPLS-DA analysis showing the differences between the intracellular content of the PET and glucose fermentation, each point corresponds to the overall metabolite profile of one sample (A), volcano plot glucose vs PET showing significant y differences in intracellular metabolites during the fermentation, in green metabolites with higher concentration on PET, in red metabolites with higher concentration on glucose, each point corresponds to a metabolite (B) 98

Figure 3-21: Heat map of the ten metabolites from the cell pellet which had significantly decreased or increased on PET and glucose. In blue the highest peak area measured, in red the lowest. 100

Figure 3-22: Graph to show peak area of the terephthalic acid in the supernatant of both F grown in SMMmodFm at 30℃, with 1% glucose and 1% PET powder (F on PET condition) and cell free PET control 101

Figure 3-23 : Bar chart to show peak area of the glucose present in the supernatant during fermentations grown in SMMmodFm at 30℃, with 1% glucose (glucose condition) , 1% glucose and 1 % PE film (PE condition) 102

Figure 3-24: OPLS-DA analysis showing the metabolite distribution in the extracellular content from the PE (gold) and glucose (light blue) fermentation, each point corresponds to the overall metabolite profile of one sample (A), volcano plot representing metabolites with significant increases and decreases concentration on glucose vs PE, in green metabolites with higher concentration on PE, in red metabolites with higher concentration on glucose, each point corresponds to a metabolite (B) 104

Figure 3-25: Heat map of the metabolites of interest showing differences between the PE and glucose in the supernatant. In blue the highest peak area measured, in red the lowest. 107

Figure 3-26: OPLS-DA analysis showing the metabolite distribution in the extracellular content from the PE (orange) and glucose (green) fermentation, each point corresponds to the overall metabolite profile of one sample (A), volcano plot representing metabolites with significant increases and decreases concentration on glucose vs PE, in green metabolites with higher concentration on PE, in red metabolites with higher concentration on glucose, each point corresponds to a metabolite (B) 109

Figure 3-27: Heat map of the significant metabolites between the glucose and PE condition detected in the intracellular content. In blue the highest peak area measured, in red the lowest 111

Figure 3-28: OPLS-DA analysis showing the metabolite distribution in the extracellular content from the PE (gold) and PET (dark blue) fermentation, each point corresponds to the overall metabolite profile of one sample (A), volcano plot representing metabolites with significant increases and decreases concentration on PET vs PE, in green metabolites with higher concentration on PET, in red metabolites with higher concentration on PE, each point corresponds to a metabolite(B). 113

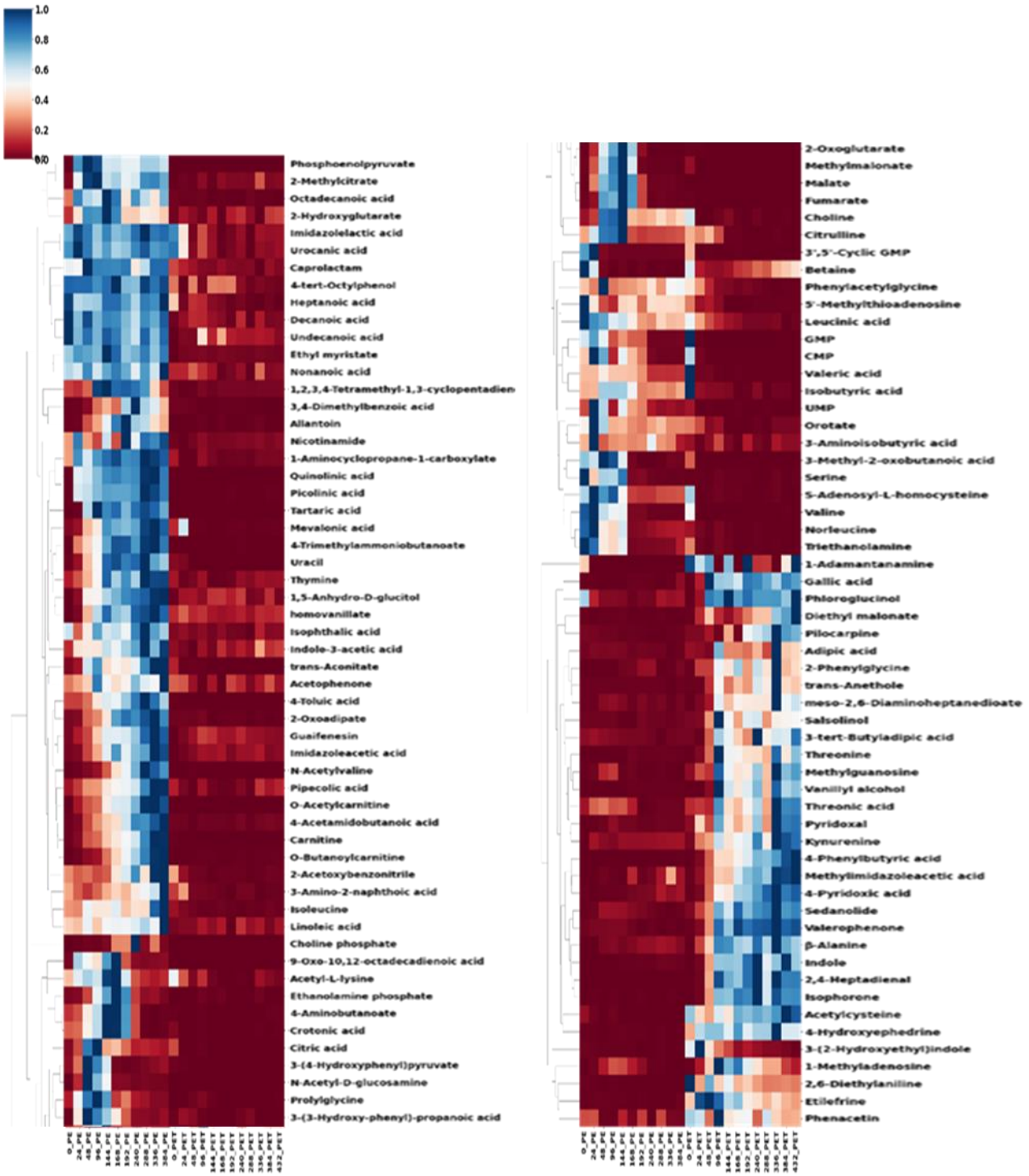


Figure 3-29 : Heat map of the significant metabolites between the PET and PE condition detected in the supernatant. In blue the highest peak area measured, in red the lowest. 115

Figure 3-30 : OPLS-DA analysis showing the metabolite distribution in the extracellular content from the PE (orange) and PET (yellow) fermentation, each point corresponds to the overall metabolite profile of one sample (A), volcano plot representing metabolites with significant increases and

decreases concentration on PE vs PET in green metabolites with higher concentration on PE, in red metabolites with higher concentration on PET, each point corresponds to a metabolite(B). 117

Figure 3-31 : Heat map of the significant metabolites between the PET and PE condition detected in the intracellular content. In blue the highest peak area measured, in red the lowest. 118

Figure 3-32 : Graph to show CFU count for *Streptomyces* sp. F on ethylene glycol (EG) and terephthalic acid (TPA) 120

Figure 3-33 : Volcano plots showing statistically significant genes upregulated on PET (in green) and upregulated on glucose (in red) on glucose at 96 hours (A), at 144 hours (B) and at 240 hours (C) 122

Figure 3-34 : Cluster network to show of genes overexpressed on PET, cluster of gene involved in the “sulphur metabolism” (A), false discovery rate = $1*10^{-10}$, cluster of gene involved in the biosynthesis of arginine and leucine (B), false discovery rate = $2*10^{-5}$. 123

Figure 3-35 : Cluster network to show genes significantly overexpressed on glucose, cluster of gene involved in the tetracycline biosynthesis (A), false discovery rate = 0.04, cluster of gene part of the “ABC transport” system (B), false discovery rate = $3*10^{-7}$, cluster of gene presenting a protease activity (C), false discovery rate = $1*10^{-5}$ 125

Figure 3-36. Volcano plot to show genes which were upregulated on PE (in green) and upregulated on glucose (in red) at 96 hours (A), at 144 hours (B) and at 240 hours (C) 126

Figure 3-37 : Volcano plots showing statistically significant genes expression for growth on PE (in green) and PET (in red) at 96 hours (A), at 144 hours (B) and at 240 hours (C) 128

Figure 3-38 : : Cluster network of genes overexpressed on PET, cluster of genes involved in sulphur metabolism (A), false discovery rate $1*10^{-9}$, cluster of genes involved in the biosynthesis of arginine and leucine (B), false discovery rate $2*10^{-4}$. 129

Figure 3-39 : Network cluster of genes overexpressed on PE, cluster of genes involved in fatty acid biosynthesis (A), false discovery rate = $3*10^{-7}$, cluster of genes involved in the biosynthesis tetracycline biosynthesis (B), false discovery rate = $6*10^{-6}$. 130

Figure 3-40 : Predicted metabolic pathway involved PET degradation in *Streptomyces* sp. F with the key reactions highlighted in bold. 131

Figure 3-41 : Predicted pathway involved in the metabolism of the by-products of PE degradation 133

Figure 4-1: Steps of the PacBio sequencing reaction, (1) interaction of a fluorescently labeled nucleotide with the active site of the polymerase, (2) excitation of the fluorescent dye, allowing the identification of the base, (3) the dye linker is cleaved from the nucleotide and diffused out of the ZMW, ending the fluorescence signal, (4) the polymerase moves towards its next position, (5) a new base fluorescently labelled nucleotide interact with the active site, restarting the fluorescence pulse. The figure is taken from Rhoads & Au, 2015 and Rank et al., 2009. 137

Figure 4-2 : Schematic representation of the genome of *Streptomyces* sp. F 139

Figure 4-3: Schematic to show the degradation of vanillin, phthalate and terephthalate (Kanehisa & Goto, 2000, from Kegg consulted on 18/08/2022) 144

Figure 4-4: Degradation pathway of ethylene glycol (Kanehisa & Goto, 2000, from Kegg consulted on 18/08/2022) 147

Figure 4-5 :Phylogenetic tree of the *pedH* gene 149

Figure 4-6: Degradation pathway of fatty acids in *Streptomyces fulvissimus* (Kanehisa & Goto, 2000, from Kegg consulted on 18/08/2022) 150

4.3.4.1 Figure 4-7 :Phylogenetic tree of PETase homologs Computational Modelling of the F-PETase enzyme 154

Figure 4-8 : Structural model of the F-PETase, in green the structured part of the model and in red the unstructured part 155

Figure 4-9 : Crystal structure of a PET hydrolase R103G/S131A mutant in complex with HEMT from *Ideonella sakaiensis*, PDB: 5XH3 (Han *et al.*, 2017) 156

Figure 4-10 : Model of the F-PETase in complex with an oligomer of PET, with an arrow showing the position of Phe 255. 157

Figure 4-11: Active site of the PETase from *Ideonella sakaiensis* (PDB: 5XJH) (Han *et al.*, 2017), in red, and the active site of F-PETase, in blue. HMET has been added from the structure of PETase (PDB: 5XH3) (Han *et al.*, 2017). 158

Figure 4-12 : Crystal structure of the MHETase from *Ideonella sakaiensis* in complex with BHET, lid domain in dark grey (PDB: 6JTT) (Sagong *et al.*, 2020)..... 160

Figure 4-13: Model of the F-MHETase in complex with BHET, lid domain in dark grey..... 160

Figure 4-14 : Secondary structure of the lid domain of I-MHETase (in red) and F-MHETase (in blue)..... 161

Figure 4-15 : Comparison of the secondary structure of the active site of the I- MHETase (in red) and F-MHETase (in blue), active amino acids are shown as stick models with hydrogen bonds between the catalytic triad (Knott *et al.*, 2020)..... 162

Figure 4-16 : Amino acids interacting with the substrate in the active site of the I-MHETase (in red) and F-MHETase (in blue), with catalytic amino acid in bold 163

Figure 4-17: Phylogenetic tree of the LadA homologous genes found in *Streptomyces* sp. F 165

Figure 4-18: Sequence alignment of LadA from *G. thermodenitrificans* and F-LadA1 and A2, amino acid residues involved in FMN binding are labelled with

a black arrow, putative active pocket residue are in red rectangle (Li *et al.*, 2008)..... 166

Figure 4-19 : Phylogenetic tree of laccases from *Rhodococcus* sp. and the laccase homolog found in *Streptomyces* sp. F..... 167

Figure 4-20 : Sequence alignment of the laccase enzymes from *R. ruber* and *R. opacus* and the homologous sequence from *Streptomyces* sp. F, the copper binding motif found in the laccase from C208 is highlighted with black arrows (Zampolli et al., 2021)..... 168

List of tables

Table 1-1 : List of technics used in the characterisation of plastic degradation 38

Table 1-2: List of reported mutant PETase enzymes 45

Table 1-3 : List of other enzymes with reported PET degradation activity ... 46

Table 1-4 : List of several antibiotics produced industrially using *Streptomyces* sp. 56

Table 2-1: composition of PCR reaction mix 63

Table 2-2 : PCR thermocycler condition used in this work 63

Table 3-1: Growth rate of *Streptomyces* sp. F on glucose 81

Table 3-2: Growth rate of *Streptomyces* sp. reported in the literature..... 82

Table 3-3: List of samples taken during the fermentation of *Streptomyces* sp. F on glucose. 83

Table 3-4: Growth rate of *Streptomyces* sp. F during the fermentation on PET 87

Table 3-5: Growth rate of *Streptomyces* sp. F during fermentation on PE... 90

Table 3-7: Growth rate of *Streptomyces* sp. F on the monomeric product of PET degradation, ethylene glycol (EG) and terephthalic acid (TPA)..... 120

Table 3-8 : Table showing the number of genes significantly overexpressed on both PET and glucose throughout the fermentation 122

Table 3-9: Table to show the number of gene significatively overexpressed on both PE and glucose throughout the fermentation 127

Table 3-10 :Table to show the number of genes significatively overexpressed on both PE and PET. 128

Table 4-1 :Comparison between the genome of *Streptomyces* sp. and *Streptomyces* sp. F. 140

Table 4-2 : ANTISMASH analysis of the genome of *Streptomyces* sp. F .. 141

Table 4-3 :List of homologous genes involved in aromatic degradation pathways which were detected in the genome of *Streptomyces* sp. F..... 146

Table 4-4: Homologous genes involved in degradation of ethylene glycol identified in the genome of *Streptomyces* sp. F 149

Table 4-5 : List of homologous genes involved in the fatty acid degradation identified in the genome of *Streptomyces* sp. F 151

Table 4-6 : Homologous PET degrading enzymes detected in the genome of *Streptomyces* sp. F 153

Table 4-7: Characterisation of the signal peptide of the protein F-PETase 155

Table 4-8 : Homologous MHETase enzymes detected in the genome of *Streptomyces* sp. F 159

Table 4-9 : List of homologous genes detected in *Streptomyces* sp. F with potential PE degradation activity..... 164

Abbreviation

BGC	Biosynthetic gene clusters
BHET	Bis(2-hydroxyethyl)-terephthalic acid
CFU	Colony forming unit
DSC	Differential Scanning Calorimetry
EG	Ethylene glycol
FTIR	Fourier-Transform infrared spectroscopy
GC-MS	Gas chromatography-mass spectrometry
GI	Genetic element
HGT	Horizontal gene transfer
HPLC	High performance liquid chromatography
HT-GPC	High Temperature Gel Permeation Chromatography
ICL	Isocitrate lyase
IPA	Isopropanol
LCC	Leaf Compost Cutinase
LC-MS	Liquid chromatography-mass spectrometry
MCO	Multicopper oxidases superfamily
MHET	Mono(2-hydroxyethyl)-terephthalic acid
MP	Microplastic
MT	Million tonnes
NADH	Nicotinamide adenine dinucleotide
NP	Nanoplastic
OPLS-DA	Orthogonal Projections to Latent Structures Discriminant Analysis
ORF	Open reading frame
PBS	Polybutylene succinate
PCA	Protocatechuic acid
PCR	Polymerase chain reaction
PE	Polyethylene
PEF	Polyethylene furandicarboxylate
PE-HD	High density PE
PE-LD	Low density PE
PE-LLD	Linear Low Density PE
PET	Polyethylene terephthalate
PKS	Polyketide synthase
PS	Polystyrene
PTM	Polycyclic tetramate macrolactams
PUR	Polyurethane
PVC	Polyvinyl chloride
RT-PCR	Reverse transcription polymerase chain reaction
SEM	Scanning electron microscopy
SFM	Soya Flour Mannitol media
TCA	Tricarboxylic acid cycle
TPA	Terephthalate
XRD	X-ray Diffraction

1 Introduction

1.1 Plastics: a modern material which has led to a global crisis

1.1.1 A history of Plastic

The first plastic ever produced was created in 1862 by Alexander Parkes, its name was Parkesine (Rasmussen, 2021). The first semi-synthetic plastic used cotton fibre as a feedstock and was reasonably commercially successful. The first synthetic plastic was created in 1907 by Leo Baekeland, termed Bakelite (Crespy, Bozonnet and Meier, 2008). However, the industrial production of plastic only really started in 1950, with 2 million tonnes (MT) of plastic produced in a year (Geyer, Jambeck and Law, 2017). Since then, the plastic industry has seen rapid growth and expansion, with a compound annual growth rate of 8.4% between 1950 and 2015 (Geyer, Jambeck and Law, 2017). It is estimated that 8.3 billion tonnes of plastic have been produced since 1950 (Brooks, Wang and Jambeck, 2018). In 2019, the worlds plastic production reached 368 MT, and is still expected to grow (EuropePlastics, 2020).

Plastics are polymers, usually separated into two different families: thermoplastics and thermosets (EuropePlastics, 2020). The thermoplastics are plastics that can be melted when heated and hardened when cooled (EuropePlastics, 2020). These characteristics are reversible. The thermosets are plastics, which undergo a chemical change when heated, creating a three-dimensional network (EuropePlastics, 2020). After they are heated and formed these plastics cannot be re-melted and reformed. Within these two families, a variety of different plastics exist and have a wide range of characteristics.

The thermoplastic family contains the following plastic: Polyethylene Terephthalate (PET), Polyvinylchloride (PVC), Polystyrene (PS) and Polyethylene (PE) (EuropePlastics, 2020). PE can be subsequently divided into: High Density Polyethylene (PE-HD), Low Density Polyethylene (PE-LD) and Linear Low-Density Polyethylene (LLDPE). The thermoset family contains the following plastic: Polyurethane (PUR), Vinyl esters, Epoxy resin and other form of resins (EuropePlastics, 2020).

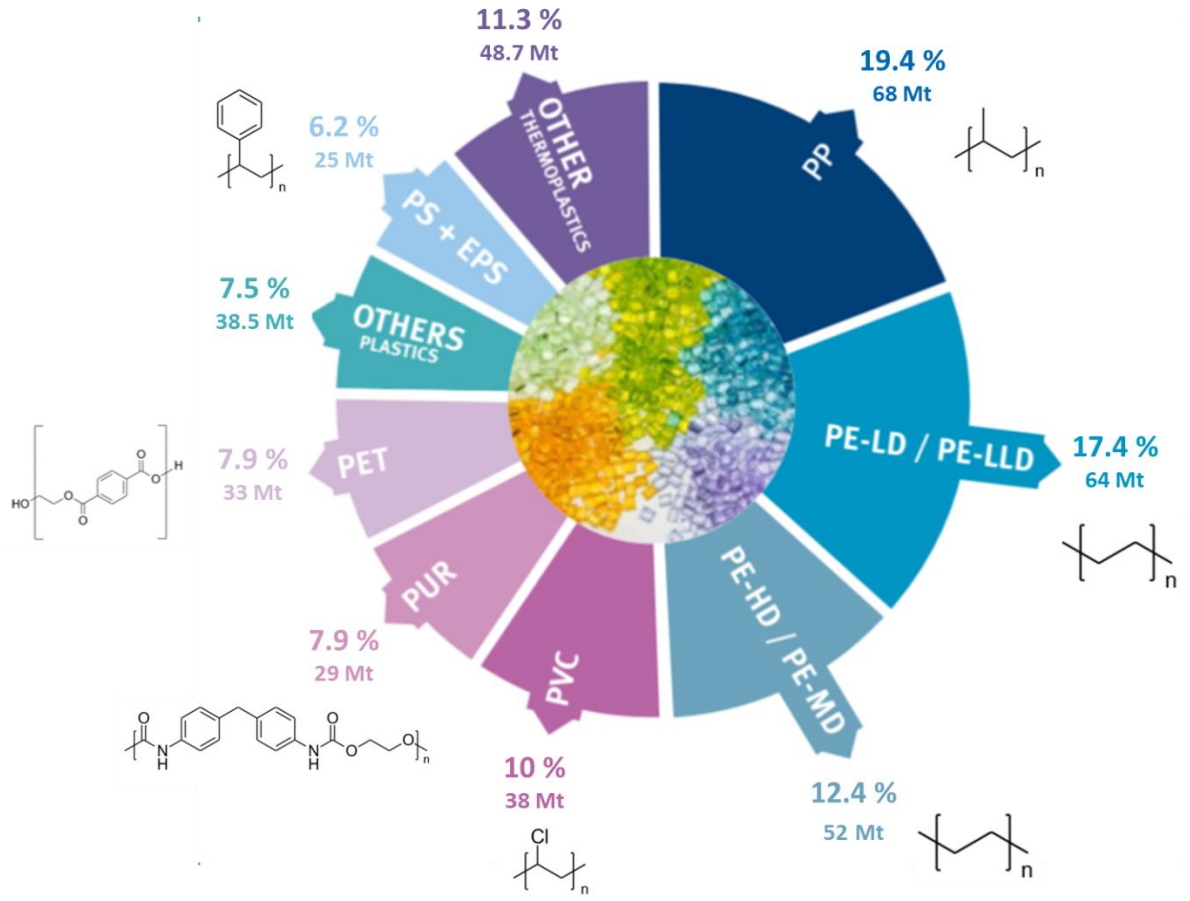


Figure 1-1: Estimated global plastic production in 2020, with estimated production of each plastic and their molecular structure. Note that the chemical structure of polyurethane is shown using a representative example and is not the only possible structure to represent this diverse polymer group (Lear et al., 2022). The category "other plastic" regroups several plastic polymers from the thermoset family such as silicone, phenolic resins, acrylic resins etc… The category "other thermoplastic", regroups several thermoplastic polymers such as polyamides, polycarbonate, poly

methyl methacrylate etc… This figure is adapted from EuropePlastics, 2020 and Lear et al., 2022.

Two forms of PE are currently leading the market (EuropePlastics, 2020): high Density PE (Figure 1B), or HD, with a low branching rate, high crystallinity, and heat resistance and low Density PE (Figure 1C), or PE-LD, with a higher branching rate, a lower crystallinity and high flexibility. The degree of branching has an impact on the crystallinity of the plastic, and therefore is suspected to have an impact on the accessibility of the polymer for the enzymatic attack (Montazer, Habibi Najafi and Levin, 2020)

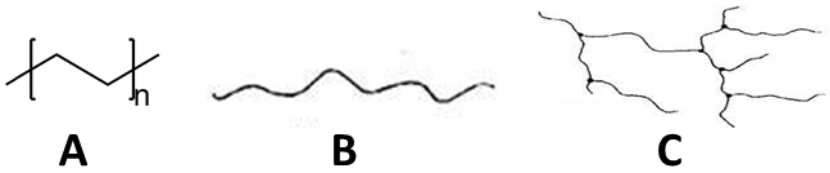


Figure 1-2: Structural formula of polyethylene (A), structure of High-Density PE (PE-HD) (B), structure of Low-Density PE (PE-LD) (C)

Plastic characteristics are highly dependent on their composition. In addition to the variety of available polymers, various additives can be blended into the resin to fine tune the characteristics of the final commercial plastic (Hahladakis *et al.*, 2018). These additives, also known as plasticizers, are numerous and enable the plastic to be endowed with a variety of characteristics, including, heat resistance (heat stabilisers), colour (pigments), UV and oxidative resistance (UV stabiliser and antioxidant) and static electricity discharge (antistatic agents) (Hahladakis *et al.*, 2018). Commercial plastic can also be formulated with filler, which accounts for up to 50% of the mass of commercial plastic (Hahladakis *et al.*, 2018). The formulation of plastic is heavily protected by patents therefore it is difficult to know the precise composition of commercial plastic (Lear *et al.*, 2022).

Plastic has significant societal benefits, which account for its popularity. Plastic represents a low-cost, easily formable, high-modulus, hydrophobic,

bio-inert material that has found a use in a wide range of consumer products. The ubiquitous presence of plastic in our everyday lives led to the coin of the term the *Plasticene*, an “age of plastic” (Haram *et al.*, 2020).

The majority of the plastics currently produced are from the thermoplastic family, estimated at 70% of global plastic production (EuropePlastics, 2020). The most produced plastic is PE, with all its variations (PE-HD, PE-LD and PE-LLD), which account for 30 % of plastic production. The second is PP, with around 20% of the total production. PET accounts for around 8% of production (EuropePlastics, 2020)

In Europe, four industries are responsible for the largest share of the plastic market. The biggest consumer is the packaging industry, with 40% of the European plastic market (EuropePlastics, 2020). The second, the building and construction industry, consumes over 20% of plastic. Finally, the automotive and electronics industry account for 10 and 6% of the European market (EuropePlastics, 2020).

The packaging industry also has the most diverse plastic needs. Whilst the building industry relies heavily on PVC and PUR, the packaging industry consumes significant levels of PET, PP and PE (EuropePlastics, 2020).

In addition, to plastic volume and diversity, a significant proportion of the plastic used by the packaging industry is single use. It is estimated that over 70% of this plastic ends up in the environment, with over 40 % being landfilled (World Economic Forum, 2016; Geyer, Jambeck and Law, 2017). An additional 32% is not properly managed and “leaks” into the environment, this “leak” is either due to a lack of collection system or due to the mismanagement of the plastic waste (illegal dumping) (World Economic Forum, 2016). At least 8 million tonnes of plastics leak into the ocean each year (Jambeck *et al.*, 2015)

1.1.2 Recycling, is it a viable solution to the plastic problem?

Despite the creation of the recycling logo more than 40 years ago, globally only 9% of plastic has been collected and effectively recycled (Brooks, Wang and Jambeck, 2018). In addition, recycling itself is far from being perfect. The process has several stages: collection, transport, cleaning, sorting of the plastic waste and finally recycling (World Economic Forum, 2016). Each stage represents a cost both economically and environmentally, for example the collection and transport stages require an efficient waste collection and management infrastructure. This first stage of the plastic recycling process is vital to prevent leakage of plastic into the environment (World Economic Forum, 2016). However, it also requires heavy investment in both infrastructure and manpower. Despite having an advanced collection system, Europe and the United States still leak over 170, 000 tonnes of plastic material into the ocean each year (Jambeck *et al.*, 2015). In addition to a strong plastic waste management, plastic recycling also requires the separation of each type of plastic, for each plastic waste to enter its own recycling process. The sorting step is by far the most complex step in the plastic recycling process, limited by both the identification of the plastic and the increase of different plastic on the same product (World Economic Forum, 2016).

Plastic waste represents a low-value commodity, each step in the preparation before recycling is an additional burden. The costs prior to direct recycling represent an investment that recycled plastic is not able to support, hindering the economic viability of the recycling process. (World Economic Forum, 2016)

A good example of the limitation of plastic recycling is PET. PET, used in beverage bottles, is by far the most recycled plastic, however, even its success is limited (World Economic Forum, 2016). Highlighting the difficulties that the plastic recycling industry is facing. Globally, around half of PET plastic is collected for recycling (World Economic Forum, 2016). The presence of a variety of additives, as well as other contaminants, prevent the properties of the plastic being conserved during the recycling process. For example, if water molecules are present during the recycling process, it can lead to hydrolytic chain cleavage of the polymer, decreasing the viscosity of

the resin to a level, which would not allow bottles to be blown (Damayanti and Wu, 2021). Moreover, chemical contamination can happen during the normal lifetime of the plastic bottle. For example, heavy metal (lead, nickel, cadmium and antimony) can be found in the labels, inks and adhesives of PET plastic bottle (Whitt *et al.*, 2013; Damayanti and Wu, 2021). As the consumption of heavy metals can represent a serious risk to human health, without additional treatment to remove trace heavy metals from the PET waste, the recycled PET cannot be used for food grade application, and therefore a plastic bottle (Whitt *et al.*, 2013).

Therefore, most of the recycled PET is used for lower-value applications (World Economic Forum, 2016). Only 7% of the PET currently collected is recycled bottle-to-bottle (World Economic Forum, 2016). In 2019, only around 3.5% of the globally produced PET had been recycled into a form, which allowed more than one recycling cycle (World Economic Forum, 2016). In addition to the poor retention of PET plastic, the current method of recycling PET plastic is limited in the number of times it can be utilised. After several recycling process, the PET cannot be reprocessed and needs to be either buried in landfill or incinerated (World Economic Forum, 2016). Both elements question the long-term efficiency of PET recycling.

In addition to the economic difficulties of recycling, political difficulties have also arisen in recent years. China, a major player in the international plastic recycling market, decided to ban imports of plastic waste at the start of 2018 (Wen *et al.*, 2021). It is estimated that both China and Hong Kong imported more than 70 % of all plastic waste produced since 1992 (Brooks, Wang and Jambeck, 2018). With Hong Kong acting as an entry-port into China: in 2016, 63% of its imports went directly to China (Brooks, Wang and Jambeck, 2018). This ban, known as the “China Shock” had a massive ripple effect on the international plastic waste market. Firstly, the global trade of plastic decreased by more than 45 % (Wen *et al.*, 2021). Secondly, other plastic waste importing countries increased their importation of plastic waste. Especially Southeast Asian countries, who tripled their importation of waste plastic (Wen *et al.*, 2021). Thirdly, the main plastic waste producer, Europe and the United states, had to increase the quantity of plastic being buried in

landfill or burned (Wen *et al.*, 2021). Although, early reports of the effect of the ban indicate an overall positive environmental impact in the longer term (Wen *et al.*, 2021), this ban has completely restructured the international plastic waste market and has led to a crisis in the management of plastic waste (Joltreau, 2022). Following the ban, other Southeast Asian countries (Malaysia, Vietnam, India and Thailand) were overwhelmed by plastic waste importation and had to implement import restrictions (Joltreau, 2022). Others have seen their importation of plastic waste dramatically increased. For example, Turkey has seen a 20 fold increase of plastic waste imports between 2016 and 2020 (Joltreau, 2022)

The recycling industry is still failing to collect all the plastic waste. With a recycling rate of around 30 %, Europe has the best global recycling rate (Geyer, Jambeck and Law, 2017; EuropePlastics, 2020). The 70% of plastic which remains has two different fates, the first one is incineration, also known as “Energy recovery” (EuropePlastics, 2020). As plastics are carbon-based polymers, they can be burned to produce energy. Around 40% of the plastic collected in Europe is used to “recover” energy (Geyer, Jambeck and Law, 2017; EuropePlastics, 2020). The rest of the plastic, around 25%, is buried in landfill (Geyer, Jambeck and Law, 2017; EuropePlastics, 2020).

Other technologies have been developed to divert plastic waste from landfill. However, only one reached the industrial scale: pyrolysis. Pyrolysis relies on a simple principle: the degradation of organic materials using high heat treatment in the absence of oxygen (Qureshi *et al.*, 2020). This process typically yields a mixture of molecules in the form of gas, liquid, or solid (char or wax) (Qureshi *et al.*, 2020). This method is promising because it allows for energy recovery from waste and generates a wide spectrum of products (Fernández, Arenillas and Menéndez, 2011). However, this method is not energy efficient, due to the high heat content carried over by the hot gas leaving the process, gas which can reach up to 1000°C at the exhaust of the process (Bocci *et al.*, 2014). To reduce the energy deficiency of the process, another pyrolysis approach has recently received more traction: microwave pyrolysis (Bocci *et al.*, 2014). Since microwave energy can be delivered directly to the plastic waste due to its dielectric properties (Qureshi *et al.*, 2020). It allows

for more volumetric heating of the material, which limits the energy loss and increases by several orders of magnitude the heating rate (Bocci *et al.*, 2014; Qureshi *et al.*, 2020). This method allows a better control of the heating, a better control of the pyrolysis process and therefore a better management of the expected products (Khaghanikavkani, 2013). However, pyrolysis of plastic waste still suffers from multiple challenges, the two main problems are the lack of consistency in the waste feed and the lack of specificity in the products (Fernández, Arenillas and Menéndez, 2011; Bocci *et al.*, 2014). Both of those limitations can be resolved, by sorting the plastic before the process and by purifying the desired product. However, both require additional steps in the pyrolysis process, and would limit the economic viability of the process.

The low recycling rates are problematic for several reasons. The first, being the energy allocated to the production of the plastic. Over 90% of virgin plastics are derived from fossil feedstocks, which accounts for 9% of global oil consumption (World Economic Forum, 2016). If the growth of plastic continues as expected, it will account for 20% of the global oil consumption by 2050 (World Economic Forum, 2016). The second being accumulation of plastic in the environment, either through leakage or burial in landfill. The impact of plastic on the environment is very evident and has severe consequences for both aquatic and terrestrial life . (Ballerini, Andrady and Cole, 2018; Brandon, Jones and Ohman, 2019).

1.1.3 Plastic degradation in the environment: Biotic vs abiotic degradation.

Plastic is an extremely recalcitrant material and takes several decades, if not centuries, to degrade in the environment (Chamas *et al.*, 2020; Ghatge *et al.*, 2020). However, plastic is not immune to degradation in the environment several different natural mechanisms help to degrade plastic (Chamas *et al.*, 2020). These mechanisms can be divided into two categories: abiotic and biotic (Chamas *et al.*, 2020).

Abiotic degradation results from non-biological degradation mechanisms. There are four different abiotic mechanisms, which can act in synergy to accelerate plastic degradation: mechanical degradation, light degradation, thermal degradation and chemical degradation (Lucas *et al.*, 2008). Mechanical degradation results from compression, tension and/or shear forces (Lucas *et al.*, 2008). It is this mechanism which degrades large pieces of plastic into smaller pieces of plastic, eventually resulting in the production of microplastics.

Light degradation is dependent on the photosensitivity of the plastic; it is thought to have the most impact on abiotic degradation (Lucas *et al.*, 2008; Danso, Chow and Streit, 2019). Energy carried by the photon creates an unstable state in the plastic. This instability can create a variety of effects on the plastic polymer: oxidation, cross-linking, chain scission, which leads to degradation (Lucas *et al.*, 2008).

Thermal degradation occurs when a polymer is transformed from solid to liquid, this is >250℃ for PET (Jog, 1995), and <95℃ for PE (Kumar Sen and Raut, 2015). These temperatures are rarely achieved in the environment, the impact of temperature is therefore limited to the glass temperature of the plastic in order to facilitate its degradation (Lucas *et al.*, 2008).

Exposure to chemicals such as atmospheric pollutants or agrochemicals can lead to changes in polymer properties. Oxygen is one of the most potent species, which plays a key role in the degradation of plastic (Lucas *et al.*, 2008). Oxidative degradation often works in synergy with photo degradation, resulting in the formation of free radicals (Lucas *et al.*, 2008). Water plays a key role in the hydrolysis of polymers, especially polyester polymers. Its reactivity depends on temperature, pH and the crystallinity of the polymer (Lucas *et al.*, 2008).

Biotic degradation results from biological mechanisms which lead to the degradation of plastic (Chamas *et al.*, 2020). Different degrees of biotic degradation include bio-deterioration, a superficial degradation that modifies the mechanical, physical and chemical properties of the plastic (Lucas *et al.*, 2008). It does not result in significant degradation of the plastic since the

degradation is mainly focused on the surface. Bio-fragmentation, is a lytic phenomenon which leads to the formation of lower molecular weight polymers (Lucas *et al.*, 2008). This type of degradation leads to the complete depolymerisation of the plastic, to its monomers.

As stated earlier, commercial plastic uses additives embedded in the plastic to limit the different forms of abiotic degradation, which results in the abiotic degradation being less effective. However, there is now an increased effort to facilitate degradation using additives which facilitate photodegradation and/or biotic degradation. Additives including pro-oxidant molecules, such as TiO_2, are used to promote photo-degradation (Thomas and Sandhyarani, 2013). The addition of bio-available carbon, such as starch (Lee *et al.*, 1991; Pometto, Lee and Johnson, 1992; El-Shafei *et al.*, 1998), is also used to promote biotic degradation.

1.1.4 The impact of plastic on the environment

Even though plastic has only been produced for a few decades, large amounts of plastic are already found in the environment (Lear *et al.*, 2021). In 2015, it was estimated that more than 4900 MT of plastic have been discharged into the environment since 1950 (Geyer, Jambeck and Law, 2017). Due to its inherent resistance, plastic is not rapidly degraded and accumulates in the environment.

The environmental risks of plastic pollution fall into three categories: physical, chemical and biological pollution (Ballerini, Andrady and Cole, 2018). Physical pollution results from the mechanical and physical characteristics of the plastic, which results in entanglement and perforation of the digestive tract (Li *et al.*, 2021). Chemical pollution results from the leaching of chemicals for example plasticizers, monomers, additives, fillers and colourants (Li *et al.*, 2021) . Biological harm results from the loss of native species from the food web, such as bacteria and invertebrates, as communities adapt to plastic. The “plastisphere”, was coined to represent the

microbial community on plastic debris, it is a relatively new concept and studies are ongoing to try and measure the impact plastic is having on the broader ecosystem (Zettler, Mincer and Amaral-Zettler, 2013; Amaral-Zettler, Zettler and Mincer, 2020; Rüthi *et al.*, 2020).

In addition to macroplastic pollution, micro and nano plastics are also under increasing scrutiny. Microplastics (MPs) are small particles of plastic, the size definition is still non-uniform. However, the National Oceanic and Atmospheric Administration defined MPs as plastic particles smaller than 5 mm and nanoplastics (NPs) as plastic particles smaller than 1 mm (Table 1-3) (Arthur, Baker and Bamford, 2009).

Category of plastic particle	**Diameter of plastic particle**	**Typical size of affected organism**
Macroplastic	>25 mm	vertebrates, birds (Franeker, Heubeck and Stienen, 2005)
Mesoplastic	5-25 mm	birds, fish (Boerger *et al.*, 2010)
Microplastic	1-5 mm	fish, crustaceans (Boerger *et al.*, 2010)
Nanoplastic	<1 mm	mussel, plankton

Figure 1-3 : Categorisation of the plastic particles and their main effects on organisms. This figure is adapted from Essel et al., 2015

Two different processes result in the production of MPs and NPs: these being environmental release following the utilisation of plastic products and secondly the degradation of macroplastics (Sundt, Schulze and Syversen, 2014).

The primary source of MPs and NPs is very varied given the number of available plastics; several sources have been identified. Synthetic textiles are considered the main source of primary MPs and NPs, through the abrasion

and shedding of fibres, especially during the washing process (Boucher and Friot, 2017). MPs coming out of synthetic textiles are made of a mix of polyester, polyethylene, acrylic and elastane (Essel *et al.*, 2015). The second main source of MPs is the abrasion of tyres(Sundt, Schulze and Syversen, 2014). While driving, tyres erode and particles from the outer part of the tyre are produced. The outer part is usually made of a mix of styrene butadiene rubber, natural rubber and other additives (Sundt, Schulze and Syversen, 2014). These two sources account for more than half of the estimated global production of MPs (Boucher and Friot, 2017).

The only industry currently intentionally producing MPs is the cosmetic industry. The industry was recently criticized for using MPs in their products: especially exfoliating products using “microbeads” of plastic (Essel *et al.*, 2015; Bashir *et al.*, 2021). However, due to public pressure, major cosmetic companies pledged to eliminate MPs from their formulations, especially in Europe (Guerranti *et al.*, 2019).

Secondary MPs result from the degradation of larger pieces of plastic. The main source for this type of MPs is the ocean, where both mechanical and light degradation (UV) are responsible for breaking up plastic. The quantification of this type of MPs is particularly challenging, since it depends on several factors, which are in themselves hard to quantify (e.g. the impact of mechanical degradation due to waves, impact of UV degradation, impact of biofouling) (Waldman and Rillig, 2020).

The fate of MPs and the impact they may have on the ecosystem are still not adequately understood and this remains a very active research area (Thompson *et al.*, 2004; Browne *et al.*, 2011; Karbalaei *et al.*, 2018; Bashir *et al.*, 2021). One thing is certain, MPs are ubiquitous in the environment, especially in the marine environment, and could be considered as a pollutant of concern (Browne *et al.*, 2011; Farady, 2019). Despite the current lack of evidence for direct toxicity. MPs have been shown to have a negative effect on various species. Zebra fish, *Danio rerio*, fed with polystyrene MPs for 7days, presented early sign of early inflammatory responses in their liver associated with significant changes in their metabolomics (Lu *et al.*, 2016).

Furthermore, another study showed that Zebra fish, *Danio rerio,* treated with polystyrene NPs during their development had a significantly slower heart rate (bradycardia) although this did not result in an increase in their mortality, deformity or pericardial development (Buchakjian *et al.*, 2018). While research of the negative impact of MPs is still ongoing, so far 663 species have been reported as being negatively impacted by MPs (Essel *et al.*, 2015)

In addition of the hazards posed by MPs, NPs are emerging as a pollutant representing an “unknown” risk for the human health (Karbalaei *et al.*, 2018; Ng *et al.*, 2018; Rist *et al.*, 2018). In 2022, reports of the first detection of NPs in human blood were published (Leslie *et al.*, 2022). However, no comment about its risk have been made thus far.

1.2 . Biodegradation of plastic

Microorganisms have been shown to degrade plastics with varying levels of evidence for this in the literature. Two plastics have received a lot of attention from the scientific community: polyethylene (PE) and polyethylene terephthalate (PET). Together they represent over 40% of the plastic currently produced (EuropePlastics, 2020; Geyer et al., 2017). Therefore, they make up the bulk of plastic collected in the environment.

The level of characterisation done on the degradation of both plastics is very different. PET degradation is well-established, with the mechanism and the enzymes responsible for the depolymerisation fully characterized (Yoshida *et al.*, 2016; Tournier *et al.*, 2020). However, PE degradation is still in its infancy with details missing on the key enzymes involved in the degradation mechanism (Ghatge *et al.*, 2020) .

1.2.1 The technical limitations with assessing the biotic degradation of plastic

Various papers have been published evaluating the growth of microorganisms on plastic, with varying degrees of characterisation on the plastic degradation. The following species have been reported to degrade polyethylene terephthalate: *Bacillus* (Yang, Yang, W. Wu, *et al.*, 2014) *sp., Fusarium sp.* (Müller *et al.*, 2005)*, Ideonella sp.* (Yoshida *et al.*, 2016)*, Thermobifida sp* (Then *et al.*, 2015a) *and Pseudomonas sp.* (Carr, Clarke and Dobson, 2020), on polyethylene: *Bacillus sp.* (Kumar Sen and Raut, 2015)*, Pseudomonas sp.* (Nowak *et al.*, 2011) *Rhodococcus sp., Klebsiella sp* (Awasthi, Srivastava and Singh, 2017).

One of the main limitations with evaluating growth is the ambiguity around what the organism is actually growing on, as stated earlier commercial plastics are a blend of a variety of different molecules, including polymer, fillers, plasticizers and other additives (Hahladakis *et al.*, 2018; Li *et al.*, 2021). Therefore, screening based on growth alone could introduce bias.

Furthermore, several studies have utilised pre-treated plastic, also called “weathered plastic”. The pre-treatment usually consists of treating the plastic with UV light, mimicking natural “photodegradation”(Montazer, Habibi Najafi and Levin, 2019; Mohanan *et al.*, 2020). However, UV is known to chemically modify and disrupt the structure of the polymer (Bonhomme *et al.*, 2003). Therefore, detection of plastic degrading organism on treated plastic does not imply that the organism itself can degrade the plastic. However, it could imply that the organism may play a role in the degradation of the plastic, with abiotic degradation assisting with the biodegradation, making the plastic more accessible to the microorganism (Bonhomme *et al.*, 2003; Zheng, Yanful and Bassi, 2005).

Several methods are commonly used to assess plastic degradation, however they are not all equal, when it comes to demonstrating degradation. They fall into two main categories: the first category, being methods which assess the direct degradation of the plastic (tensile strength, molecular weight distribution, mass measurement), the second method which assess the effect of the plastic on the microorganism (growth, detection of specific metabolites).

Mass measurement, also known as gravimetric measurement is by far the most common approach to assess plastic degradation (Ghatge *et al.*, 2020; Montazer, Habibi Najafi and Levin, 2020). This method is simple: the plastic mass is measured before and after biological treatment. The degradation is assessed by the diminution of the mass of the plastic after biological treatment. However, this approach suffers from several flaws: firstly, a mass diminution does not necessarily demonstrate polymer degradation has occurred. Such mass diminution could be the result of a loss of non-polymeric molecules, such as additives or fillers. Secondly, biofilm formation and biofouling can negatively impact the measurement, by adding biological mass on the surface of the plastic.

Fourier-transform infrared (FTIR) is a spectrometric analysis which analyses the surface of the plastic, it is also commonly utilised to evaluate plastic degradation. This analysis relies on the reflection of the infrared spectrum on the surface of the plastic. The reflectiveness of the infrared spectrum is dependant of the chemical function present on the surface of the plastic (Nandiyanto, Oktiani and Ragadhita, 2019). The decrease of the reflectiveness for specific wavelengths allows the identification of functional groups on the plastic surface (Montazer, Habibi Najafi and Levin, 2019). This method is particularly useful due to its affordability and reliability (Celina *et al.*, 1997; Restrepo-Flórez, Bassi and Thompson, 2014). However, the method is particularly sensitive to biological contamination, especially if the plastic sample has not been properly cleaned (Weber, Pusch and Opatz, 2017).

The molecular weight of the polymer can also be assessed using High Temperature Gel Permeation Chromatography (HT-GPC). The polymer is solubilized in a solvent, in which the polymer molecular chains, when dissolved, form into coils (Neira-Velázquez *et al.*, 2013). Separation of the polymer molecular chains relies on a size exclusion column: the larger the size of the chains the quicker they are eluted. The column is maintained at high temperature (up to 140 C)(Lee *et al.*, 1991) in order to facilitate the solubilisation of polymeric chains (Neira-Velázquez *et al.*, 2013). This

technique is used for plastic with relatively long polymer chains, such as PE (Hadad, Geresh and Sivan, 2005; Ghatge *et al.*, 2020).

Other technics, such as Differential Scanning Calorimetry (DSC) and X-ray Diffraction (XRD), have been used to assess the crystallinity of the plastic sample (Table 1-1) (Amini *et al.*, 2004; Sajwan, Aggarwal and Singh, 2008; Ghatge *et al.*, 2020). DSC is a thermodynamical technique in which the amount of energy required to increase or decrease the temperature of the sample is measured (Gill, Moghadam and Ranjbar, 2010). This precise calorimetric technique is particularly applied to monitor the changes in phase transition and is therefore routinely used to assess the crystallinity of solid samples (Gill, Moghadam and Ranjbar, 2010). XRD is a spectrometry method which relies on the different pattern of refraction of X-rays on different phases of the sample (amorphous or crystalline) (Bunaciu, Udriştioiu and Aboul-Enein, 2015). From the diffraction pattern, the characteristics of the crystal (size, preferred orientation of crystal, crystal defects etc) in the sample can be measured (Bunaciu, Udriştioiu and Aboul-Enein, 2015).

Tensile testing (also called inston) can be used to characterise the mechanical characteristics of plastic (Table 1-1). The principle is simple: a tensile test applies tensile (pulling) force to a material and measures the specimen's response to the stress (Xiao, 2008). By doing this, tensile tests determine how strong a material is and how much it can elongate. Tensile test is a standardized procedure, and requires specialised equipment, however one test can give multiple useful characteristics of the plastic : tensile strength; strain energy and % elongation (Xiao, 2008).

A quick method to assess the hydrophobicity/ hydrophilicity of a surface is to perform a measure of contact angles (Schuster, Schvezov and Rosenberger, 2015) (Table 1-1). The angle of the drop on the plastic surface is directly linked to the hydrophobicity of the surface. It is mainly used in the study of biodegradation of PE, since the surface of PE is particularly hydrophobic (Awasthi *et al.*, 2017). Therefore, a diminution of the angle of the drop is recognized as an increase of the hydrophilicity of the surface, which is indicative of an oxidation at the surface (Ghatge *et al.*, 2020).

While DSC, XRD, instron and contact angle measurement are useful techniques in the characterisation of plastic samples, the detection of changes in the characteristic of the plastic informs very little on the mechanism of the degradation (Table 1-1) (Ghatge *et al.*, 2020; Lear *et al.*, 2022).

Analytical techniques, such as HPLC, LC-MS and GC-MS, are also routinely utilised to detect the degradation products of the plastic (Pirillo, Pollegioni and Molla, 2021) (Table 1-1). PET degradation studies have used these techniques given the monomeric degradation products are already known (de Swart and Zimmerman, 2009; Ronkvist, Xie, Lu and Richard A Gross, 2009; Han *et al.*, 2017; Austin *et al.*, 2018; Pirillo, Pollegioni and Molla, 2021). However, for the majority of plastics, the degradation products are unknown, which makes the use of these analytical methods more limited, especially for bio-resistant plastics such as PE (Ghatge *et al.*, 2020).

Technic used	**Changes in PE**	**Measured characteristic**	**Reference**	**Pro**	**Con**
FTIR	Functional group on the surface	Detection of keto-carbonyl function, ester-carbonyl function	Nandiyanto et al., 2019; Yang et al., 2014a	Easy to set up	Prone to biological contamination, limited characterisation of the degradation
Measure of contact angles	Hydrophobicity /Hydrophilicity	Contact angle with surface of plastic	Awasthi, Srivastava, Singh, et al., 2017; Ghatge et al., 2020	Easy to set up	Requires specific equipment Indirect correlation with biodegradation
HT-GPC	Molecular weight distribution	Changes in the molecular weight	Hadad et al., 2005; B. Lee et al., 1991	Characterisation of the polymer molecule	Requires specific equipment Indirect correlation with biodegradation
XRD/ DSC	Crystallinity	Crystallinity; Melting temperature;	Ghatge et al., 2020	Characterisation of the polymer crystallinity	Requires specific equipment

					Indirect correlation with biodegradation
SEM	Surface topography	Modification topography	Austin et al., 2018; Ren et al., 2019; Tournier et al., 2020	Easy and fast	Limited degradation characterisation, with potential for misidentification
Instron	Mechanical properties	Tensile strength; strain energy; % elongation and	El-Shafei et al., 1998; B. Lee et al., 1991	Cheap and fast	Requires specific equipment Indirect correlation with biodegradation
Gravimetric analysis	Consumption of the polymer	Weight loss		Very easy	Prone to misidentification
HPLC, GC-MS, LC-MS	N/A	Detection of degradation by-product		Detection of degradation by-products, Direct estimation of the degradation	Requires having target molecule

Table 1-1 : List of technics used in the characterisation of plastic degradation.

There have been calls from the scientific community to standardise the measurements for plastic degradation (Kumar Sen and Raut, 2015; Chamas *et al.*, 2020; Ghatge *et al.*, 2020; Montazer, Habibi Najafi and Levin, 2020; Lear *et al.*, 2021). Two experiments have been reported as “the gold standard” for the assessment of plastic degradation, especially for plastic where monomeric degradation is unknown. Firstly, the use of ^{13}C labelled plastic labelled PE already exists, allowing the carbon to be traced from the plastic through the monomers and into metabolism (Sander, Kohler and McNeill, 2019). The second “gold standard” experiment is the detection of CO_2 resulting from the active metabolism of the organism on plastic. It is particularly useful for studying plastic degradation in a complex setting, such as monitoring degradation by a microbial community or evaluating plastic degradation in soil or compost (Fontanella *et al.*, 2010; Nowak *et al.*, 2011).

However, both methods have their own limitations. The use of labelled plastic is primarily limited by the price of labelled plastic, a gram can cost upwards of £2000, which is very expensive. Thus far there has been no reports of this being used in the literature. The main limitation of using CO_2 detection is the lack of specificity, i.e., which carbon is used in the metabolism. It does not prove that the carbon came from the degradation of the plastic. It is therefore not usually used as a measure of degradation on its own and is often combined with other methods to validate plastic degradation (Gyung Yoon, Jeong Jeon and Nam Kim, 2012).

1.2.2 Polyethylene terephthalate biodegradation

Polyethylene terephthalate (PET), is the most produced polyester in history (Geyer, Jambeck and Law, 2017; EuropePlastics, 2020), with an estimated 70 million tonnes produced every year (Austin *et al.*, 2018). PET is a copolymer of ethylene glycol and terephthalate (Figure 1-4). The high ratio of aromatic compounds reduces the chain mobility, and makes PET a difficult polyester to hydrolyse (Austin *et al.*, 2018). PET is used in two different forms: resin and fibre. Both forms have the same chemical formula but differ in their properties by the addition of specific additives (Geyer, Jambeck and Law, 2017).

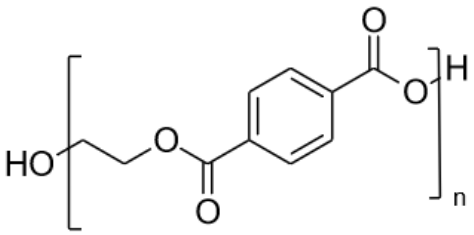


Figure 1-4 : Skeletal structure of polyethylene terephthalate (PET)

The first enzymes able to degrade aromatic polyesters were described in 2005, two cutinases isolated from *Thermobifida fusca* (*Tf*Cut1 and *Tf*Cut2),

which showed some activity against PET (Müller *et al.*, 2005). Both enzymes were able to decrease the weight of the PET film by 30-50% in 3 weeks (Müller *et al.*, 2005). Further *in vitro* characterisation work suggested that their activity was around 0.07 $mg_{terephthalate}$ h^{-1} mg_{enzyme}^{-1} (Tournier *et al.*, 2020). However, in 2016 the first organism able to grow on PET was described, and subsequently the first enzyme which specifically targeted PET was identified (Yoshida *et al.*, 2016).

1.2.2.1 PETase enzyme

Isolated from a PET recycling plant, *Ideonella sakaiensis* was the first organism capable of actively growing and degrading PET for use as its sole carbon source (Yoshida *et al.*, 2016). It is also able to metabolize the monomeric breakdown products of PET, terephthalic acid (TPA) and ethylene glycol (EG) (Yoshida *et al.*, 2016). Two enzyme were reported to be responsible for the degradation of PET: PETase and MHETase (Yoshida *et al.*, 2016). Interestingly, both enzymes have different substrates, the PETase enzyme was only active on PET, resulting in the production of mono(2-hydroxyethyl)-terephthalic acid (MHET), bis(2-hydroxyethyl)-terephthalic acid (BHET) and TPA (Figure 1-4), with a preference for MHET (Yoshida *et al.*, 2016). The PETase has also shown activity against other aromatic polyesters, such as polyethylene furandicarboxylate (PEF), but not against aliphatic or semi aromatic polyesters, such as polybutylene succinate (PBS) and polylactic acid (PLA) (Austin *et al.*, 2018). The MHETase only showed activity on MHET, with a reported k_{cat} of 31 ± 0.8 s^{-1} and a k_{cat}/K_m of 4200±370 s^{-1} mM-1, and no reported activity against PET (Yoshida *et al.*, 2016, 2021). The synergetic relationship between the PETase and the MHETase enables the organism to break down PET.

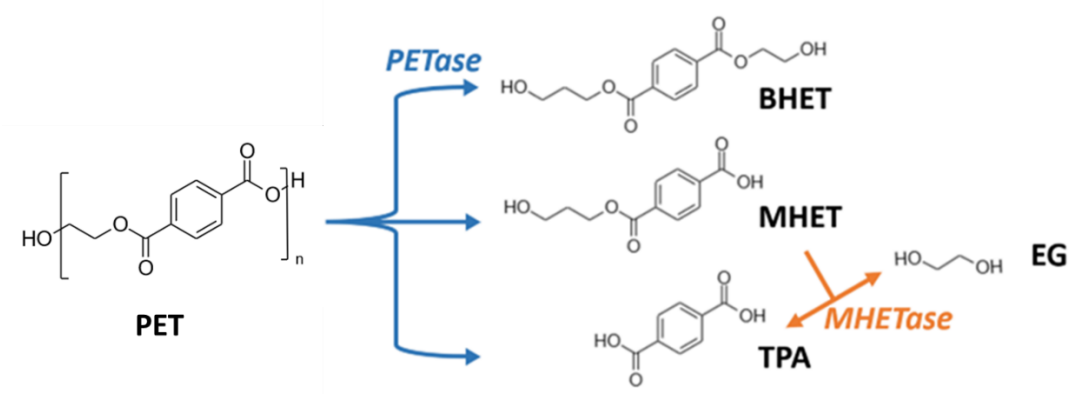


Figure 1-5 : PETase catalyses the depolymerization of PET to terephthalic acid (TPA), bis(2-hydroxyethyl)- TPA (BHET) and mono(2-hydroxyethyl)-TPA (MHET). MHETase converts MHET to terephthalic acid and ethylene glycol (EG)

.

The PETase enzyme exhibits a canonical α/β-hydrolase structure, with a core consisting of eight β-strands and six α-helices (Figure 1-5 C). The MHETase enzyme exhibits a similar general structure, with a α/β-tannase structure (Figure 1-5 B and D). The main difference between PETase and MHETase structure is the presence of lid in MHETase, comprised of 23 α helices.

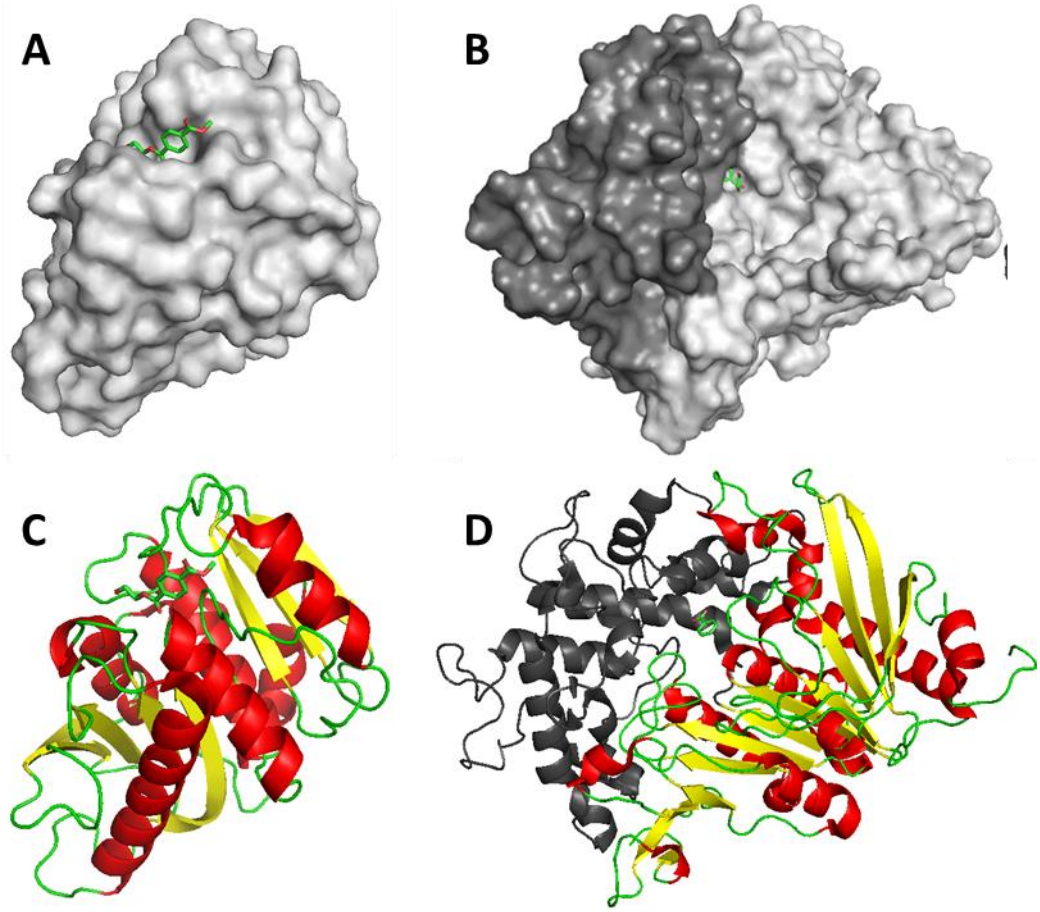


Figure 1-6 : (A) Crystal structure of a PET hydrolase R103G/S131A mutant in complex with HEMT from *Ideonella sakaiensis*, PDB: 5XH3 (Han *et al.*, 2017)**, (B) Crystal structure of the MHETase from *Ideonella sakaiensis* in complex with BHET, lid domain in dark grey, PDB: 6JTT** (Sagong *et al.*, 2020)**, (C) Secondary structure of a PET hydrolase R103G/S131A mutant in complex with HEMT from *Ideonella sakaiensis*, in yellow the β-strands and in red the α-helices PDB: 5XH3** (Han *et al.*, 2017)**, (D) Secondary structure of the MHETase from Ideonella sakaiensis in complex with BHET, lid domain in dark grey, in yellow the β-strands and in red the α-helices, PDB: 6JTT** (Sagong *et al.*, 2020)

The PETase has some sequence similarity with other bacterial cutinases, especially cutinases from *Thermobifida fusca*, with 52% sequence identity. The expression of the PETase enzyme is only triggered by PET, and not by the addition of TPA and BHET (Yoshida *et al.*, 2016).

Multiple PETase mutants have been engineered with improved activity utilising different mutagenesis strategies. The first report of an improved PETase enzyme was in 2018, Austin *et al.* reconstructed a more canonical cutinase, by narrowing the binding cleft. The double mutant

PETase^{S238F,W159F} showed an increased activity against both amorphic and crystallised PET (Austin *et al.*, 2018) (Table 1). Multiple mutants have been reported since, to obtain these mutants two different mutagenesis strategies strategy were utilised. Firstly, a strategy based on structure-guided site-directed mutagenesis, focusing on a few amino acids chosen because of their structural position. Site saturation mutagenesis, was then used to produce a large number of mutants (Joo *et al.*, 2018; Ma *et al.*, 2018; Son *et al.*, 2019, 2020) (Table 1). The second approach utilised computational methods based on protein homology to explore the homologous sequences, identifying conserved residues and assessing their role in activity (Cui *et al.*, 2021; Meng *et al.*, 2021; Lu *et al.*, 2022). Several algorithms have been used to engineer PETase mutants: “MutCompute” (Lu *et al.*, 2022),”Premuse” (Meng *et al.*, 2021) and GRAPE (Cui *et al.*, 2021) (Table 1-2). Despite utilising different methodologies, the approaches all focused on stabilisation of the protein. Using a variety of strategies including finding consensus amino acids (Premuse) (Meng *et al.*, 2021), and assessing the effect of the mutation by minimisation of the statistical energy function (GRAPE) (Cui *et al.*, 2021). Alternatively, by using a trained convolutional neural network to optimise the local chemical microenvironments of amino acids (MutCompute) (Lu *et al.*, 2022).

FAST-PETase, the mutant designed by the neural network MutCompute, exhibits the highest PETase activity recorded (Lu *et al.*, 2022) (Table 1-2). The crystal structure of FAST-PETase, PDB: 7SH6, did not reveal any mutation directly involved in the active site (Lu *et al.*, 2022). Instead, the five mutations are all involved in newly formed, stabilising residue interactions (Figure 1-7). The N233K mutation creates an ionic interaction with E204 and establishes an intramolecular salt bridge (Figure 1-7 (vi)). The side chain of the glutamine R224Q, forms a hydrogen bond with the carbonyl group of S192 (Figure 1-7 (iv)). Finally, the S121E mutation recruits a water molecule to create new a hydrogen-bonding network with H186 and N172 (Figure 1-7 (ii)).

Mutation strategy	Mutations	Results	Reasoning	Reference
Mimicking the active site of a homologous enzyme	S238F, W159F	Increased activity by 17% compared to WT at 30°C, increased activity towards more crystalline substrates	Promoting substrate binding: increased π-stacking interactions Allowed PET molecule to sit deeper within the active site	Austin et al., 2018
Mimicking the active site of a homologous enzyme	S121E, D186H, S242T, N246D	Increased Tm by 9.8°C, increased activity by 58-fold, compared to WT at 37°C	Promoting substrate binding: increased the hydrophobicity of binding pocket, formation of a salt bridge to aid stability	Son et al., 2019
Use computational methods based on protein homology to increase protein thermostability	S214H, W159H, S188Q, R280A, A180I, G165A, Q119Y, L117F, T140D	Increased Tm by 22°C, enzyme active at 50°C and 60°C (WT inactive at these temperatures)	Promoting substrate binding: increased hydrophobicity of binding pocket Promoting thermal stability with new electrostatic interactions and better hydrophobic packing of the protein	Cui et al., 2021
Use computational methods based on protein homology to increase protein thermostability and activity	W159H, F229Y	Increased Tm by 10.4°C, increased activity by 40-fold, compared to WT at 40°C	Promoting substrate binding: increased π-stacking interactions and formation of a salt bridge to aid stability	Meng et al., 2021
Use computational methods based on protein homology to increase	S121E D186H R224Q N233K R280A	Improved activity 1.5-fold against the best PET degrading enzyme	Promoting thermal stability using intramolecular salt bridges,	Lu et al., 2022

protein thermostability and activity		Improved activity against crystallised substrates		

Table 1-2: List of reported mutant PETase enzymes

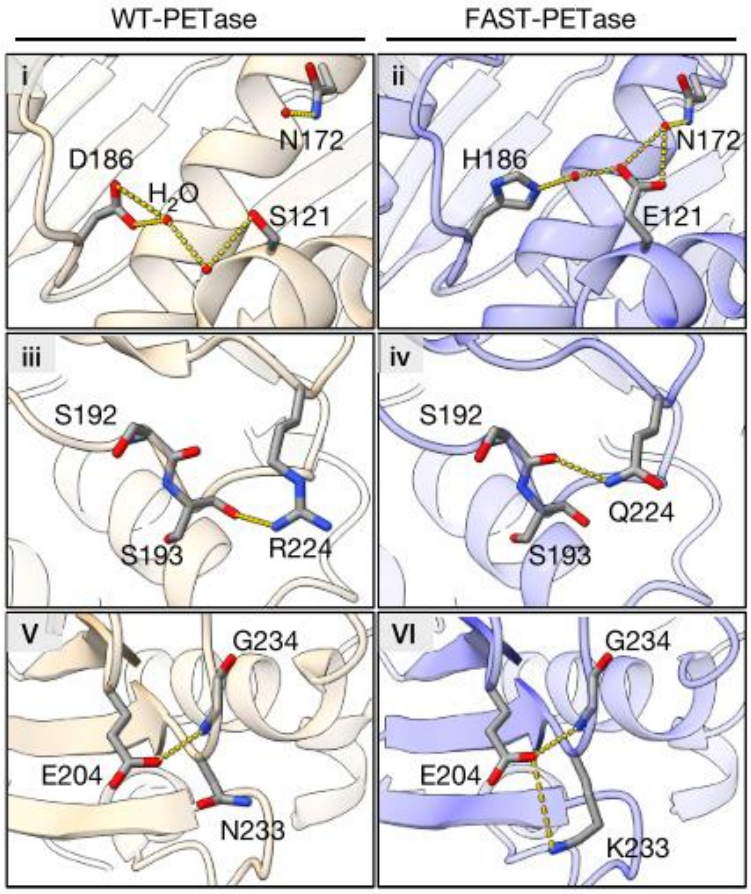


Figure 1-7 :Predicted mutations from MutCompute algorithm stabilize FAST-PETase (I–VI). Structural comparison between (I, III, V) WT PETase (tan-coloured cartoon model, PDB code 5XJH) and (II, IV, VI) FAST-PETase (blue-coloured cartoon model, PDB code 7SH6) near the predicted mutation sites (S121E, R224Q, N233K, respectively). Hydrogen-bonding and salt bridge interactions are shown and highlighted as yellow dotted lines. The figure is taken from Lu et al., 2022.

1.2.2.2 PET degradation utilising cutinases

The degradation of PET has been reported in a variety of organisms including *Thermobifida* sp. and *Streptomyces* sp. utilising an array of enzymes (Table 1-2). All the reported PET degrading enzymes share similarity in their sequences and their structures (Herrero Acero *et al.*, 2011; Yoshida *et al.*, 2016; Austin *et al.*, 2018; Almeida, Rincón, Jackson and Alan D. W. Dobson, 2019).The overall structure of the cutinases are very similar with the structure of *Ideonella sakaiensis* PETase. Especially the hydrophobic region surrounding the catalytic site, which is hypothesized to participate in the adsorption of the enzyme on PET (Kawai, Kawabata and Oda, 2019). Moreover, the different enzymes all result in the same degradation products: BHET, HMET, TPA and EG, which suggests a similar degradation mechanism (Kawai, Kawabata and Oda, 2019).

Enzyme	**Organism**	**Sequence ID**	**Results**	**Reference**
TfCut1	*Thermobifida fusca KW3*	CBY05529.1	≤11% weight loss	Then et al., 2015
TfCut2	*Thermobifida fusca KW3*	CBY05530.1	≤12% weight loss	Then et al., 2015
Thc_Cut 1	*Thermobifida cellulosilytica DSM44535*	ADV92526.1	Detection of monomer: MHET, TPA	Herrero Acero et al., 2011
Thc_Cut 2	*Thermobifida cellulosilytica DSM44535*	ADV92527.1	Detection of monomer: MHET, TPA	Herrero Acero et al., 2011
Leaf Compost Cutinase (LCC)	*Uncultured bacterium*	AEV21261.1	≤5% weight loss	Sulaiman et al., 2012
FsC	*Fusarium vanettenii*	N/A	≤5% weight loss	Ronkvist et al., 2009
Sub1	*Streptomyces scabiei*	A0A5P3LVN0	Detection of monomer: TPA	Jabloune et al., 2020
SM14est	*Streptomyces sp.* SM14	A0A679PDB4	Activity against PCL	Almeida et al., 2019

Table 1-3 : List of other enzymes with reported PET degradation activity

1.2.2.3 Bio-recycling of PET as an economically viable process

Protein engineering of the PETase enzyme led to the creation of mutants with an activity sufficient to sustain a PET bio-recycling process. Carbios is the first company to have developed an enzymatic recycling process, using a Leaf Compost Cutinase (LCC) mutant, to degrade PET into TPA and EG at a commercial scale (Tournier *et al.*, 2020). Following this another recycling process with potential commercial application was recently published, which uses a mutant PETase enzyme (Lu *et al.*, 2022).

Tournier *et al* showed that the recycled TPA can repolymerise to form a recycled PET. The recycled PET resin exhibited similar viscosity (0.75 dl g−1) and average molecular weight (36,650 g mol−1) to those of PET synthetised by petrochemical TPA (evaluated number average molecular weight 38,390 g mol−1 and intrinsic viscosity 0.78 dl g−1) (Tournier *et al.*, 2020). Moreover, after being re-blown the recycled PET bottle presented similar mechanical properties than the petrochemical one (Tournier *et al.*, 2020). This would be the first biological-recycling process for which the recycled plastic exhibits similar characteristic than petrochemical PET. This opens the possibility of a circular economy for PET plastic (Tournier *et al.*, 2020).

However, both of those recycling process suffer the same problem: they both focus on the recuperation of the TPA, which would require the use of de novo EG to reform PET. Moreover, the price of the recycled PET is significatively more expensive than the de novo PET, which questions the economic viability of the process (Crownhart, 2021).

1.2.3 Polyethylene biodegradation

Polyethylene is the most commonly utilised plastic (Geyer, Jambeck and Law, 2017; EuropePlastics, 2020), with an estimated 2700 million tonnes produced since 1950 (Geyer, Jambeck and Law, 2017). PE is a polymer of ethylene, which forms a continuous chain of carbon. The stability of the carbon-carbon bonds and the lack of an exposed reactive group makes it

difficult to degrade. PE can be found in different forms, depending on the polymerisation process , and the degree of branching, which results in variability in the characteristic of the polymer (density, melting point, flexibility, etc) (Sam *et al.*, 2014).

Comparison of the different reports about the biodegradation of PE is complex. While more than 20 bacterial species have been reported to degrade PE including *Staphylococcus* sp.(Nowak *et al.*, 2011), *Bacillus* sp. (Sudhakar *et al.*, 2008), *Brevibacillus* sp. (Hadad, Geresh and Sivan, 2005) and more than 10 fungal species *Aspergillus* sp. (Volke-Sepúlveda *et al.*, 2002), *Penicillium* sp. (Volke-Sepúlveda *et al.*, 2002), *Fusarium* sp. (Fontanella *et al.*, 2010) to varying degrees (Ghatge *et al.*, 2020). A direct comparison of the efficacy of the PE degradation remains challenging due to the difference in the experimental conditions: type of plastic used, treatment of plastic, media used, and the differing techniques used to measure the degradation.

The biodegradation of PE has been extensively studied (Kumar Sen and Raut, 2015; Ghatge *et al.*, 2020; Montazer, Habibi Najafi and Levin, 2020), yet despite this the biodegradation process remains uncharacterised. It is thought that both abiotic and biotic factors contribute to the degradation process, but their co-involvement still needs to be assessed (Montazer, Habibi Najafi and Levin, 2020).

Perhaps most problematic in the characterisation of the biodegradation of PE is the utilisation of different sources of PE. There is a lack of standardisation of the type PE used (Kumar Sen and Raut, 2015; Ghatge *et al.*, 2020; Montazer, Habibi Najafi and Levin, 2020). Reports of PE biodegradation used generally 3 types of PE: commercial PE, pre-treated PE and virgin PE.

1.2.3.1 Biodegradation of commercial PE

The label “commercial PE” is used for PE which contains additives. While this grouping is the most representative of the type of PE present in the

environment, the presence of additives makes it impossible to differentiate the degradation of the PE polymer from the degradation of additives (Ghatge *et al.*, 2020).

Several reports have tried to facilitate the degradation of PE by changing the composition of PE. The addition of bioavailable carbon sources, such as starch (Lee *et al.*, 1991; Pometto, Lee and Johnson, 1992; El-Shafei *et al.*, 1998) and synthetic aliphatic polyester (Nowak *et al.*, 2011) have been used to promote bio-degradation. Despite this addition, the PE biodegradation detected is limited. The gravimetric measurement showed very little significant decreases in the mass of the PE film, in fact the mass of the PE film increased (Lee *et al.*, 1991; El-Shafei *et al.*, 1998). Other degradation assessments such as tensile strength and elongation break demonstrated some degree of degradation, but this was not significant (Lee *et al.*, 1991; El-Shafei *et al.*, 1998). The best degradation reported to date was with a modified PE plastic which had 17% weight loss after 225 days of incubation, using a consortium of soil bacteria, mainly composed of *Bacillus* sp. (Nowak *et al.*, 2011). Interestingly, the mass loss detected is still less than the than quantity of bio-available aliphatic polyester added in the PE plastic (30%) (Nowak *et al.*, 2011)

1.2.3.2 Biodegradation of pre-treated PE

The pre-treatment of PE allows for the initial degradation of PE using abiotic degradation mechanisms. Two types of pre-treatments are utilised in the plastic degradation field: UV and thermal pre-treatment. The UV pre-treatment consists of exposing the PE to UV rays, for a more or less time (from 5 to 60 hours) (Santo, Weitsman and Sivan, 2013; J. Zhang *et al.*, 2020) This pre-treatment is usually used as both a decontamination method and an abiotic degradation to “weather” PE (Lucas *et al.*, 2008). The thermal pre-treatment consists of placing the plastic in a hot environment (70℃) for long period of time (up to 10 days) (Awasthi, Srivastava and Singh, 2017). While this method does not decontaminate the plastic, it “ages” the plastic

and allows abiotic degradation of PE to take place (Awasthi, Srivastava and Singh, 2017).

Awasthi et al. reported that HDPE following thermal treatment was degraded by *Klebsiella pneumoniae*, in 60 days, with an 18.4% weight loss and a 60% decrease in tensile strength (Awasthi *et al.*, 2017). A strain of *Aspergillus flavus* sp. exhibited PE degrading ability on UV pre- treated PE with a mass loss of 3.9025 ± 1.18% and a significant decrease in the molecular weight of PE (J. Zhang *et al.*, 2020). Purified laccases from *Rhodococcus ruber* was able to reduce the average molecular weight of UV pre-treated PE, by up to 20 % (Santo, Weitsman and Sivan, 2013).

While the pre-treatment could be an efficient way to facilitate the degradation of PE in an industrial setting (Lear *et al.*, 2022), it is not recommended for the characterisation of PE degrading organism/enzymes (Wei and Zimmermann, 2017; Ghatge *et al.*, 2020). Pre-treatment can have a significant impact on the biodegradation of PE and could lead to an overestimation of the actual PE biodegradation ability measured (Lear *et al.*, 2022).

1.2.3.3 Biodegradation of virgin, non-treated, PE

Yang et al. reported in 2014 the isolation of two bacterial strains able to grow using PE as the sole carbon source (Yang, Yang, W.-M. Wu, *et al.*, 2014). *Enterobacter asburiae* YT1 and *Bacillus sp.* YP1 are to date the first organisms able to degrade PE with no pre-treatment. However, the degradation detected from their growth is still limited: they both degraded the surface of PE film, both increased the O/C ratio on the surface of the plastic, which is generally considered as a proof of oxidation of the PE plastic (Yang, Yang, W.-M. Wu, *et al.*, 2014). YT1and YP1 degraded respectively approximately 6.1 ± 0.3% and 10.7 ± 0.2% of the mass of PE film in 60 days (Yang, Yang, W.-M. Wu, *et al.*, 2014).

While encouraging, these results are still considered by some researchers as not enough to consider YT1 and YP1 as plastic degrading organisms, because of slow degradation rate (Lear *et al.*, 2022)

1.2.4 Bioplastics

Conventional plastic is polluting the environment in response to this alternatives have been sought to petrochemical based plastics, these are termed bioplastics (Rosenboom, Langer and Traverso, 2022). Bioplastics are defined as plastics manufactured from bio-based polymers. They are often composed of multiple materials, which have different properties and applications. The European bioplastics define a bioplastic as being a material or product derived from bio based or a product which is biodegradable (European Bioplastics, 2018). Bio based materials or products are derived from biomass (Figure 8) (European Bioplastics, 2018).

Currently, bio-based plastics are generally produced from carbohydrate-rich biomass, such as corn or sugarcane, or oily plants (Rosenboom, Langer and Traverso, 2022). A “biodegradable” plastic is defined as a plastic which is capable of being degraded through the biological activity of microorganisms (Figure 8). A “compostable” plastic, a subclass of “biodegradable” plastic, is a plastic which degrades to form water, carbon dioxide and biomass (Rosenboom, Langer and Traverso, 2022). Therefore, both the compostability and the biodegradability, of a polymer depend on the microbial and chemical environment of the plastic (European Bioplastics, 2018; Rosenboom, Langer and Traverso, 2022).

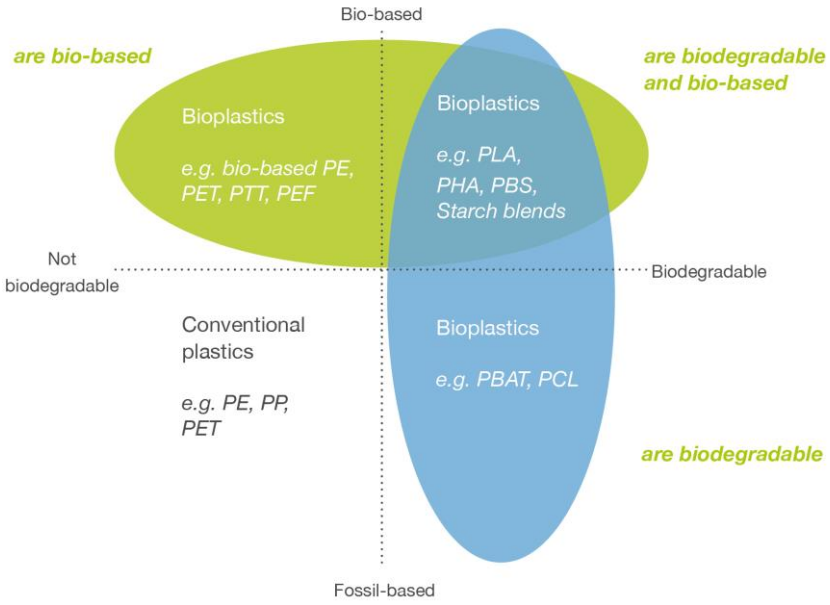


Figure 8: diagram highlighting the difference between the conventional plastics and the different types of "bioplastics". The figure is taken from European Bioplastics, 2018

Therefore, the term "bioplastic" can cover a large variety of plastic including non-biodegradable biobased plastics such as bio-PE or bio-PET, biodegradable petrol-based plastic, like polycaprolactone (PCL), and bio-based biodegradable plastic, like starch blends or polylactic acid (PLA) (Figure 8). This variety in the definition of a bioplastic can be misleading and does not necessarily mean that they are really bioplastics, in that they are made from biomaterial and can degrade in the environment (Rosenboom, Langer and Traverso, 2022).

1.3 Streptomyces sp.

1.3.1 Streptomyces as potential plastic degraders

Streptomyces sp. have been reported to degrade several complex large polymeric macromolecules including chitin, cellulose and lignin (Rodríguez-Fonseca *et al.*, 2021). Several of the enzymes involved in the degradation of lignin have been reported to be able to degrade artificial

polymers (Lee *et al.*, 1991; Pometto, Lee and Johnson, 1992; Ehara *et al.*, 2000; Fujisawa, Hirai and Nishida, 2001).

In addition of being able to degrade natural polymers, several *Streptomyces* sp*.* have been reported to be active on PET and PE.

1.3.1.1 Streptomyces as potential PET degrader

PET degradation relies on enzymes that are very similar to the ones involved in the degradation of cutin, a polymer found in leaves (Tournier *et al.*, 2020). Multiple strains of Streptomyces have been reported to be able to degrade PET, with various characterisation of the degradation.

The overexpression of PETase enzymes has been used in at least two cases to characterise PET degradation by Streptomyces (Almeida, Rincón, Jackson and Alan D.W. Dobson, 2019; Jabloune *et al.*, 2020). Almeida et al overexpressed a homolog of the *Ideonella sakaiensis* PETase and looked for activity on polycaprolactone, also referred as PCL, a widely used PET substitute, to determine degradation activity. PCL is a soluble aliphatic polyester, easier to manipulate than PET, usually used in clearance assays (Jun *et al.*, 1994; Goldberg, 1995; Cho *et al.*, 2011). But no direct evidence of PET degradation was reported (Almeida, Rincón, Jackson and Alan D.W. Dobson, 2019).

Jabloune *et al.* characterised a suberinase enzyme, Sub1, which has direct activity against suberin and cutin. The characterisation of PET included the detection of TPA. The addition of a non-ionic surfactant, such as Triton, improved the activity of the Sub1 enzyme against PET, a behaviour more related to lipase enzymes than cutinases enzymes (Jabloune *et al.*, 2020). Despite the increase in activity, the Sub1 enzyme did not exhibit a strong activity against PET, with 200 µg/mL of TPA detected after 20 days of enzymatic treatment (Jabloune *et al.*, 2020).

Farzi *et al.*, reported an unidentified strain of *Streptomyces* sp*.* able to degrade commercial PET (Farzi, Dehnad and Fotouhi, 2019). However, the characterisation of the degradation was limited, commercial plastic contains

additives which can also fuel growth and no monomeric breakdown products were detected. Moreover, the surface of the film did not show significant degradation (Farzi, Dehnad and Fotouhi, 2019).

Despite tentative evidence of *Streptomyces* sp. being able to degrade PET, an in-depth characterisation of the degradation process remains elusive.

1.3.1.2 Streptomyces as potential PE degraders

PE degradation, although not fully characterized, is hypothesised to rely on a variety of successive reactions leading to the oxidation of PE (Ghatge *et al.*, 2020). Several strains of *Streptomyces* sp. have been reported to degrade PE, however the level of characterisation of this degradation varies (Rodríguez-Fonseca *et al.*, 2021). One of the main limitations remains the standardisation of the plastic sample and degradation measurements.

Initial reports of PE degradation by Streptomyces used PE blended with starch (Lee *et al.*, 1991; El-Shafei *et al.*, 1998). Characterisation of the rate of PE degradation is difficult as it is not clear if it was only the starch which was been degraded, a more likely scenario.

More recent reports of PE degradation utilising *Streptomyces* sp. have been published. *Streptomyces* sp. have been found to be part of consortiums growing on PE in various environment (Huerta Lwanga *et al.*, 2018; Huang *et al.*, 2019; Rüthi *et al.*, 2020; Lear *et al.*, 2021). Moreover, a few Streptomyces strains able to degrade PE have been published, however the level of characterisation of the degradation is limited (Kannahi and Sudha, 2013; Shahnawaz, Sangale and Ade, 2016; Shao *et al.*, 2019). In each report, the degradation is characterised by a combination of gravimetric measurements (Kannahi and Sudha, 2013), FTIR analysis (Shahnawaz, Sangale and Ade, 2016) and SEM pictures (Shao *et al.*, 2019). Methods which have been criticized for their bias (Kumar Sen and Raut, 2015; Chamas *et al.*, 2020; Ghatge *et al.*, 2020; Montazer, Habibi Najafi and Levin, 2020; Lear *et al.*, 2021).

1.3.2 Streptomyces Life cycle and Morphology

Streptomyces sp. are part of the actinobacteria phyla and the order Actinomycetales (Romano and Nickerson, 1956). This genus is characterized by a high G+C content, typically >70%, with a large linear chromosome (>8 Mb) (de Lima Procópio *et al.*, 2012). Streptomyces is a genus of Gram-positive bacteria; they can undergo filamentous growth similar to fungi and are strictly aerobic (Xu *et al.*, 2022). *Streptomyces* sp. have a complex life cycle, which involves morphological differentiation (Yagüe *et al.*, 2013; Chater, 2016). This differentiation involves the formation of aerial hyphae that can differentiate into a chain of spores (Figure 1-9). This complex phenomenon is usually referred to as “sporulation”. Sporulation is generally triggered when the organism faces a stress condition such as nutrient or oxygen limitation (Yagüe *et al.*, 2013).

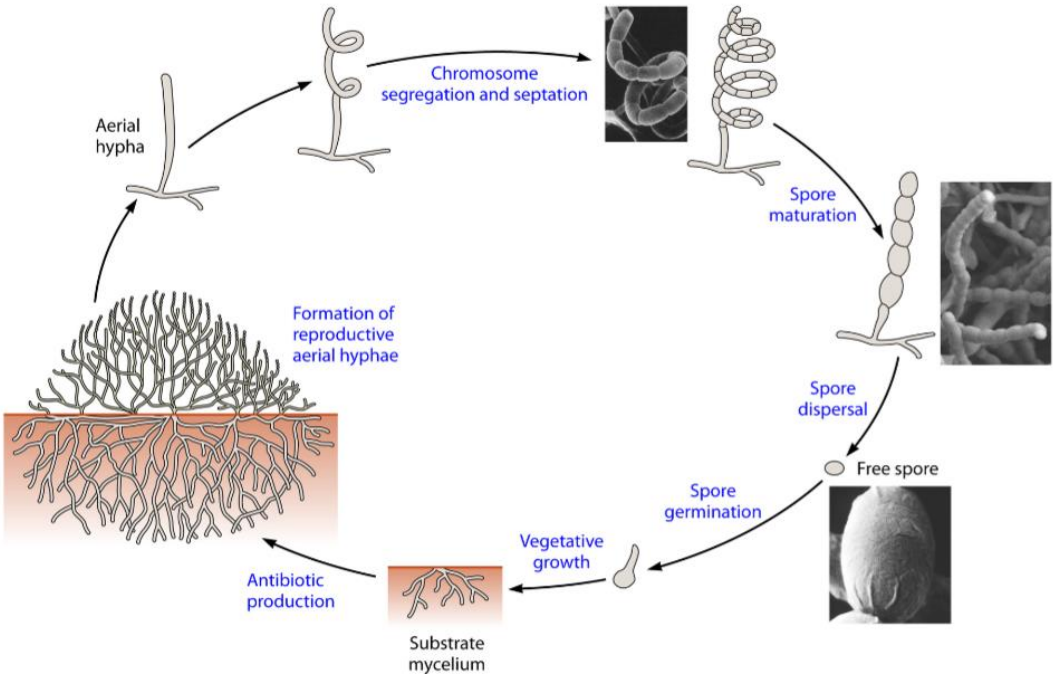


Figure 1-9 : Schematic representation of the life cycle of Streptomyces. This figure is taken from Barka et al., 2016

In addition of its complex life cycle, *Streptomyces* are a powerhouse of secondary metabolite production, which have a wide range of bioactivities (Z. Zhang *et al.*, 2020; Xu *et al.*, 2022). It is estimated that *Streptomyces sp*. are

responsible for producing more than 50% of the 11,900 known microbial antibiotics (Borodina, Krabben and Nielsen, 2005) and are used to produce more that 70 % of industrially relevant antibiotics (Table 1-3) (Kitani *et al.*, 2011).

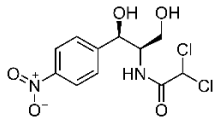
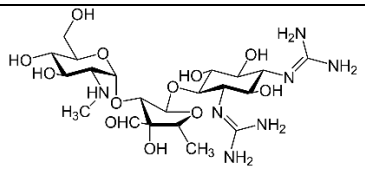
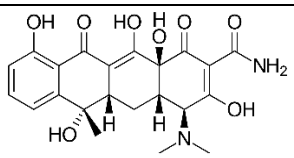
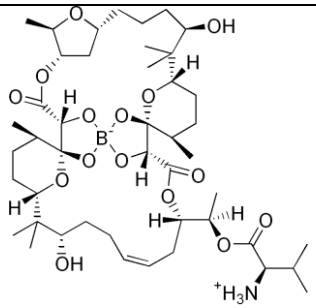
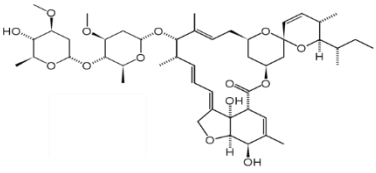
Antibiotic	**strains**	**Chemical structure of the antibiotic**	**Reference**
Chloramphenicol	*S. venezuela*		Fernández-martínez et al., 2014
Streptomycin	*S. griseus*		Distler et al., 1987
Tetracycline	*S. rimosus*		Petković et al., 2017
Boromycin	*S. antibioticus*		Chen et al., 1981
Ivermectin B1a	*S. avermitilis*		Deng et al., 2019

Table 1-4 : List of several antibiotics produced industrially using *Streptomyces* sp.

Streptomyces sp. are ubiquitous in a wide variety of environments and constitute up to 50% of the total population of soil actinomycetes (Flärdh and Buttner, 2009). *Streptomyces* sp. has a versatile metabolism and can utilise a variety of different macromolecules (cellulose, lignin, agar and

chitin) (Chater *et al.*, 2010) and aromatic compounds (vanillin, benzoate, catechol) (Hae-Reun, Hyun-Joo and Eung-Soo, 2000; Menendez-Bravo *et al.*, 2017; Khalil *et al.*, 2019).

1.4 Project aim and objectives

We recently isolated a *Streptomyces* sp. from a wall in Warwick which was shown to have some activity on both commercial PET and PE. This is the first time this phenomenon has been reported.

The aim of this project is to provide a comprehensive understanding of the metabolic and enzymatic degradation of virgin PET and PE by *Streptomyces.* sp.

Objectives.

Determine the growth rates of the *Streptomyces* sp. on virgin PET and PE in shake flasks and fermentation.

Characterisation of the metabolic pathways involved in the degradation of virgin PET and PE utilising metabolomic and transcriptomic analysis.

Genomic sequencing and bioinformatic analysis to identify key enzymes and metabolic pathways for the degradation of PET and PE.

The work presented in this thesis is a first step towards understanding how this remarkable microorganism can grow on both PET and PE.

Chapter 3 presents the characterisation of the plastic degradation using commonly used methodology such as the characterisation of the growth rate and SEM analysis of the surface of plastic. Moreover, thanks to a multi-layer analysis approach, relying on both metabolomics and transcriptomics, the metabolic pathways involved in the degradation of virgin PET and PE were characterised.

Chapter 4 presents the characterisation of the genome of the *Streptomyces* sp. isolate. The identification of the metabolic pathways enabling the growth on plastic degradation by-product as well as potential enzyme candidates for plastic degradation. When possible, structural comparisons have been conducted on the plastic degrading enzyme candidate, to infer their activity

2 Materials and Methods

2.1 Media

2.1.1 Minimal medium

2.1.1.1 Modified minimal medium (SMMmod)

Modified minimal medium (SMMmod) was a modified version of the previously described minimal medium (SM) (T Kieser *et al.*, 2000).

SMMmod medium was used to grow *Streptomyces* sp. in shake flasks with both glucose and plastic as the carbon source and contained 2.4 mM $MgSO_4$ x 7 H_2O, 0.5mM NaH_2PO_4, 0.5 mM K_2HPO_4, 50 mM NH_4Cl, 25 mM TES buffer and 1mL/L of trace element solution. The trace element solution was composed of 46 mM H_3BO_3, 9 mM $MnCl_2$ x $4H_2O$, 0.77 mM $ZnSO_4$ x $7H_2O$, 1.6 mM Na_2MoO_4 x $2H_2O$, 0.3 mM $CuSO_4$ x 5 H_2O and 0.17 mM Co $(NO_3)_2$ x $6H_2O$. The pH was set to 7.2. SMMmod was supplemented with either 0.1% (w/v) of glucose or 0.1% (w/v) of glucose and 1% (w/v) of plastic.

2.1.1.2 SMMmod fermentation media (SMMmodFm)

SMMmod was used for the fermentation, the basic recipe was the same as the one detailed above except for the addition of 27nM $CaCl_2$. This medium was supplemented with 1% (w/v) of glucose and 1% (w/v) of plastic. The concentration of glucose was increased to 1%(w/v) to ensure a sufficient biomass to detect the plastic degradation.

2.1.1.3 M9 medium

M9 minimal medium was used to assess the ability of *Streptomyces* sp. to grow using either terephthalic acid (TPA) and/or ethylene glycol (EG) as the sole carbon source. It contained 40 mM Na_2HPO_4 x 2 H_2O, 22 mM KH_2PO_4, 8.6 mM NaCl, 18.7 mM NH_4Cl, 2 mM $MgSO_4$, 100 μM $CaCl_2$ and 1 mL/L of trace element solution (the same composition as used in the SMMmod medium). M9 media was supplemented with 0.1 % (w/v) of TPA and 1 % (v/v) of EG.

2.1.2 Rich medium

2.1.2.1 GYM medium

GYM medium (T. Kieser *et al.*, 2000) was used to routinely grow *Streptomyces* sp. GYM contains 4 g/L glucose, 4 g/L yeast extract and 10 g/L malt extract. The pH was set at 7.2. To grow *Streptomyces* sp. for DNA extraction, GYM was further supplemented with 0.5 % (w/v) of glycine (Nikodinovic, Barrow and Chuck, 2003).

2.1.2.2 Soya Flour Mannitol (SFM) medium

SFM medium was used to grow Streptomyces on solid agar plates. SFM is composed of 20 g/L agar, 20 g/L mannitol and 20 g/L soya flour, sourced from Holland and Barrett (T. Kieser *et al.*, 2000).

2.1.3 General chemicals

Except otherwise stated, all chemical compounds were purchased from Sigma-Aldrich.

Except otherwise stated, all plastics used were virgin plastic purchased from Goodfellow.

2.2 Biological manipulation

2.2.1 List of organisms used in this study

One isolate was used in this work, which was previously isolated from a wall in Warwick, *Streptomyces* sp.F.

2.2.2 Culture growth

Streptomyces sp. F was grown on GYM at 30 °C unless otherwise stated. Liquid cultures were agitated at 125 rpm and typically grown at 10-20% of the volume of a 250 mL baffled flask equipped with a membrane screw cap to allow optimal oxygenation.

2.2.3 Bacterial storage

Spore suspensions were used for long-term storage of *Streptomyces sp.* Briefly, spores were collected from a plate, after 96 h of growth, by scrapping the plate with a spreader and resuspending in 2-3 ml of 20% glycerol. The spore suspension was centrifuged for 3 min at 1400 rpm, the supernatant discarded and replaced by 500 µL of fresh 20% glycerol. After preparation, all the vials were stored at -80 ºC.

2.3 Molecular procedures

2.3.1 Extraction and purification of chromosomal DNA

Genomic DNA was extracted from *Streptomyces* sp. S using a Zymo Research® *Quick* DNA Kit, according to the manufacturer's instructions. The protocol for DNA extraction from Gram-positive bacteria was utilised.

2.3.2 List of primer used

For the identification of *Streptomyces* isolates several house-keeping genes as well as 16S rRNA genes were sequenced. Primer names and sequences are described in Table 2.

Gene	Primer name	Sequence	Amplicon size	reference
16S	16S_F	ACAAGCCCTGGAAACGGGGT	1074	Rintala et al., 2001
	16S_R	ACGTGTGCAGCCCAAGACA		
rpoB	rpoBP_F	GAGCGCATGACCACCCAGGACGTCGAGGC	994	Guo et al., 2008
	rpoBP_R	CCTCGTAGTTGTGACCCTCCCACGGCATGA		
trpB	trpB_F	GCGCGAGGACCTGAACCACACCGGCTCACACAAGATCAACA	822	Guo et al., 2008
	trpB_R	TCGATGGCCGGGATGATGCCCTCGGTGCGCGACAGCAGGC		
recA	recA_F	CCGCRCTCGCACAGATTGAACGSCAATTC	913	Guo et al., 2008
	recA_R	GCSAGGTCGGGGTTGTCCTTSAGGAAGTTGCG		
atpD	atpD_F	GTCGGCGACTTCACCAAGGGCAAGGTGTTCAACACC	998	Guo et al., 2008
	atpD_R	GTGAACTGCTTGGCGACGTGGGTGTTCTGGGACAGGAA		

Table 2: Sequencing primers used in this study.

2.3.3 Dreamtaq-polymerase colony PCR (cPCR) for sequencing

All polymerase chain reactions (PCR) were performed in Sapphire 0.2 mL thin-walled, flat cap PCR tubes using a Biometra Trio (AnalytikJena©, Jena, Germany) PCR thermocycler. All PCR-amplified DNA was analysed via agarose gel electrophoresis.

cPCR was performed to amplify genes from isolates for sequencing. Promega GoTaq™ G2 Green Master Mix was used routinely in 15 µL reactions. For *Streptomyces* isolates, a single colony was picked using a toothpick and resuspended in 10 µL of nuclease-free water in a PCR tube, then boiled for 10 min. 5 µL of the boiled material was subsequently added to 10 µL of the pre-made master mix with GoTaq™ G2 Green Master Mix and the adequate primer pair (Table 3).

Component	
DreamTaq Green® PCR Master Mix (2x)	7.5 µL
Forward primer (~17 µM)	0.5 µL
Reverse primer (~17 µM)	0.5 µL
Template DNA	5 µL
Nuclease-free water	0.5 µL
DMSO 100%	1 µL
Total reaction volume	15 µL

Table 2-1: composition of PCR reaction mix

Despite different primers being utilised the same PCR program was used.

Step		**Temperature**	**Duration**
Initial denaturation		95 °C	10 min
10 cycles	Denaturation	95 °C	30 seconds
	Annealing	55 °C	40 seconds
	Extension	72 °C	60 seconds / kb
25 cycles	Denaturation	95 °C	30 seconds
	Annealing	60 °C	40 seconds
	Extension	72 °C	60 seconds / kb
Final extension		72 °C	10 minutes
Hold		14 °C	∞

Table 2-2 : PCR thermocycler condition used in this work

2.3.4 DNA analysis via agarose gel electrophoresis

1% agarose gels were prepared by mixing 1 g technical grade agarose (Sigma) per 100 mL 1X TAE buffer (40 mM Tris base; 0.1% (v/v) glacial acetic acid; 1 mM EDTA) and melting the mixture at high heat for 2/3 min. SYBR® Safe DNA gel stain (Thermo-Fisher Scientific®) was added at a final concentration of 10 µL/mL to visualise DNA bands on the gel. Samples from DreamTaq PCR reactions were either directly loaded on agarose gels or

supplemented with NEB® 6X Purple Gel Loading Dye prior to loading on the gel and running using 1X TAE as running buffer, at 100 V, (400 mA) for 40-60 minutes and visualised using a UV transilluminator (Gel Doc™). DNA size was estimated by comparison with a NEB® 2-log DNA ladder.

2.3.5 Extraction and purification of DNA from agarose gel

DNA bands of appropriate size were excised from the agarose gel using a blue light transilluminator (BT Lab Systems©). DNA was extracted using either the QIAquick® or Monarch® Gel Extraction Kit according to the manufacturer's instructions. DNA was eluted in 13 µL of nuclease free water.

2.3.6 Quantification of nucleic acids

DNA concentrations were measured using a BioMate™ 3S Spectrophotometer (Thermo Fisher Scientific, Waltham, MA, United States), using high purity water or elution buffer from extraction kits as blank. One µL of each sample was loaded onto the device and absorbance at 260 nm and 280 nm was measured. DNA maximal absorbance is at 260 nm whereas proteins absorb preferentially at 280 nm. The 260/280 ratio was used to measure sample purity. A ratio of ~1.8 was generally accepted as "pure" for DNA (Sambrook, Fritsch, and Maniatis 1989).

2.4 SEM picture

SEM microscopy was used to assess the degradation of both the PE and PET film. After 21 days submerged in media with and without cells the polymer films were rinsed with water. Polymer films were cut to small pieces around ~10 mm in diameter and dried at 60 °C until the water was completely removed. Samples were mounted on aluminium stubs using carbon tape. Gold was applied on the sample, as sputter coating. SEM imaging was performed using an FEI Quanta 650 ESEM instrument under

low vacuum (0.45 torr) operating with a gaseous solid-state detector. Imaging was performed with a beam-accelerating voltage of 15 keV.

2.5 Fermentation on plastic

2.5.1 Fermentation conditions

Growth of the *Streptomyces* sp. F was assessed using fermentation in SMMmod fermentation medium. Precultures were prepared in 500 mL baffled shake flasks by inoculating spores from a fresh plate into 200 mL of GYM medium. These cultures were incubated at 30 °C, 250 rpm for 48 hours.

The fermentations were carried out in an Eppendorf® bioreactor system, with a working volume of 2000 mL. Both the pH and dissolved oxygen (DO) were controlled by the Eppendorf controller, using 1 M HCL and 1 M KOH to control pH at 7.2. Fermentations were performed for 14 to 21 days, with samples taken every 2-3 days. Those sample were further analysed using LC-MS and transcriptomic analysis.

2.5.2 LC-MS analysis

Samples were analysed in a Dionex UltiMate 3000-QExactive LC-HRMS/MS (quadrupole-orbitrap MS) equipped with a ZICpHILIC, (4.6x150mm) column. Analysis was carried out with constant mobile phase of 20 mM ammonium carbonate, with a flow rate set to 300 µL/min. The run time was set at 15 min and the injection volume at 5 µL.

Identification analysis was carried out with Compound Discoverer 3.1 SP1 (Thermo Fisher Scientific). Metabolite identification was performed using both accurate mass and retention time against 268 standard and TPA to match sample metabolites against multiple databases. Further analysis using

accurate mass values were performed against *mz*Cloud and *mz*Valut databases.

2.6 Genome data mining

2.6.1 Extraction and purification of chromosomal DNA

Genomic DNA was extracted from *Streptomyces* sp.F using a Zymo Research® *Quick* DNA Kit, according to manufacturer's instructions. The protocol for DNA extraction from Gram-positive bacteria was utilised.

2.6.2 Genome sequencing

The genome of *Streptomyces* sp FS was extracted using a Zymo Research® *Quick* DNA Kit and sequenced *de novo*, using Pac-Bio methodology, by Novogene (South Plainfield, NJ), with a sequencing depth >10. The sequence of the genome was collected after the alignment and merging of the sequencing reads.

2.6.3 Transcriptomic analysis

Streptomyces sp.F was subject to fermentation as described above. Samples were collected at 96-, 144- and 240-hours post-inoculation. Every sample collected was prepared for transcriptomic analysis using RNAprotect Cell Reagent® (Quiagen), following manufacturer's instructions. All sample were stored at -80 °C after the last centrifugation step. RNA extraction and subsequent transcriptomic analysis were performed by Genewiz (South Plainfield, NJ).

Using the data received from Genewiz, transcripts with statistical importance were defined as having a Log2>2 and P-value<0.05. Visualisation of gene cluster was performed using STRING software (Szklarczyk *et al.*, 2019)

2.6.4 ANTISMASH analysis

The detection of secondary metabolite clusters was performed using ANTISMASH 6.0 (Blin *et al.*, 2021). This software allows the genome-wide identification, annotation, and analysis of secondary metabolite biosynthesis gene clusters in bacterial genomes.

2.6.5 BLAST analysis

In silico metabolic capability of an organism can be assessed using tblastn (https://blast.ncbi.nlm.nih.gov) to detect homologous genes already described in the literature. A homologous gene is considered a good candidate if the E-value < 10^{-5} and an identity cover > 30%.

2.6.6 Modelling of PETase

A model of the three-dimensional structure of F-PETase was produced using AlphaFold2 (Jumper *et al.*, 2021). The most accurately predicted structure model was obtained using “five models” and “MMseqs2” mode. The model was refined and protonation states assigned using H++ server (Gordon *et al.*, 2005). This refined model was solvated and subjected to extensive molecular dynamics (MD) simulations using Amber20. Protein-ligand molecular docking was carried out using GOLD, using the refined protein model as the receptor and PET tetramer as the ligand. All residues within 10 Å of the catalytic Serine residue in the receptor were defined as the binding site. The receptor

residues were kept fixed while the ligand was treated as fully flexible during docking.

From this treatment a model of F-PETase with ligand was generated and compared to an already known structure of PETase using the visualization software Pymol.

2.6.7 Modelling of MHETase

A model of the three-dimensional structure of F-MHETase was produced using SWISS-PROT modelling software (Waterhouse *et al.*, 2018). The modelling was homology based using already published 3D structure of MHETase from *Ideonella sakaiensis* (Sagong *et al.*, 2020). Visualisation and comparison of the structure were done using Pymol.

3 Chapter 3 Characterisation of the biodegradation of PE and PET

3.1 Introduction

Streptomyces sp. have a versatile metabolism and can utilise a variety of different macromolecules (cellulose, lignin, agar and chitin) (Chater *et al.*, 2010) and aromatic compounds (vanillin, benzoate, catechol) (Hae-Reun, Hyun-Joo and Eung-Soo, 2000; Menendez-Bravo *et al.*, 2017; Khalil *et al.*, 2019).

Streptomyces sp. are capable of degrading a large variety of natural polymers, including cellulose, lignin, agar and chitin (Chater *et al.*, 2010; Rodríguez-Fonseca *et al.*, 2021) (Rodríguez-Fonseca *et al.*, 2021) . Their ability to degrade natural polymers has led to renewed interest in their ability to degrade artificial polymers, with studies to date focusing on their ability to potentially degrade PE and PET (Ehara *et al.*, 2000; Almeida, Rincón, Jackson and Alan D.W. Dobson, 2019; Farzi, Dehnad and Fotouhi, 2019).

However, despite current efforts to resolve the mechanisms responsible for the degradation, the mechanism and subsequent degradation by-products still remain largely unknown for PE (Farzi, Dehnad and Fotouhi, 2019).

Several microorganisms have already been identified in the literature, which have been shown to degrade a range of different plastics. However, these studies are limited to the identification of individual strains, which are capable of degrading one type of plastic (Ghatge *et al.*, 2020; Mohanan *et al.*, 2020; Ru, Huo and Yang, 2020). Most of the reports in the literature to data have focused on the plastic having similar chemistry. Austin at al reported that the PETase enzyme, a hydrolase isolated from *Ideonella sakaiensis,* can function on both PET and PEF (polyethylene furanoate) (Austin *et al.*, 2018). However, this is based on the enzyme and the fact that PET and PEF are related. (Figure 3-1)

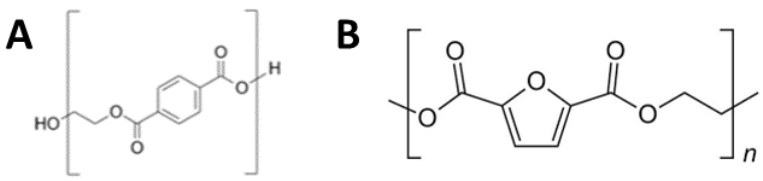


Figure 3-1 : Chemical structure of PET (A) and PEF (B)

The PETase enzyme has not been shown to degrade other non-related plastic, for example PE. In fact thus far, no organism has been identified which is capable of degrading multiple plastics.

Research efforts are underway to engineer microorganisms which are capable of degrading multiple different types of plastic simultaneously. These include the European project MIX-UP (Ballerstedt *et al.*, 2021). This project aims to engineer a Pseudomonas chassis, which is able to degrade multiple types of plastic (Ballerstedt *et al.*, 2021). Ongoing efforts are also focused on engineering microbial consortia, capable of working together to degrade plastics and utilise the monomers to generate high value products (Edwards *et al.*, 2022). The discovery, or the targeted engineering, of an organism able to degrade different types of plastic would be a first step towards an economically viable process for the utilisation of mixed plastic waste.

The recycling of mixed plastic waste is currently a problem, even the most advanced technologies in plastic recycling still require sorting the plastic before usage. This step is a major bottleneck in the economic viability of any plastic recycling process (Singh *et al.*, 2021). This is the reason of the importance of the European project MIX-UP (Ballerstedt *et al.*, 2021), if successful the industrial biodegradation of mixed plastic would be made possible, this would alleviate one of the major economical caveats of plastic recycling (Singh *et al.*, 2021).

Chapter 3 will evaluate the plastic degrading ability of a novel Streptomyces strain, which had been previously shown to grow on commercial PET and PE. A small-scale approach in shake flasks, was taken to evaluate growth on virgin PE and PET and to assess the physical degradation of both the PE and PET. A second approach was then utilised, fermentation was performed

at 2L scale with both PE and PET as feedstocks, allowing the process to be standardized and to increase reproducibility. Samples were taken from the fermenter for metabolomic and transcriptomic analysis.

3.2 Phylogenetic Identification of the Streptomyces isolate

The Streptomyces known as *Streptomyces* sp. F was previously isolated from soil in Warwickshire by Dr Bryan. The isolate had been shown to grow on both commercial PET (plastic bottle) and commercial PE (plastic bag). However, the isolate had yet to be fully characterised.

To identify the isolate, 16S sequencing was performed. The 16S rRNA gene has been a mainstay of sequence-based bacterial analysis for several years, providing taxonomic resolution at both the species and strain level (Newsome *et al.*, 2004). Current 16S primers either target the 16S variable region or the entire gene, with the preference being for sequencing the whole gene, which increases the taxonomic resolution (Newsome *et al.*, 2004). Individual colonies of *Streptomyces* sp. F were boiled in water and PCR reactions were set up using the universal 16S primers: pA (AGAGTTTGATCCTGGCTCAG) and pH (AAGGAGGTGATCCAGCCGCA) (Edwards *et al.*, 1989) (Figure 3.2)

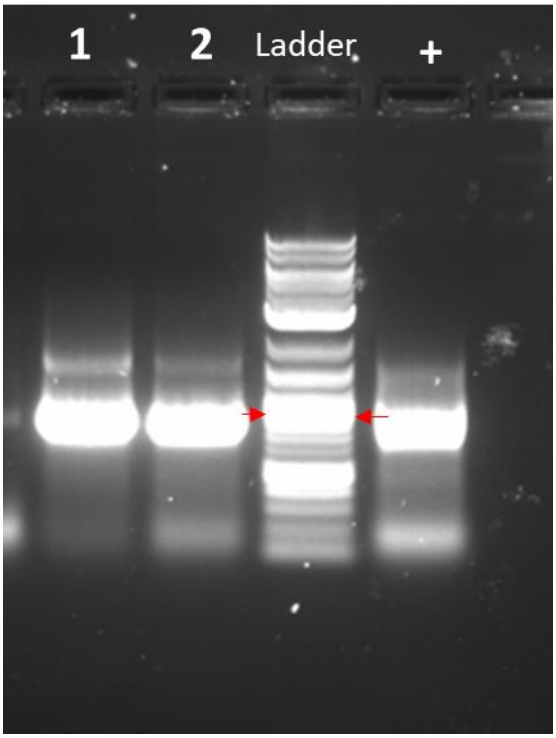


Figure 3-2 : Picture of the electrophoresis gel of the 16S PCR of *Streptomyces* sp. F (Well 1 and 2), with a ladder (1 kb fragment marked with red arrow) and a positive control (+)

The band was excised from the gel, and the DNA was extracted utilising the Qiagen gel extraction kit as detailed in section 2.3.5. The DNA was subsequently sent for sequencing (Eurofins) and analysed in BLASTn. The 16S sequence was shown to be closely related to *Streptomyces fulvissimus* with 99.27% homology (Figure 3.3).

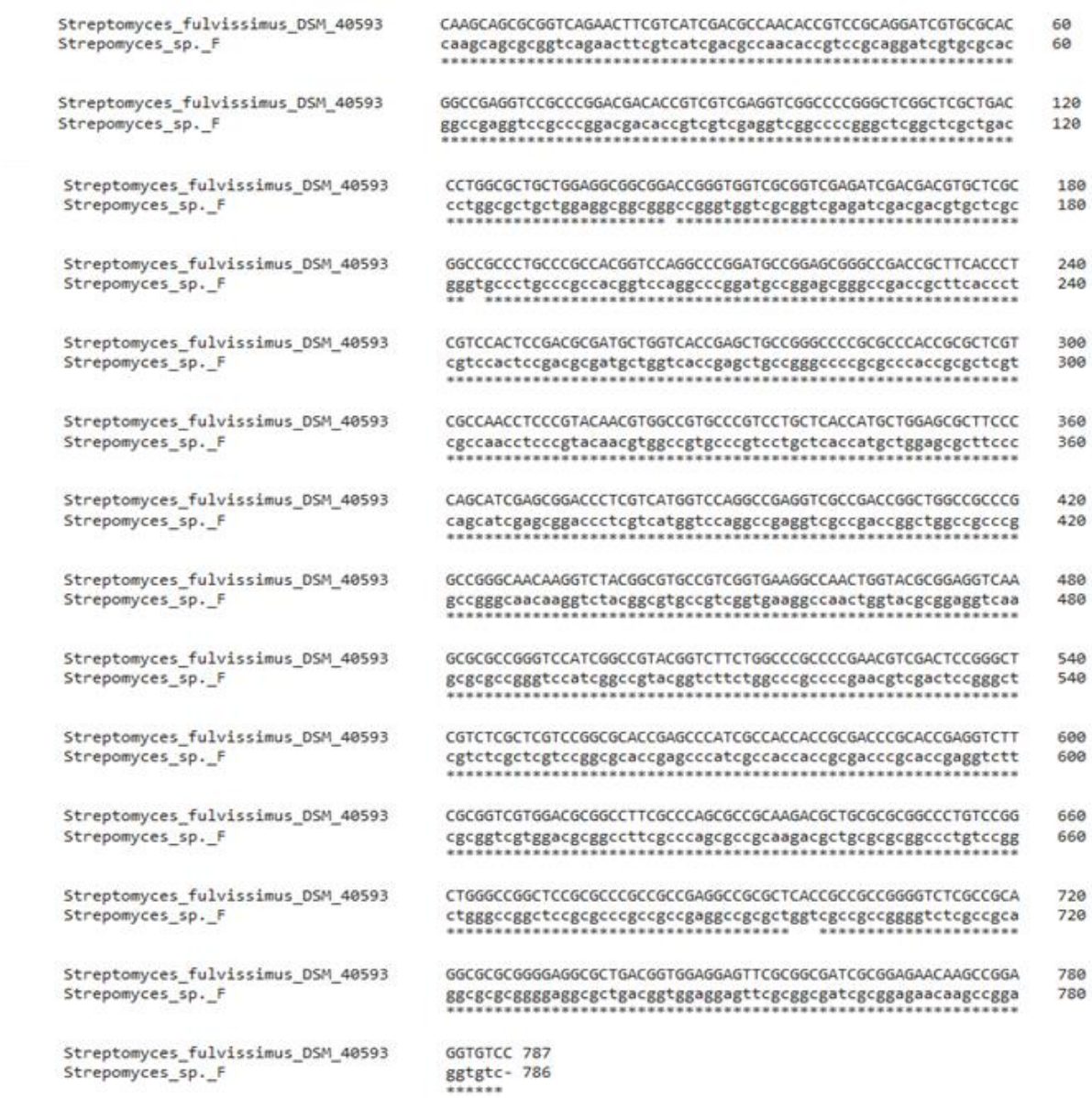


Figure 3-3 : Alignment of the 16S region of *Streptomyces* sp. F and *Streptomyces fulvissimus* DSM 40593

Typically sequences with >95% homology represent the same genus, while sequences with 97% identity are indicative of the same species (Johnson *et al.*, 2019). Phylogenetic analysis, utilising Clustal Omega and visualized using the one click tool on phylogeny.fr, demonstrated that *Streptomyces* sp. F is closely related to *Streptomyces fulvissimus* (Figure 3.4).

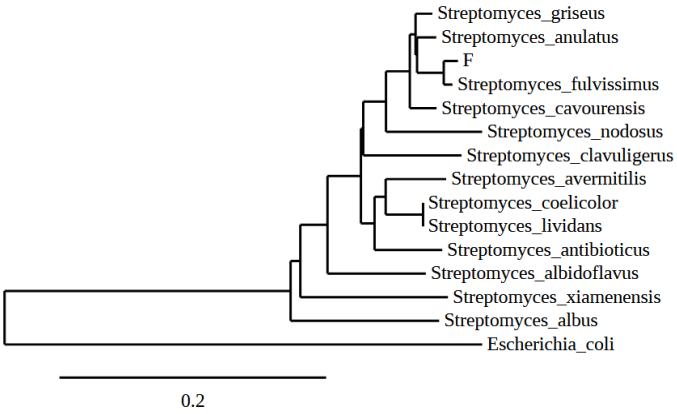


Figure 3-4: Phylogenetic tree of 16S

It has previously been reported that the identification of *Streptomyces* sp. can be difficult when utilising the 16S sequence alone (Guo *et al.*, 2008) due to poor resolution being unable to distinguish between closely related species. Multilocus sequence analysis (MLSA) is commonly utilised for species identification and determining phylogenetic relationships between *Streptomyces* sp. The following gene sequences are commonly utilised *atpD* (ATP synthase delta subunit), *gyrB* (DNA gyrase subunit B), *recA* (recombinase A), *rpoB* (RNA polymerase subunit) and *trpB* (tryptophan biosynthesis) (Guo *et al.*, 2008). PCR was utilised to amplify the *atpD, recA, rpoB,* and *trpB* genes from *Streptomyces* sp. F (Figure 3.5).

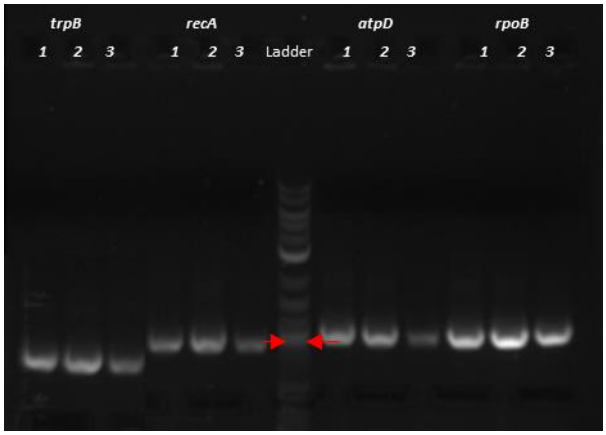


Figure 3-5 : Picture of the electrophoresis gel of the PCR of *trpB, recA, atpD* and *rpoB* (in triplicate), with a ladder (1 kb fragment marked with red arrow)

The PCR products were gel extracted as above and sent to sequencing. Phylogenetic analysis utilising clustal Omega and visualized using the one click tool on phylogeny.fr confirmed that *Streptomyces* sp. F was a synonym

of *Streptomyces fulvissimus.* Given its close positioning with *Streptomyces fulvissimus* in the phylogenetic trees (Figure 3.6).

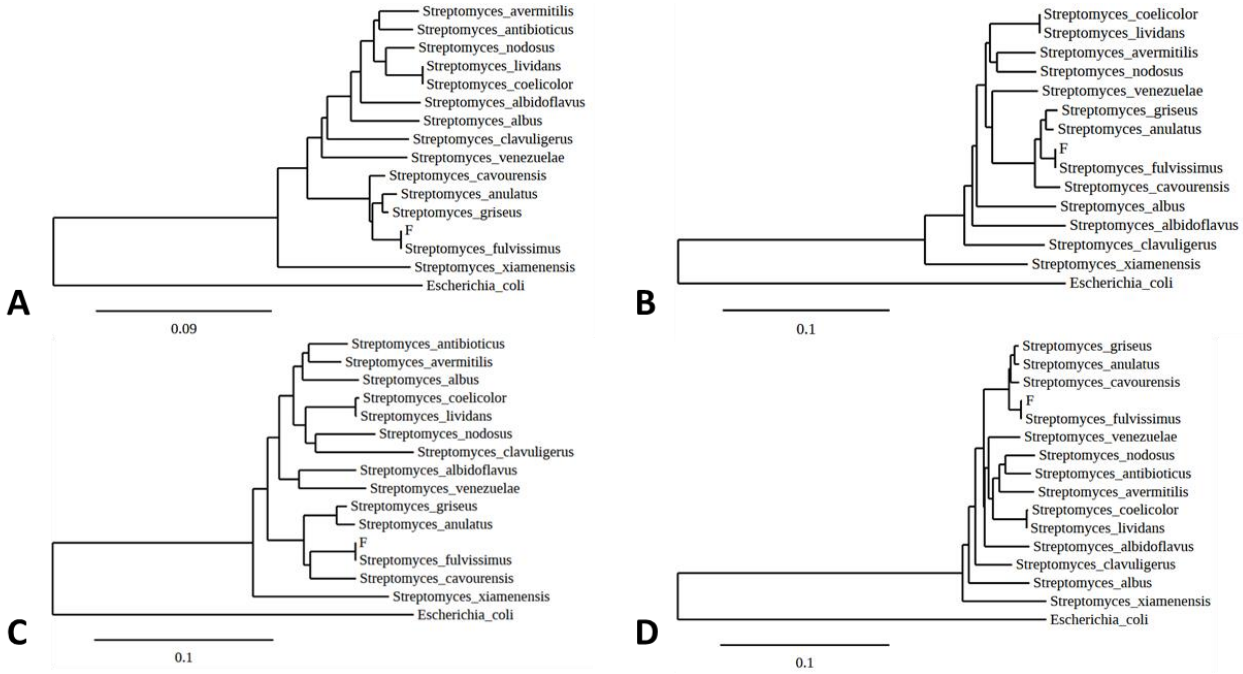


Figure 3-6 :Phylogenetic tree for different genes: *recA* (A), *atpD* (B), *tprB* (C) and *rpoB* (D)

3.3 Evaluation of the growth of *Streptomyces* sp. F on virgin PET and PE. of plastic degradation

3.3.1 Evaluation of growth of *Streptomyces* sp. F on PET and PE

Streptomyces sp. F has already been shown to grow on both commercial PET and PE. However, basing growth purely on commercial plastics can be problematic, given they contain plasticisers and other chemicals. These make it difficult to assess if the bacteria are truly growing on the plastic itself or the added chemicals. Therefore, it has become more desirable to assess growth on virgin plastic with no chemical additives. *Streptomyces* sp. F was grown in shake flasks with SMM modified media, a minimal media commonly utilised for Streptomyces as detailed in section 2.1.1.1. PET and PE virgin plastic film purchased from Goodfellows were cut into square of 4X4 cm (or 0.5 g of plastic film) and added to the flasks.

Four different conditions were tested in the shake flasks to characterise the plastic degradation: PET film and glucose (termed PET), PE film and glucose, (termed PE), glucose (termed glucose) and a carbon negative control (termed media only). To kick-start metabolism and enable an increase in cell density, a small amount of glucose, 0.01% was added to the PET, PE and media control cultures. Each experiment was done in triplicate.

Samples were taken every 3-4 days; the samples were subject to serial dilution and plated directly onto SFM plate and incubated for 3 days. Individual colonies were counted, and the numbers were used to calculate the colony forming unit (CFU). *Streptomyces* sp. are filamentous organisms, which means conventional techniques such as turbidity or optical density (OD) cannot be utilised to measure cell growth. Typically, dry cell weight (DCW) is utilised to measure filamentous cell growth. However, the presence of plastic in the experimental setup, made DCW difficult to assess. Therefore, CFU counts were chosen as a suitable method to assess the number of viable cells and hence growth. However, this method is not perfect, *Streptomyces* sp. can sporulate, which could result in an artificial increase in CFU counts (Chater, 2016).

Figure 3-7 clearly shows some significant differences between the different conditions, surprisingly the CFU counts were higher when the cells were grown on both PET and PE. The error bars are high, which is probably due to the lack of homogeneity in the flasks: biomass was attached to the plastic as well as to the side of the flasks.

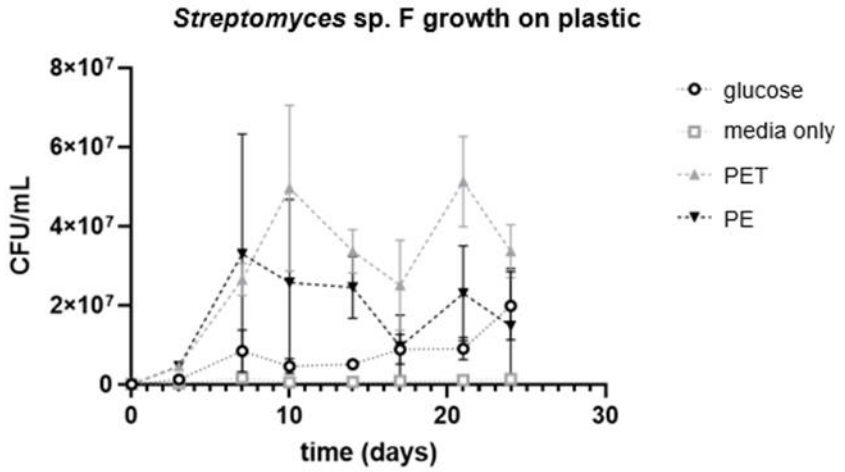


Figure 3-7 : Graph to show CFU counts from *Streptomyces* sp. F on media only, PET, PE and glucose. Grown in flaks, in SMMmod media at 30℃,

3.3.2 SEM Analysis of the plastic film from PET and PE

After 28 days of growth on the PET and PE film, the individual films from each individual condition were cleaned with water and allowed to dry ready for SEM analysis. The plastic was cut to coupon sized ~10 mm of diameter, mounted on stubs using carbon tape and then coated in gold. The SEM sample preparation and analysis was performed by Denise McLean. This analysis allowed the detection of surface modifications on the plastic film, but the preparation of the plastic film did not allow for the preservation of cell structure or biofilm formation.

For each of the plastics, a control was used to assess the impact of the experimental conditions on degradation. This control was subject to the same experimental conditions (temperature, RPM, sterilisation technique, submerged in media)

Analysis of the PE film showed several holes in the plastic (Figure 3-8), with a clear difference between the control (Figure 3-8 A) and the PE film with the bacteria (Figure 3-8 B).

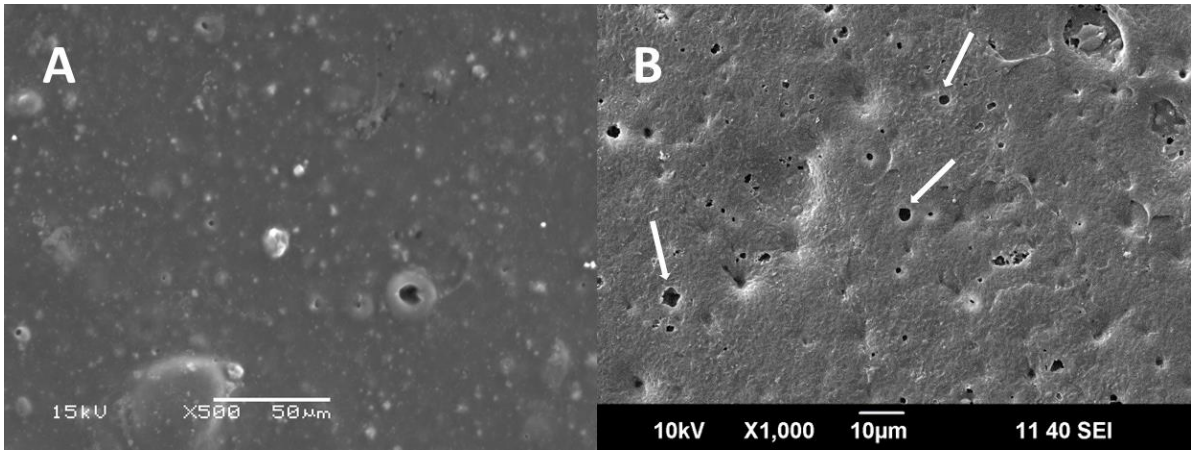


Figure 3-8: SEM picture showing virgin PE film: media only control (A) and film from the "PE" condition, grown in SMMmod media at 30℃, with 0.1% glucose and 1 % PE film (B). White arrows depict the holes.

The detection of modifications on the surface of the plastic is a good indication of PE degradation, this is limited to the surface of the plastic, the initial step in PE degradation.

Similar, modifications were seen on the surface of the PET film (Figure 3-9), with clear differences between the control (Figure 3-9 A) and PET from the cells (Figure 3-9 B). The degradation pattern is comparable with what has already been published, though this is less pronounced (Austin *et al.*, 2018).

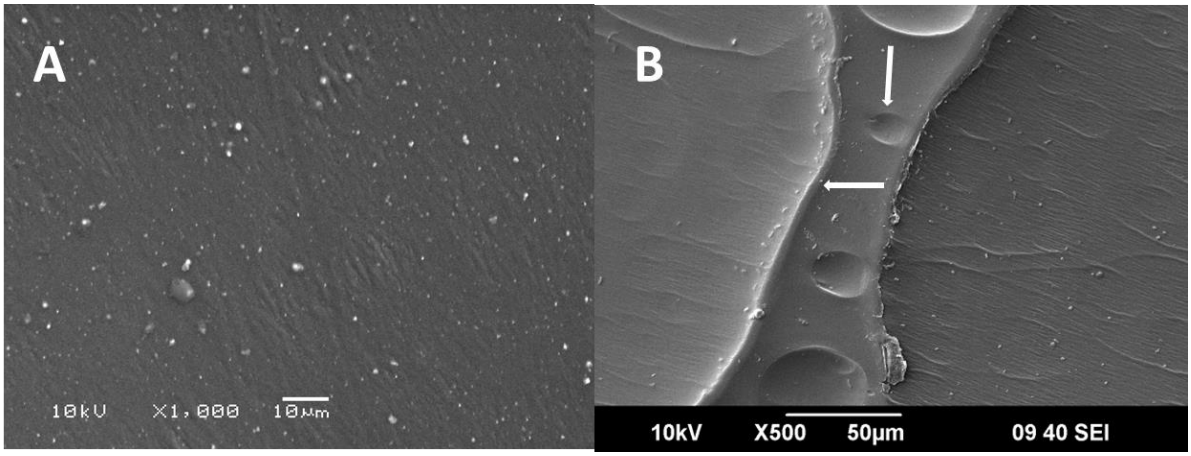


Figure 3-9: SEM images of virgin PET film: control (A) and film from the "PET" condition, grown in SMMmod at 30℃, with 0.1% glucose and 1 % PET film (B). White arrows depict the holes.

.

3.4 Characterisation of the growth of *Streptomyces F* on PET and PE plastic in Fermentation

Shake flasks are typically utilised for small scale optimisation, given they are easy to handle. However, shake flasks typically have a limited supply of oxygen and important parameters such as pH and temperature are difficult to control. Therefore, growth of *Streptomyces* sp. F was evaluated at fermentation scale on PET and PE on SMMmodFm, Glucose (10 g/L) was added to each of the three fermentations this was added to kick start the fermentation and increase the biomass. A control fermentation was also included utilising glucose as the sole carbon source. For the two fermentations on plastic, in addition to glucose, PET and PE powdered plastic (Goodfellow) was added at 10 g/L to each of the fermenters. All the fermentations were performed at 30C, in a carbon-free modified version of the SMM media. Each fermentation was monitored closely, and both the pH and the OD were regulated, pH = 7.2 and the OD>30%. Growth was evaluated using CFU counts, and samples were taken every 48-72 hours. Samples were also taken for LC-MS and transcriptomic analysis.

3.4.1 Evaluation of *Streptomyces* sp. F on glucose

To directly compare the growth rate of *Streptomyces* sp. F on plastic, cells were grown on glucose. The fermentation was done in batch, batch fermentation involves the substrate and nutrients being added together at time point 0 and the vessel then proceeds until maximum product concentration is achieved. Both fed batch and batch are commonly utilised to grow Streptomyces, fed batch involve the feeding of carbon and supplements into the culture during the duration of the process. During the growth of *Streptomyces* sp. F the colour of the media changed. Changes in colour usually relate to growth changes as the cell moves into stationary phase, this correlates with the onset of secondary metabolism in Streptomyces such as the production of polyketides, peptides and polyketide peptide hybrids (Lacey

and Rutledge, 2022). At the end of the growth period the broth was a dark brown colour (Figure 3-10).

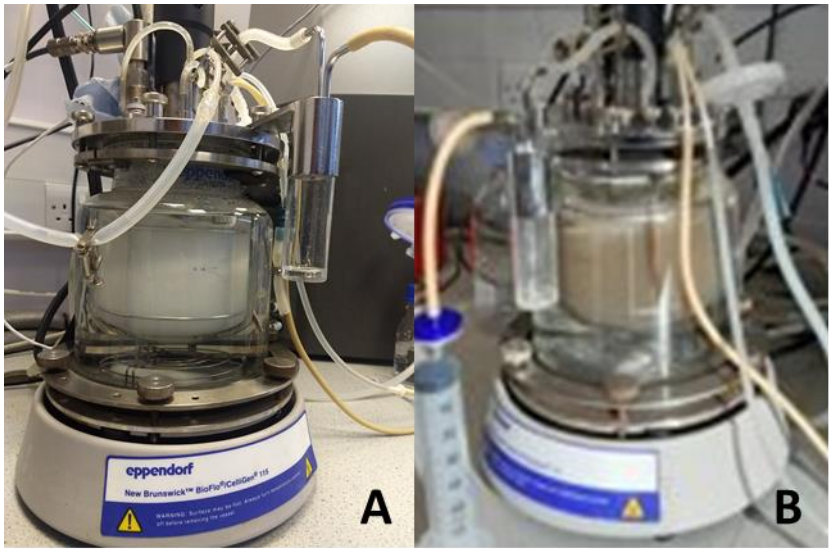


Figure 3-10: Differences between the colour of the fermentation with *Streptomyces* sp. F on SMMmodFm at 30℃, with 1% glucose after 24 hours (A) and after 216 hours (B)

Streptomyces sp. F reached a maximum biomass between 144 and 168 hours, with a viable count of around $1*10^8$ CFU/mL (Figure 3-11). After 168 hours the growth decreased. (Figure 3-11). Microscopy was used to validate cellular growth and confirm that the cells were still filamentous and not forming spores. Spores were detected after 144 hours. Interestingly, the amount of viable cells decreased after 168 hours this may be due to some of the spores getting stuck on the surface of the fermenter.

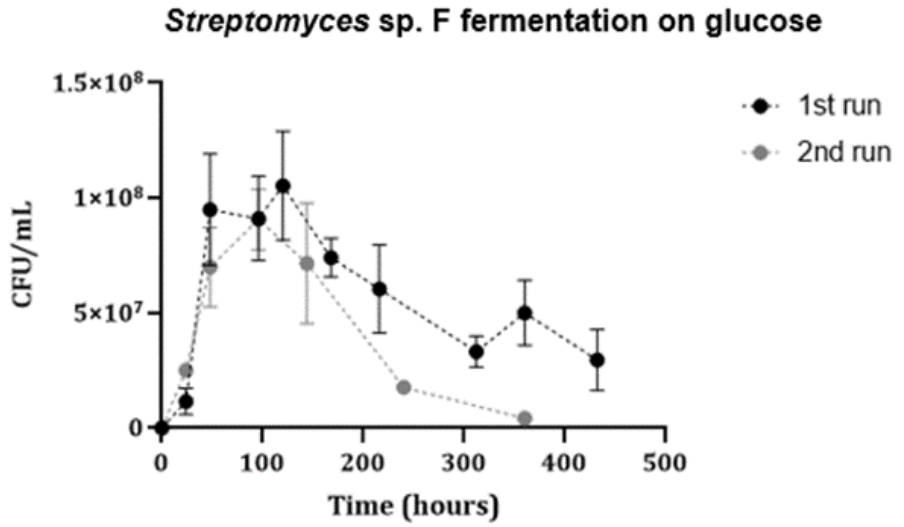


Figure 3-11: Graph to show growth of *Streptomyces* sp. F in SMMmodFm at 30℃, with 1% glucose.

The growth rate of *Streptomyces* sp. F on glucose was calculated (Table 3-1).

		μ (h^{-1})	Lower 95%	Upper 95%	P.value	Coefficient of determination (R^2)
1st run	μ on glucose	0.052	0.009	0.114	7.357 e-02	0.893
2nd run	μ on glucose	0.055	0.003	0.113	5.487 e-02	0.893

Table 3-1: Growth rate of *Streptomyces* sp. F on glucose

Direct comparisons with the literature are problematic, due to different media utilisation. Minimal media for the growth of Streptomyces usually contains varied carbon sources which are used to promote the production of specific secondary metabolites (Flowers and Williams, 1977; Untrau-Taghian *et al.*, 1995; Kiviharju *et al.*, 2007; Koepff *et al.*, 2018).

Growth rates already reported in the literature for *Streptomyces* are dependent on both the species and the growth condition. The growth rate of *Streptomyces* sp. is generally considered to be slow with a maximum growth rate (μ value) between 0.06 h^{-1} and 0.6 h^{-1}. *Streptomyces* sp. F had a growth rate of 0.055 h^{-1} (Table 3-2) on glucose which is consistent with the rest of

the literature, however it is still among the slowest growers. This could be due to the fact that the strain is an environmental isolate and is not adapted to growth on sugar, it may also have specific media requirements which would need to be further validated and optimised.

Organism	**Media name**	**Carbon source used**	**Growth rate (h^{-1})**	**Reference**
S. peucetis	ET 1	Glucose Soy peptone Yeast extract …	μmax > 0.1	Kiviharju et al., 2007
S. ambofaciens	N/A	Dextrin	μmax = 0.06	Untrau-Taghian et al., 1995
Streptomyces sp.	GCA CCP	Casamino acid Yeast Extract Asparagine Proline	0.2< μ < 0.6	Flowers & Williams, 1977
Streptomyces Lividans	AA-00	Glucose	μmax =0.2	Koepff et al., 2018
Streptomyces F	SMM mod	Glucose	μmax = 0.05	This work

Table 3-2: Growth rate of *Streptomyces* sp. reported in the literature.

Table 3-3 shows a breakdown of the different time points collected and the destination of each sample.

	1st run		2nd run		
Time point (hours)	**CFU counts**	**LC-MS analysis**	**CFU counts**	**LC-MS analysis**	**Transcriptomic analysis**
0	✓	✓	✓	✓	
24	✓	✓	✓	✓	✓
48	✓	✓	✓	✓	
96	✓	✓	✓	✓	✓
144	✓	✓	✓	✓	✓
168	✓	✓	✓	✓	
192	✓	✓		✓	
240	✓	✓	✓	✓	✓
288	✓	✓		✓	
336	✓	✓	✓	✓	
384	✓	✓	✓	✓	

Table 3-3: List of samples taken during the fermentation of *Streptomyces* sp. F on glucose.

3.4.2 Fermentation Characterisation of the growth of *Streptomyces* sp. F on polyethylene terephthalate

Following the successful validation of growth on PET in a shake flask, the growth of *Streptomyces* sp. F was characterised in fermentation utilising virgin PET and glucose. Glucose (10 g/L) was utilised to ensure a reasonable level of biomass could be generated to enable plastic degradation based on the shake flask results. Virgin PET from Goodfellows was utilised at 10 g/L. This concentration was chosen as it was deemed low enough to avoid having an adverse impact on the fluid mechanics of the broth, but at a sufficient concentration to promote the degradation of the plastic. Plastic powder was chosen to maximise surface area and to minimise the mechanical stress in the glass vessel. The PET powder was sterilised via autoclaving, due to its high melting temperature (>250℃) (Jog, 1995). However, the glass transition temperature for PET is around 70℃ (Jog, 1995), which is lower than the temperature reached during the sterilisation process. Therefore, autoclaving would have had an impact on the crystallinity of the PET powder but would not have an impact on the chemical composition or chemical stability of the plastic.

To characterize the growth of *Streptomyces* sp. F on PET, fermentations were done in triplicate. Samples were taken either every 48 or 72 hours, and utilised for CFU counts, and LC-MS analysis as described in Table 3-4. Samples were also taken in triplicate for the transcriptomic analysis.

The initial fermentation resulted in *Streptomyces* sp. F forming a biofilm in the fermenter after 48hrs of growth. This is very atypical behaviour for Streptomyces (Figure 3-12 A). The biofilm formation made it very difficult to collect samples, which meant no CFU analysis and no LC-MS analysis. *Streptomyces* sp. F did not show any obvious signs of stress or early sporulation during this fermentation. Microscopy analysis confirmed that PET

particles were imbedded in the mycelia of *Streptomyces* sp. F (Figure 3-12 B).

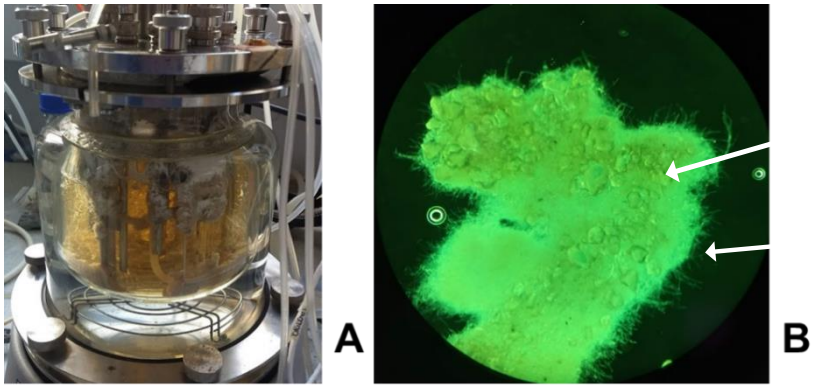


Figure 3-12: Fermentation of *Streptomyces* sp. F on on SMModFm at 30℃, with 1% glucose and 1 % PET powder after 72 h (A), microscopic observation of mycelia embedded in the PET particles after 72 h (B)

Biofilm formation in *Streptomyces* sp. is very rare , and there are very few reports of biofilm formation in the literature (Morales, Ocampo and Zambrano, 2007; El Othmany *et al.*, 2021). Despite the small number of studies, a few key elements in the formation of the biofilm have been described. In the model organism, *Streptomyces coelicolor*, attachment of the cells is hypothesised to be mediated by a gene encoding a cellulose synthase like gene, *cslA* (de Jong *et al.*, 2009). Another report using *Streptomyces coelicolor* as the model showed that media composition also plays a very important role in the cells ability to form a biofilm. For example minimal media with mannitol as a carbon source has been shown to promote attachment (Winn *et al.*, 2014).

Following the surprising biofilm formation in the first fermentation, two further repeats were set up using the same conditions. This time no biofilm formation was observed in the two vessels, the broth colour changed during the fermentation, to a dark brown colour this was also observed in the fermentation on glucose. This colour change coincided with the latter stages of the growth cycle and subsequent entry into stationary phase (Figure 3-13).

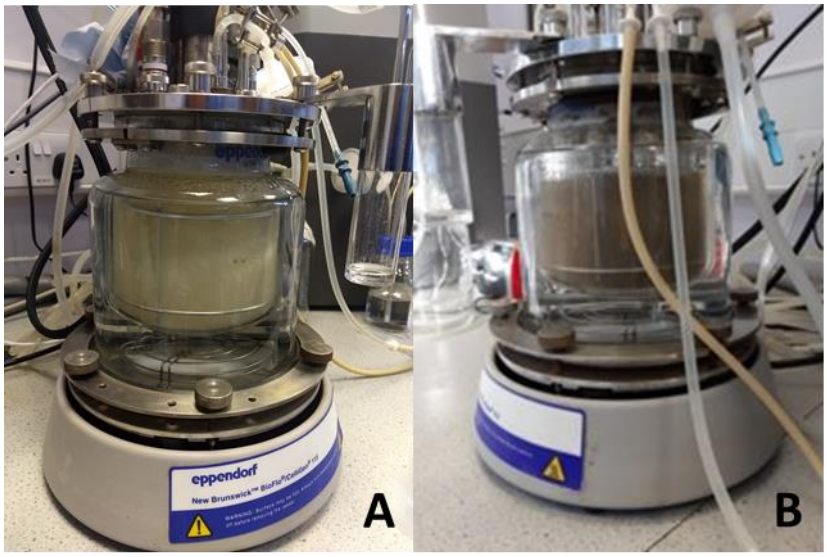


Figure 3-13: Fermentation of *Streptomyces* sp. F on SMMmodFm at 30℃, with 1% glucose and 1 % PET powder after 48 h (A) and after 312 hours (B)

The two consecutive fermentations were run for between 780 hours and 384 hours for the 2nd and 3rd runs respectively. The 3rd fermentation did not reach stationary phase. Unfortunately, this fermentation had to be stopped earlier than desired due to technical constraints.

The fermentation of *Streptomyces* sp. *F* on PET clearly had two distinct phases of growth. The first growth phase was dominated by the consumption of glucose testing with glucose strips demonstrated that the glucose had run out after 200 hours (Figure 3-14) A second growth phase was seen after 200 hrs, which was attributed to PET degradation and growth on the subsequent monomers.

A maximum viable count was reached for the 2nd run after 600 hours, with around $5*10^7$ CFU/mL. For the 3rd run the maximum growth rate was reached after only 360 hours, with around $4*10^7$ CFU/ mL. A decrease in the viable cell count was not detected in either run suggesting that *Streptomyces* sp. F had not started to sporulate.

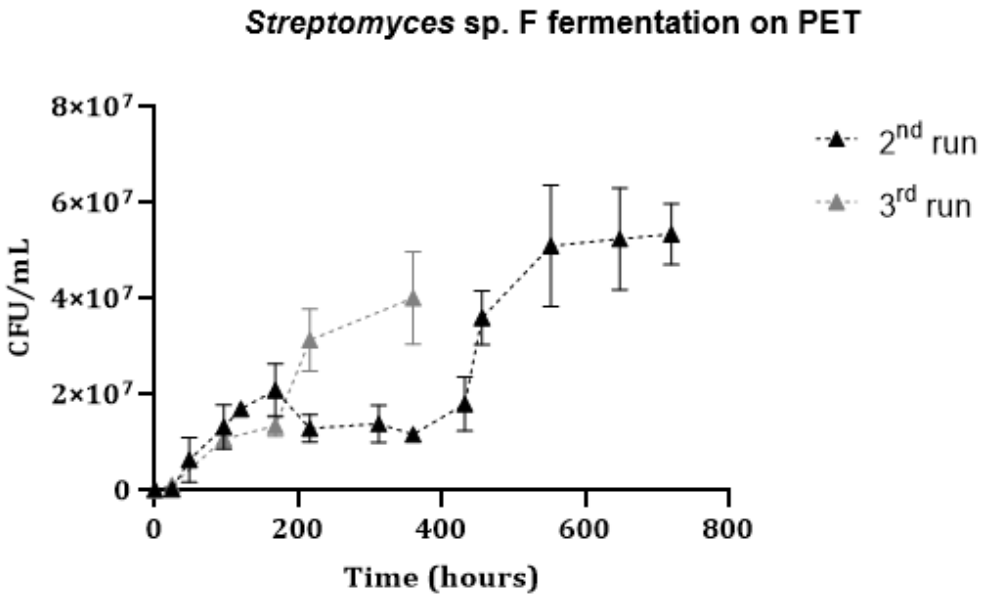


Figure 3-14: Graph to show growth of *Streptomyces* sp. F in SMMmodFm at 30℃, with 1% glucose and 1 % PET powder.

The maximum growth rate was calculated for both PET and glucose, both fermentation runs were similar. The specific growth rate μ for the fermentation the 1st phase of growth on glucose was between 0.04 h^{-1} and 0.06 h^{-1} and for the 2nd growth phase on PET it was between 0.008 h^{-1} and 0.005 h^{-1} (Table 3-4). The growth rate for the 1st phase of growth on glucose was very similar to the growth rate determined during the fermentation of *Streptomyces* sp. F on glucose as the sole carbon source (Table 3-1). This is further proof that the initial stages of growth are linked to the consumption of glucose. The second growth phase being due the consumption of the monomeric breakdown products of PET.

		μ (h-1)	**Lower 95%**	**Upper 95%**	**P.value**	**Coefficient of determination (R2)**
1st run	μ on glucose	0.040	0.040	0.074	3.17E-02	0.829
	μ on PET	0.008	0.003	0.012	1.77E-02	0.965

2nd run	μ on glucose	0.060	0.023	0.143	6.88E-02	0.733
	μ on PET	0.005	0.002	0.008	1.68E-02	0.943

Table 3-4: Growth rate of *Streptomyces* sp. F during the fermentation on SMMmodFm at 30℃, with 1% glucose and 1 % PET powder

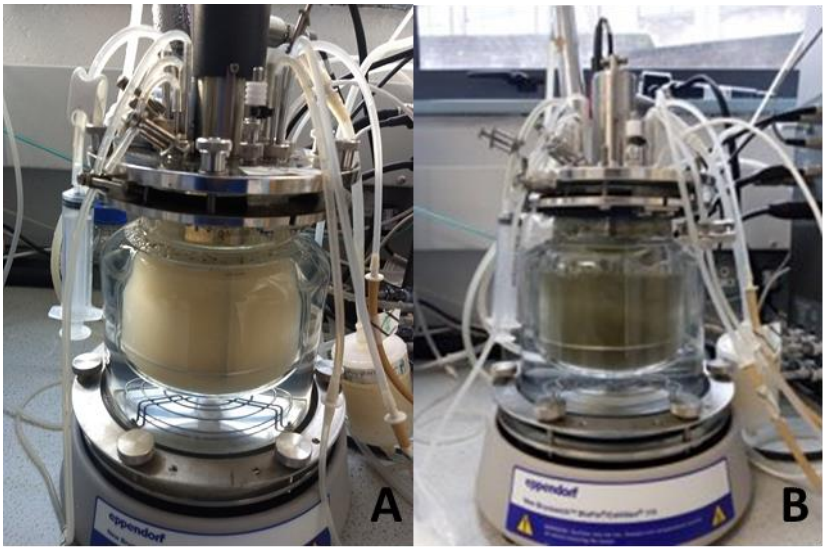
Microscopic analysis confirmed that mycelia were detected throughout all phases of the fermentation on PET, even after 200 hours. The detection of mycelia is an important observation as it demonstrates that the cells are active even after the glucose has been consumed (200 hours). The formation of spores would suggest that the cells are carbon starved and therefore are not able to break the PET. It is also important as the detection of mycelia demonstrates that the increase in the CFU count is not the result of sporulation but an indication that PET is used by *Streptomyces* sp. F as a carbon source.

3.4.3 Characterisation of the growth of *Streptomyces* sp. F on PE

The PE fermentations were carried out as detailed in section 3.4.2, utilising two different carbon sources PE and glucose to maximise biomass. Virgin PE was utilised from Good fellows at 10 g/L. PE has a low temperature resistance, with degradation starting at 95℃ (Ghatge *et al.*, 2020), therefore a different sterilisation method had to be used. To sterilise the PE powder, the powder had to be washed with 70 % isopropanol (IPA) solution. Moreover, due to its hydrophobicity in water, the solution of 70% IPA was also used to transfer the sterilised PE powder into the vessel prior to the fermentation. The solvent was eliminated by running the fermentation for 24-hours at 30 ^{oC} with 2L/min of air flow, before inoculation.

To characterize the growth of *Streptomyces* sp. F on PE, two replicate fermentations were performed. As for the previous fermentations on PET, samples were taken every 48 or 72 hours, for CFU counts, LC-MS analysis and transcriptomic analysis. For both runs, the fermentations had to be stopped at 384 hours, due to technical constraints and access to the fermentation vessels.

As previously reported on both PET and glucose the broth changed colour, however on PE the broth was dark green compared to the dark brown colour seen on PET (Figure 3-15).



s

Figure 3-15: Fermentation of *Streptomyces* sp. F on SMMmodFm at 30°C, with 1% glucose and 1 % PE powder after 48 h (A) and after 384 h (B)

The first 200 hours of fermentation of *Streptomyces F* on PE was different to the first 200 hrs of growth seen on both PET and glucose, even though the cells had access to glucose (Figure 3-16). A specific growth rate of 0.02 h^{-1} (Table 3-6) was calculated, this growth rate was smaller than the one observed on both the PET fermentation (Table 3-4), and the glucose fermentation (Table 3-1). Moreover, the growth rate had a very poor coefficient of determination, R^2<0.90, and statistical significance, p-value>0.05 (Table 3-6). Microscopic analysis confirmed that the cells were healthy, as mycelia could be detected. The addition of PE in the fermentation seems to impact on the growth of *Streptomyces* sp. F and perhaps on its ability to utilise glucose possibly through some feedback inhibition. The reasons for this behaviour are not fully understood and may also be due to mechanical stress caused by the PE powder.

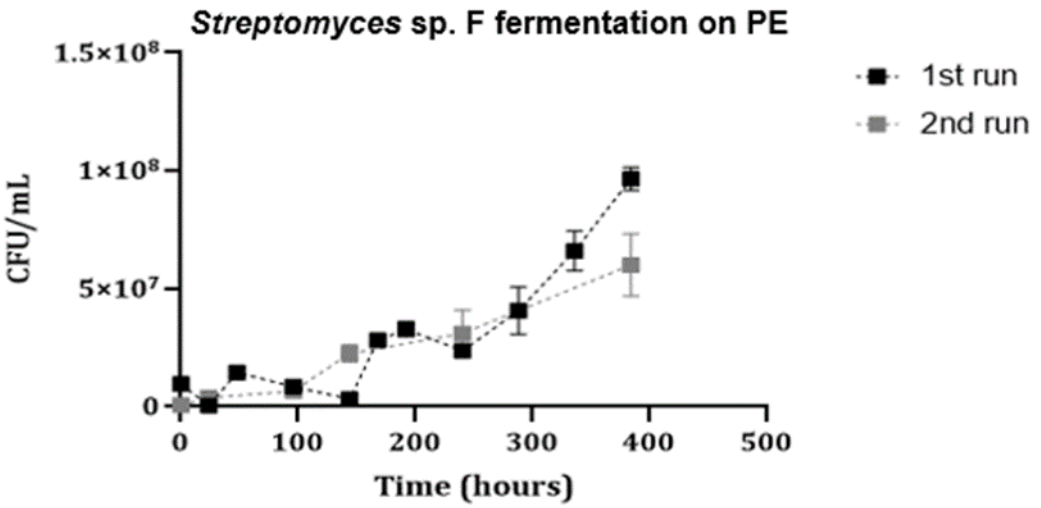


Figure 3-16: Graph to show CFU count from the fermentations of *Streptomyces* sp. F in SMMmodFm at 30℃, with .1% glucose and 1 % PE powder.

Following the consumption of glucose after 200 hrs, the growth seemed to increase steadily (Figure 3-16). However, the growth rate was very slow with a specific rate of 0.0041-0.0057 h^{-1} (Table 3-5). Despite its very low value, the regression used to extract the growth rate had a significant p-value, p-value<0.05 (Table 3-5), with a high coefficient of determination, R^2>0.99 (Table 3-5). This low growth rate could be expected since PE degradation is hypothesized to produce fatty acid like compounds, which would result in a slower growth rate than on glucose.

The increased growth detected after 200 hours of fermentation is an indication that *Streptomyces* sp. F can grow on PE as a sole carbon source. However, a deeper understanding of the mechanism and the metabolism of *Streptomyces* sp. F is required to confirm how this growth occurs and what impact PE has on glucose metabolism.

		μ (h^{-1})	***Lower 95%***	***Upper 95%***	**p-value**	**Coefficient of determination (R^2)**
1st run	μ on glucose	0.010	-0.101	0.121	7.38E-01	0.069
	μ on PE	0.005	0.002	0.012	2.94E-03	0.994

2nd run	μ on glucose	0.021	-0.151	0.192	3.70E-01	0.069
	μ on PE	0.004	0.000	0.008	5.25E-02	0.993

Table 3-5: Growth rate of *Streptomyces* sp. F during fermentation on SMMmodFm at 30℃, with 1% glucose and 1 % PE powder.

3.5 Metabolomics analysis of the supernatant and cell pellet of *Streptomyces* sp. F on PET and PE

Untargeted LC-MS can detect a wide variety of different molecules; from one sample hundreds of different metabolites can be identified and quantified. Untargeted LC-MS approaches enable the visualisation and analysis of the entire metabolism of one organism, also called the metabolome (Tweeddale, Notley-McRobb and Ferenci, 1998). Metabolomic analysis of both the pellet and the supernatant would allow a more detailed understanding of the changes in the metabolome on PET and PE to be evaluated. Such analysis would enable the detection of increased concentrations of metabolites and would help to identify potential degradation by-products. To analyse the intra and extracellular metabolites from *Streptomyces* sp. F grown on both PET and PE both untargeted and targeted metabolomics was utilised.

However, untargeted approaches can also have several drawbacks (Seger, 2012). The first being that identification is based on a direct comparison to a collection of databases. The two parameters used to identify the peak are the retention time (Rt) of the molecule from the liquid chromatography and the mass-to-charge ratio (m/z) detected by the mass spectrometer. From these two parameters, each peak is identified by comparison to the different databases (Vinaixa *et al.*, 2016). However, if the peaks have unknown retention times and mass-to-charge ratios, they will remain unknown and will not be included in the rest of the analysis (Vinaixa *et al.*, 2016). Moreover, some peaks can be misidentified due to their Rt and m/z being too close to another previously reported metabolite (Vinaixa *et al.*, 2016).

In addition of the untargeted approach, a more targeted LC-MS approach was used for a small number of specific target molecules associated with the degradation of PET and PE. This approach is based on standards and enables molecules to be clearly detected in the samples. The following metabolites were selected terephthalic acid, one of the monomers of PET breakdown, nicotinic acid, and quinolic acid, molecules which are known to be involved in the reduction power of the cell and could be present in PE degradation.

All the samples were from biological replicates and each biological replicate had a corresponding technical replicate. Technical replicates provide a better statistical evaluation. The data discussed below is quantitative, but no calibration curves were done, instead the arbitrary peak was utilised. Orthogonal Projections to Latent Structures Discriminant Analysis (OPLS-DA) analyses were used to represent the changes in the metabolome throughout the fermentation. Volcano plots were used to represent the number of significantly different metabolites between the two conditions, and heat maps were used to represent the peak area of the metabolites of interest.

3.5.1 Metabolomic analysis: PET vs glucose

As stated previously, *Streptomyces* sp. F was grown using glucose as the sole carbon source and PET and glucose. It is therefore important to differentiate the metabolic activity on glucose from the activity on PET. In order to do a comprehensive comparison was made between the metabolic data from *Streptomyces* sp. F grown on both glucose and PET.

3.5.1.1 Glucose consumption rates

Glucose consumption was monitored in both the glucose only and the glucose and PET fermentation, using both glucose sticks and LC-MS. In both conditions, the glucose was completely consumed around 168 hours. The

presence of PET did not significantly impact on the glucose consumption rate (p-value>0.05) and the glucose had been completely consumed by 168 hours (Figure 3-17). Therefore, any growth detected after 200 hours during the fermentation on PET (Figure 3-14) cannot be the result of the consumption of glucose. This growth strongly suggests that Streptomyces *sp. F* can utilise PET to sustain its growth.

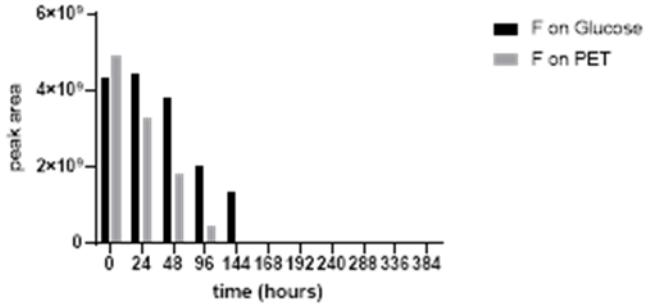


Figure 3-17 : Bar chart to show peak area of the glucose present in the supernatant during both the fermentation of *Streptomyces* sp. F on glucose and PET

3.5.1.2 Comparison of the supernatant from fermentation on glucose and glucose and PET

Samples were collected from the fermenter and centrifuged; the supernatant was added to an equal volume of methanol. The samples were then analysed via LC-MS by Laudina Safo. OPLS-DA was used to group the data sets according to 2 dimensions (Worley and Powers, 2012). The data was used to assess the metabolomic differences between the two supernatants from the fermentation (Worley and Powers, 2012). The acceptable empirical value is denoted as the quality assessment (Q^2) > 0.5 (Worley and Powers, 2012). Statistical relevance can also be assessed via the use of R^2X and R^2Y, which corresponds to the coefficient of determination of the model according to both the X and Y axis (Worley and Powers, 2012). The value to infer the significance of the modelling is empirically described as >0.5 (Worley and Powers, 2012). For the OPLS-DA analysis to be considered

statistically significant both the Q^2 and the coefficient of determination (R^2) need to be superior to 0.5.

The OPLS-DA analysis performed on the supernatant from the fermentation had a $Q^2>0.5$ and $R^2>0.5$. This analysis allowed for the direct comparison of metabolite profiles between samples. There was a clear difference between the metabolite profile of the glucose vs the PET supernatant (Figure 3-18 A). Stark differences in the metabolic profile start around 48 hours (2days) (Figure 3-18 A), interestingly this is before all the glucose has been utilised, which occurs at 144 hours (6 days) (Figure 3-17). This would indicate that the cell has already started to break down the PET while co-utilising the glucose.

A volcano plot (Figure 3-18 B) was used to detect metabolites which had a significant change in their concentration (p-value<0.05) and log fold change of 2 with a log2 ratio > 2. The volcano plot identified nine metabolites of interest which either significantly decreased (7) or increased (2).

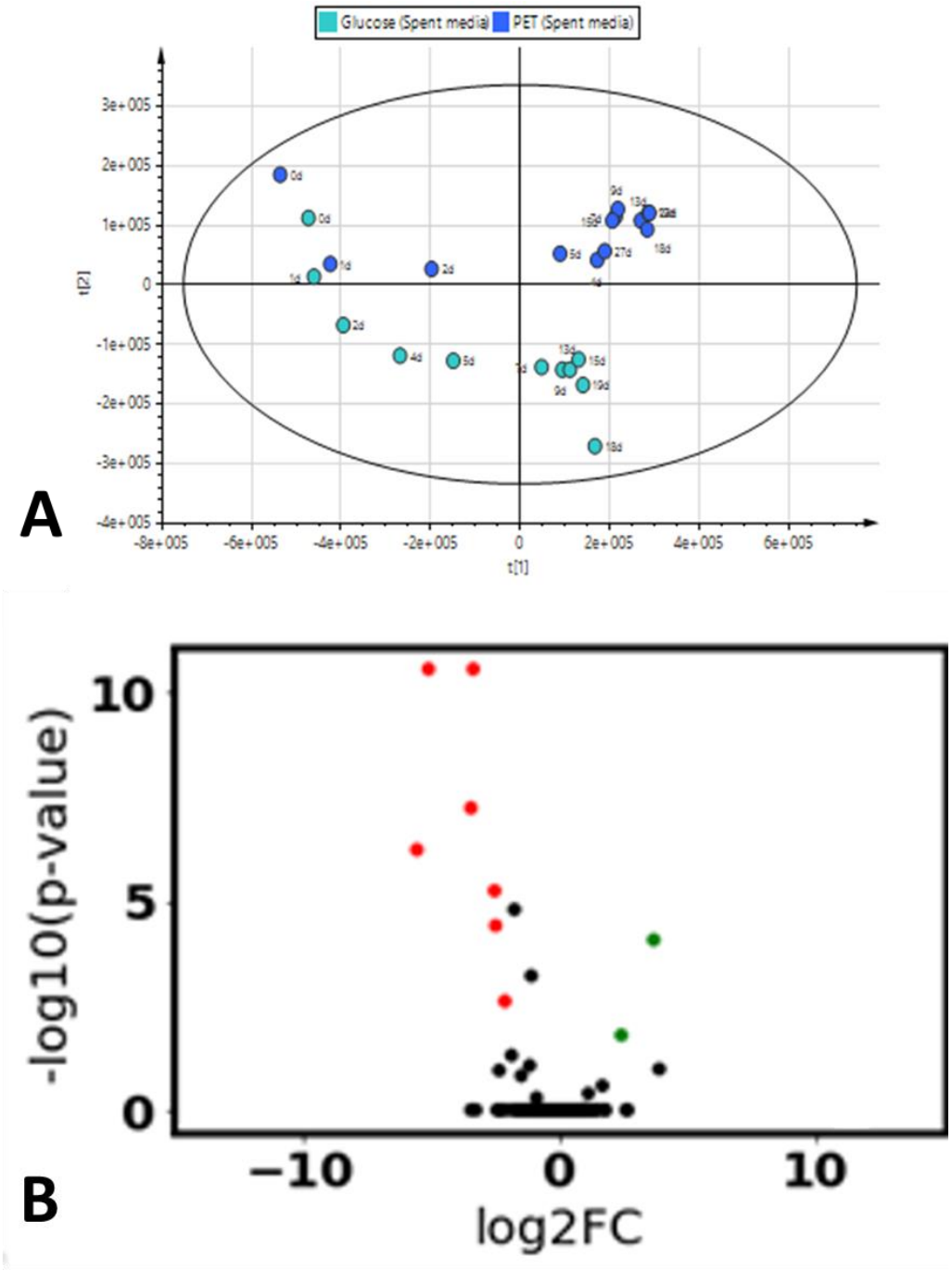


Figure 3-18: OPLS-DA analysis showing the differences between the glucose (light blue) and PET (dark blue) supernatant throughout the fermentation, each point corresponds to the overall metabolite profile of one sample(A), volcano plot of glucose Vs PET showing significant increases and decreases in extracellular metabolites during the fermentation, in green metabolites with higher concentration on PET, in red metabolites with higher concentration on glucose, each point corresponds to a metabolite (B)

The statistically significant metabolites identified from the volcano plot were utilised to generate a heat map, using a Python program written by Dr Nicole Pearcy. This heat map was used to analyse the nine metabolites in more detail (Figure 3-19). The scale was standardized, using the peak area with a value between 0 and 1, 1 being the highest peak area observed under both conditions. From this analysis, two classes of metabolites were identified, ones with enrichment on PET and ones with enrichment on glucose.

All of the metabolites enriched on glucose (phenacetin, mevalonic acid, octadecanoic acid, ethyl myristate, heptanoic acid, 4-toluic acid and homovanillate) share a similar dynamic in their concentration (Figure 3-19). Their concentration reached a maximum peak between 96 to 144 hours, then their concentration decreased (Figure 3-19). For example, the heptanoic acid concentration increased 4-fold in the first 144 hours, before decreasing later in the fermentation. Only two metabolites were enriched on PET: 2-aminooctanedioic acid and galacturonate (Figure 3-19).

While no specific pathway has been identified to explain the metabolite dynamic, this dynamic is specific to glucose and PET (Figure 3-18 B and 3-19). The key metabolite terephthalic acid will be discussed more specifically below.

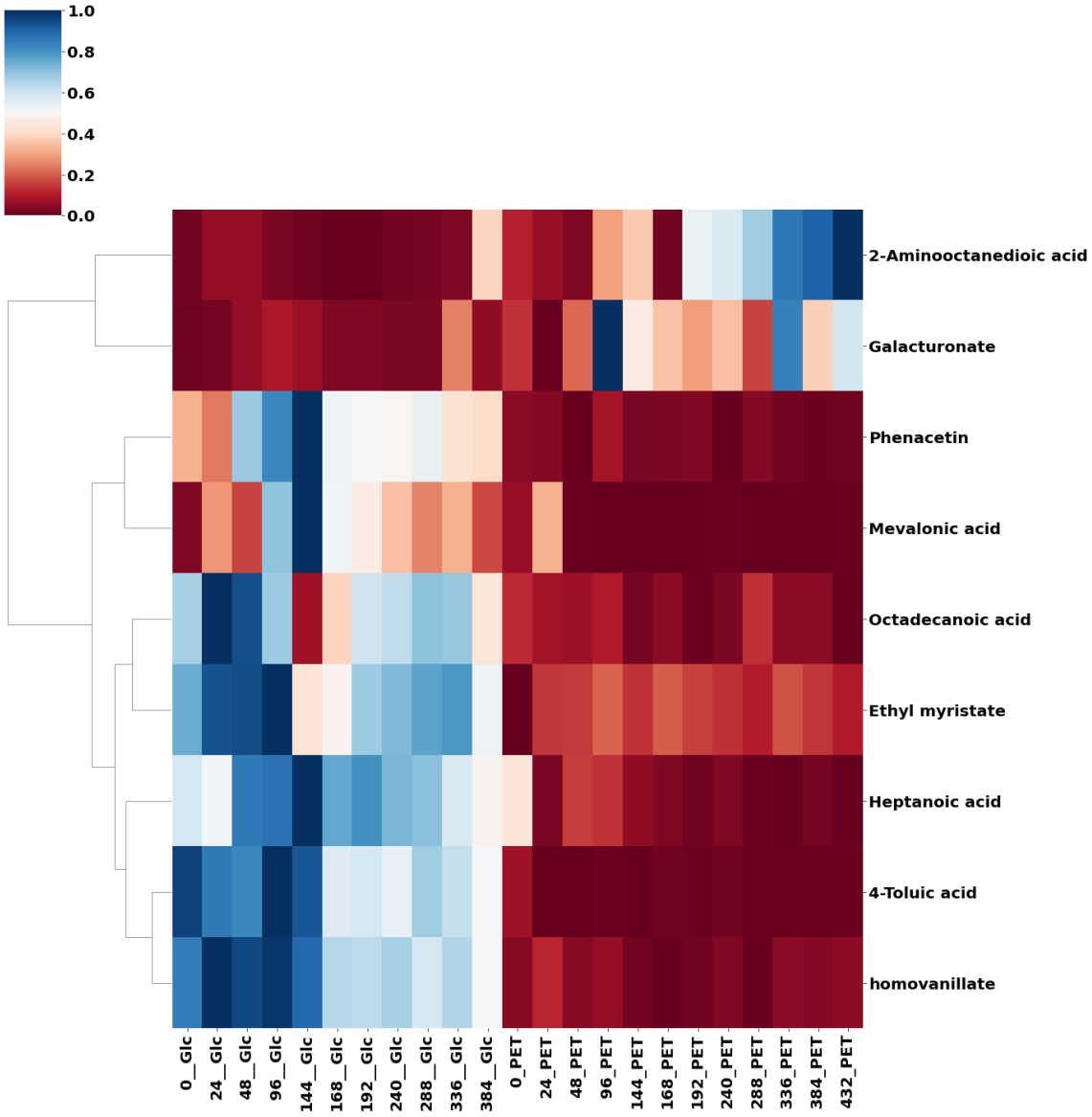


Figure 3-19: Heat map of the nine metabolites which had either increased or decreased concentrations on both PET and glucose in the supernatant. In blue the highest peak area measured, in red the lowest.

3.5.1.3 Comparison of the cell pellet from PET and glucose

The pelleted cells were added to 100% ice cold methanol and the pellet was resuspended and the cells were left on ice for 1 hr. The samples were then diluted to 50% methanol in water, centrifuged and analysed via LC-MS by Laudina Safo. Both OPLS-DA analysis and a volcano plot were used to evaluate the changes in the intracellular metabolite concentration from the

fermentation on both glucose and PET. The OPLS-DA had a Q^2 and R^2> 0.5 and showed a distinctive difference between the intracellular metabolites from both the glucose and the PET conditions, with a clear distinction being seen from very early in the fermentation (Figure 3-20 A).

A volcano plot (Figure 3-20 B) was used to detect metabolites, which had a significant increase or decrease in their concentration (p-value<0.05) depicted as the log fold change (with a log2 ratio > 2). The analysis highlighted 10 metabolites of interest, 6 which decreased on the PET vs the glucose and 4 which increased, the remaining metabolites did not significantly change.

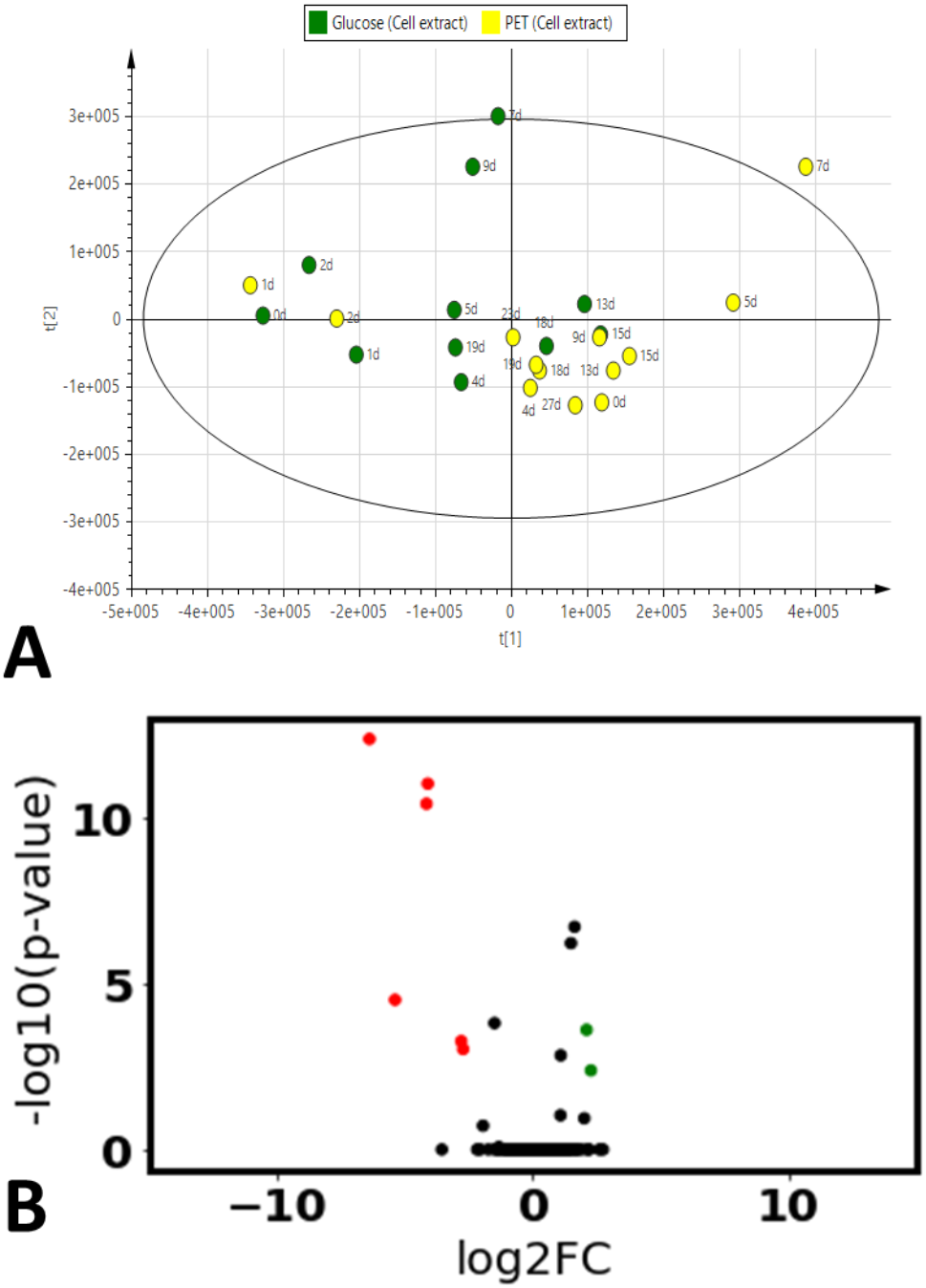


Figure 3-20: OPLS-DA analysis showing the differences between the intracellular content of the PET and glucose fermentation, each point corresponds to the overall metabolite profile of one sample (A), volcano plot glucose vs PET showing significant y differences in intracellular metabolites during the fermentation, in green metabolites with higher concentration on PET, in red metabolites with higher concentration on glucose, each point corresponds to a metabolite (B)

Utilising the statistically significant metabolites from the volcano plot a heat map was constructed, the scale was standardized, from 0 to 1. From this

analysis, two groupings of metabolites were identified: metabolites enriched on glucose (7) and metabolites enriched PET (3).

The metabolites enriched on glucose (4-toluic acid, octadecanoic acid, 3-(2 Hydroxyethyl) indole, nicotinamide, 4-carboxyphenylglycine, phenacetin and homovanillate) share a similar dynamic in their concentration: first there was an initial increase in the concentration, with a peak around 96-168 hours, followed by a decrease in the concentration (Figure 3-21). For example, for homovanillate the concentration increased 2-fold between 0 and 96 hours and after 144 hours its concentration decreased 5-fold (Figure 3-21).

While no specific pathway has been identified to explain the metabolite dynamic, it is specific to glucose and PET (Figure 3-20 B and 3-21).

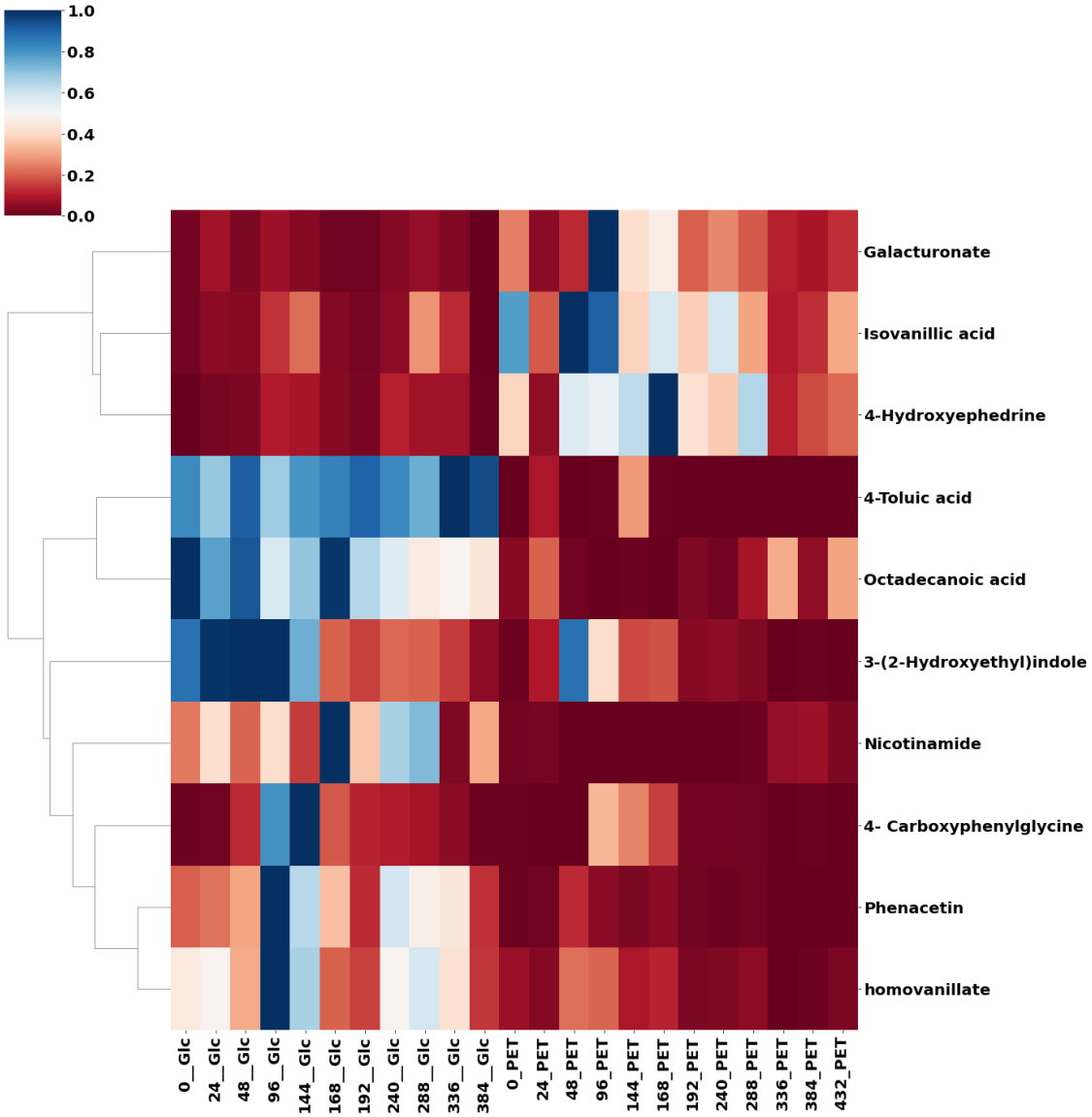


Figure 3-21: Heat map of the ten metabolites from the cell pellet which had significantly decreased or increased on PET and glucose. In blue the highest peak area measured, in red the lowest.

3.5.1.4 Detection of PET monomer terephthalate acid

To detect the specific breakdown products of PET, a targeted LC-MS approach was utilised. The supernatant was extracted as detailed above. One of the key molecules associated with the degradation of PET is TPA (Wei and Zimmermann, 2017). In order to test that PET degradation was not

due to mechanical stress in the fermentation, a control cell-free fermentation (PET-control) was performed. A small number of samples were taken for LC-MS analysis 0 hours, 96 hours, 336 hours, and 456 hours. Targeted LC-MS analysis was performed on both the control and the PET fermentations, using biological replicates and technical replicates.

TPA was detected in both the PET fermentation and the PET control. However, the peak area in the PET control was stable over time and does not increase as expected between 0 hours and 456 hours (Figure 3-22). If mechanical shearing was responsible for the degradation, then the concentration would be expected to increase over time. In the PET fermentation, an increase in the peak area was detected (Figure 3-22). The TPA concentration increased from 96 hours to 432 hours, which surpassed the glucose depletion, at 144 hours (Figure 15). The presence of increased TPA in the PET supernatant clearly shows that *Streptomyces* sp. F can degrade PET.

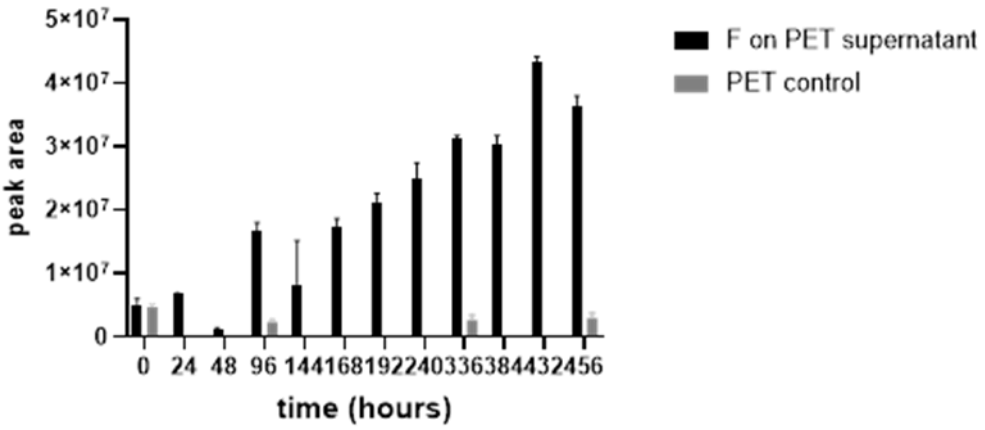


Figure 3-22: Graph to show peak area of the terephthalic acid in the supernatant of both F grown in SMMmodFm at 30℃, with 1% glucose and 1% PET powder (F on PET condition) and cell free PET control

3.5.2 Metabolomics analysis: PE vs glucose

As stated previously, *Streptomyces* sp. F was grown using glucose as the primary carbon source, in both the PE and glucose fermentations. It is

therefore important to differentiate the metabolite levels in both the PE and the glucose supernatant and cellular pellets. In order to do this a comprehensive comparison was made between the metabolism of *Streptomyces* sp. F on both glucose and PE using untargeted metabolomics.

3.5.2.1 Glucose consumption

The glucose concentration was monitored throughout the fermentation for both the glucose only control and the PE/glucose fermentation using a combination of glucose test strips and targeted LC-MS analysis. The identification of the peak was confirmed using a standard.

Under both conditions, the glucose was completely consumed at 168 hours (Figure 3-23). The presence of PE did not have a significant impact on the glucose consumption (p-value>0.05). However, the consumption of glucose during the first 144 hours of the fermentation did not significantly increase growth (Figure 3-16, Table 3-5). Moreover, growth increased after 200 hours on PE (Figure 3-16, Table 3-5) which was not related to the consumption of glucose.

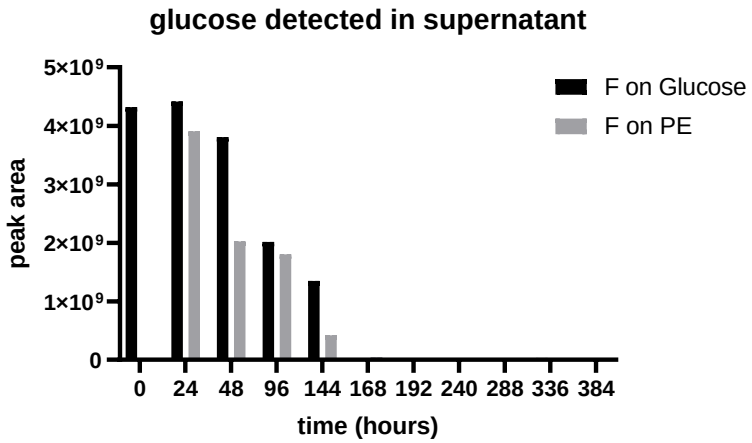


Figure 3-23 : Bar chart to show peak area of the glucose present in the supernatant during fermentations grown in SMMmodFm at 30°C, with 1% glucose (glucose condition) , 1% glucose and 1 % PE film (PE condition)

3.5.2.2 Comparison of the extracellular content

Untargeted metabolomics was utilised to compare the supernatant from both the glucose and the PE fermentation. The supernatant was extracted in methanol as described above and analysed on the LC-MS. There was a clear difference between the metabolite composition of the supernatant from the PE and the glucose fermentation.

Both the OPLS-DA analysis and a volcano plot were used to evaluate the changes in the extracellular composition of the fermentations on glucose and PE. The OPLS-DA had a Q^2 and R^2> 0.5, which demonstrated a clear difference in the extracellular metabolite content for the PE (Figure 3-24 A). The differences in the metabolic profile were seen after 168 hours (7d) (Figure 3-24 A).

A volcano plot (Figure 3-24 B) was used to detect metabolites which had a significant increase or decreases in their metabolite concentration (p-value<0.05) with a log fold change greater than 2 (with a log2 ratio > 2). The analysis identified more than 50 metabolites of interest, which has significant increases or decreases on glucose vs PE.

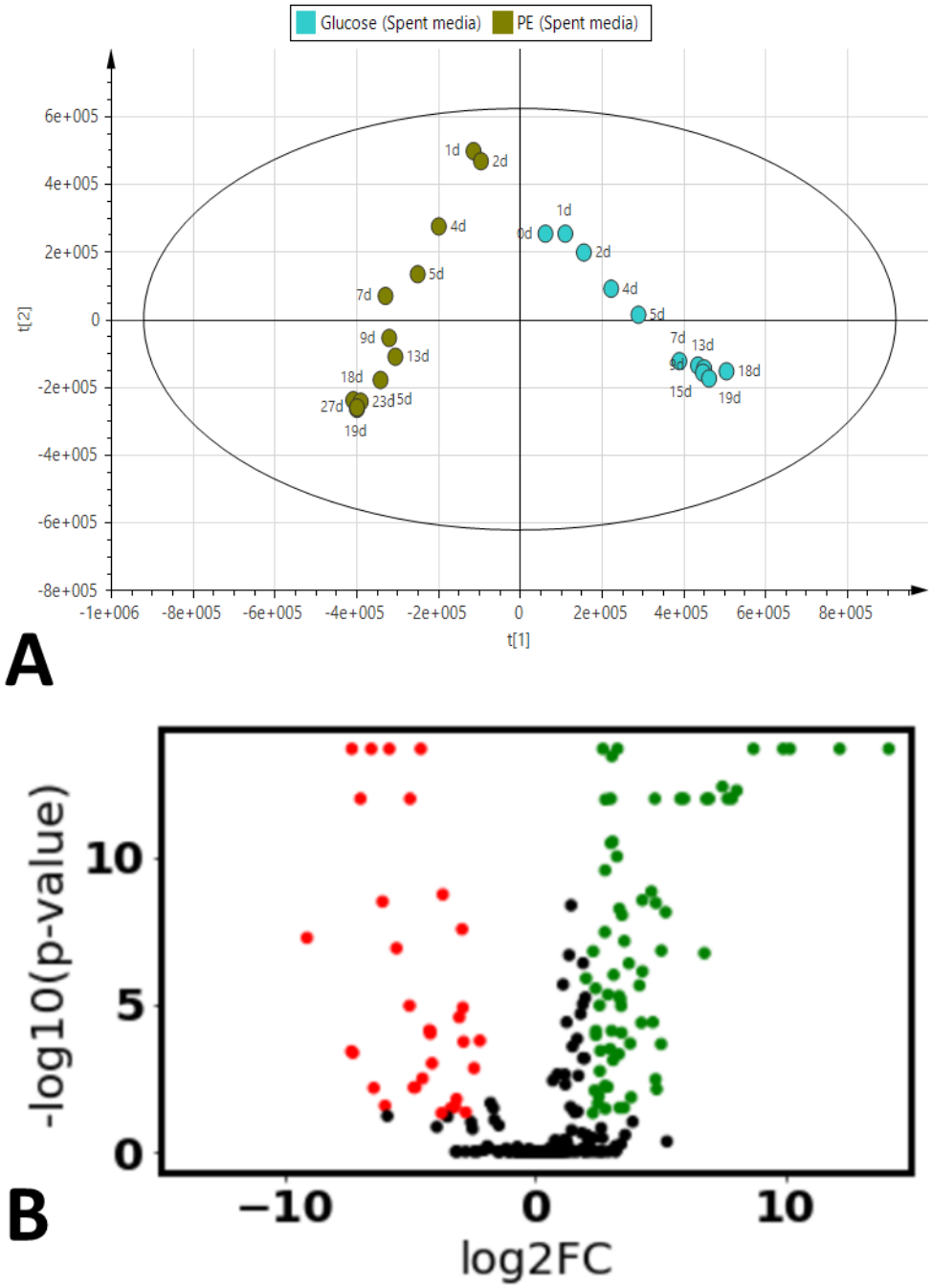


Figure 3-24: OPLS-DA analysis showing the metabolite distribution in the extracellular content from the PE (gold) and glucose (light blue) fermentation, each point corresponds to the overall metabolite profile of one sample (A), volcano plot representing metabolites with significant increases and decreases concentration on glucose vs PE, in green metabolites with higher concentration on PE, in red metabolites with higher concentration on glucose, each point corresponds to a metabolite (B)

From the metabolites of interest with statistical significance (p-value<0.05 and log2>2), a heat map was constructed, the scale was standardized, from

0 to1. From this analysis, three grouping of metabolites were identified: metabolites enriched on glucose (33) (Figure 3-25), metabolites enriched on PE with no decrease in concentration (40) (Figure 3-25), and metabolites enriched on PE with a decrease in concentration (31) (Figure 3-25),

The first group contained 33 metabolites which were enriched on glucose, far more than during the comparison between glucose vs PET (Figure 3-18 B and 3-19). Several aliphatic compounds were also present in this grouping, such as 2, 4-heptadienal, suberic acid, adipic acid and 3-tert-butyladipidic acid, their concentration increased after 168 hours (from 6 to 30-fold increase) (Figure 3-25).

The second group contained 40 metabolites. This group contains metabolites which initially increased in their concentration, but after 168-196 hours there was a rapid decrease. Several TCA compounds (pyruvate, fumarate, malate and citric acid) were part of this group. In the case of fumarate, in the first 168 hours a 100-fold increase was detected, followed by a 200-fold decrease between 168 and 360 hours (Figure 3-25). A similar pattern was seen for pyruvate (4-fold increase, followed by a 200-fold decrease), malate (1200-fold increase, followed by a 700-fold decrease) and citric acid (250-fold increase, followed by a 10-fold decrease) (Figure 3-25).

The third and last group contained metabolites enriched on PE, which had a consistent increase in their concentration. This grouping contained metabolites belonging to several different pathways: fatty acid transport chain, biosynthesis of nicotinamide adenine dinucleotide and fatty acids.

Carnitine related compounds were identified in this group. Carnitine concentration had increased 100-fold during the fermentation, O acetyl-carnitine concentration had increased 350-fold and O butyl-carnitine had increased 240-fold (Figure 3-25). Carnitine has multiple functions in the cell, the most prominent being related to fatty acid transportation in micro-organisms (Wargo and Meadows, 2015; Longo, Frigeni and Pasquali, 2016). Several reports have shown that bacteria, such as *Pseudomonas* sp. are able to metabolise acylcarnitine and use it for growth (Kleber *et al.*, 1978; Meadows and Wargo, 2013)

Metabolites related to the fatty acid and other carbonated chain were also part of the third grouping (Figure 3-25). These are of particular interest, since they are hypothesised to be degradation products of PE (Bonhomme *et al.*, 2003; Restrepo-Flórez, Bassi and Thompson, 2014). Long carbon chains with various degrees of oxidation were detected: linoleic acid, octadecanoic acid, 9-oxo-10, 12-octadecadienoic acid, 2-oxoadipate, a well as shorter carbon chain: tartaric acid (Figure 3-25). The 2-oxoadiapte concentration increased by 300-fold during the course of the fermentation, octadecanoic acid increased by 3-fold, 9-oxo-10, 12-octadecadienoic acid increased by 30-fold and tartaric acid concentration increased by 100-fold (Figure 3-25)

PE had a significant impact on the extracellular metabolites in the fermentation broth, with over 100 metabolites significantly increased or decreased (Figure 3-24 B). This could be due to the degradation of PE.

Moreover, the detection of metabolites involved in central carbon metabolism indicates that cellular activity is continuing throughout the fermentation (Figure 25). This is a clear indication that *Streptomyces F* can degrade PE and is able to metabolise the by-products of PE degradation.

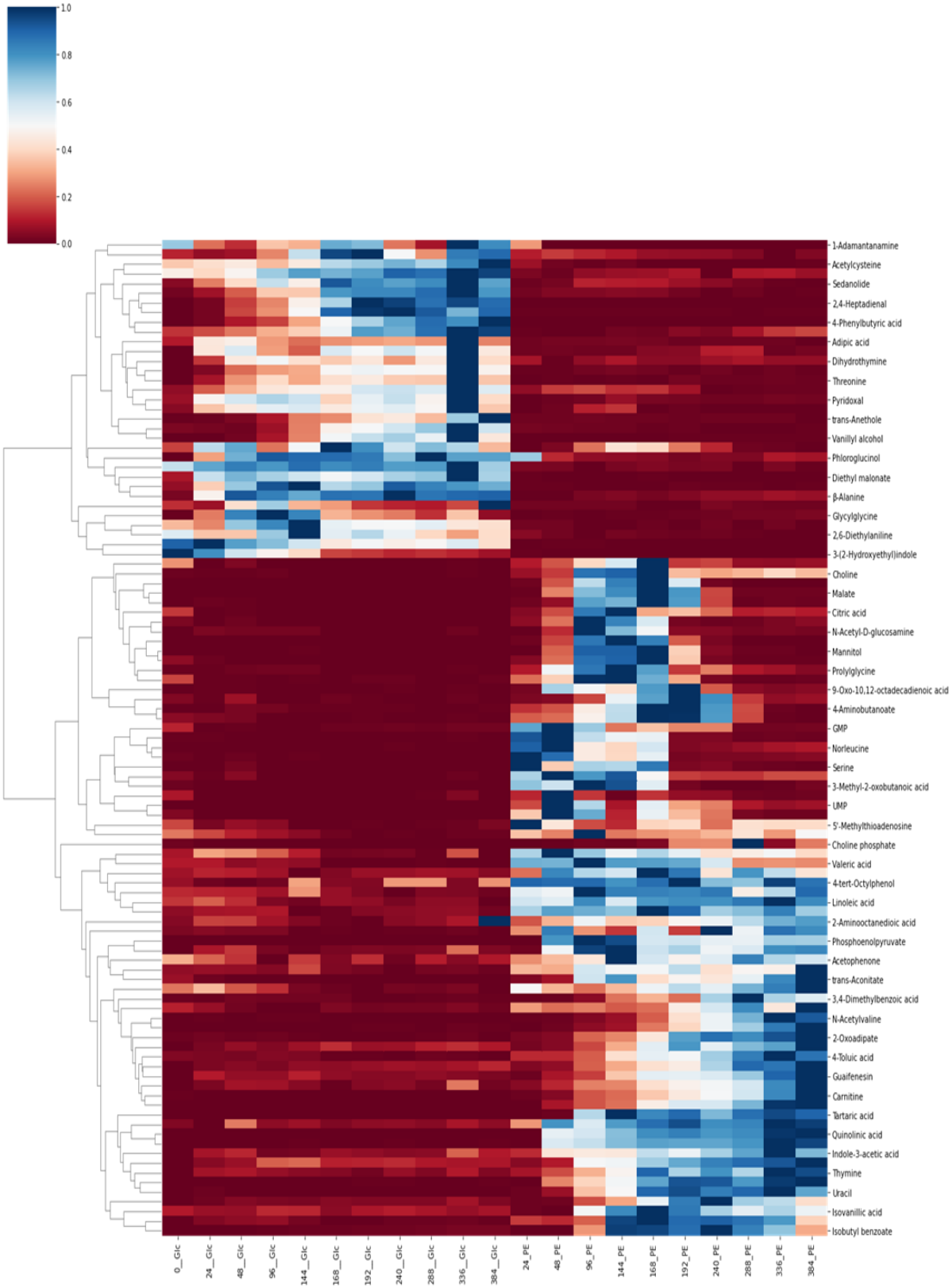


Figure 3-25: Heat map of the metabolites of interest showing differences between the PE and glucose in the supernatant. In blue the highest peak area measured, in red the lowest.

3.5.2.3 Comparison of the intracellular content

The cell pellet was extracted utilising cold methanol as detailed above, after dilution in water, the samples were subject to LC-MS. Both the OPLS-DA analysis and a volcano plot were used to analyse the changes in the intracellular composition of the fermentation on glucose and PE. For the OPLS-DA, both Q^2 and R^2> 0.5. There was a clear shift in the intracellular metabolite concentration in the cells when grown on PE (Figure 3-26 A). The change in intracellular metabolite concentration started after 96 hours (4d) and stabilized after 216 hours (9d) (Figure 3-26 A).

A volcano plot (Figure 3-27 B) was used to detect metabolites of interest with an increase or decrease in metabolic activity (p-value<0.05 and log2 ratio > 2). Twelve metabolites were identified with either increasing or decreasing metabolite concentration.

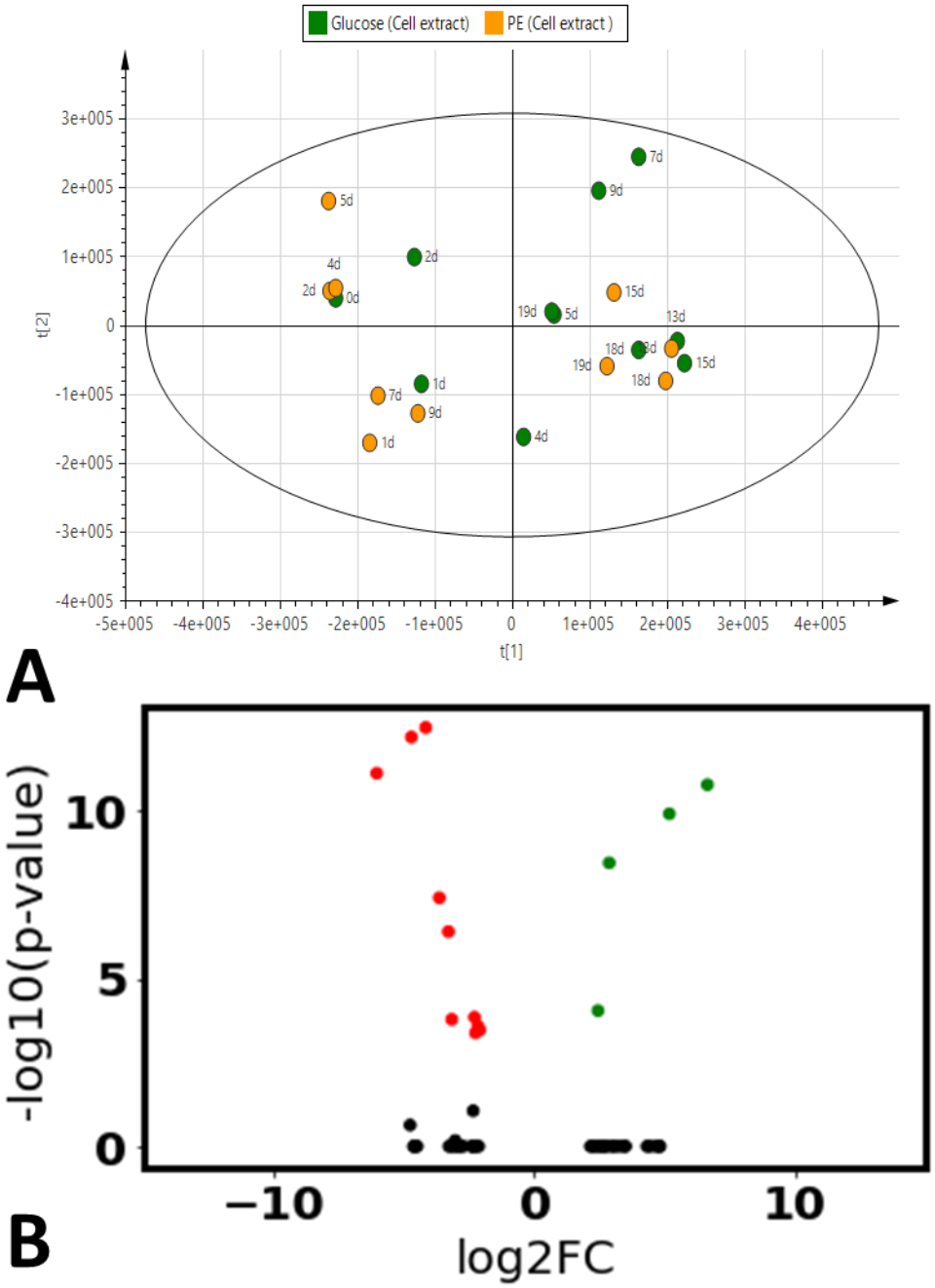


Figure 3-26: OPLS-DA analysis showing the metabolite distribution in the extracellular content from the PE (orange) and glucose (green) fermentation, each point corresponds to the overall metabolite profile of one sample (A), volcano plot representing metabolites with significant increases and decreases concentration on glucose vs PE, in green metabolites with higher concentration on PE, in red metabolites with higher concentration on glucose, each point corresponds to a metabolite (B)

Utilising the statistically significant metabolites (p-value<0.05 and log2>2), a heat map was constructed, the scale was standardized, from 0 to1. From this analysis, two groups of metabolites were identified: metabolites enriched on glucose (5) (Figure 3-278), and metabolites enriched on PE (4) (Figure 3-27),

Metabolites enriched on PE, included both quinolinic acid and picolinic acid (Figure 3-27). Both metabolites are part of NADH biosynthesis, suggesting there is an increase in the reducing power of the cell. This is further supported by an increased concentration of nicotinamide on glucose, a key intermediate in the biosynthesis of NADH (Figure 3-27).

Metabolites enriched on glucose, include 4-Toluic acid, which is only enriched on the glucose condition (Figure 3-15 and 3-23 and 3-27).

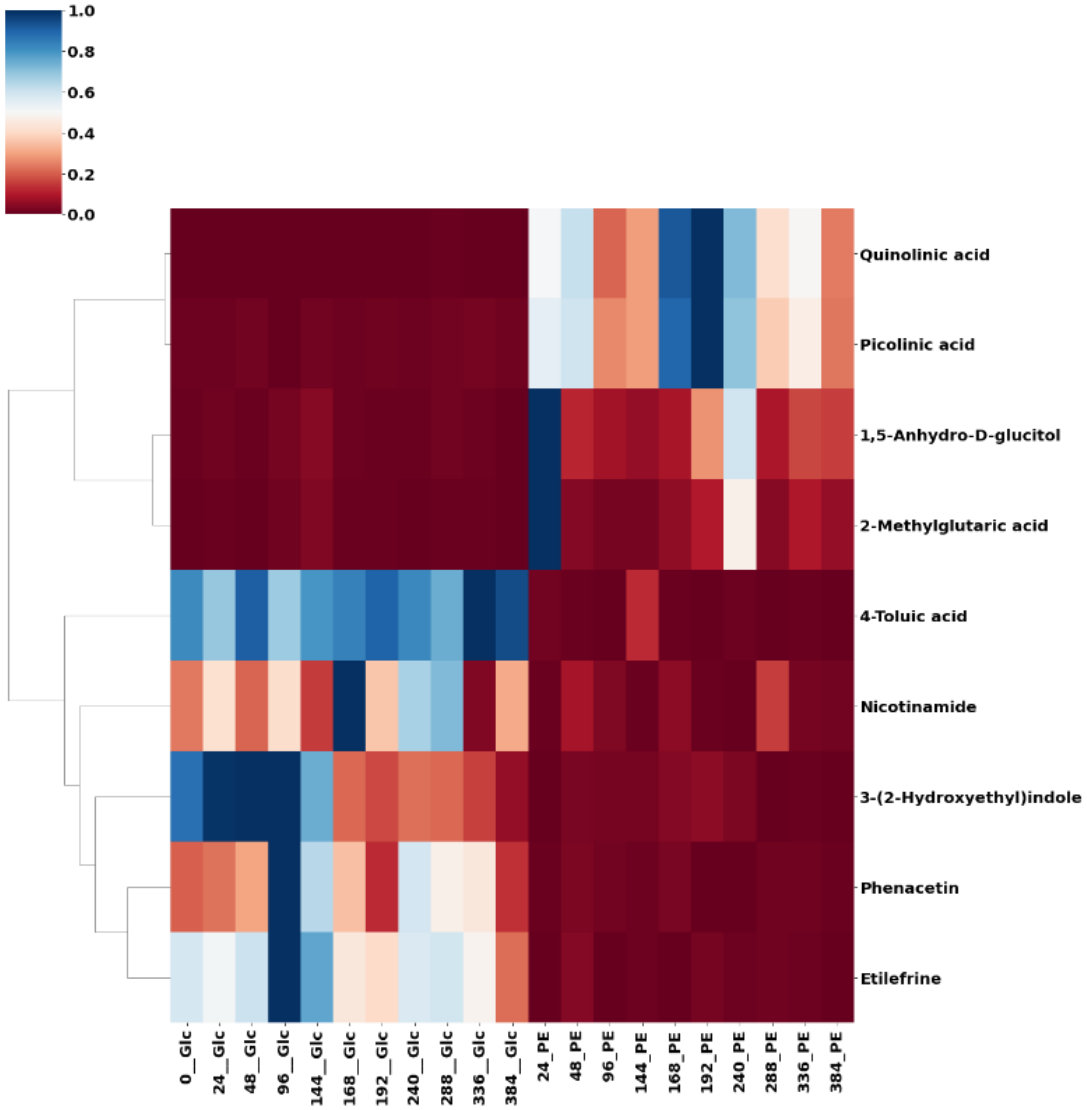


Figure 3-27: Heat map of the significant metabolites between the glucose and PE condition detected in the intracellular content. In blue the highest peak area measured, in red the lowest

3.5.3 Metabolomics analysis: PE vs PET

A final comparison was made between the two plastics, PET and PE to see if specific differences could be seen in the metabolite levels. The extracted metabolites were subject to LC-MS analysis.

3.5.3.1 Comparison of the extracellular content

OPLS-DA analysis and a volcano plot were used to detail the changes in the extracellular composition of the fermentations on both PET and PE. Both the Q^2 and R^2> 0.5, demonstrating a shift in the metabolite pattern following growth on PE growth (Figure 3-28 A). Changes in the metabolite profile and concentration typically started after 168 hours (7d) and stabilized after 216 hours (9d) (Figure 3-28 A). A volcano plot (Figure 3-28 B) was used to highlight metabolites of interest with a log fold increase of greater than 2 (p-value<0.05 and log2 ratio > 2). This analysis highlighted more than a hundred metabolites of interest.

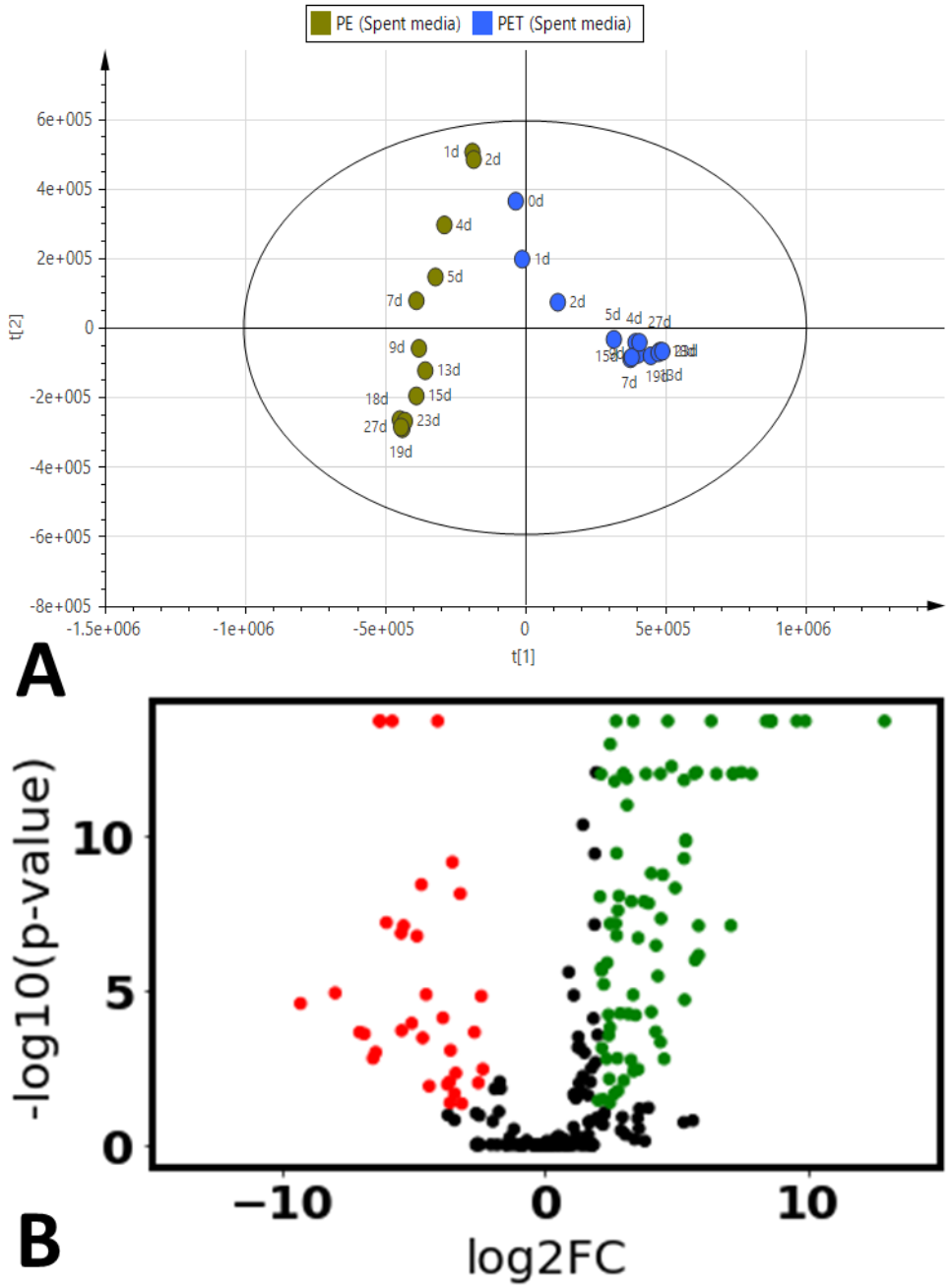


Figure 3-28: OPLS-DA analysis showing the metabolite distribution in the extracellular content from the PE (gold) and PET (dark blue) fermentation, each point corresponds to the overall metabolite profile of one sample (A), volcano plot representing metabolites with significant increases and decreases concentration on PET vs PE, in green metabolites with higher concentration on PET, in red metabolites with higher concentration on PE, each point corresponds to a metabolite(B).

From the metabolites of interest with statistical significance (p-value<0.05 and log2>2), a heat map was constructed, the scale was standardized, from 0 to1. From this analysis, >100 metabolites of interest have been identified.

From this analysis, three grouping of metabolites were identified: metabolites enriched on PET (33) (Figure 3-30), metabolites enriched PE with no decrease of concentration (45) (Figure 3-29), and metabolites enriched PE with decrease of concentration (34) (Figure 3-29).

The first grouping contains 33 metabolites with an enrichment on the PET condition, a similar number that during glucose vs PE comparison (Figure 3-25 B and 3-26) Several aliphatic compounds were present in this grouping, such as 2,4-heptadienal, suberic acid, adipic acid and 3-tert-butyladipidic acid, they share a similar dynamic of their concentration: an increase of their concentration after 168 hours (from 3 to 100-fold increase) (Figure 3-29).

The second and third grouping contains similar metabolites than during the glucose vs PE comparison (3.5.2.2). It is due to the lack of significant metabolic changes between the PET and glucose condition (3.5.1.2).

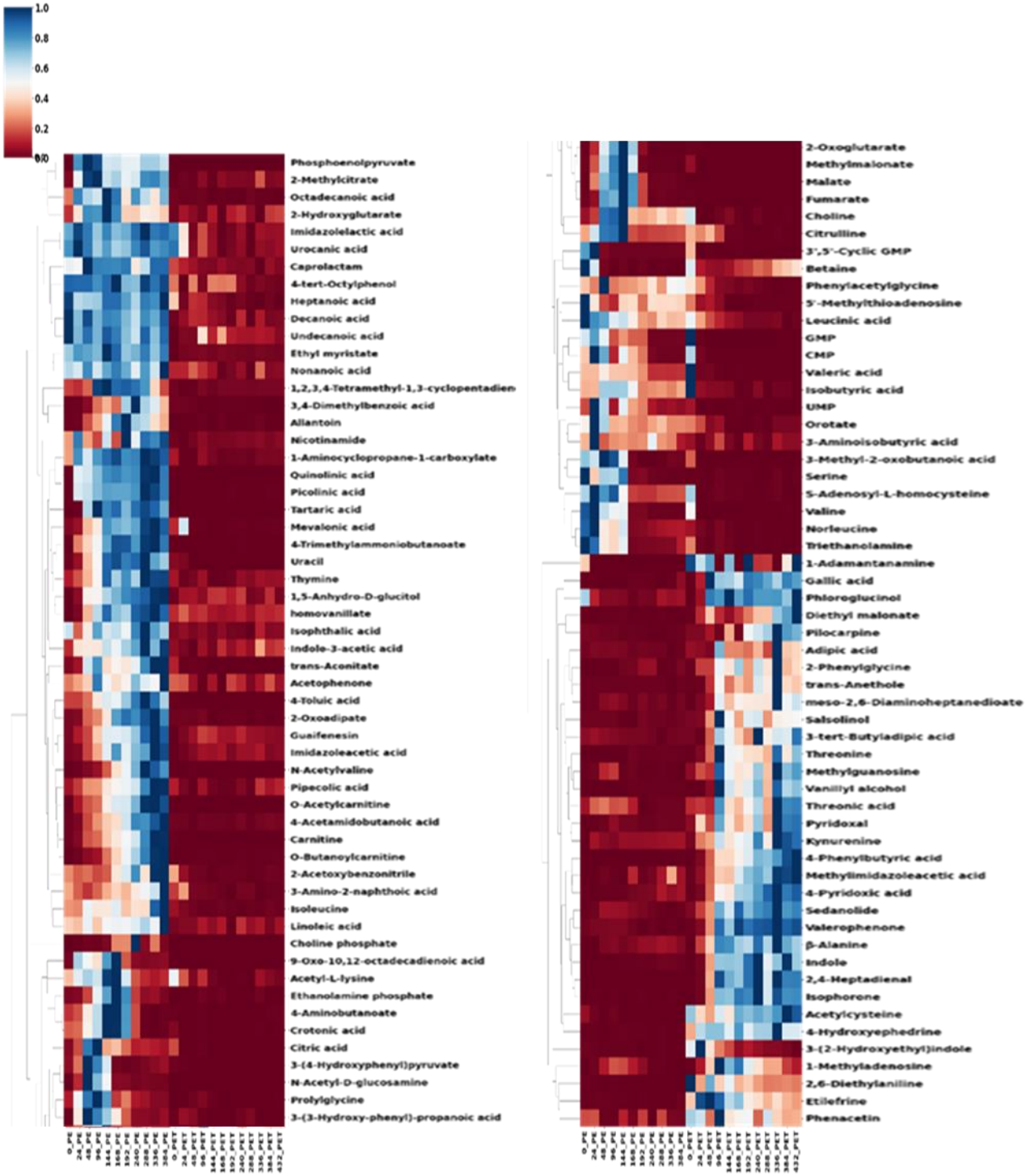


Figure 3-29 : Heat map of the significant metabolites between the PET and PE condition detected in the supernatant. In blue the highest peak area measured, in red the lowest.

3.5.3.2 Comparison of the intracellular content

OPLS-DA analysis was utilised initially, and a volcano plot was generated to describe the changes in the extracellular composition of the fermentation on PET and PE. The OPLS-DA, date had a Q^2 and R^2> 0.5, demonstrating a change in the metabolic profile under both conditions (Figure 3-30 A). The metabolic shift on PE started after 168 hours (7d) and stabilized after 288 hours (13d) (Figure 3-30 A). A volcano plot (Figure 3-30 B) was used to detect metabolites of with significant changes in their concentration, with a log fold increase above 2 (p-value<0.05 and log2 ratio > 2). The subsequent analysis highlighted 9 metabolites of interest.

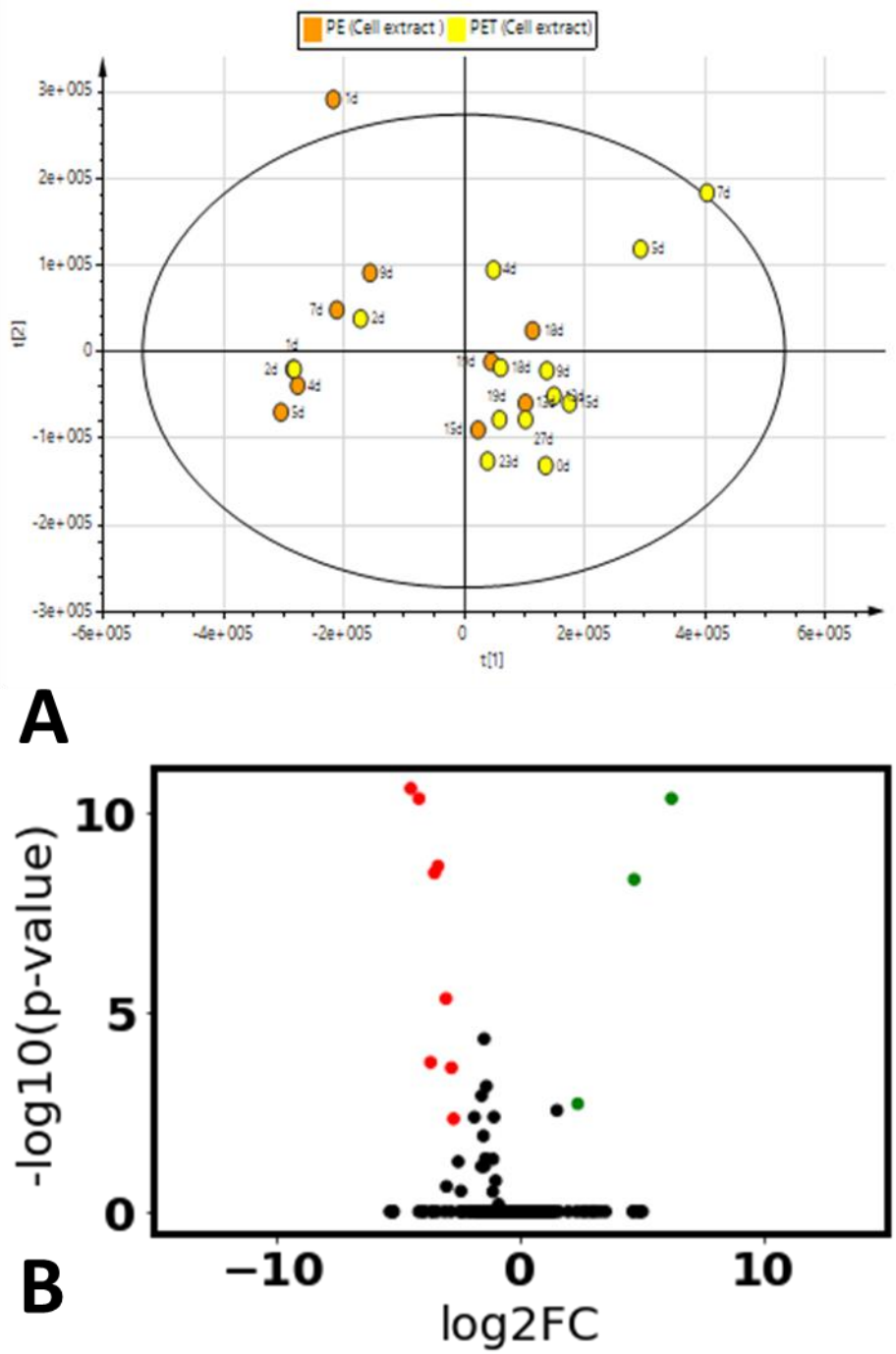


Figure 3-30 : OPLS-DA analysis showing the metabolite distribution in the extracellular content from the PE (orange) and PET (yellow) fermentation, each point corresponds to the overall metabolite profile of one sample (A), volcano plot representing metabolites with significant increases and decreases concentration on PE vs PET in green metabolites with higher concentration on PE, in red metabolites with higher concentration on PET, each point corresponds to a metabolite(B).

From the metabolites of interest with statistical significance (p-value<0.05 and log2>2), a heat map was constructed, the scale was standardized, from

0 to1. From this analysis, 9 metabolites of interest have been identified (Figure 3-31).

The comparison of the intracellular metabolite of interest between PE and PET revealed the same metabolites than during the glucose vs PE comparison (3.5.2.3). This is most likely due to the metabolic similarity between PET and glucose condition, as seen previously (3.5.1.3)

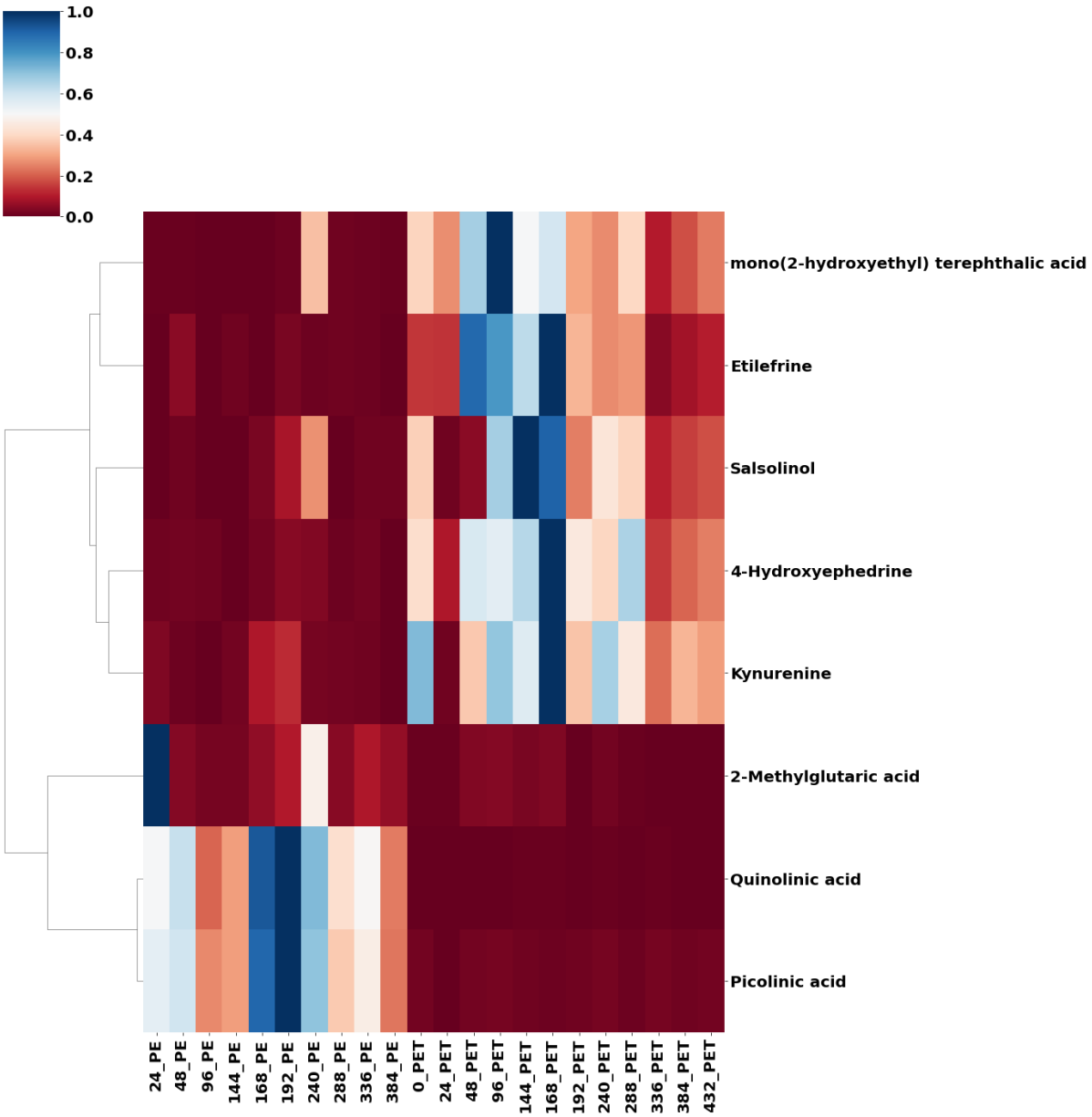


Figure 3-31 : Heat map of the significant metabolites between the PET and PE condition detected in the intracellular content. In blue the highest peak area measured, in red the lowest.

3.6 Characterisation of the growth of *Streptomyces* sp. F on the monomeric breakdown products of PET

3.6.1 Characterisation of the growth of *Streptomyces* sp. F on TPA and EG

To further demonstrate that *Streptomyces* sp. F could grow on PET, cells were grown on the monomeric breakdown products of PET, TPA and EG in shake flasks.

Growth was conducted on media where both TPA (0.1% W/V) and EG (1% V/V) were the only carbon sources. Growth tests were performed in triplicate, and the CFU count was used to assess the growth.

Streptomyces sp. F was able to grow on both TPA and EG initially up to 97 hours, this could be due to carry over of inoculum. After the initial growth period, the CFU count began to decrease on TPA. Due to this decrease, the monitoring of the growth on TPA was stopped after 192 hours (Figure 3-32). For EG, a second growth phase was detected after 168 hours. The growth rate was calculated for both phases of growth (Table 13). This indicates that *Streptomyces* sp. F can utilise EG as a sole carbon source.

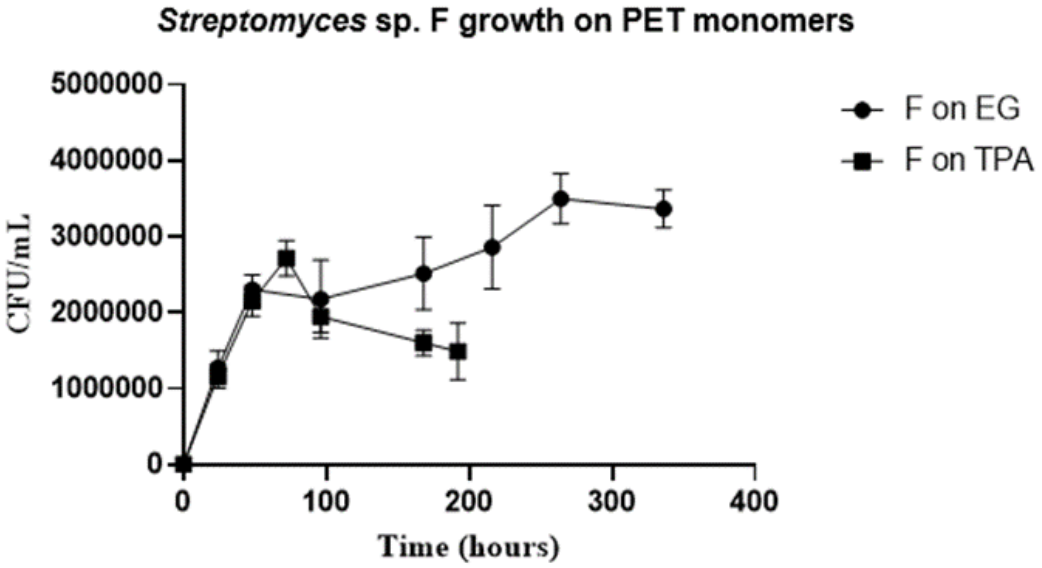


Figure 3-32 : Graph to show CFU count for *Streptomyces* sp. F on ethylene glycol (EG) and terephthalic acid (TPA)

	μ (h^{-1})	***Lower 95%***	***Upper 95%***	**p-value**	**Coefficient of determination (R^2)**
μ on EG	0.0049	0.002	0.007	1.57E-02	0.9917
μ on TPA	N/A	N/A	N/A	N/A	N/A

Table 3-6: Growth rate of *Streptomyces* sp. F on the monomeric product of PET degradation, ethylene glycol (EG) and terephthalic acid (TPA)

3.7 Transcriptomic analysis of *Streptomyces* sp. F on PET and PE.

Samples collected from the fermentation at 96 hours, 144 hours and 240 hours were also utilised for transcriptomic analysis, to look at genetic responses to growth on PET and PE. These time points were selected as they represent the different stages of growth on plastic; the growth on glucose (96 hours), the transition between the growth from glucose to plastic (144 hours) and the growth exclusively on plastic (240 hours).RNA later was added to the cell pellets and after one hour the pellets were frozen at -80, the

cells were then sent to GeneWiz for RNA extraction and analysis. The samples were done in triplicate.

The transcriptomic analysis was done using direct comparisons between glucose vs PET, glucose vs PE and PET vs PE. A further comparison was also done against growth phase, this was important given the different growth rates of the cells. The data was overlaid onto the genome of *Streptomyces fulvissimus* for two reasons, firstly, *Streptomyces* sp. F was identified as being closely related to this strain and secondly the absence of a genome for this strain. A volcano plot was utilised to identify the gene candidates which had a significant increase or decrease in expression i.e. log2 > 2 and a p-value < 0.05. Utilizing these genes, a network analysis was done using STRING.

3.7.1 Transcriptomic analysis of *Streptomyces* sp. F on PET

A direct comparison was made between the transcriptomic data collected from growth on glucose and PET, utilising the same growth phase.

In the 96-hour sample when glucose was still present in the media there was already a significant difference in the transcript level between the two cells (Figure 3-34), with more than 200 genes identified (Table 3-8). This clearly demonstrates that PET is already having an impact even while the cell is still co-utilising glucose. It also strongly suggests that the changes in expression are not due to starvation stress as the cells still have glucose. At 144 hours, there was a significant increase in the number of genes overexpressed on PET compared to glucose, 800 genes in total (Figure 3-34 and Table 3-8). This highlights that the cell is undergoing a significant shift in its regulatory network following glucose depletion (Figure 3-18). Over 500 genes were differentially regulated once the cells were growing on PET (Figure 3-34, Table 3-8).

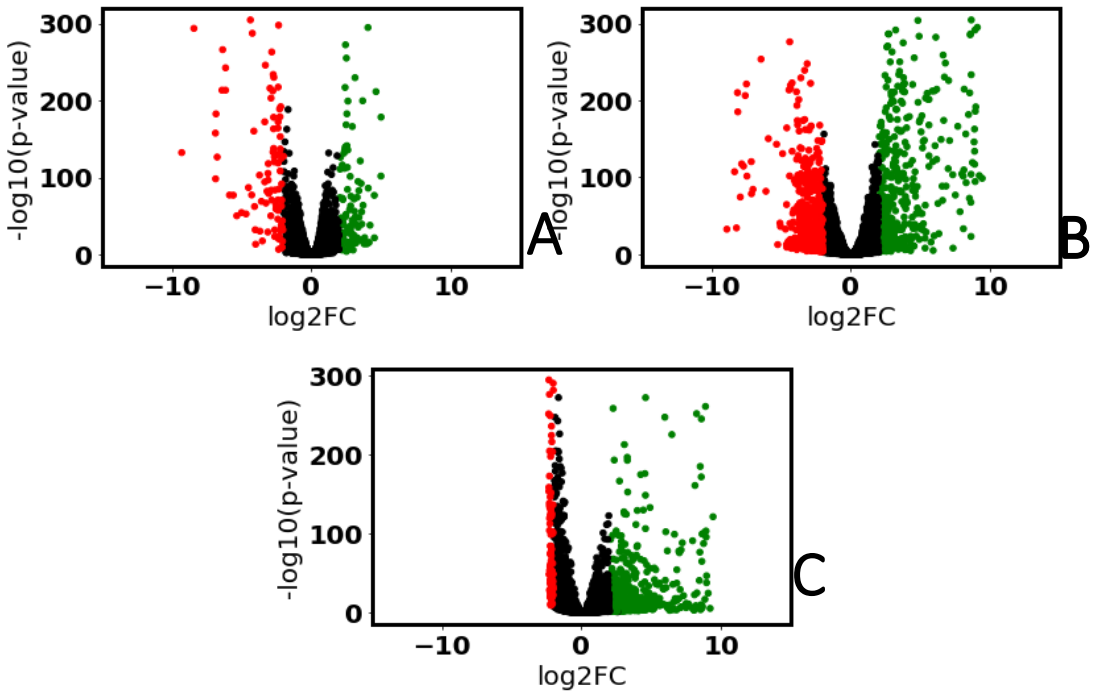


Figure 3-33 : Volcano plots showing statistically significant genes upregulated on PET (in green) and upregulated on glucose (in red) on glucose at 96 hours (A), at 144 hours (B) and at 240 hours (C)

	Number of gene overexpressed on glucose	**Number of gene overexpressed on PET**
1st sample: 96 hours	115	104
2nd sample: 144 hours	434	439
3rd sample: 240 hours	327	156

Table 3-7 : Table showing the number of genes significantly overexpressed on both PET and glucose throughout the fermentation

Utilizing the most significantly expressed genes a network analysis was done using STRING. From these networks, two enriched pathways were detected on PET. A gene cluster involved in sulphur metabolism was detected at 144 hours and 240 hours (Figure 3-35 A), with a false discovery rate of $1*10^{-10}$. This upregulation in sulphur metabolism could be due to key enzymes being expressed in the glyoxylate shunt and isocitrate lyase (*icl*). This enzyme

requires a thiol function for its activity (Rehman and McFadden, 1997). Given the cell can grow on EG which utilises the glyoxylate shunt, a higher demand for thiol containing compounds would arise in the cell. This in turn may lead to an increase in sulphur metabolism in the cell, resulting in an overexpression of the pathway.

Another cluster was also detected after 240 hours. This cluster contained genes involved in the 2-oxocarboxylic acid metabolism pathway (Figure 3-35 B). This pathway had a false discovery rate of $2.3*10^{-5}$. It includes multiple genes involved in the biosynthesis of several amino acids including arginine, valine, leucine and isoleucine. The enrichment of this pathway is detected only at the later stage of the fermentation, at 240 hours. This is evidence that *Streptomyces F* still has an active metabolism even after the glucose has been depleted, at 144 hours (Figure 3-18).

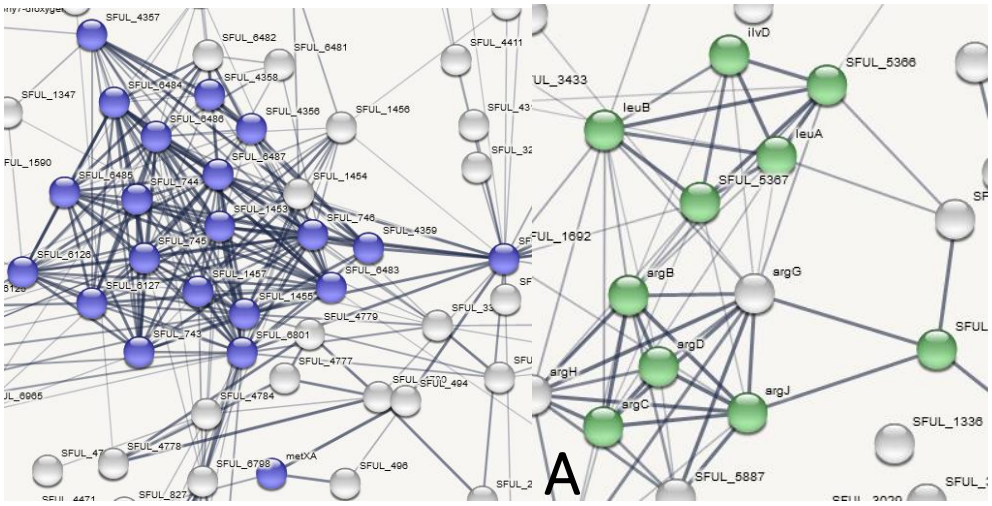


Figure 3-34 : Cluster network to show of genes overexpressed on PET, cluster of gene involved in the "sulphur metabolism" (A), false discovery rate = $1*10^{-10}$, cluster of gene involved in the biosynthesis of arginine and leucine (B), false discovery rate = $2*10^{-5}$.

A large number of genes are also overexpressed on glucose only, three main gene clusters were identified using STRING. The first cluster, detected at 144 hours, contained genes involved in tetracycline biosynthesis, with a false discovery rate of 0.04 (Figure 3-36 A). The production of antibiotics has been reported in *Streptomyces sp.* and is most commonly related to the onset of secondary metabolism, typically induced by a carbon starvation (SEJINY,

1991; Chater, 2016). The overexpression of this cluster may be triggered by the consumption of glucose, triggering secondary metabolism. The second cluster contained genes which were related to the ABC transport system (Figure 3-36 B). This cluster is detected at 240 hours only, with a false discovery rate of $3*10^{-7}$. The third cluster contained genes with a protease activity (Figure 3-36 C). The overexpression of both of the last two clusters might be a response to carbon starvation: the second cluster to get all the carbonated compounds in the medium and the third to try to recycle the protein present in the medium.

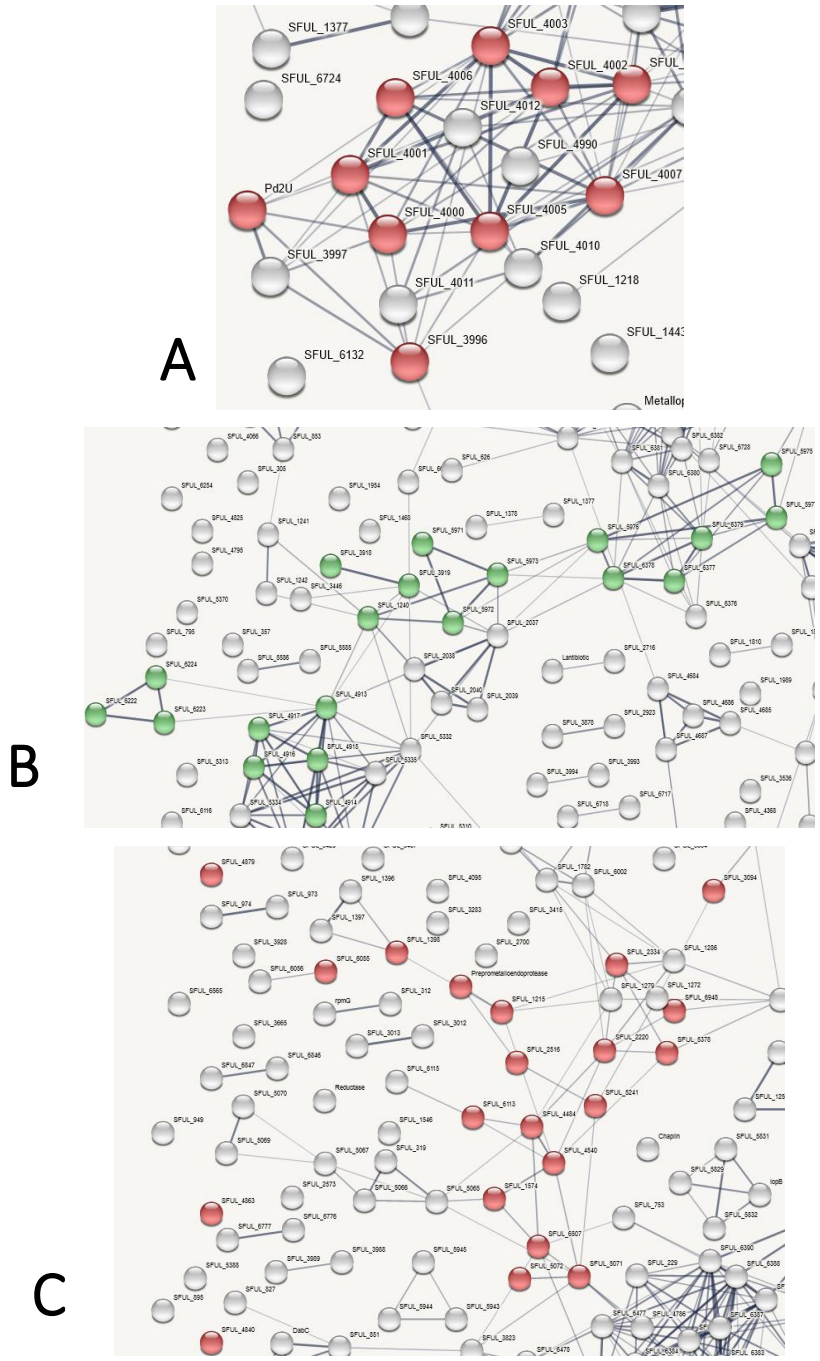


Figure 3-35 : Cluster network to show genes significantly overexpressed on glucose, cluster of gene involved in the tetracycline biosynthesis (A), false discovery rate = 0.04, cluster of gene part of the "ABC transport" system (B), false discovery rate = $3*10^{-7}$, cluster of gene presenting a protease activity (C), false discovery rate = $1*10^{-5}$.

3.7.2 Transcriptomic comparison of growth on PE vs Glucose

The transcriptomic data was compared between glucose and PE, using the same time point, to ensure the same growth phase can be assessed, which

enabled the detection of genes which are upregulated or downregulated on PE throughout the fermentation.

The direct comparison between the transcriptomic data on glucose and PE condition allowed the detection of a few genes being overexpressed on both conditions (Figure 3-37 and Table 3-9). Surprisingly, this number was far lower than the ones observed in the previous comparison between PET and glucose (Table 3-8 and 3-9): 50 genes in total. This would indicate that the transcriptional network does not change significantly between growth on PE and glucose Network analyses performed on the overexpressed genes, did not show any significantly enriched pathways.

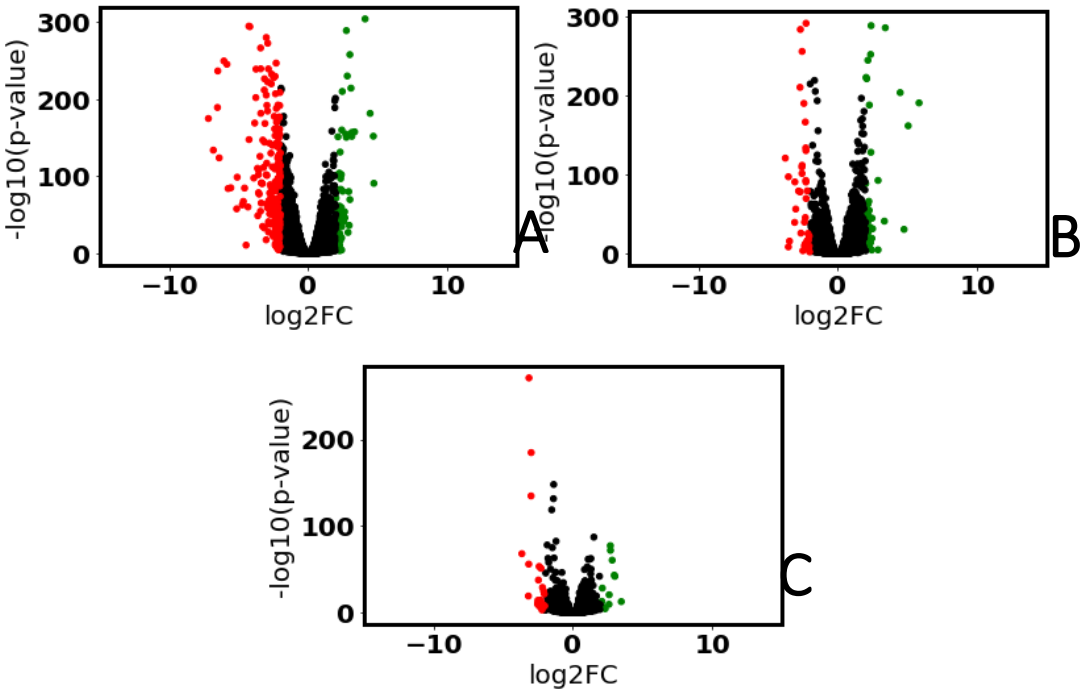


Figure 3-36. Volcano plot to show genes which were upregulated on PE (in green) and upregulated on glucose (in red) at 96 hours (A), at 144 hours (B) and at 240 hours (C)

	Number of gene overexpressed on glucose	Number of gene overexpressed on PE
1st sample: 96 hours	229	55
2nd sample: 144 hours	41	47
3rd sample: 240 hours	30	12

Table 3-8: Table to show the number of gene significatively overexpressed on both PE and glucose throughout the fermentation

The similar transcriptional behaviour of *Streptomyces* sp. F on PE is surprising given that the growth was very different (Figure 10 and 15), and there where clear differences in the metabolite levels (Figure 24 and 26).

3.7.3 Transcriptomic comparison between growth on PET vs PE

A final comparison was made between PET and PE at the same growth phases to identify differentially regulated genes between the two plastics.

The comparison of the transcriptomic data between PET and PE identified a small number of genes which were overexpressed in both conditions (Figure 3-38, Table 3-10). At 96 hours, there were very few genes which were statistically significant with 50 genes being overexpressed (Table 3-10).

At 144 hours, there was a significant difference between the transcriptional profile with over 700 genes having differential expression levels (Table 3-10). This was similar to what was observed in the comparison between PET and glucose (Table 3-8).

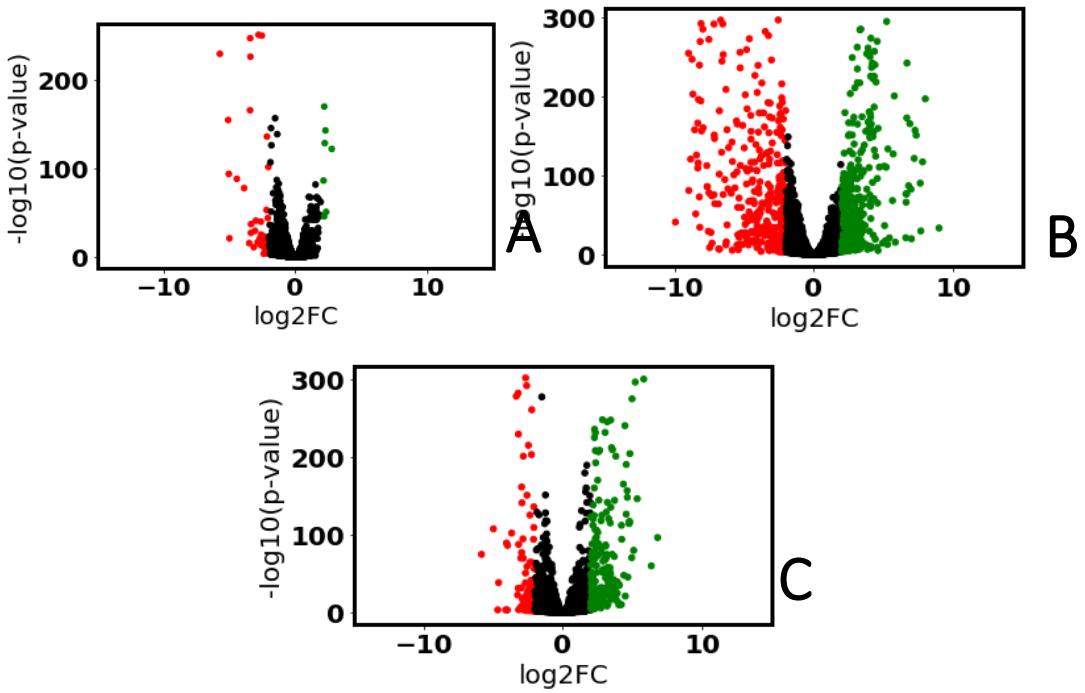


Figure 3-37 : Volcano plots showing statistically significant genes expression for growth on PE (in green) and PET (in red) at 96 hours (A), at 144 hours (B) and at 240 hours (C)

	Number of gene overexpressed on PE	**Number of gene overexpressed on PET**
1st sample: 96 hours	7	43
2nd sample: 144 hours	359	377
3rd sample: 240 hours	209	116

Table 3-9 :Table to show the number of genes significatively overexpressed on both PE and PET.

Network analysis was performed, using STRING. The genes overexpressed on PET vs PE were similar to those already identified as being overexpressed on glucose. Two key enriched pathways were detected: the

first contained genes involved in the metabolism of sulphur (false discovery rate of $1*10^{-9}$) and the second contained genes involved in the biosynthesis of several amino acids (false discovery rate of $2*10^{-4}$) (Figure 3-39). Both clusters have already been detected in the comparison between the PET and glucose (Figure 33).

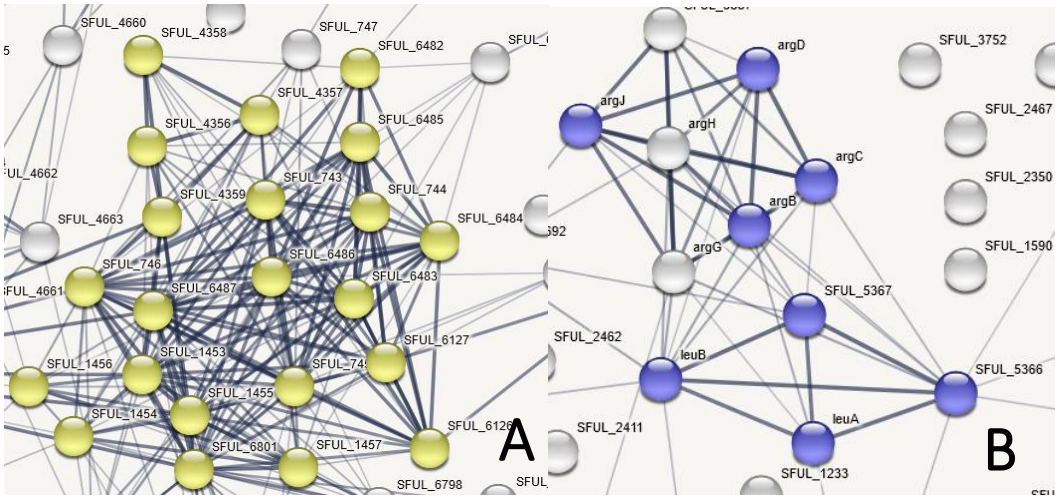


Figure 3-38 : : Cluster network of genes overexpressed on PET, cluster of genes involved in sulphur metabolism (A), false discovery rate $1*10^{-9}$, cluster of genes involved in the biosynthesis of arginine and leucine (B), false discovery rate $2*10^{-4}$.

The genes overexpressed on PE were also similar to the ones previously detected on glucose and PET. This is to be expected due to the similar transcriptional behaviour of *Streptomyces* sp. F on both glucose and PE (Table 3-9). From the list of overexpressed genes, a cluster of genes involved in the biosynthesis of tetracycline was detected, with a false discovery rate of $6*10^{-6}$ (Figure 3-40 B). However, a new cluster was identified with a false discovery rate of $3*10^{-7}$. This cluster contained genes involved in the biosynthesis/degradation of fatty acids (Figure 3-40 A). The enrichment of this pathway is a proof of metabolic activity in the fatty acid pathway on PE and concurs with the hypothesised mechanism of the degradation of PE.

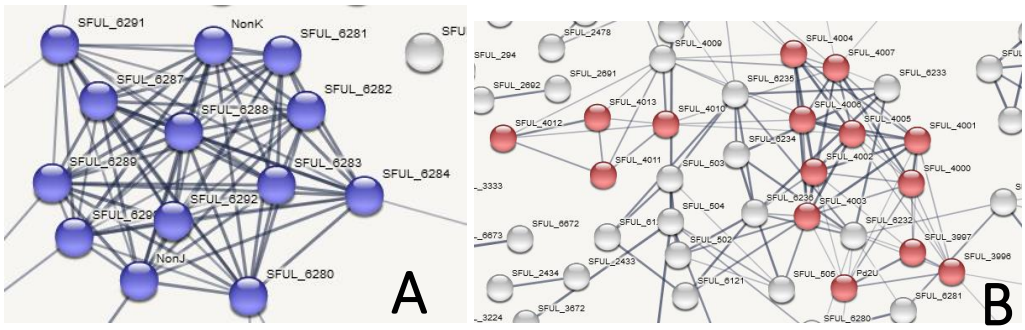


Figure 3-39 : Network cluster of genes overexpressed on PE, cluster of genes involved in fatty acid biosynthesis (A), false discovery rate = $3*10^{-7}$, cluster of genes involved in the biosynthesis tetracycline biosynthesis (B), false discovery rate = $6*10^{-6}$.

3.8 Discussion

This work is the first characterisation of PET and PE degradation using a multi-omics analysis approach. Using a wide range of techniques, the behaviour of *Streptomyces* sp. F has been characterized on both PE and PET. The use of both metabolomics and transcriptomics enabled a global approach in the characterisation of plastic degradation. To date, no description of an organism degrading plastic using multi-omics analysis has been published in the literature. This global approach in the characterisation has helped to inform hypothesis on the mechanisms which play a part in the degradation of both PE and PET.

3.8.1 Degradation of PET by *Streptomyces* sp. F

Streptomyces sp. F can utilise one of the PET monomers, EG (Figure 3-32). The growth of *Streptomyces* sp. on ethylene glycol has been previously described (Ghogare and Gupta, 2012). Growth on EG involves part of the glyoxylate shunt pathway and the biosynthetic degradation pathway for ethylene glycol (Figure 3-41). Interestingly, the growth rate of *Streptomyces* sp. F on ethylene glycol was very similar to the 2nd growth phase seen in the

fermentation on PET (Table 3-4, Table 3-7), confirming that this strain can utilise EG as a carbon source.

TPA was also detected during the fermentation on PET (Figure 3-23). Yet *Streptomyces* sp. F was unable to grow on TPA as a sole carbon source, presumably due the fact that it is missing the necessary metabolic pathway.

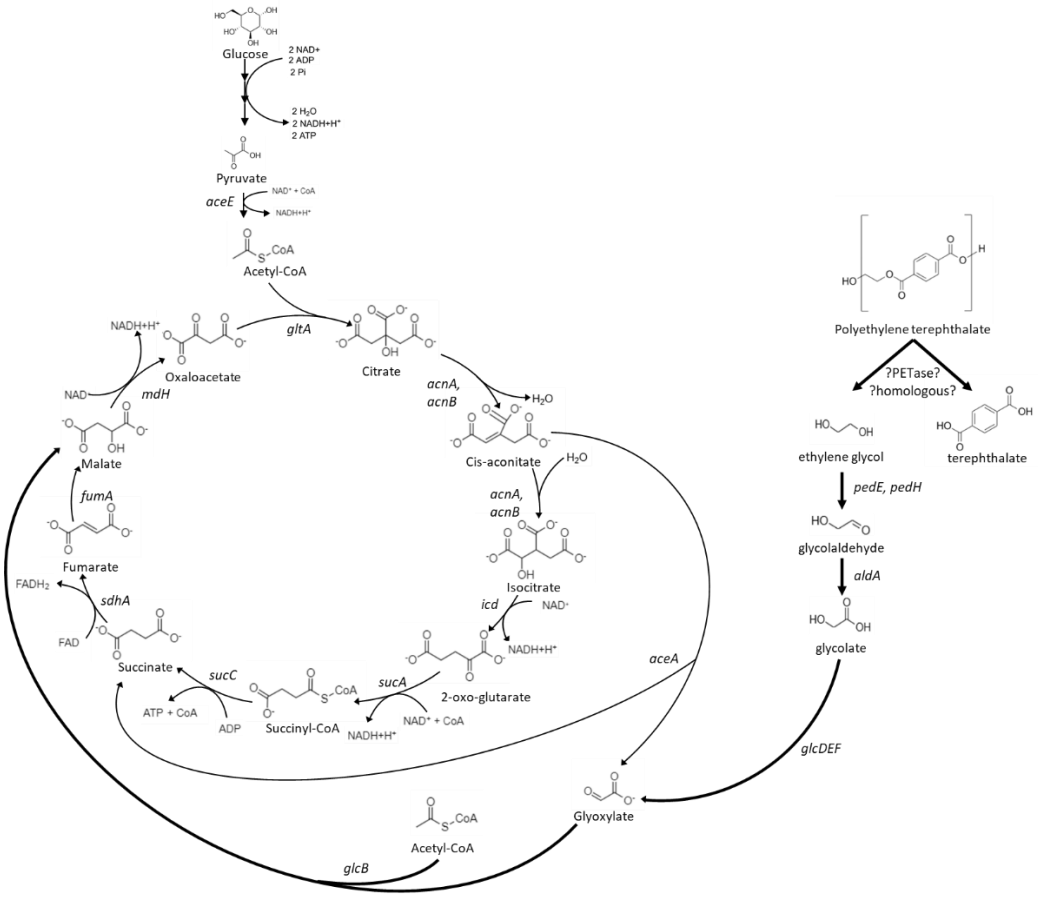


Figure 3-40 : Predicted metabolic pathway involved PET degradation in *Streptomyces* sp. F with the key reactions highlighted in bold.

Interestingly, the metabolomic analysis did not show any major changes in the metabolism of *Streptomyces* sp. F on glucose or PET (Figure 3-19 B and 3-21 B). This could be the result of the metabolic connection between central carbon metabolism and the ethylene glycol degradation pathway (Figure 3-

41). The small metabolomic changes are very different to the major changes observed in the transcriptomic data where more than 800 genes were differentially expressed (Table 3-8), especially the over-expression of multiple genes involved in sulphur metabolism.

3.8.2 Degradation of PE by Streptomyces sp. F

In contrast to PET degradation, PE degradation is not fully understood. One of the main difficulties is the variety of PE utilised in studies to date (Restrepo-Flórez, Bassi and Thompson, 2014; Ghatge *et al.*, 2020). However, despite the variety in the substrate, a general understanding of the mechanism of the degradation of PE has been hypothesised (Ghatge *et al.*, 2020). The first step of PE degradation is thought to involve the oxidation of the carbon chain of PE, either by addition of a hydroxy or a ketone group. Following the first oxidation, a series of oxidation steps leads to the production of by-product molecules with either carboxylic, ketone or alkene chemical groups (Bonhomme *et al.*, 2003; Restrepo-Flórez, Bassi and Thompson, 2014).

The fermentation of *Streptomyces* sp. F on PE led to an interesting growth dynamic, specifically the absence of an exponential growth phase in the first 200 hours (Figure 3-17), despite normal glucose consumption (Figure 3-18). Moreover, the metabolomics analysis detected a very specific group of metabolites linked to the presence of PE. The first is the detection of a variety of carboxylic compounds in the supernatant: heptanoic acid, nonanoic acid, decanoic acid and undecanoic acid (Figure 24 and 28). The second is the detection of TCA-related compounds in the supernatant: pyruvate, malate, fumarate, and citric acid (Figure 24 and 28). The third is the detection of carnitine-related compounds: carnitine, O-acetylcarnitine and O-butanoylcarnitine (Figure 24 and 28). The fourth is the detection of compounds involved in the biosynthesis of NADH: picolinic acid and quinolinic acid (Figure 24 and 28). The last two compounds have been confirmed using commercial standards and a targeted LC-MS approach. The

hypothesised metabolic pathway is shown below for *Streptomyces* sp. F on PE (Figure 3-42)

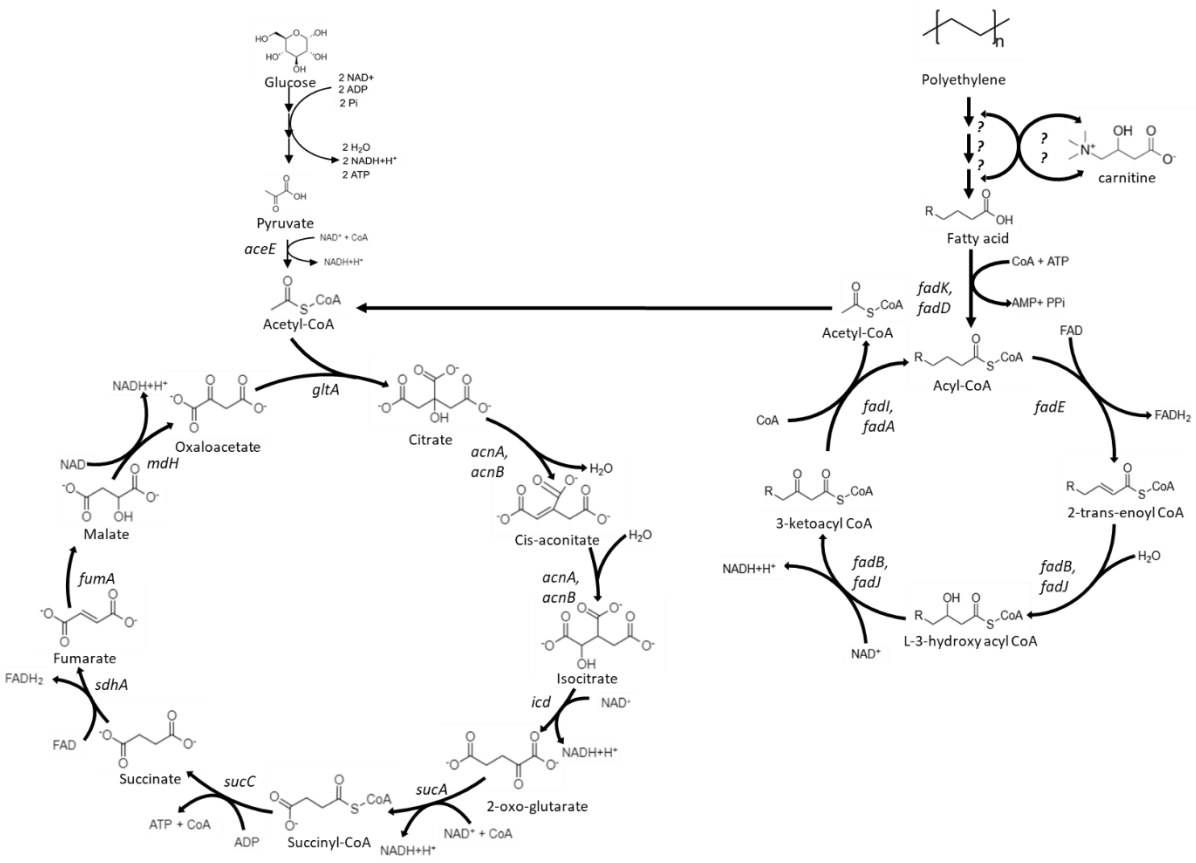


Figure 3-41 : Predicted pathway involved in the metabolism of the by-products of PE degradation

The lack of growth in the first 200 hours of fermentation on PE (Figure 3-17) could be explained by metabolic strain. This metabolic strain could be supported by the exportation of TCA-related compounds found in the supernatant (Figure 3-26 and 3-30). This would indicate an important flux towards the TCA cycle, which could be the result of different metabolic pathways bringing carbon to the TCA cycle at the same time. This might be due to the simultaneous activity of both glycolysis, degrading glucose, and the β oxidation pathway, degrading fatty acid compounds (Figure 3-42). Both these pathways led to the production of acetyl-CoA, which is involved in the TCA cycle. The simultaneous activity of these two pathways might result in metabolically stressing the cell, which would have a negative impact on the

growth rate of *Streptomyces* sp. F. Moreover, once the glucose had been depleted, at 168 hours (Figure 3-18), the metabolic strain was alleviated, and growth occurred (Figure 3-17). Following glucose depletion, the TCA-related compounds were very quickly consumed, with a complete depletion at 240 hours (Figure 3-26 and 3-30).

In addition of the detection of TCA-related compounds, several other types of molecules involved in the metabolism of aliphatic compounds were detected: carboxylic compounds, carnitine-related compounds, and NADH-related compounds (Figure 3-26 and 3-30). These molecules steadily increased throughout the fermentation (Figure 3-26 and 3-30). It has been hypothesised that PE degradation results in the production of carboxylic acid compounds (Restrepo-Flórez, Bassi and Thompson, 2014; Ghatge *et al.*, 2020). Moreover, carnitine has been described as a molecule facilitating the transport of fatty acid molecules (Wargo and Meadows, 2015; Longo, Frigeni and Pasquali, 2016). Finally, the metabolization of fatty acids is done through the β-oxidation pathway, which requires a large pool of reducing power (Figure 3-42). This may be a clear indication that PE is degraded into fatty acid compounds which are metabolised by *Streptomyces* sp. F through the β-oxidation pathway, by the carnitine fatty acid transport system (Figure 3-42).

4 Chapter 4 Genomic Sequencing and Bioinformatic Analysis to Identify key Enzymes and Metabolic Pathways for the Degradation of PET and PE in *Streptomyces* sp. F

4.1 Introduction

Chapter 3 confirmed that *Streptomyces* sp. F can grow on PE and PET using both as sole carbon sources. Furthermore metabolomics and transcriptomic confirmed that the growth on PET and PE resulted in significant changes to the cellular physiology. However, the transcriptomic analysis relied on a direct comparison to *Streptomyces fulvissimus,* which may mean some regions of the genome are excluded from the analysis. To help elucidate the enzymes and pathways involved in the degradation process, the genome of *Streptomyces* sp. F was sequenced, enabling bioinformatics analysis and comparative analysis to de done between known plastic degrading bacteria and *Streptomyces* sp. F.

Since the release of the first fully sequenced bacterial genome in 1995 (Teng *et al.*, 2017), the post genomic ere has undergone a radical transformation (Land *et al.*, 2015). During the 1990s and early 2000s, microbial genome sequencing relied heavily on random shotgun approaches to sequence genomes. These approaches were both laborious and labour intensive, given the need to clone individual gene fragments, sequence and assemble. In the last decade whole genome sequencing has progressed to utilising a number of high throughput short read technologies, which began with the introduction of the 454-pyrosequencing platform (Margulies *et al.*, 2005). The market is now dominated by the Illumina platform, offering high quality genome sequences, with high fidelity reads at lower costs (Goodwin, McPherson and McCombie, 2016). The Illumina platform utilises synthesising technologies where fluorescently labelled nucleotides are incorporated into DNA strands. The method provides accurate base by base sequencing, which significantly reduces errors and enables up to 750 Gb data to be processed by sequencing run (Teng *et al.*, 2017). Despite these advantages, Illumina is

limited by a number of factors, including the short read lengths of the sequences, which range from 25-300 bases. This can lead to incomplete assembly, furthermore, repetitive elements and genome duplications also impact (Miller, Koren and Sutton, 2011). There is also the potential for GC bias, making it difficult to sequence large GC rich genomes using Illumina.

Pacific Biosciences introduced the first PacBio sequencing platform to the market in 2011, which utilised single molecule real-time (SMRT) technology capable of real time sequencing of individual polymerase molecules (Eid *et al.*, 2009). The SMRT technology is based on zero-mode waveguides (ZMWs), these optical nanostructures are embedded in a thin film which is capable of confining an excitation volume. This enables single molecule fluorescence experiments to be conducted at physiologically relevant concentrations of the biomolecule (Plénat, Yoshizawa and Fourmy, 2017). In this case the DNA polymerase is bond to the nanophotonic confinement structures, and the DNA is synthesised from the template within an array of ZMWs, using fluorescently labelled nucleotides. Each of the four nucleotides is labelled with a different dye, so they have a specific emission spectrum. As a nucleotide is interacting with the polymerase (Figure 4-1-1), a light pulse is produces to identify the base (Figure 4-1-2). After the incorporation of the base, the dye is released, ending the fluorescence pulse (Figure 4-1-3). The polymerase then moves to the next position (Figure 4-1-4), interacting with the next nucleotide to be incorporated, restarting the fluorescence pulse (Figure 4-1 5). The simultaneous detection of individual fluorophores can then be visualised in real-time from each ZWF as the DNA is synthesised.

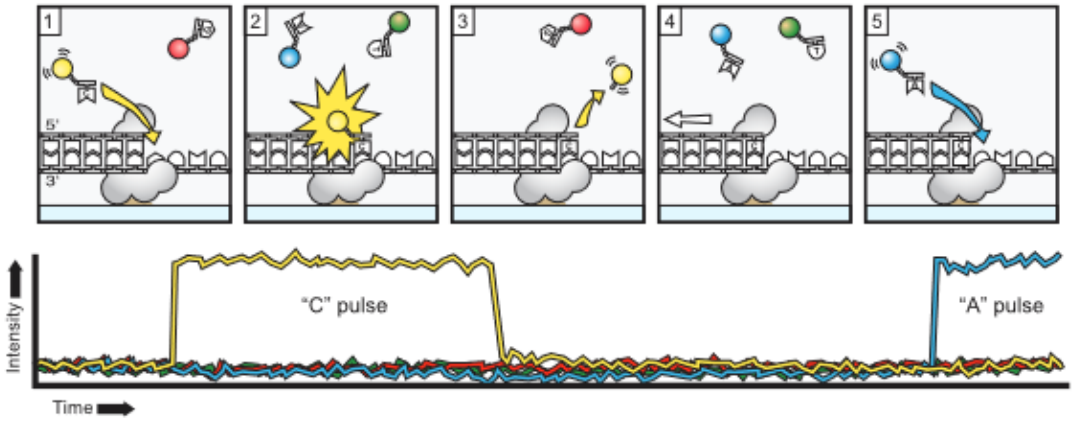


Figure 4-1: Steps of the PacBio sequencing reaction, (1) interaction of a fluorescently labeled nucleotide with the active site of the polymerase, (2) excitation of the fluorescent dye, allowing the identification of the base, (3) the dye linker is cleaved from the nucleotide and diffused out of the ZMW, ending the fluorescence signal, (4) the polymerase moves towards its next position, (5) a new base fluorescently labelled nucleotide interact with the active site, restarting the fluorescence pulse. The figure is taken from Rhoads & Au, 2015 and Rank et al., 2009.

The advantage being that the DNA does not need to be amplified, which circumvents some of the major problems with Illumina, allowing for longer read lengths, typically around 2,500 to 23,000 bases and less bias. However, PacBio is plagued by errors, with error rates of 10% being reported, these are typically indel events, caused by the short time intervals between nucleotide incorporation, which impacts on fluorophore detection. Software and chemistry improvements have helped to increase the accuracy of the reads and reduce the error rates (Rhoads and Au, 2015). Hybrid sequencing strategies are being adopted for complex bacterial genomes, combining the accuracy of short reads with the data on genomic structure from longer reads (De Maio *et al.*, 2019). This approach has been particularly useful for the sequencing and assembly of high GC genomes with a high incidence of repetitive sequences such as those found in *Streptomyces* sp. (Albuquerque *et al.*, 2021).

4.2 Genome Sequencing of *Streptomyces* sp. F

Streptomyces sp. F was identified as being closely related to *Streptomyces fulvissimus* from the 16s sequence in Chapter 3. *Streptomyces fulvissimus* was sequenced in 2013 and consists of a single linear chromosome of 7, 905,758 bp, with a GC content of 71.5%. The genome was found to be smaller than other model Streptomyces, for example, S*. coelicolor* A3 (2) has a genome of 8.7Mbp, *S. avermitilis* MA-4680, 9.0 mega base pair (Mbp) and S*. griseus* IFO13350 8.5 Mbp (Myronovskyi *et al.*, 2013). Analysis of the *S. fulvissimus* genome revealed 6952 predicted open reading frames, 73 tRNA genes and 6 rRNA gene clusters. Genomic DNA was extracted from *Streptomyces* sp. F using the Zymo Research *Quick*-DNA fungal/bacterial kit. DNA integrity was validated via agarose gel-electrophoresis, the DNA was shown to be of good quality with no RNA contamination. Sample purity was confirmed via spectrometry, the 260/230nm ratio being greater than 2 and the 260/280nm ratio 1.8-2.0. The DNA was subsequently sent to Novogene for sequencing via PacBio and assembly.

Streptomyces sp. F was shown to have a linear chromosome of 8.5 Mbp and a GC content of 71.2% (Figure 4-2). Due to IP surrounding *Streptomyces* sp. F, the whole genome sequence cannot be included in this thesis.

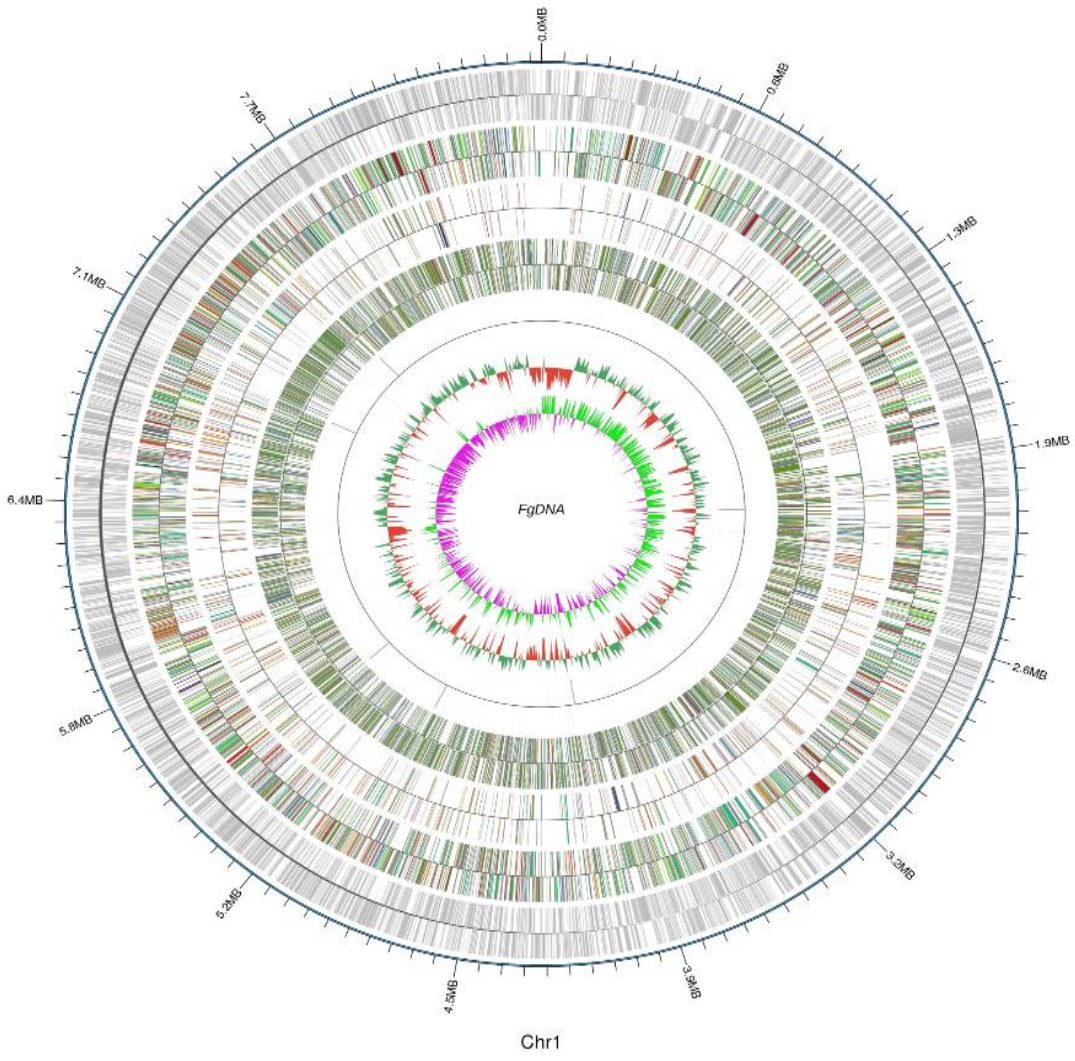


Figure 4-2 : Schematic representation of the genome of *Streptomyces* sp. F

A direct comparison between the genome of *Streptomyces* sp. F and other published genomes from others *Streptomyces* sp. demonstrates that they are very similar i.e. the genome of *Streptomyces* sp. F is in the range of what could be expected from a *Streptomyces* sp. (Table 4-1). The number of protein coding genes detected in the genome of *Streptomyces* sp. F was 7463, comparable to other published genomes (ranging from 6925 to 7825) (Table 4-1). Moreover, *Streptomyces* sp. F has 34 natural product biosynthetic gene clusters (BGCs), again similar to others *Streptomyces* sp. (ranging from 21 to 32) (Table 4-1).

Organism	*Streptomyces. F*	*Streptomyces coelicolor A3(2)*	*Streptomyces venezuelae ATCC10595*	*Streptomyces fulvissimus*
Assembled genome size				
Genome Size:	8,538,214	8,667,507	7,871,449	7,905,758
GC content	71.2 %	72.1%	72.5%	71.5 %
Chromosome topology	Linear	Linear	Linear	Linear
Number of genes				
Protein coding genes	7463	7825	7,700	6925
Natural product BGCs	34	21	27	32
Genetic elements				
Extrachromosomal elements	0	0	0	0
Prophages	5	N/A	N/A	N/A
Genomic islands	19	N/A	N/A	N/A
Reference	This work	Bentley et al., 2002	Lee et al., 2020	Myronovskyi et al., 2013

Table 4-1 :Comparison between the genome of *Streptomyces* sp. and *Streptomyces* sp. F.

4.2.1 Analysis of the secondary metabolite clusters in the genome of *Streptomyces* sp. F utilising ANTISMASH

An ANTISMASH analysis was performed on the genome of *Streptomyces* sp. F enabling the detection and identification of natural product biosynthetic pathways (Blin *et al.*, 2021). ANTISMASH analysis revealed that the genome of *Streptomyces* sp. F contained multiple natural product clusters. Several of these clusters have already been identified and characterised in the literature, these include examples from the lanthipeptide class, some non-ribosomal peptides, and some polyketide synthases (Table 4-2).

Among these metabolites, several antibiotics were also detected: lanthibiotics, a class of lanthionine-containing peptides, with several AmfS-related pathway (Repka *et al.*, 2017), polycyclic tetramate macrolactams (PTM), an antibiotic resulting of the polyketide synthase (PKS) pathways (Nivina *et al.*, 2019) and bacteriocin (Benítez-Chao *et al.*, 2021) (Table 4.2). Moreover, the biosynthetic pathways for ectoine, a chemical with industrial

application (Zhao *et al.*, 2019; Pérez *et al.*, 2021), was also detected (Table 4-2).

metabolic class	Number of clusters	Example of most similar pathway	Similarity of the most similar pathway
Ectoine	1	ectoine	100%
Lanthipeptide	3	AmfS	100%
Melanin	1	melanin	100%
Siderophore	2	desferrioxamin B	100%
Polyketide synthase biosynthesis pathway (PKs)	9	Polycyclic Tetramate Macrolactams (PTM)	100%
Terpene	6	Isorenieratene, geosmine	100%
Other	6	keywimysin	100%
Non-Ribosomal Peptides (NRPs)	6	streptobactin	94%
Bacteriocin	2		
TOTAL	34		

Table 4-2 : ANTISMASH analysis of the genome of *Streptomyces* sp. F.

4.3 Detection of the degradation pathways involved in the degradation of PE and PET

Based on the previous candidates identified for both PET and PE degradation, a BLAST search was performed on *Streptomyces* sp. F using the standard nucleotide program TBLASTN.TBLASTN aligns protein sequences to the nucleotide database (Gertz *et al.*, 2006; Opperdoes and Lemey, 2009). However, this method suffers from bias. The main one being that each nucleotide sequence contains more than one coding region in the same or different translation frames. One nucleotide sequence could translate into 6 different possible protein sequences, due to the 6 different translation frames. As a result, most of the hypothetical amino acid sequences which get translated to nucleotide sequences do not correspond to any protein at all (Gertz *et al.*, 2006). Accentuating this bias, TBLASTN does not consider the Open Reading Frame (ORF) of the nucleotide sequence. The accumulation of hypothetical translated protein sequence increases the chance of false positive hits (Gertz *et al.*, 2006).

Despite those biases, TBLASTN is widely used to associate proteins with genetic sequences with a minimal impact of the GC content (Opperdoes and Lemey, 2009). This method maximises the chances of finding a homologous candidate in the genome of *Streptomyces* sp. F*.* Although it must be stated that detection of a homologous gene in the genome, does not confer activity. A cut-off of 30 % of homology is widely reported as being significant enough to ensure a 90% chance of homology (Rost, 1999). Moreover, an E-value of 10^{-3} would ensure a false positive chance of 1/1000 (Gertz *et al.*, 2006). Those cut-off values were used to select homologous candidates. Sequences below this threshold did not share significant homology and were not likely to be directly related and/or sharing the same activity.

.

A small number of candidate genes were selected for each plastic based on the literature. For PET, the PETase enzyme and MHETase were selected for the degradation of PET. The MHETase and PETase enzymes originated from *Ideonella sakaiensis* (Yoshida *et al.*, 2016). Other PETase candidates were also utilised in the analysis, these included LCC from an unknown prokaryotic organism (Tournier *et al.*, 2020), and two hydrolases from *Thermobifida fusca* (Müller *et al.*, 2005). For PE, various laccases and peroxidases were selected as these candidates are among the enzymes thought to break down PE (Ghatge *et al.*, 2020).

To evaluate the monomeric degradation pathways from both PET and PE, pathways were selected from the literature as a guide. For PET, the monomeric breakdown products are TPA and EG. The TPA degradation pathway can be separated in two steps, the degradation of TPA into protocatechuic acid (PCA) and the subsequent metabolization of PCA in to the TCA cycle. For the first part the *tphA* and *tphB* genes from *Comamonas sp*, where selected as a guide A strain identified in the literature as E6, was selected for the degradation of TPA into PCA (Sasoh *et al.*, 2006). Genes involved in the further conversion of PCA into the TCA cycle were selected based on the two different conversion routes; the meta-cleavage of the aromatic ring, relying of the *ligV* and *ligM* genes (MASAI *et al.*, 2007), or the

ortho-cleavage of the aromatic ring, relying on *pcaG* and *pcaH* (Guevara *et al.*, 2019; Tan *et al.*, 2022). For PE, the expected degradation products are hypothesized to be long carbon chains, the expected metabolization pathway is therefore the fatty acid degradation pathway (Ghatge *et al.*, 2020; Zampolli *et al.*, 2021), relying on a series of genes to degrade the long carbon chain into acetyl-coA (Bombelli and Howe, 2017).

4.3.1 Characterisation of the degradation pathways of aromatic compounds

Streptomyces sp. are known to be able to degrade a variety of aromatic compounds. These include vanillin-related compounds, such as cinnamic acids (Khalil *et al.*, 2019), benzoate-related compounds (Hae-Reun, Hyun-Joo and Eung-Soo, 2000) and catechol (Menendez-Bravo *et al.*, 2017). Moreover, Streptomyces sp. are also capable of degrading lignin (Fuchs, Boll and Heider, 2011; Kumar and Chandra, 2020; Riyadi *et al.*, 2020; Tan *et al.*, 2022). It is interesting to note that all these degradation pathways are funnelled into one key metabolite: PCA. If an organism does not have the pathways to utilise PCA, it would be therefore impossible for it to grow on a large variety of aromatic compounds. (Fuchs, Boll and Heider, 2011)

The degradation of vanillin has previously been described in *Streptomyces* sp. (Nishimura, Kawakami and Otsuka, 2018). The most common pathway for vanillin degradation utilises the vanillin dehydrogenase *vdh or ligV* and the vanilate-O-demethylase, *vanA, vanB and ligM* (Figure 4-3). The degradation of phthalate has been described in multiple organisms (Vamsee-Krishna and Phale, 2008; Zhang *et al.*, 2013; Boll *et al.*, 2020). However, to date no *Streptomyces* sp. have been reported that have this ability. The most common phthalate degradation pathways consist of a phthalate 4,5-dioxygenase (*phtA)*, a phthalate 4,5-cis-dihydrodiol dehydrogenase (*phtB*) and a 4,5-dihydroxuphthalate decarboxylase (*phtC*) (Figure 4-3). The degradation of terephthalate has been reported in several organisms, including *Bacillus* sp (Karegoudar and Pujar, 1985), *Pseudomonas* sp.,

Chryseobacterium sp., *Burkholderia* sp. (Aksu *et al.*, 2021) and *Arthrobacter* sp. (Zhang *et al.*, 2013; Aksu *et al.*, 2021). However, this pathway has not been identified in any *Streptomyces* sp. The degradation pathway for TPA comprises several genes: a terephthalate transporter (*tphC*), a terephthalate 1,2-dioxygenase oxygenase (*tphA*) and a 1,2-dihydroxy-3,5-cyclohexadiene-1,4-dicarboxylate dehydrogenase (*tphB*) (Figure 4-3). Sasoh et al, have shown that the expression of *tphA* and *tphB* seems to be the only necessary enzyme for the conversion of TPA into PCA (Sasoh *et al.*, 2006)

Protocatechuate is then linked to central metabolism by two different pathways: 3.4-dioxygenation of protocatechuate (*pcaG, pcaH)* and the 4,5-dioxygenation of protocatechuate (*ligA, ligB*) (Figure 4-3).

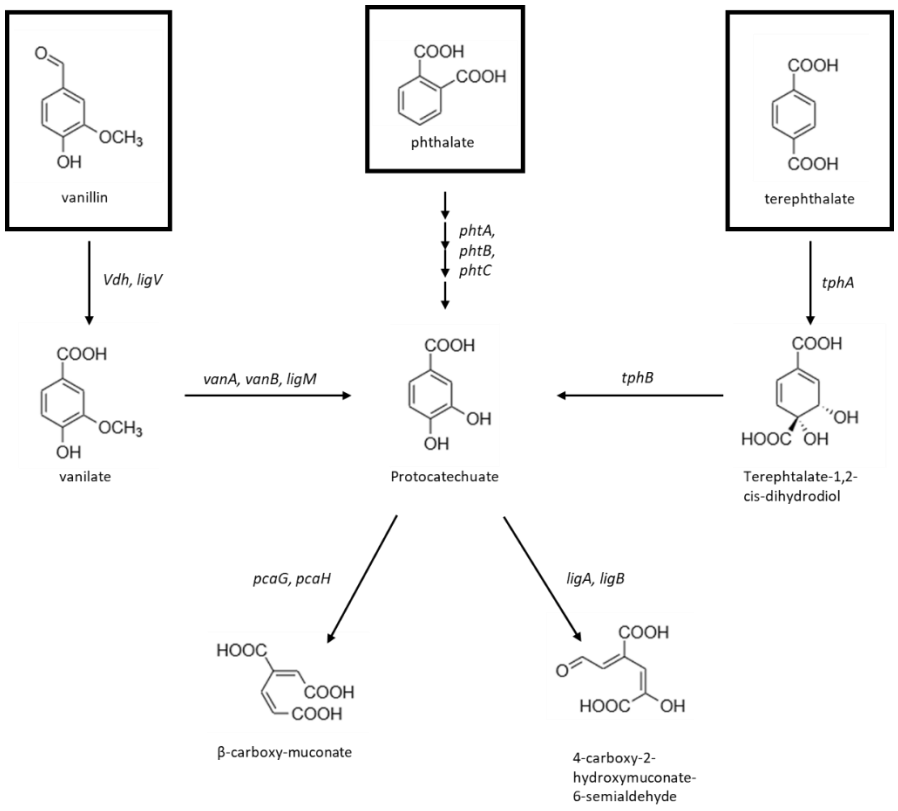


Figure 4-3: Schematic to show the degradation of vanillin, phthalate and terephthalate (Kanehisa & Goto, 2000, from Kegg consulted on 18/08/2022)

Using TBLASTN, several homologous genes were detected in the genome of *Streptomyces* sp. F. Genes involved in the degradation of both vanillin and phthalate were detected, with E value of $>10^{-3}$ for *vanA, vanB, ligV* and *ligM*. The E-value is a metric for the significance of an alignment in a homology

The identity cover for *vdh*, *vanA* and *vanB* was very low (>30%) and below the thresholds published in the literature, which consider a good viable cut-off should fall between values of greater than 90%. ANI values which fall below this level are often seen as false negative matches and experimental validation would be needed to confirm that the above genes can function in this role.

No genes were detected for TPA degradation (Table 4-3). In addition, a potential degradation pathway for PCA was detected with a single homologous gene identified in the genome which shared some homology with both *pcaG* and *pcaH*, with an E-value< 10^{-5} and identity cover >30 %. Again, both the E-value and the percentage homology were very low below the usual threshold of >90%. The formation of an active enzyme responsible for the 3,4-dioxygenation of protocatechuate requires both the alpha (*pcaG*) and beta (*pcaH)* subunits. However, the gene detected here is a single homologous gene (ORF 4416), therefore it may not be able to perform the reaction. This is further supported by growth experiments conducted on aromatic compounds including PCA done by Dr Spence: demonstrating that *Streptomyces* sp. F cannot grow on PCA.

Moreover, the transcriptomic analysis showed that only 3 gene candidates were overexpressed on both PE and PET. On PE, ORF 2902, a homologue of *phtC*, ORF 5945, a homologue of *vanB*, and ORF 4416, a homologue of *pcaG* and *pcaH*, were overexpressed. On PET, ORF 4181, a homologue of *vdh,* ORF 2902, a homologue of *phtC*, and ORF 5945, a homologue of *vanB*, were overexpressed.

Gene	organism	ORF in F	E value	Identity cover (%)	Expression gene PE Vs Glucose	Expression gene PET Vs Glucose
vdh	*Streptomyces coelicolor*	3708	0	87	1.91	0.87
		4181	$5e^{-05}$	32	1.84	4.30
		2735	$2e^{-04}$	25	-0.87	-0.81
ligV	*Sphingobium sp. (strain NBRC 103272 / SYK-6)*	6762	$9e^{-97}$	37	-0.32	-1.32

		4428	$9e^{-92}$	36	0.26	-1.01
		284	$1e^{-72}$	32	0.30	-2.92
ligM	*Sphingobium sp. (strain NBRC 103272 / SYK-6)*	2126	$4e^{-16}$	24	0.52	0.32
vanA	*Pseudomonas sp. (strain HR199 / DSM 7063)*	7330	$4e^{-16}$	29	-0.98	-2.17
		342	$1e^{-06}$	36	-0.61	0.18
phtA1	*Terrabacter sp. (strain DBF63)*	7330	$3e^{-04}$	37	-0.98	-2.17
phtA2	*Terrabacter sp. (strain DBF63)*	5302	$8e^{-03}$	31	0.52	0.07
phtB	*Terrabacter sp. (strain DBF63)*	6875	$2e^{-18}$	31	-0.41	0.10
		3559	$9e^{-18}$	32	-5.09	-3.96
		4750	$1e^{-17}$	35	-0.27	0.19
phtC	*Terrabacter sp. (strain DBF63)*	6321	$9e^{-07}$	33	0.20	0.44
		2902	$5e^{-05}$	28	3.35	2.08
vanB	*Pseudomonas sp. (strain HR199 / DSM 7063)*	5945	$6e^{-60}$	40	3.11	2.09
		7724	$1e^{-11}$	27	-2.58	-2.68
pcaG	*Pseudomonas putida*	4416	$2e^{-06}$	31	6.18	1.78
pcaH	*Pseudomonas putida*	4416	$3e^{-08}$	31	6.18	1.78
tphA	*Comamonas sp. Strain E6*	NA			NA	NA
tphB	*Comamonas sp. Strain E6*	NA			NA	NA
ligA	*Sphingobium sp. (strain NBRC 103272 / SYK-6)*	NA			NA	NA
ligB	*Sphingobium sp. (strain NBRC 103272 / SYK-6)*	NA			NA	NA

Table 4-3 :List of homologous genes involved in aromatic degradation pathways which were detected in the genome of *Streptomyces* sp. F. The expression level of each gene is presented by the Log2 of the ratio of gene expression. A log2>2 means that the gene is significatively over-expressed on the plastic (PET/PE). A log2<-2 means that the gene is significantly overexpressed on glucose.

Genomic analysis of the genome of *Streptomyces* sp. F identified some homologous genes involved in aromatic degradation. However, none of the genes identified in the genomic analysis were upregulated on plastic, specifically PET. Therefore, during the degradation of PET, *Streptomyces* sp. F must grow solely on ethylene glycol, as no candidates for TPA degradation could be detected. This supports the growth data presented in Chapter 3,

where *Streptomyces* sp. F was unable to grow on TPA but could sustain growth on EG.

4.3.2 Characterisation of the degradation pathway for ethylene glycol (EG)

The metabolization of EG has already been described in a variety of organisms, including *Sphingomonas macrogoltabidus, Alcaligenes xylosoxidans* (Kawai, 1995), as well as in consortium of bacteria from rhizosphere (Carnegie and Ramsay, 2009). However, the best characterised strains remains *Pseudomonas putida* (Mückschel *et al.*, 2012; Franden *et al.*, 2018; Li *et al.*, 2019). *Streptomyces* sp. have also been shown to utilise ethylene glycol as a carbon source however the pathway used for the metabolization of EG has not been fully characterized in *Streptomyces* sp. (Ghogare and Gupta, 2012).

The degradation pathway for EG relies on a series of oxidation reactions which produce glyoxylate (Figure 4-4). Several enzymes are responsible for these oxidation reactions: *pedH,* a dehydrogenase, *aldA,* a glycolaldehyde dehydrogenase, and *glcDEF,* which make up the three subunits of the glycolate oxidase (Figure 4-4). The glyoxylate is then converted to malate via the malate synthase *aceB*. The activity of the four enzymes is enough to ensure growth from ethylene glycol (Pandit, Harrison and Mahadevan, 2021)

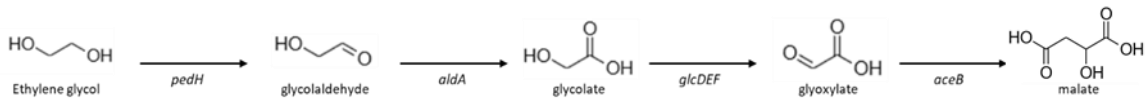


Figure 4-4: Degradation pathway of ethylene glycol (Kanehisa & Goto, 2000, from Kegg consulted on 18/08/2022)

Using the same methodology detailed above and four candidate genes from the EG pathway, *pedH*, *aldA*, *glcDEF* and *aceB*, as a reference, a full EG pathway was detected in *Streptomyces* sp. F. Both the e-value and the percentage identity remained low (Table 4-4): *pedH* (E-value= $2e^{-04}$, identity cover= 35 %), *aldA,* (E-value= $5e^{-93}$, identity cover= 39%), *glcD,* (E-value= $5e^{-93}$, identity cover= 35 %), *glcE,* (E-value= $2e^{-09}$, identity cover= 33 %), *glcF* (E-value= $6e^{-10}$, identity cover= 34%) and *aceB* (E-value< $1e^{-250}$, identity cover= 48 %). However, despite being detected, this pathway is not over-expressed on PET. Only one homolog of *glcE* is over-expressed on PE. This could simply be due to the fact that the transcriptomic data is overlaid on *S. fulvissimus* and not *Streptomyces* sp. F, or that another pathway is used to metabolise EG.

Moreover, the different genes homolog found in *Streptomyces* sp. F were not clustered together, therefore are not part of one operon. Thus, supporting the hypothesis that another EG degradation pathway might be used.

Streptomyces sp. F has previously been shown to grow utilising EG as the sole carbon source, Chapter 3 section 3.6.1. Bioinformatics analysis has demonstrated that the EG pathway shares some similarities to pathways already identified in the literature. However, the ethylene glycol genes were not overexpressed on PET compared to glucose. This may suggest that an alternative ethylene glycol pathway is being used in *Streptomyces* sp. F.

Gene	organism	ORF in F	E value	Identity cover (%)	Expression gene PE Vs Glucose	Expression gene PET Vs Glucose
pedH	*Pseudomonas putida*	3190	$2e^{-04}$	35	0.21	-0.26
aldA	*Pseudomonas putida*	2771	$5e^{-93}$	38	0.18	0.03
		1928	$2e^{-88}$	37	-0.47	-0.56
		1936	$2e^{-86}$	35	1.23	1.33

glcD	*Escherichia coli (strain K12)*	5046	$1e^{-93}$	39	1.23	1.33
		3309	$9e^{-42}$	31	1.16	1.43
		6997	$5e^{-25}$	26	-0.22	0.23
glcF	*Escherichia coli (strain K12)*	3309	$6e^{-10}$	34	1.16	1.43
		818	$3e^{-09}$	32	0.48	-1.65
		6997	$4e^{-08}$	32	-0.22	0.23
glcE	*Escherichia coli (strain K12)*	5046	$2e^{-09}$	33	0.64	0.28
		7621	$2e^{-04}$	29	2.27	1.92
aceA	*Pseudomonas putida*	1335	0	48	0.35	-0.04
		7379	$1e^{-157}$	44	1.64	1.76

Table 4-4: Homologous genes involved in degradation of ethylene glycol identified in the genome of *Streptomyces* sp. F. The expression level of each gene is presented by the Log2 of the ratio of gene expression. A log2>2 means that the gene is significantly over-expressed on the PET or PE. A log2<-2 means that the gene is significantly overexpressed on glucose.

PedH, is a pyrroloquinoline quinone (PQQ)-dependent alcohol dehydrogenase, which plays a crucial role in the degradation of EG (Mückschel *et al.*, 2012), being the first enzyme in the pathway. Phylogenetic analysis (Figure 4-5) was utilised to determine the evolution of the *pedH* gene, homologous sequences were aligned using ClustalW and a tree was constructed using the one click tool from phylogeny.fr. The *pedH* gene from *Streptomyces* sp. F shares a common ancestory with *P. putida* but is more closely aligned with genes from other *Streptomyces* sp. which despite being classified as PQQ dependent enzymes, have no dehydrogenase activity (Figure 4-5).

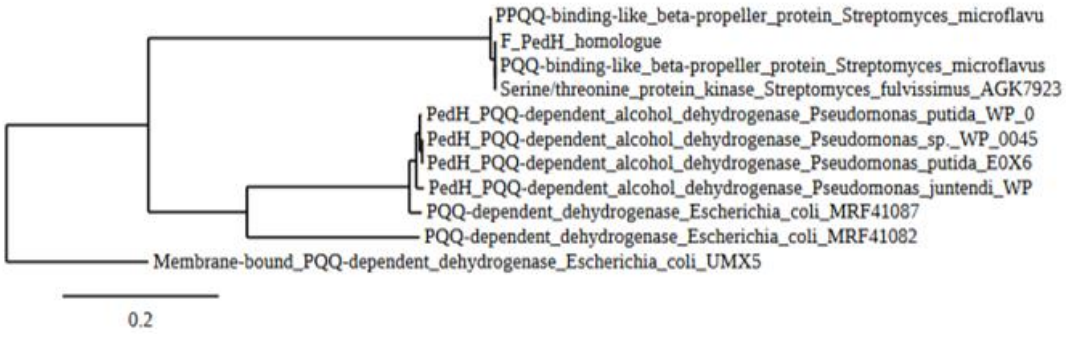


Figure 4-5 :Phylogenetic tree of the *pedH* gene

4.3.3 Bioinformatic analysis of potential PE degradation pathways

The degradation of PE is thought to produce a variety of different molecules, all based on hydrocarbon oligomers, with various degrees of oxidation (Ghatge *et al.*, 2020). The main pathway thought to be involved in the metabolization of the monomers of PE degradation is the β-oxidation pathway, which is the pathway for the degradation of fatty acids (Figure 4-6).

Fatty acid degradation relies on a cycle of successive oxidation reactions which release reductive power, in the form of NADH and $FADH_2$, and acetyl-CoA (Figure 4-6). This cycle relies on four enzymes which are responsible for fatty acid degradation: *fadE*, acyl-CoA dehydrogenase, *fadB*, fatty acid oxidation complex subunit beta, *fadA*, ketoacyl-CoA thiolase and *fadK*, a fatty acid CoA ligase (Figure 4-6).

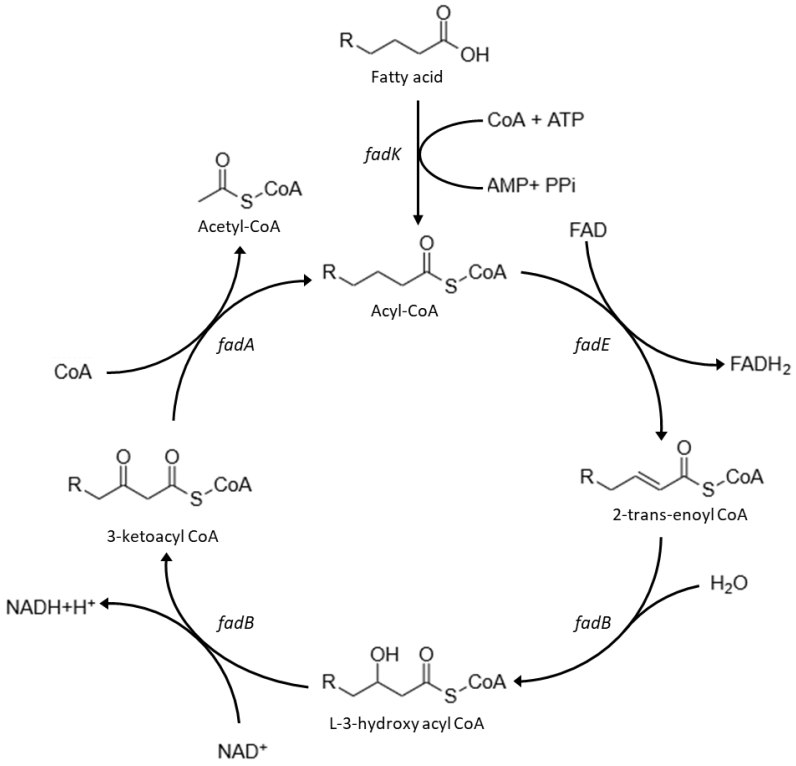


Figure 4-6: Degradation pathway of fatty acids in *Streptomyces fulvissimus* (Kanehisa & Goto, 2000, from Kegg consulted on 18/08/2022)

BLASTN searches identified a number of homologous genes in *Streptomyces* sp. F (Table 4-5). The E-values and identity coverage were mixed with some good homology, for example *fadE,* (E-value< $1e^{-250}$, identity cover= 86%), which had the highest value. Although still below the threshold of 90%. The remaining genes had lower values, *fadB,* (E-value= $1e^{-110}$, identity cover= 69%), *fadA,* (E-value= $1e^{-121}$, identity cover= 49%) and *fadK* (E-value= $4e^{-06}$, identity cover= 40%).

The transcriptomic analysis showed that genes involved in fatty acid degradation were upregulated on both PE and PET, these included: ORF 6518, a homologue of *fadK*, ORF 6521, a homologue of *fadE*, ORF 3294, a homologue of *fadB* and ORF 6153, a homologue of *fadA*. . Both ORF 6518 and 6521 were shown to be clustered together in the genome, which could indicate that they are part of the same operon. However, ORF 6153 and 3294 are too far apart to be part of an operon with the rest of the pathway.

Gene	**organism**	**ORF in F**	**E value**	**Identity cover (%)**	**Expression gene PE Vs Glucose**	**Expression gene PET Vs Glucose**
fadK	*Streptomyces coelicolor*	3234	$4e^{-06}$	40	1.54	-0.18
		1082	$6e^{-06}$	30	0.17	0.19
		6518	$1e^{-5}$	36	3.89	2.19
fadE	*Streptomyces coelicolor*	6521	0	86	3.92	2.57
		6500	$4e^{-39}$	30	1.34	0.92
		1171	$2e^{-33}$	26	0.37	0.78
fadB	*Streptomyces coelicolor*	3294	$1e^{-110}$	69	2.88	2.08
		7559	$3e^{-23}$	34	0.08	-1.33
		2752	$4e^{-22}$	35	0.21	2.28
fadA	*Streptomyces coelicolor*	6153	$1e^{-121}$	49	0.69	1.40
		5804	$7e^{-96}$	45	2.57	1.64
		908	$1e^{-89}$	41	1.35	-0.40

Table 4-5 : List of homologous genes involved in the fatty acid degradation identified in the genome of *Streptomyces* sp. F. The expression level of each gene is presented by the Log2 of the ratio of gene expression. A log2>2 means that the gene is

significantly over-expressed on PET and PE. A log2<-2 means that the gene is significatively overexpressed on glucose.

Fatty acid metabolism has been well characterised in *Streptomyces* sp. (Arabolaza *et al.*, 2008; Comba *et al.*, 2013; Menendez-Bravo *et al.*, 2017). Several enzymes have already been identified in the literature for the degradation of both PE and PET. Several of the PETase candidates have been shown to degrade PET, while the PE degradation enzymes remain largely speculative (Ghatge *et al.*, 2020).

4.3.4 Bioinformatic characterisation of the PETase homologous found in the genome of *Streptomyces sp. F*

Several PET degradation enzymes have already been identified and characterised, all of the ones identified to date have a similar structure and activity (Han *et al.*, 2017; Austin *et al.*, 2018; Tournier *et al.*, 2020). From the ones identified so far, two have the best activity: the PETase from *Ideonella sakaiensis* (Austin *et al.*, 2018) and the Leaf-branch compost cutinase (LCC) enzyme isolated from an unknown prokaryotic organism in a compost heap (Tournier *et al.*, 2020).

BLASTN was used to identify, two homologous genes in the genome of *Streptomyces* sp. F, open reading frame (ORF) 6120 and 7664. BLAST searches and alignments with the PETase from *I. sakaiensis*, identified ORF 6120 as having the closest homology, although both the e-value ($< 1e^{-60}$) and the percentage similarity (46%) were low. Further comparisons with both the LCC enzyme and the hydrolase enzyme yielded better homology results, but the identity remained low (Table 4-6). A second candidate, ORF 7664, was identified with some similarity to both the cutinase and the hydrolase with an E-value of $<3e^{-5}$ and a percentage match of 36 % (Table 4-6). Given ORF 6120 has more sequence similarity to the candidates already described in the literature this was chosen for further analysis. From now on, ORF 6120 will be referred to as *petF* and its enzyme will be referred to as F-PETase.

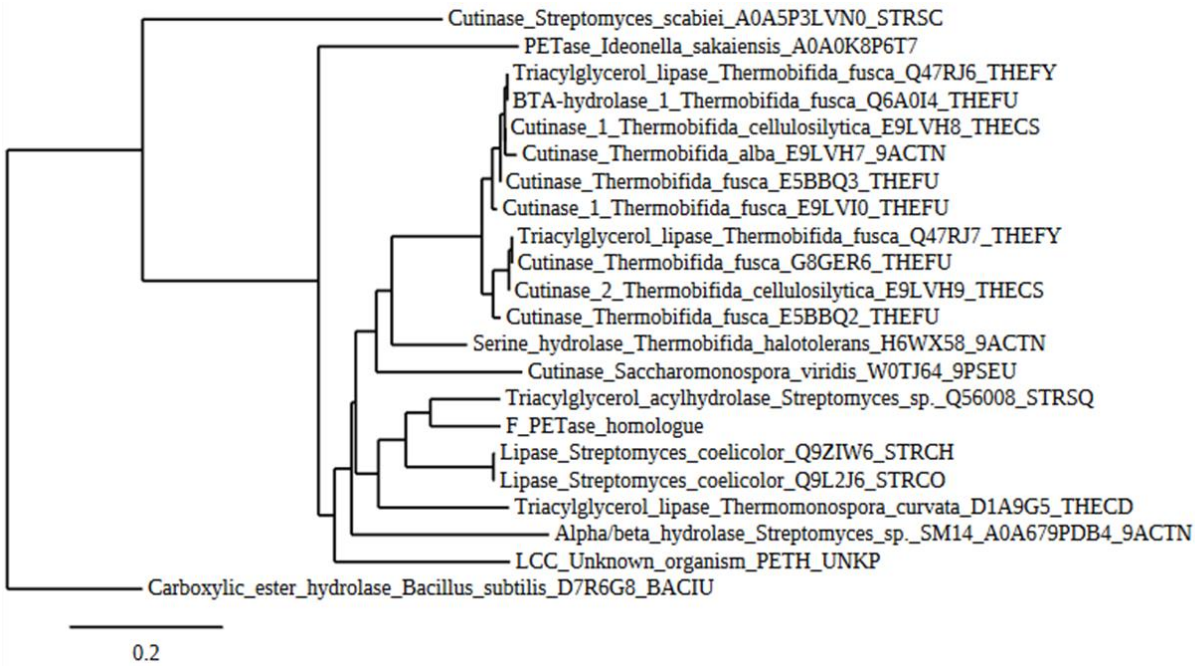
Surprisingly, there was no significant upregulation of the PETase homolog on PET. However, this could simply be due to the fact that the transcriptomic data is overlaid on *S. fulvissimus* and not *Streptomyces* sp. F, it is also possible that limited time point sampling may have also meant that the initial upregulation on PET was missed. The F PETase may also be constitutively expressed, due to its role in the cell.

Protein name	**Organism**	**ORF in *Streptomyces* sp. F**	**E value**	**Identity cover (%)**	**Reference**	**Expression gene PE Vs Glucose**	**Expression gene PET Vs Glucose**
Poly(ethylene terephthalate) hydrolase (PETase)	*Ideonella sakaiensis*	6120	6e-67	46	Yoshida et al., 2016	-0.42	-0.20
Leaf-branch compost cutinase (LCC)	Unknown prokaryotic organism	6120	3e-89	66	Tournier et al., 2020	-0.42	-0.20
		7664	3e-05	36		0.60	0.16
Hydrolase (TfCut1)	*Thermobifida fusca*	6120	1e-107	62	Müller et al., 2005	-0.42	-0.20
		7664	5e-06	27		0.60	0.16
Hydrolase (TfCut2)	*Thermobifida fusca*	6120	1e-107	61	Müller et al., 2005	-0.42	-0.20
		7664	3e-07	29		0.60	0.16

Table 4-6 : Homologous PET degrading enzymes detected in the genome of *Streptomyces* sp. F. The expression level of each gene is presented by the Log2 of the ratio of gene expression. A log2>2 means that the gene is significantly over-expressed onPET and PE. A log2<-2 means that the gene is significantly overexpressed on glucose.

Phylogenetic analysis was done using sequences closely related to the PETase from *Streptomyces* sp. F. Sequences were aligned via Clustal W and the tree was constructed using the one click tool from phylogeny.fr. The F-PETase clearly shares a common ancestor with the *I. sakaiensis* enzyme, but the enzyme has diverged overtime and now sits in a separate clade, being more closely related to lipases (Figure 4-7). It is also related to the hydrolase from *Streptomyces* sp. SM14 (Almeida, Rincón, Jackson and Alan D.W. Dobson, 2019), the two hydrolases from *T. fusca* (Müller *et al.*, 2005), and the LCC enzyme (Tournier *et al.*, 2020). The outgroup used was an ester hydrolase enzyme from an isolate of *Bacillus subtilis*. This enzyme has been reported as being able to degrade an oligomer PET, but shares very little

homology with the other studied PETase (Ribitsch *et al.*, 2011).



4.3.4.1 Figure 4-7 :Phylogenetic tree of PETase homologs Computational Modelling of the F-PETase enzyme

A model was constructed for the structure of the F-PETase homolog, ORF 6120, utilising AlphaFold2 software (Jumper *et al.*, 2021). The model was constructed by Dr Marko Hanzevacki. The model allows for a direct comparison to be made between other published structures and the PETase homologue from *Streptomyces* sp. F. Visualisation and comparison of the model was done using Pymol software (Schrödinger, L. & DeLano, W., 2020. PyMOL, Available at: http://www.pymol.org/pymol.)

From the model, two distinct structural components could be detected (Figure 4-8). The first part, highlighted in green, has a stabilised structure, the second part, in red, is not stable (Figure 4-8). This section of the enzyme could be a signal peptide used by *Streptomyces* sp. F to export the protein out of the cell.



Figure 4-8 : Structural model of the F-PETase, in green the structured part of the model and in red the unstructured part

Analysis was performed using SignalP-6.0 software, which looks for signal peptides in proteins. The software predicted the presence of a Sec signal peptide on the protein (Table 4-7). The Sec or general secretory pathway is ubiquitous and essential for the export of proteins into and through the plasma membrane (Tsirigotaki *et al.*, 2017). Proteins are cleaved via the Signal peptidase I (Sec/SPI) (Table 4-7). The cleavage site is predicted to be between Ala46 and Ala47, with a probability of 0.81 (Table 4-7). The size of the signal peptide corresponds to the unstructured part of the F-PETase (Figure 4-8). For this reason, the signal peptide region of the protein was excluded from the structural analysis.

Signal peptide type		**Likelihood**
Sec/SPI		0.8706
Cleavage site	**Motif**	**Probability**
46-47	AQA-AA	0.815806

Table 4-7: Characterisation of the signal peptide of the protein F-PETase

4.3.4.2 Comparison between the structure of the F-PETase and the PETase from Ideonella sakaiensis

Protein-ligand molecular docking was carried out on the F-PETase using an oligomer of the PETase from *I. sakaiensis*. The model was then directly compared to the published model of the *Ideonella sakaiensis* PETase.

The structure of the PETase from *Ideonella sakaiensis* has been resolved both with and without the ligand (Han *et al.*, 2017). The comparison between the structure of the PETase from *Ideonella sakaiensis* and the F-PETase revealed several similarities. These included the presence of a pocket and the ability of this pocket to stabilise either the HMET or PET oligomer (Figure 4-9 and 4-10). The main difference between the two pockets is the presence of a phenylalanine at position 255, which could provide additional π-stacking and enable hydrophobic interactions to adjacent terephthalate moieties. This stabilisation is supported by the short distance between the terephthalate moieties and Phe208, ranging between 3.5 and 4.2 Å (Figure 4-10). Moreover, the presence of phenylalanine at this position has been shown to improve the degradation activity of the PETase enzyme from *Ideonella sakaiensis* (Austin *et al.*, 2018).

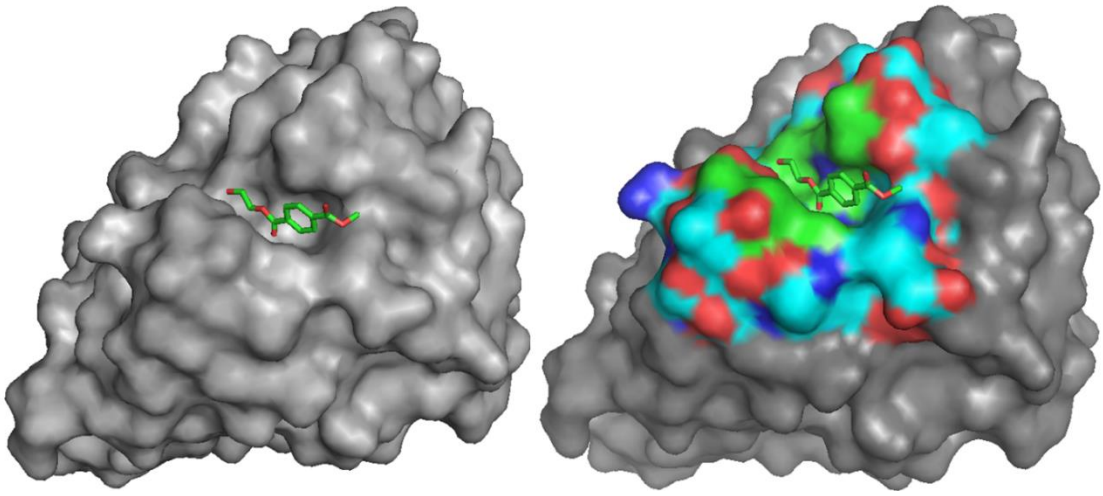


Figure 4-9 : Crystal structure of a PET hydrolase R103G/S131A mutant in complex with HEMT from *Ideonella sakaiensis*, PDB: 5XH3 (Han *et al.*, 2017)

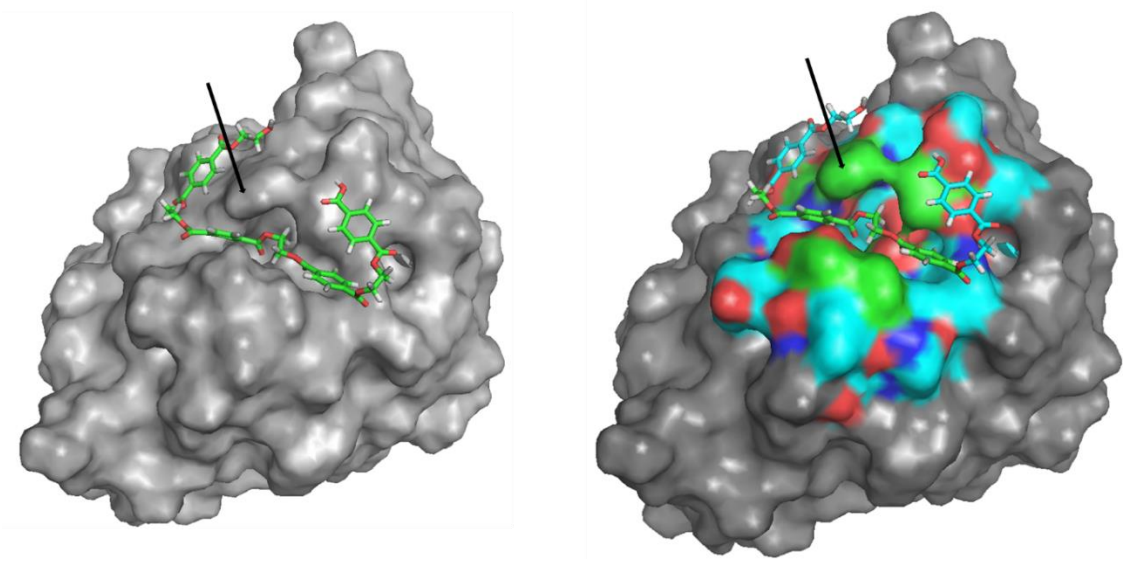


Figure 4-10 : Model of the F-PETase in complex with an oligomer of PET, with an arrow showing the position of Phe 255.

A direct comparison between the active sites of both the I-PETase and F-PETase revealed a very similar structure (Figure 4-11). The catalytic triad is composed of the following residues, histidine (His 237 for I-PETase and His 207 for F-PETase), aspartate (Asp 176 for I- PETase and Asp 175 for F-PETase) and serine (Ser 131 for I-PETase and Ser 129 for F-PETase). The residues can all be found in the active site of both enzymes at similar positions. The similar positioning of these key amino acids in the active site indicates that the F-PETase could perform a similar activity to the PETase from *Ideonella sakaiensis.*

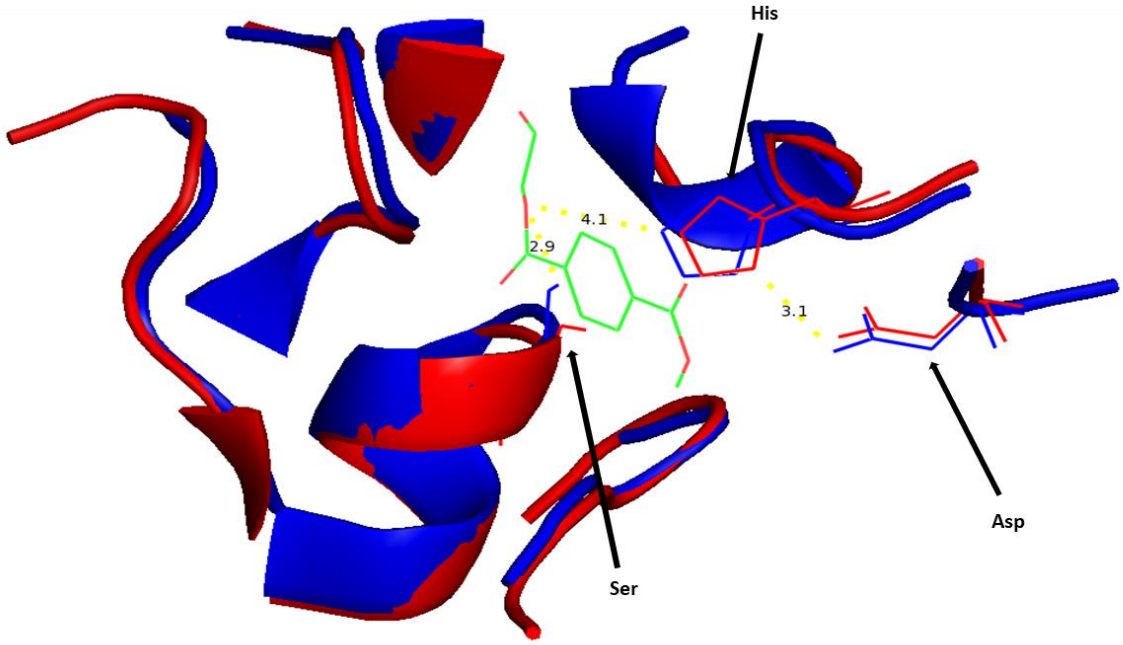


Figure 4-11: Active site of the PETase from *Ideonella sakaiensis* (PDB: 5XJH) (Han *et al.*, 2017)**, in red, and the active site of F-PETase, in blue. HMET has been added from the structure of PETase (PDB: 5XH3)** (Han *et al.*, 2017)**.**

4.3.5 Characterisation of the MHETase homologous found in the *Streptomyces sp. F*

4.3.5.1 Identification and characterisation of the MHETase homolog in Streptomyces sp. F

The PETase enzyme is not the only enzyme needed for the degradation of PET in *Ideonella sakaiensis,* the by-products of the PETase enzyme are degraded by a second enzyme the MHETase (Yoshida *et al.*, 2016). This enzyme has specific activity against MHET, the monomeric form of PET (Yoshida *et al.*, 2016; Sagong *et al.*, 2020). This dual enzymatic system allowing for the degradation of PET is specific to *Ideonella sakaiensis* and has not been reported in other organisms. The engineering of a dual enzyme system was reported in 2016, Barth et al. used two different polyester hydrolases (LCC and TfCut2) with one carboxylesterase (TfCa) to degrade PET (Barth *et al.*, 2016). The addition of the carboxylesterase, mimicking the

reaction of the MHETase, which had a very positive impact on the degradation rate of the PET.

Using the BLASTN methodology, a homologous gene was identified in the genome of *Streptomyces* sp. F, which shared some similarity to the MHETase from *I. sakaiensis* (Table 4-8).

The transcriptomic analysis showed that the MHETase homolog was not significantly overexpressed on PET. However, as for the PETase homolog, this could simply be due to the fact that the transcriptomic data is overlaid on *S. fulvissimus* and not *Streptomyces* sp. F, or that the initial upregulation on PET was missed. The F MHETase may also be constitutively expressed, due to its role in the cell.

Protein name	organism	ORF in F	E value	Identity cover (%)	Reference	Expression gene PE Vs Glucose	Expression gene PET Vs Glucose
Mono(2-hydroxyethyl) terephthalate hydrolase (MHETase)	*Ideonella sakaiensis*	2144	$5e^{-04}$	40	Yoshida et al., 2016	1.72	0.97

Table 4-8 : Homologous MHETase enzymes detected in the genome of *Streptomyces* sp. F. The expression level of the homologous gene is presented by the Log2 of the ratio of gene expression. A log2>2 means that the gene is significantly over-expressed on PET and PE. A log2<-2 means that the gene is significantly overexpressed on glucose.

4.3.5.2 Computational Modelling of the F-MHETase

A direct comparison between the structure of the I-MHETase and the F-MHETase was performed. A model of the F-MHETase (Figure 4-13) was constructed using the structure of the *Ideonella sakaiensis* MHETase (Figure 4-12). The structure of the MHETase from *Ideonella sakaiensis* have been resolved on multiple occasions with different ligands (Sagong *et al.*, 2020). Both I-MHETase and F-MHETase have a similar overall structure, with two separate domains, a core domain and a lid domain (Figure 4-12 and 4-13) (Knott *et al.*, 2020). The active site is situated between the lid domain and the

core domain, a major difference between the I-MHETase and the F-MHETase is the accessibility of the active site. In the case of I-MHETase, the active site is covered by parts of the lid domain, creating a “buried” active site (Figure 4-12). For the F-MHETase, the lid domain does not cover the active site, creating a larger more accessible active site (Figure 4-13).

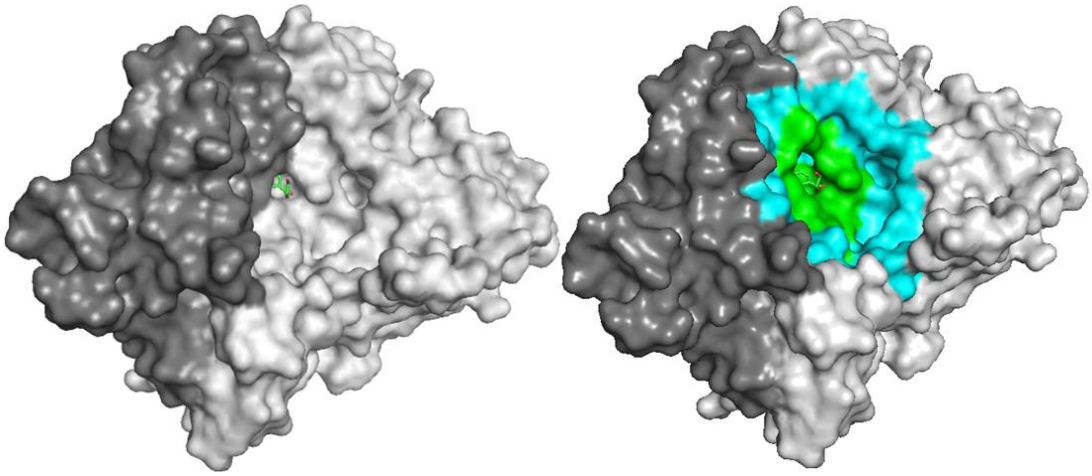


Figure 4-12 : Crystal structure of the MHETase from *Ideonella sakaiensis* in complex with BHET, lid domain in dark grey (PDB: 6JTT) (Sagong *et al.*, 2020)

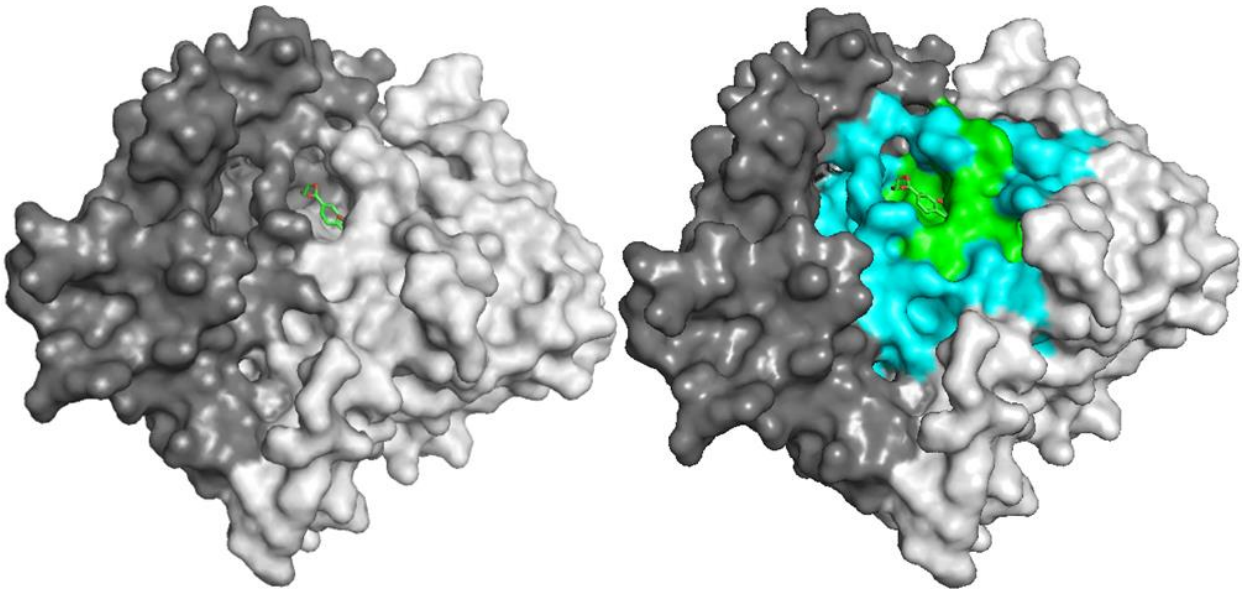


Figure 4-13: Model of the F-MHETase in complex with BHET, lid domain in dark grey

4.3.5.3 Comparison of the structure of the F-MHETase and the MHETase from Ideonella sakaiensis

One key difference between the PETase and the MHETase is the presence of this lid domain. These domains have been shown to play a crucial role in the specificity of the MHETase, with a lidless version of the MHETase having a reduced activity against MHET, which was shown to be 1000 fold lower than the lidded MHETase (Knott *et al.*, 2020).

The lid domain of I-MHETase contains eight α helices, whereas the F-MHETase only has 6 α helices, including 4 short helices (Figure 4-14). Due to the differences in the lid domain, the active site of both enzymes has a different structure (Figure 4-15). MHETase-I has an α helix which participates in the stabilisation of the substrate (Figure 4-14), whereas the F-MHETase does not have this structure (Figure 4-14 and 4-15).

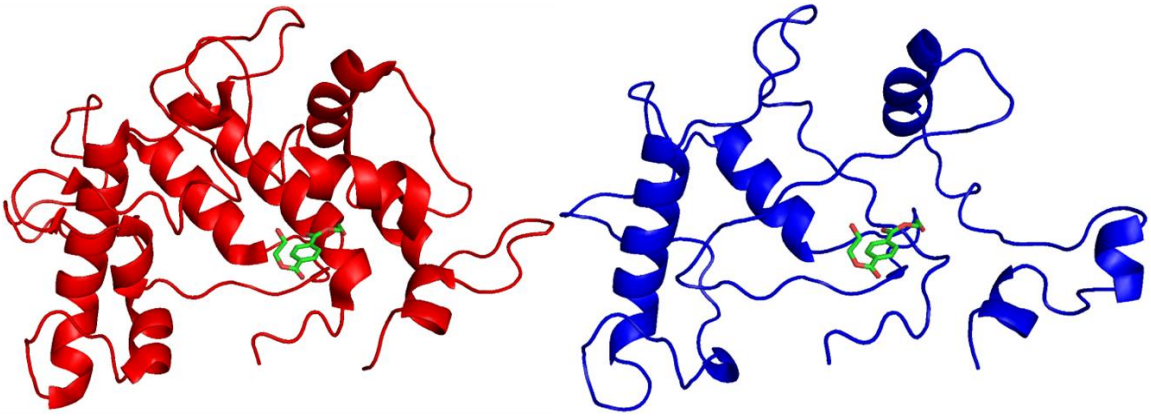


Figure 4-14 : Secondary structure of the lid domain of I-MHETase (in red) and F-MHETase (in blue)

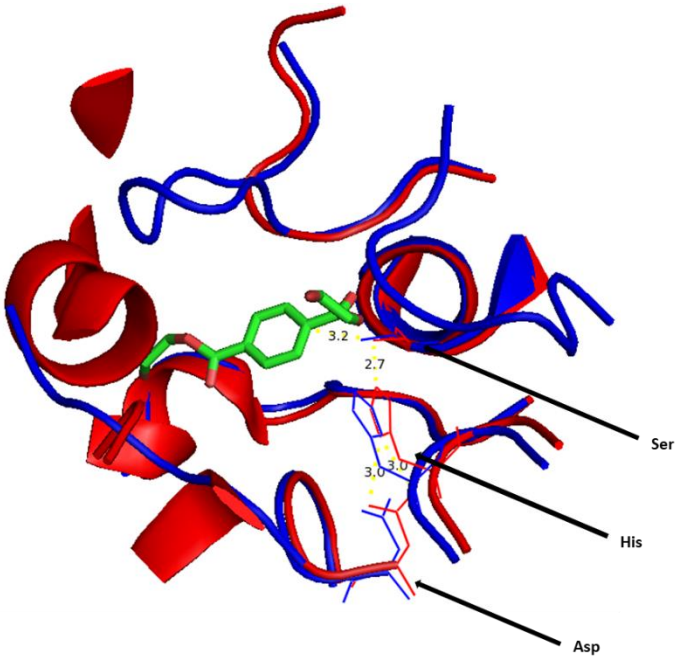


Figure 4-15 : Comparison of the secondary structure of the active site of the I-MHETase (in red) and F-MHETase (in blue), active amino acids are shown as stick models with hydrogen bonds between the catalytic triad (Knott *et al.*, 2020)

Despite sharing similar catalytic triad positions (Figure 4-15), the I-MHETase and the F-MHETase do not share the same amino acids which interact directly with the substrate. The I-MHETase has nine amino acids which stabilise the substrate (Figure 4-16): these being S225, E226, L254, R411, S416, H528 and D492 (Knott *et al.*, 2020). The F-MHETase only has 7 amino acids which interact closely with: G119, S202, T203, Y235, D416, Y418 and H455 (Figure 4-16). There is also less hydrogen bonds in the active site of the F-MHETase, this could have an impact on the stabilisation of the substrate and therefore on the activity of the enzyme.

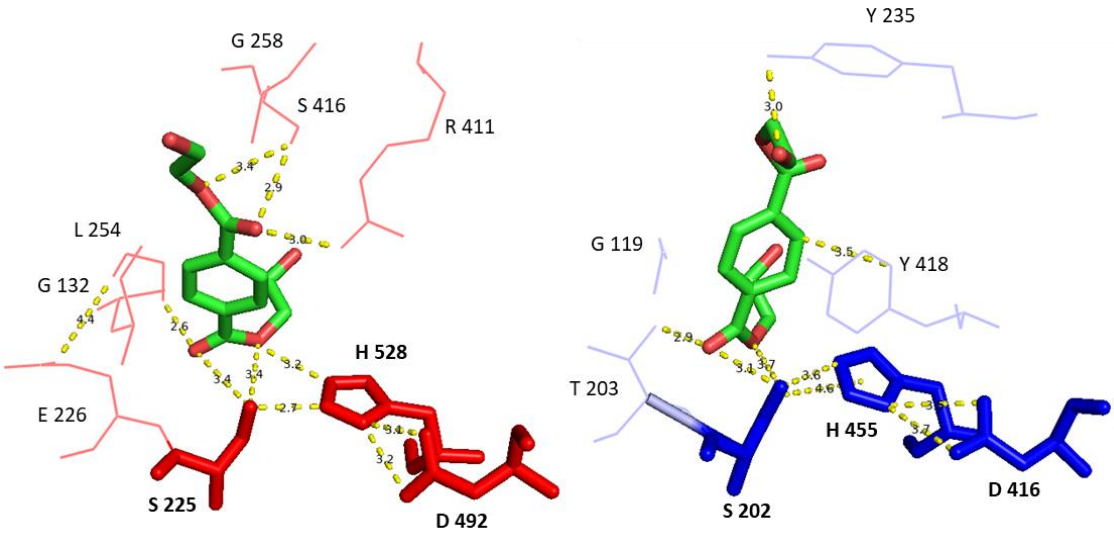


Figure 4-16 : Amino acids interacting with the substrate in the active site of the I-MHETase (in red) and F-MHETase (in blue), with catalytic amino acid in bold

4.3.6 Bioinformatic analysis of the enzymes responsible for the degradation of PE

Thus far no enzymes have been fully characterised which degrade PE. However, several enzymes have been reported in the literature which may be responsible for the degradation of PE. These include laccases, peroxidases, monoxygenases and the dioxygenase, AlkB (Ghatge *et al.*, 2020). The BLASTN methodology was used to identify potential homologs in the genome of *Streptomyces* sp. F.

Sequence BLAST searches identified two homologs in the genome, the monooxygenase, *ladA* and a laccase. The LadA monooxygenase utilizes a terminal oxidation pathway to convert long-chain alkanes (up to at least C(36) to their corresponding primary alcohols (Feng *et al.*, 2007; Li *et al.*, 2008). Laccases belongs to the superfamily of multicopper oxidases (MCO's) a diverse group of enzymes comprising many proteins, which have different substrate specificities and diverse biological functions (Janusz *et al.*, 2020).

Two homologous of the monooxygenases (*ladA*) were identified in the genome, both the e-value (<$1e^{-50}$) and the percentage identity (>30%) were low (Table 4-9). One of the laccase homologs had a significant E-value (1e-116), but the percentage identity remained low (47%).

None of the previous gene candidates for PE degradation were upregulated on PE. This could mean one of two things: the expression of PE degrading enzymes already identified in the literature is not dependant on the presence of PE. Or that PE degradation is not carried out by the candidate genes already suggested in the literature and *Streptomyces* sp. F relies on another type of enzyme to degrade PE. Alternatively, it could simply have been missed due to the fact that the host genome was not utilised for the analysis.

Protein name	**organism**	**ORF in F**	**E value**	**Identity cover (%)**	**Reference**	**Expression gene PE Vs Glucose**	**Expression gene PET Vs Glucose**
AlkB	*Pseudomonas putida GPo1*	N/A			Beilen et al., 2001		
	Streptomyces coelicolor	N/A			Saadoun & Alawawdeh, 2008		
ladA (monooxygenase)	*Geobacillus thermodenitrificans*	1393	$2e^{-76}$	29	Feng et al., 2007; Li et al., 2008	-0.35	1.18
ladA (monooxygenase)	*Geobacillus thermodenitrificans*	600	$1e^{-75}$	29	Feng et al., 2007; Li et al., 2008	-1.75	-1.07
Laccase	*Rhodoccocus ruber*	5898	$1e^{-116}$	47	Santo et al., 2012	-1.61	-0.63
Mnp (manganese peroxidase)	*Phanerochaete chrysosporizun*	N/A			Bao et al., 1994; Ehara et al., 2000		

Table 4-9 : List of homologous genes detected in *Streptomyces* sp. F with potential PE degradation activity. The expression level of each gene is presented by the Log2 of the ratio of gene expression. A log2>2 means that the gene is significantly over-expressed on PET and PE. A log2<-2 means that the gene is significantly overexpressed on glucose.

4.3.6.1 Comparison of F-LadA and LadA from Geobacillus thermodenitrificans

As stated previously, LadA is a monooxygenase belonging to the flavin-dependent hydroxylases group. This group of enzymes can oxidise a variety of aromatic substrates and plays an important role in the degradation of lignin and other phenolic compounds (Chenprakhon, Wongnate and Chaiyen, 2019). LadA has been reported as able to degrade long chain alkanes (Feng *et al.*, 2007), and has been reported as a candidate gene for the degradation of polyethylene.

Phylogenetic analysis using Clustal Omega (Sievers *et al.*, 2011) revealed that the two LadA homolog in *Streptomyces* sp. F form separate clades, F-LadA1 with other flavin dependent oxidoreductases from Streptomyces species and F-LadA2 with FMN dependent oxygenases. Although both diverged from a common ancestor neither are directly related to LadA from *G. thermodenitrificans* (Figure 4-17). This divergence in the sequence could be the sign that the monooxygenase family contains a large variety of potential PE degrading enzymes (Ghatge *et al.*, 2020)

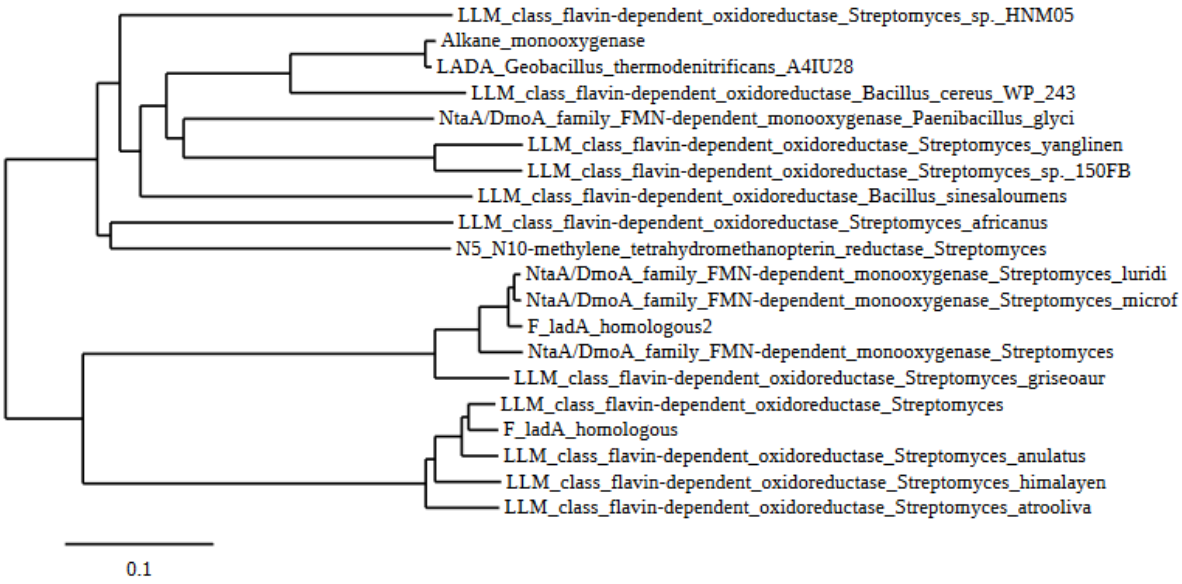


Figure 4-17: Phylogenetic tree of the LadA homologous genes found in *Streptomyces* sp. F

Sequence alignment between the F-LadA1 and A2 and other LadA homologs revealed some sequence similarity in the active site. Six out of the 10 amino acids were conserved in the active site (Figure 4-18, black arrow). However, several amino acids (H138, W348 and F349) which are essential for the

binding of FMN were not present in F-LadA1 and A2 (Figure 4-18, red rectangle).



Figure 4-18: Sequence alignment of LadA from *G. thermodenitrificans* and F-LadA1 and A2, amino acid residues involved in FMN binding are labelled with a black arrow, putative active pocket residue are in red rectangle (Li *et al.*, 2008)

4.3.6.2 Comparison of the F-laccase and the laccase from Rhodoccocus ruber

Laccases are multi-copper oxidases that catalyse the oxidation of one electron to a wide range of aromatic compounds (Arregui *et al.*, 2019). The reaction generally involves one electron, which goes through a series of sequential oxidation reactions, eventually leading to the total reduction of O_2 to H_20 (Arregui *et al.*, 2019). Laccases have been reported in the literature as potential PE degrading enzymes, especially those found in *Rhodococcus sp.* (Santo, Weitsman and Sivan, 2013; Zampolli *et al.*, 2021). The laccase from

R. opacus R7 was shown to increase its transcript abundance when grown on PE (Zampolli *et al.*, 2021).

Phylogenetic analysis demonstrated that the F-laccase, although diverging from a common ancestor, does not form a clade with the laccases cited in the literature as potential PE degrading enzymes (Figure 4-19). F-laccase is part of a clade which has sequences specific to laccases from other *Streptomyces* sp. (Figure 4-19).

Moreover**,** a multi sequence alignment between the F-laccase and other laccases shown to degrade PE demonstrated that the F-laccase shares key amino acid residues which are present in the copper binding motif (Figure 4-20).

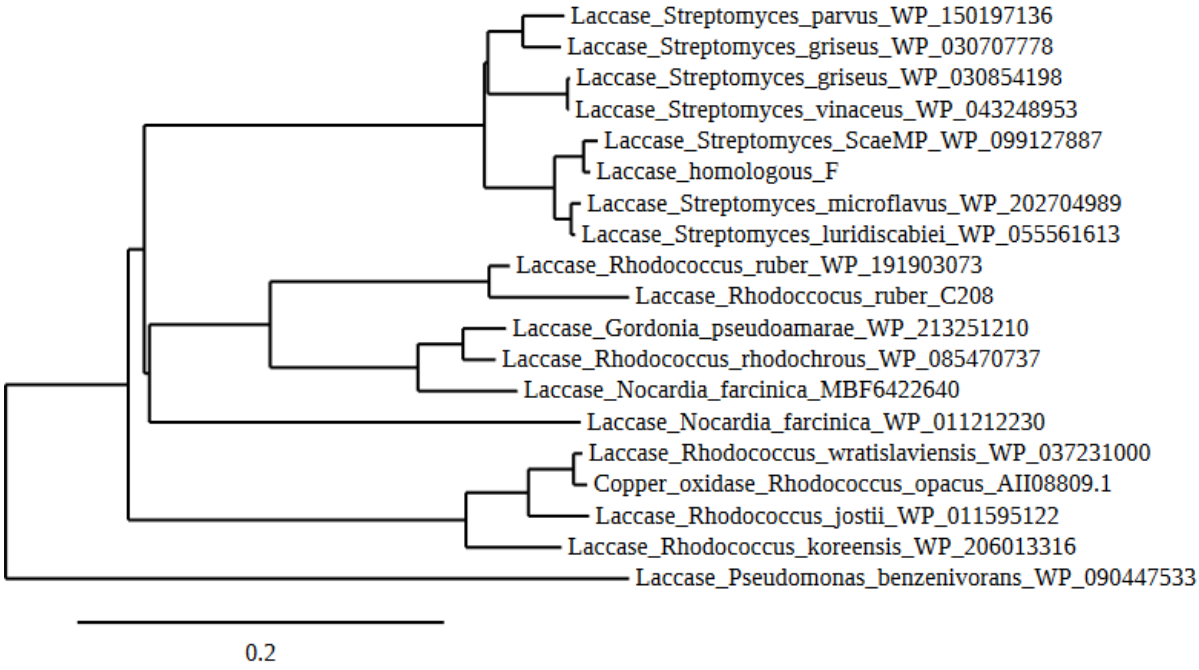


Figure 4-19 : Phylogenetic tree of laccases from *Rhodococcus* sp. and the laccase homolog found in *Streptomyces* sp. F.



Figure 4-20 : Sequence alignment of the laccase enzymes from *R. ruber* and *R. opacus* and the homologous sequence from *Streptomyces* sp. F, the copper binding motif found in the laccase from C208 is highlighted with black arrows (Zampolli et al., 2021)

4.4 Discussion

Genomic analysis of S*treptomyces* sp. F confirmed the identification of isolate *F* as a *Streptomyces sp.* closely related to *S. fulvissimus*. The genome size and GC content were consistent with other *Streptomyces* sp. Genetic elements (GIs) were identified which were related to genome instability, a documented phenomenon in *Streptomyces sp.* (Leblond and Decaris, 1994; Volff and Altenbuchner, 1998). GIs are also known to contribute to genome evolution enabling horizontal gene transfer (HGT) in many bacterial species (Dobrindt *et al.*, 2004), including *Streptomyces sp.* (Bentley *et al.*, 2002; Ikeda *et al.*, 2003). Moreover, the natural product clusters or BGCs are often located at the ends of the chromosome, where genetic rearrangement is common, in particular in the GI (Leblond and Decaris, 1994; Dobrindt *et al.*, 2004; McDonald and Currie, 2017). The high number of BGCs found in *Streptomyces* sp. F, 34 in total, might be a direct result of the high number of GIs detected. The analysis of the BGCs, using ANTISMASH, revealed several interesting features for potential industrial use. Several biosynthetic pathways were detected, such as potential antibiotics (AmfS, PTM) (Table 4-2).

Furthermore, a PETase homolog was identified in the genome of *Streptomyces* sp. F. Structural comparisons between the F-PETase and the PETase from *Ideonella sakaiensis* revealed some structural similarities. With the key amino acids involved in the catalytic triad being shared between the

two enzymes (Figure 4-11). In addition to a very similar active site, the F-PETase has a phenylalanine (Phe 255) next to the pocket containing the active site, which has previously been shown to improve PETase activity (Austin *et al.*, 2018). The similarity between the two enzymes is suggestive of the function of the F-PETase, but it is also interesting to note the differences between the two and the fact that the F-PETase aligns more closely with hydrolases than with cutinases.

This illustrates the variety of enzymes reported as PET degrading enzymes. While they share the same reaction, the breaking of ester bond using a water molecule, they are part of different family of enzymes (lipase (Wang *et al.*, 2008), cutinase (Yoshida *et al.*, 2016), hydrolase). This may suggest that the variation in seen in the PET degrading enzymes is not evolutionary and instead may result from promiscuous activity against the PET polymer.

Bioinformatic analysis identified some potential candidate enzymes and pathways involved in the degradation of PE. Although this is speculative given the lack of data on the degradation of PE in the literature. Multiple homologs were identified in the genome of *Streptomyces* sp. F (Table 4-9). Interestingly, two monooxygenases were identified, which may suggest how PE degradation progresses in this strain. Several monooxygenases have been reported in the literature as the enzymes involved in the degradation of PE, through the oxidation of carbon chains (Feng *et al.*, 2007; Li *et al.*, 2008; Wang and Shao, 2013). A laccase was also detected in the genome of *Streptomyces* sp. F, sequence alignments confirmed that it shared a similar copper binding motif to of other laccases previously reported to be PE degrading enzymes (Santo, Weitsman and Sivan, 2013; Zampolli *et al.*, 2021). While a similar copper binding motif might not be sufficient to qualify as a potential PE degrader, this motif is shared with many other laccases (Janusz *et al.*, 2020), it is indicative of a similar activity on potential similar substrate.

An analysis on the aromatic metabolic pathways confirmed that *Streptomyces* sp. F is unable to grow using aromatic compounds such as terephthalate and vanillic acid. The lack of any enzyme homologs in the

genome confirmed the experimental data seen in Chapter 3. The absence of enzymes involved in the degradation of PCA, a key metabolite in the aromatic degradation (Fuchs, Boll and Heider, 2011), is surprising. *Streptomyces* sp. play an important role in the degradation of biological material, they are known for their metabolic versatility (Hae-Reun, Hyun-Joo and Eung-Soo, 2000; Hodgson, 2000; Saadoun *et al.*, 2008; Khalil *et al.*, 2019). Several *Streptomyces* sp. have been reported to grow using an array of aromatic compounds (Balachandran *et al.*, 2012; Khalil *et al.*, 2019) and to degrade lignin (Riyadi *et al.*, 2020; Tan *et al.*, 2022), a polymer formed from phenyl-propane units (Fuchs, Boll and Heider, 2011). The absence of an active β-ketoadipate pathway, preventing the growth on most aromatic compounds, is therefore most peculiar.

One of the main enzymes of this pathway is protocatechuate 3,4-dioxygenase, encoded by the *pcaG* and *pcaH* genes. Only one of the subunits was detected in the genome of *Streptomyces F* (Table 4-3), although the percentage identity was low, suggesting that this has potentially evolved to be a new hybrid version or more likely, the enzyme is not a protocatechuate 3,4-dioxygenase. This is supported by the fact that *Streptomyces* sp. F cannot grow on PCA (Spence unpublished). Despite the absence of a TPA degradation pathway, there was a pathway for EG degradation, which has also been verified experimentally (Chapter 3). The percentage identity was low, but the presence of the pathway and the growth data prove that *Streptomyces* sp. F can use EG as a sole carbon source, albeit very inefficiently. A structural comparison of the enzymes involved in the degradation of EG in *Streptomyces* sp. F and *Pseudomonas putida* would be interesting. It could reveal differences in the mechanism of the degradation of EG.

5 The sequencing of the genome of *Streptomyces* sp. F enabled several potential PET and PE candidate enzymes and pathways to be uncovered. Validating the TPA and ethylene glycol growth data presented in Chapter 3. It

would be interesting to re-evaluate the expression data from Chapter 3 pathways on both PET and PE against the fully sequenced genomes, given the size differences between the two to further identify potential gene candidates. Discussion

Streptomyces sp. have been studied extensively for the production of secondary metabolites. They represent an industrial chassis producing most of the antibiotics used to date. New interest has recently arisen about their ability to degrade challenging material, such as lignin. Several reports of *Streptomyces* sp. degrading PE and PET have been recently published. However, the degradation of both PE and PET are still not fully characterised in these strains.

The overall aim of this study was to characterise the first organism able to degrade two plastics PE and PET. The discovery of such an organism will help gain valuable information about the degradation mechanism of both plastics.

Chapter 3 demonstrated the ability of *Streptomyces* sp. F to grow on virgin PE and PET, as well as characterising the by-products of the degradation of both plastics. Clear differences could be seen in the growth rates on PET and PE. Furthermore, both metabolomic and transcriptomic analysis showed significant differences in the metabolic and transcriptomic profile of the cells on PET and PE compared to glucose. The transcriptomics also identified a number of potential gene targets upregulated on both PET and PE which may play a role in the degradation process. Furthermore, it was shown that *Streptomyces* sp. F can utilise EG as a sole carbon source a breakdown product from PET. It was however surprisingly unable to utilise TPA. Based on the bioinformatics analysis degradation pathways were suggested for both PET and PE in this strain.

Chapter 4 details the genome sequencing of *Streptomyces* sp. F enabling the identification of several different enzyme candidates for PET and PE degradation. Furthermore, the genome sequence enabled the detection of

key metabolic pathways involved in the process such as the EG pathway, it also confirmed the absence of a TPA pathway. PETase and MHETase candidates were also identified and a structural comparison between the candidate enzymes and other published PETase and MHETase enzymes was conducted. This analysis did not reveal any major structural differences between the enzymes. In the case of PE, several potential candidates for the degradation of PE were identified in the genome of *Streptomyces* sp. F, but no structural analysis was conducted.

This study is the first characterisation of an organism able to degrade two different plastics. It has highlighted the potential of *Streptomyces* sp. in the biodegradation of plastic. Moreover, with the large number of industrially relevant bio-active compounds produced by Streptomyces, this work is a first step towards the use of plastic as a carbon feedstock for the production of high-value compounds.

5.1 Future Work

This research provides some interesting results which require further evaluation. Additional research still needs to be done to enable both PE and PET degradation to be fully characterised. The transcriptomic work should be compared to the *Streptomyces* sp. F genome to allow potential genes involved in both PET and PE degradation to be identified. Candidate enzymes could then be knocked out to assess activity or expressed in *E. coli, and* purified protein could be used for *in vitro* enzyme assays and crystallisation. Although PETase and MHETase candidates were identified in *Streptomyces* sp. F, revised transcriptomic analysis may also identify new candidates. Secretomics should also be done to identify enzymes excreted outside of the cell. Further characterisation of the plastic properties would also be valuable and could support the omics data. It would also be interesting to evaluate the growth of *Streptomyces* sp. F on both PET and PE to see how it responds to both plastics.

6 References

Aksu, D. *et al.* (2021) ‘Biodegradation of Terephthalic Acid by Isolated Active Sludge Microorganisms and Monitoring of Bacteria in a Continuous Stirred Tank Reactor’, *Brazilian Archives of Biology and Technology*, 64, pp. 1–10. doi: 10.1590/1678-4324-2021200002.

Albuquerque, P. *et al.* (2021) ‘Complete Genome Sequence of Two Deep-Sea Streptomyces Isolates from Madeira Archipelago and Evaluation of Their Biosynthetic Potential’, *Marine Drugs*, 19(11), p. 621. doi: 10.3390/md19110621.

Almeida, E. L., Rincón, A. F. C., Jackson, S. A. and Dobson, Alan D.W. (2019) ‘In silico Screening and Heterologous Expression of a Polyethylene Terephthalate Hydrolase (PETase)-Like Enzyme (SM14est) With Polycaprolactone (PCL)-Degrading Activity, From the Marine Sponge-Derived Strain Streptomyces sp. SM14’, *Frontiers in Microbiology*, 10. doi: 10.3389/fmicb.2019.02187.

Almeida, E. L., Rincón, A. F. C., Jackson, S. A. and Dobson, Alan D. W. (2019) ‘In silico Screening and Heterologous Expression of a Polyethylene Terephthalate Hydrolase With Polycaprolactone (PCL) -Degrading Activity , From the Marine Sponge-Derived Strain’, 10(October), pp. 1–14. doi: 10.3389/fmicb.2019.02187.

Amaral-Zettler, L. A., Zettler, E. R. and Mincer, T. J. (2020) ‘Ecology of the plastisphere’, *Nature Reviews Microbiology*, 18(3), pp. 139–151. doi: 10.1038/s41579-019-0308-0.

Amini, B. *et al.* (2004) ‘A model of the respiratory central pattern generator’, in *The 26th Annual International Conference of the IEEE Engineering in Medicine and Biology Society*. IEEE, pp. 4580–4583. doi: 10.1109/IEMBS.2004.1404270.

Arabolaza, A. *et al.* (2008) ‘Multiple Pathways for Triacylglycerol Biosynthesis in Streptomyces coelicolor □’, 74(9), pp. 2573–2582. doi: 10.1128/AEM.02638-07.

Arregui, L. *et al.* (2019) ‘Laccases : structure , function , and potential application in water bioremediation’, *Microbial Cell Factories*, pp. 1–33. doi: 10.1186/s12934-019-1248-0.

Arthur, C., Baker, J. and Bamford, H. (2009) *Proceedings of the International Research Workshop on the Occurrence , Effects , and Fate of Microplastic Marine Debris*, *Group*.

Austin, H. P. *et al.* (2018) ‘Characterization and engineering of a plastic-degrading aromatic polyesterase.’, *Proceedings of the National Academy of Sciences of the United States of America*, 115(19), pp. E4350–E4357. doi: 10.1073/pnas.1718804115.

Awasthi, S. *et al.* (2017) ‘Biodegradation of thermally treated low density polyethylene by fungus Rhizopus oryzae NS 5’, *3 Biotech*, 7(1), p. 73. doi: 10.1007/s13205-017-0699-4.

Awasthi, S., Srivastava, P. and Singh, P. (2017) ‘Biodegradation of thermally treated high-density polyethylene (HDPE) by Klebsiella pneumoniae CH001’, *3 Biotech*, 7(5), pp. 1–10. doi: 10.1007/s13205-017-0959-3.

Balachandran, C. *et al.* (2012) ‘Petroleum and polycyclic aromatic hydrocarbons (PAHs) degradation and naphthalene metabolism in Streptomyces sp. (ERI-CPDA-1) isolated from oil contaminated soil’, *Bioresource Technology*, 112, pp. 83–90. doi: 10.1016/j.biortech.2012.02.059.

Ballerini, T., Andrady, A. L. and Cole, M. (2018) *Plastic pollution in the ocean: what we know and what we don’t know about*, *Plastic and Ocean Platform*. doi: 10.13140/RG.2.2.36720.92160.

Ballerstedt, H. *et al.* (2021) ‘MIXed plastics biodegradation and UPcycling using microbial communities: EU Horizon 2020 project MIX-UP started January 2020’, *Environmental Sciences Europe*, 33(1), p. 99. doi: 10.1186/s12302-021-00536-5.

Bao, W. *et al.* (1994) ‘Oxidative degradation of non-phenolic lignin during lipid peroxidation by fungal manganese peroxidase’, *FEBS Letters*, 354(3), pp.

297–300. doi: 10.1016/0014-5793(94)01146-X.

Barka, E. A. *et al.* (2016) ‘Taxonomy, Physiology, and Natural Products of Actinobacteria’, *Microbiology and Molecular Biology Reviews*, 80(1), pp. 1–43. doi: 10.1128/MMBR.00019-15.

Barth, M. *et al.* (2016) ‘A dual enzyme system composed of a polyester hydrolase and a carboxylesterase enhances the biocatalytic degradation of polyethylene terephthalate films’, *Biotechnology Journal*, 11(8), pp. 1082–1087. doi: 10.1002/biot.201600008.

Bashir, S. M. *et al.* (2021) ‘Personal Care and Cosmetic Products as a Potential Source of Environmental Contamination by Microplastics in a Densely Populated Asian City’, *Frontiers in Marine Science*, 8(June), pp. 1–11. doi: 10.3389/fmars.2021.683482.

van Beilen, J. B. *et al.* (2001) ‘Analysis of Pseudomonas putida alkane-degradation gene clusters and flanking insertion sequences: evolution and regulation of the alk genes The EMBL accession numbers for the sequences reported in this paper are AJ245436 [P. putida (oleovorans) GPo1 alk g’, *Microbiology*, 147(6), pp. 1621–1630. doi: 10.1099/00221287-147-6-1621.

Benítez-Chao, D. F. *et al.* (2021) ‘Bacteriocins: An Overview of Antimicrobial, Toxicity, and Biosafety Assessment by in vivo Models’, *Frontiers in Microbiology*, 12(April), pp. 1–18. doi: 10.3389/fmicb.2021.630695.

Bentley, S. D. *et al.* (2002) ‘Complete genome sequence of the model actinomycete Streptomyces coelicolor A3(2)’, *Nature*, 417(6885), pp. 141–147. doi: 10.1038/417141a.

Blin, K. *et al.* (2021) ‘antiSMASH 6.0: improving cluster detection and comparison capabilities’, *Nucleic Acids Research*, 49(W1), pp. W29–W35. doi: 10.1093/nar/gkab335.

Bocci, E. *et al.* (2014) ‘State of Art of Small Scale Biomass Gasification Power Systems: A Review of the Different Typologies’, *Energy Procedia*, 45, pp. 247–256. doi: 10.1016/j.egypro.2014.01.027.

Boerger, C. M. *et al.* (2010) ‘Plastic ingestion by planktivorous fishes in the North Pacific Central Gyre’, *Marine Pollution Bulletin*, 60(12), pp. 2275–2278. doi: 10.1016/j.marpolbul.2010.08.007.

Boll, M. *et al.* (2020) ‘Microbial degradation of phthalates: biochemistry and environmental implications’, *Environmental Microbiology Reports*, 12(1), pp. 3–15. doi: 10.1111/1758-2229.12787.

Bombelli, P. and Howe, C. J. (2017) ‘Polyethylene bio-degradation by caterpillars of the wax moth Galleria mellonella’, *Current Biology*, 27(8), pp. R292–R293. doi: 10.1016/j.cub.2017.02.060.

Bonhomme, S. *et al.* (2003) ‘Environmental biodegradation of polyethylene’, *Polymer Degradation and Stability*, 81(3), pp. 441–452. doi: 10.1016/S0141-3910(03)00129-0.

Borodina, I., Krabben, P. and Nielsen, J. (2005) ‘Genome-scale analysis of Streptomyces coelicolor A3(2) metabolism’, *Genome Research*, 15(6), pp. 820–829. doi: 10.1101/gr.3364705.

Boucher, J. and Friot, D. (2017) *Primary microplastics in the oceans: A global evaluation of sources*. IUCN International Union for Conservation of Nature. doi: 10.2305/IUCN.CH.2017.01.en.

Brandon, J. A., Jones, W. and Ohman, M. D. (2019) ‘Multidecadal increase in plastic particles in coastal ocean sediments’, *Science Advances*, 5(9), pp. 1–7. doi: 10.1126/sciadv.aax0587.

Brooks, A. L., Wang, S. and Jambeck, J. R. (2018) ‘The Chinese import ban and its impact on global plastic waste trade’, *Science Advances*, 4(6), pp. 1–8. doi: 10.1126/sciadv.aat0131.

Browne, M. A. *et al.* (2011) ‘Accumulation of microplastic on shorelines woldwide: sources and sinks.’, *Environmental science & technology*, 45(21), pp. 9175–9. doi: 10.1021/es201811s.

Buchakjian, M. R. *et al.* (2018) ‘Independent Predictors of Prognosis Based on Oral Cavity Squamous Cell Carcinoma Surgical Margins.’,

Otolaryngology--head and neck surgery : official journal of American Academy of Otolaryngology-Head and Neck Surgery, 159(4), pp. 675–682. doi: 10.1177/0194599818773070.

Bunaciu, A. A., Udriştioiu, E. gabriela and Aboul-Enein, H. Y. (2015) 'X-Ray Diffraction: Instrumentation and Applications', *Critical Reviews in Analytical Chemistry*, 45(4), pp. 289–299. doi: 10.1080/10408347.2014.949616.

Carnegie, D. and Ramsay, J. A. (2009) 'Anaerobic ethylene glycol degradation by microorganisms in poplar and willow rhizospheres', *Biodegradation*, 20(4), pp. 551–558. doi: 10.1007/s10532-008-9244-9.

Carr, C. M., Clarke, D. J. and Dobson, A. D. W. (2020) 'Microbial Polyethylene Terephthalate Hydrolases: Current and Future Perspectives', *Frontiers in Microbiology*, 11(November 2020), pp. 1–23. doi: 10.3389/fmicb.2020.571265.

Celina, M. *et al.* (1997) 'FTIR emission spectroscopy applied to polymer degradation', *Polymer Degradation and Stability*, 58(1–2), pp. 15–31. doi: 10.1016/S0141-3910(96)00218-2.

Chamas, A. *et al.* (2020) 'Degradation Rates of Plastics in the Environment', *ACS Sustainable Chemistry & Engineering*, 8(9), pp. 3494–3511. doi: 10.1021/acssuschemeng.9b06635.

Chater, K. F. *et al.* (2010) 'The complex extracellular biology of Streptomyces', *FEMS Microbiology Reviews*, 34(2), pp. 171–198. doi: 10.1111/j.1574-6976.2009.00206.x.

Chater, K. F. (2016) 'Recent advances in understanding Streptomyces', *F1000Research*, 5(0), p. 2795. doi: 10.12688/f1000research.9534.1.

Chen, T. S. S., Chang, C. and Floss, H. G. (1981) 'Biosynthesis of boromycin', *The Journal of Organic Chemistry*, 46(13), pp. 2661–2665. doi: 10.1021/jo00326a010.

Chenprakhon, P., Wongnate, T. and Chaiyen, P. (2019) 'Monooxygenation of aromatic compounds by flavin-dependent monooxygenases', *Protein*

Science, 28(1), pp. 8–29. doi: 10.1002/pro.3525.

Cho, H. S. *et al.* (2011) 'Biodegradability and biodegradation rate of poly(caprolactone)-starch blend and poly(butylene succinate) biodegradable polymer under aerobic and anaerobic environment', *Waste Management*, 31(3), pp. 475–480. doi: 10.1016/j.wasman.2010.10.029.

Comba, S. *et al.* (2013) 'Identification and physiological characterization of phosphatidic acid phosphatase enzymes involved in triacylglycerol biosynthesis in Streptomyces coelicolor', *Microbial Cell Factories*, 12(1), p. 9. doi: 10.1186/1475-2859-12-9.

Crespy, D., Bozonnet, M. and Meier, M. (2008) '100 Years of Bakelite, the Material of a 1000 Uses', *Angewandte Chemie International Edition*, 47(18), pp. 3322–3328. doi: 10.1002/anie.200704281.

Crownhart, C. (2021) *A French company is using enzymes to recycle one of the most common single-use plastics*. Available at: https://www.technologyreview.com/2021/10/06/1036571/carbios-enzymes-recycle-plastics-pet/ (Accessed: 2 March 2023).

Cui, Y. *et al.* (2021) 'Computational Redesign of a PETase for Plastic Biodegradation under Ambient Condition by the GRAPE Strategy', *ACS Catalysis*, 11(3), pp. 1340–1350. doi: 10.1021/acscatal.0c05126.

Damayanti and Wu, H. (2021) 'Strategic Possibility Routes of Recycled PET', *Polymers*, 13(9), p. 1475. doi: 10.3390/polym13091475.

Danso, D., Chow, J. and Streit, W. R. (2019) 'Plastics: Environmental and Biotechnological Perspectives on Microbial Degradation', *Applied and Environmental Microbiology*. Edited by H. L. Drake, 85(19), pp. 1–14. doi: 10.1128/AEM.01095-19.

Deng, Q. *et al.* (2019) 'Streptomyces avermitilis industrial strain as cell factory for Ivermectin B1a production', *Synthetic and Systems Biotechnology*, 4(1), pp. 34–39. doi: 10.1016/j.synbio.2018.12.003.

Distler, J. *et al.* (1987) 'Gene cluster for streptomycin biosynthesis in

Streptomyces griseus : nucleotide sequence of three genes and analysis of transcriptional activity', *Nucleic Acids Research*, 15(19), pp. 8041–8056. doi: 10.1093/nar/15.19.8041.

Dobrindt, U. *et al.* (2004) 'Genomic islands in pathogenic and environmental microorganisms', *Nature Reviews Microbiology*, 2(5), pp. 414–424. doi: 10.1038/nrmicro884.

Edwards, S. *et al.* (2022) 'Microbial Consortia and Mixed Plastic Waste: Pangenomic Analysis Reveals Potential for Degradation of Multiple Plastic Types via Previously Identified PET Degrading Bacteria', *International Journal of Molecular Sciences*, 23(10), p. 5612. doi: 10.3390/ijms23105612.

Edwards, U. *et al.* (1989) 'Isolation and direct complete nucleotide determination of entire genes. Characterization of a gene coding for 16S ribosomal RNA', *Nucleic Acids Research*, 17(19), pp. 7843–7853. doi: 10.1093/nar/17.19.7843.

Ehara, K. *et al.* (2000) 'Polyethylene degradation by manganese peroxidase in the absence of hydrogen peroxide', *Journal of Wood Science*, 46(2), pp. 180–183. doi: 10.1007/BF00777369.

Eid, J. *et al.* (2009) 'Real-Time DNA Sequencing from Single Polymerase Molecules', *Science*, 323(5910), pp. 133–138. doi: 10.1126/science.1162986.

El-Shafei, H. A. *et al.* (1998) 'Biodegradation of disposable polyethylene by fungi and Streptomyces species', *Polymer Degradation and Stability*, 62(2), pp. 361–365. doi: 10.1016/S0141-3910(98)00019-6.

Essel, R. *et al.* (2015) *Sources of microplastics relevant to marine protection in Germany*, *Umweltbundesamt*. Available at: https://d3n8a8pro7vhmx.cloudfront.net/boomerangalliance/pages/509/attachments/original/1481157150/Sources_of_Microplastics_Relevant_to_Marine_Protection_in_German.pdf?1481157150.

European Bioplastics (2018) *Fact sheet: What are bioplastics? Material Types, Terminology and Labels - An Introduction*, *European Bioplastics:*

Berlin, Germany. Available at: https://docs.european-bioplastics.org/2016/publications/fs/EUBP_fs_what_are_bioplastics.pdf.

EuropePlastics (2020) *Plastics – the Facts 2020*. Available at: https://www.plasticseurope.org/application/files/3416/2270/7211/Plastics_the_facts-WEB-2020_versionJun21_final.pdf%0Ahttps://www.plasticseurope.org/en/resources/publications/4312-plastics-facts-2020.

Farady, S. E. (2019) 'Microplastics as a new, ubiquitous pollutant: Strategies to anticipate management and advise seafood consumers', *Marine Policy*, 104(December 2018), pp. 103–107. doi: 10.1016/j.marpol.2019.02.020.

Farzi, A., Dehnad, A. and Fotouhi, A. F. (2019) 'Biodegradation of polyethylene terephthalate waste using Streptomyces species and kinetic modeling of the process', *Biocatalysis and Agricultural Biotechnology*, 17(October 2018), pp. 25–31. doi: 10.1016/j.bcab.2018.11.002.

Feng, L. *et al.* (2007) 'Genome and proteome of long-chain alkane degrading Geobacillus thermodenitrificans NG80-2 isolated from a deep-subsurface oil reservoir', *Proceedings of the National Academy of Sciences*, 104(13), pp. 5602–5607. doi: 10.1073/pnas.0609650104.

Fernández-Martínez, L. T. *et al.* (2014) 'New Insights into Chloramphenicol Biosynthesis in Streptomyces venezuelae ATCC 10712', *Antimicrobial Agents and Chemotherapy*, 58(12), pp. 7441–7450. doi: 10.1128/AAC.04272-14.

Fernández, Y., Arenillas, A. and Menéndez, J. Á. (2011) 'Microwave Heating Applied to Pyrolysis'.

Flärdh, K. and Buttner, M. J. (2009) 'Streptomyces morphogenetics: dissecting differentiation in a filamentous bacterium', *Nature Reviews Microbiology*, 7(1), pp. 36–49. doi: 10.1038/nrmicro1968.

Flowers, T. H. and Williams, S. T. (1977) 'Measurement of Growth Rates of Streptomycetes: Comparison of Turbidimetric and Gravimetric Techniques', *Journal of General Microbiology*, 98(1), pp. 285–289. doi: 10.1099/00221287-

98-1-285.

Fontanella, S. *et al.* (2010) ‘Comparison of the biodegradability of various polyethylene films containing pro-oxidant additives’, *Polymer Degradation and Stability*, 95(6), pp. 1011–1021. doi: 10.1016/j.polymdegradstab.2010.03.009.

Franden, M. A. *et al.* (2018) ‘Engineering Pseudomonas putida KT2440 for efficient ethylene glycol utilization’, *Metabolic Engineering*, 48(June), pp. 197–207. doi: 10.1016/j.ymben.2018.06.003.

Franeker, J. A. Van, Heubeck, M. and Stienen, E. W. M. (2005) *’ Save the North Sea ’ Fulmar Study 2002-2004 : a regional pilot project for the Fulmar-Litter-EcoQO in the OSPAR area*. Available at: https://www.researchgate.net/publication/40120730_%27Save_the_North_Sea%27_Fulmar_Study_2002-2004_a_regional_pilot_project_for_the_Fulmar-Litter-EcoQO_in_the_OSPAR_area.

Fuchs, G., Boll, M. and Heider, J. (2011) ‘Microbial degradation of aromatic compounds — from one strategy to four’, *Nature Reviews Microbiology*, 9(11), pp. 803–816. doi: 10.1038/nrmicro2652.

Fujisawa, M., Hirai, H. and Nishida, T. (2001) ‘Degradation of Polyethylene and Nylon-66 by the Laccase-Mediator System’, *Journal of Polymers and the Environment*, 9(3), pp. 103–108. doi: /10.1023.

Gertz, E. M. *et al.* (2006) ‘Composition-based statistics and translated nucleotide searches: Improving the TBLASTN module of BLAST’, *BMC Biology*, 4(1), p. 41. doi: 10.1186/1741-7007-4-41.

Geyer, R., Jambeck, J. R. and Law, K. L. (2017) ‘Production, use, and fate of all plastics ever made’, *Science Advances*, 3(7), pp. 3–8. doi: 10.1126/sciadv.1700782.

Ghatge, S. *et al.* (2020) ‘Biodegradation of polyethylene: a brief review’, *Applied Biological Chemistry*, 63(1), p. 27. doi: 10.1186/s13765-020-00511-3.

Ghogare, P. D. and Gupta, S. G. (2012) ‘Degradation of Mono Ethylene

Glycol by Few Selected Microorganisms and Developed Microbial Consortium', *International Journal of Microbiological Research*, 3(2), pp. 93–98. doi: 10.5829/idosi.ijmr.2012.3.2.5380.

Gill, P., Moghadam, T. T. and Ranjbar, B. (2010) 'Differential Scanning Calorimetry Techniques : Applications in Biology and Nanoscience', pp. 167–193.

Goldberg, D. (1995) 'A review of the biodegradability and utility of poly(caprolactone)', *Journal of Environmental Polymer Degradation*, 3(2), pp. 61–67. doi: 10.1007/BF02067481.

Goodwin, S., McPherson, J. D. and McCombie, W. R. (2016) 'Coming of age: ten years of next-generation sequencing technologies', *Nature Reviews Genetics*, 17(6), pp. 333–351. doi: 10.1038/nrg.2016.49.

Gordon, J. C. *et al.* (2005) 'H++: a server for estimating pKas and adding missing hydrogens to macromolecules', *Nucleic Acids Research*, 33(Web Server), pp. W368–W371. doi: 10.1093/nar/gki464.

Guerranti, C. *et al.* (2019) 'Microplastics in cosmetics: Environmental issues and needs for global bans', *Environmental Toxicology and Pharmacology*, 68, pp. 75–79. doi: 10.1016/j.etap.2019.03.007.

Guevara, G. *et al.* (2019) 'New insights into the genome of Rhodococcus ruber strain Chol-4', *BMC Genomics*, 20(1), p. 332. doi: 10.1186/s12864-019-5677-2.

Guo, Y. *et al.* (2008) 'A multilocus phylogeny of the Streptomyces griseus 16S rRNA gene clade: use of multilocus sequence analysis for streptomycete systematics', *INTERNATIONAL JOURNAL OF SYSTEMATIC AND EVOLUTIONARY MICROBIOLOGY*, 58(1), pp. 149–159. doi: 10.1099/ijs.0.65224-0.

Gyung Yoon, M., Jeong Jeon, H. and Nam Kim, M. (2012) 'Biodegradation of Polyethylene by a Soil Bacterium and AlkB Cloned Recombinant Cell', *Journal of Bioremediation & Biodegradation*, 03(04). doi: 10.4172/2155-6199.1000145.

Hadad, D., Geresh, S. and Sivan, A. (2005) ‘Biodegradation of polyethylene by the thermophilic bacterium Brevibacillus borstelensis’, *Journal of Applied Microbiology*, 98(5), pp. 1093–1100. doi: 10.1111/j.1365-2672.2005.02553.x.

Hae-Reun, A., Hyun-Joo, P. and Eung-Soo, K. (2000) ‘Characterization of Benzoate Degradation via ortho-Cleavage by Streptomyces setonii’, *Journal of Microbiology and Biotechnology*, 10(1), pp. 111–114. Available at: https://koreascience.kr/article/JAKO200011919943847.pdf.

Hahladakis, J. N. *et al.* (2018) ‘An overview of chemical additives present in plastics: Migration, release, fate and environmental impact during their use, disposal and recycling’, *Journal of Hazardous Materials*, 344, pp. 179–199. doi: 10.1016/j.jhazmat.2017.10.014.

Han, X. *et al.* (2017) ‘Structural insight into catalytic mechanism of PET hydrolase’, *Nature Communications*, 8(1), p. 2106. doi: 10.1038/s41467-017-02255-z.

Haram, L. E. *et al.* (2020) ‘A Plasticene Lexicon’, *Marine Pollution Bulletin*, 150(August), p. 110714. doi: 10.1016/j.marpolbul.2019.110714.

Herrero Acero, E. *et al.* (2011) ‘Enzymatic Surface Hydrolysis of PET: Effect of Structural Diversity on Kinetic Properties of Cutinases from Thermobifida’, *Macromolecules*, 44(12), pp. 4632–4640. doi: 10.1021/ma200949p.

Hodgson, D. A. (2000) ‘Primary metabolism and its control in streptomycetes: a most unusual group of bacteria.’, *Advances in microbial physiology*, 42, pp. 47–238. doi: 10.1016/s0065-2911(00)42003-5.

Huang, Y. *et al.* (2019) ‘LDPE microplastic films alter microbial community composition and enzymatic activities in soil’, *Environmental Pollution*, 254, p. 112983. doi: 10.1016/j.envpol.2019.112983.

Huerta Lwanga, E. *et al.* (2018) ‘Decay of low-density polyethylene by bacteria extracted from earthworm’s guts: A potential for soil restoration’, *Science of The Total Environment*, 624, pp. 753–757. doi: 10.1016/j.scitotenv.2017.12.144.

Ikeda, H. *et al.* (2003) ‘Complete genome sequence and comparative analysis of the industrial microorganism Streptomyces avermitilis’, *Nature Biotechnology*, 21(5), pp. 526–531. doi: 10.1038/nbt820.

Jabloune, R. *et al.* (2020) ‘Enzymatic Degradation of *p*-Nitrophenyl Esters, Polyethylene Terephthalate, Cutin, and Suberin by Sub1, a Suberinase Encoded by the Plant Pathogen *Streptomyces scabies*’, *Microbes and Environments*, 35(1), p. n/a. doi: 10.1264/jsme2.ME19086.

Jambeck, J. R. *et al.* (2015) ‘Marine pollution. Plastic waste inputs from land into the ocean.’, *Science (New York, N.Y.)*, 347(6223), pp. 768–71. doi: 10.1126/science.1260352.

Janusz, G. *et al.* (2020) ‘Laccase Properties, Physiological Functions, and Evolution’, *International Journal of Molecular Sciences*, 21(3), p. 966. doi: 10.3390/ijms21030966.

Jog, J. P. (1995) ‘Crystallization of Polyethyleneterephthalate’, *Journal of Macromolecular Science, Part C: Polymer Reviews*, 35(3), pp. 531–553. doi: 10.1080/15321799508014598.

Johnson, J. S. *et al.* (2019) ‘Evaluation of 16S rRNA gene sequencing for species and strain-level microbiome analysis’, *Nature Communications*, 10(1), p. 5029. doi: 10.1038/s41467-019-13036-1.

Joltreau, E. (2022) ‘Five Years after China ’ s Plastic Import Ban Have Europeans Taken Responsibility ?’, *Briefings de l’Ifri*, p. 11. Available at: https://www.ifri.org/sites/default/files/atoms/files/joltreau_plastic_waste_after_chinas_ban_2022.pdf.

de Jong, W. *et al.* (2009) ‘Attachment of Streptomyces coelicolor is mediated by amyloidal fimbriae that are anchored to the cell surface via cellulose’, *Molecular Microbiology*, 73(6), pp. 1128–1140. doi: 10.1111/j.1365-2958.2009.06838.x.

Joo, S. *et al.* (2018) ‘Structural insight into molecular mechanism of poly(ethylene terephthalate) degradation’, *Nature Communications*, 9(1), p. 382. doi: 10.1038/s41467-018-02881-1.

Jumper, J. *et al.* (2021) ‘Highly accurate protein structure prediction with AlphaFold’, *Nature*, 596(7873), pp. 583–589. doi: 10.1038/s41586-021-03819-2.

Jun, H. S. *et al.* (1994) ‘Synthesis of copolyesters containing poly(ethylene terephthalate) and poly(ε-caprolactone) units and their susceptibility toPseudomonas sp. lipase’, *Journal of Environmental Polymer Degradation*, 2(1), pp. 9–18. doi: 10.1007/BF02073482.

Kanehisa, M. (2000) ‘KEGG: Kyoto Encyclopedia of Genes and Genomes’, *Nucleic Acids Research*, 28(1), pp. 27–30. doi: 10.1093/nar/28.1.27.

Kannahi, M. and Sudha, P. (2013) ‘Screening of polythene and plastic degrading microbes from Muthupet mangrove soil’, *Journal of Chemical and Pharmaceutical Research,* 5(8), pp. 122–127.

Karbalaei, S. *et al.* (2018) ‘Occurrence, sources, human health impacts and mitigation of microplastic pollution’, *Environmental Science and Pollution Research*, 25(36), pp. 36046–36063. doi: 10.1007/s11356-018-3508-7.

Karegoudar, T. B. and Pujar, B. G. (1985) ‘Degradation of terephthalic acid by a Bacillus species’, *FEMS Microbiology Letters*, 30(1–2), pp. 217–220. doi: 10.1111/j.1574-6968.1985.tb01015.x.

Kawai, F. (1995) ‘Bacterial degradation of glycol ethers’, *Applied Microbiology and Biotechnology*, 44(3–4), pp. 532–538. doi: 10.1007/BF00169956.

Kawai, F., Kawabata, T. and Oda, M. (2019) ‘Current knowledge on enzymatic PET degradation and its possible application to waste stream management and other fields’, *Applied Microbiology and Biotechnology*, 103(11), pp. 4253–4268. doi: 10.1007/s00253-019-09717-y.

Khaghanikavkani, E. (2013) ‘Microwave Pyrolysis of Plastic’, *Journal of Chemical Engineering & Process Technology*, 04(03). doi: 10.4172/2157-7048.1000150.

Khalil, M. *et al.* (2019) ‘The Plant Pathogenic Bacterium Streptomyces

scabies Degrades the Aromatic Components of Potato Periderm via the β-Ketoadipate Pathway', *Frontiers in Microbiology*, 10(December), pp. 1–13. doi: 10.3389/fmicb.2019.02795.

Kieser, T. *et al.* (2000) *Practical Streptomyces Genetics: A Laboratory Manual*. Edited by Illustrated. John Innes Foundation. Available at: https://streptomyces.org.uk/PracticalStreptomycesGenetics.pdf.

Kieser, T *et al.* (2000) *Practical streptomyces genetics*. John Innes Foundation. doi: 10.4236.

Kitani, S. *et al.* (2011) 'Avenolide, a Streptomyces hormone controlling antibiotic production in Streptomyces avermitilis', *Proceedings of the National Academy of Sciences*, 108(39), pp. 16410–16415. doi: 10.1073/pnas.1113908108.

Kiviharju, K. *et al.* (2007) 'A chemostat study of Streptomyces peucetius var. caesius N47', *Applied Microbiology and Biotechnology*, 73(6), pp. 1267–1274. doi: 10.1007/s00253-006-0607-z.

Kleber, H.-P. *et al.* (1978) 'Beziehungen zwischen Carnitinstoffwechsel und Fetts�ureassimilation bei Pseudomonas putida', *Archives of Microbiology*, 116(2), pp. 213–220. doi: 10.1007/BF00406039.

Knott, B. C. *et al.* (2020) 'Characterization and engineering of a two-enzyme system for plastics depolymerization', *Proceedings of the National Academy of Sciences*, 117(41), pp. 25476–25485. doi: 10.1073/pnas.2006753117.

Koepff, J. *et al.* (2018) 'Germination and Growth Analysis of Streptomyces lividans at the Single-Cell Level Under Varying Medium Compositions', *Frontiers in Microbiology*, 9(NOV), pp. 1–10. doi: 10.3389/fmicb.2018.02680.

Kumar, A. and Chandra, R. (2020) 'Ligninolytic enzymes and its mechanisms for degradation of lignocellulosic waste in environment', *Heliyon*, 6(2), p. e03170. doi: 10.1016/j.heliyon.2020.e03170.

Kumar Sen, S. and Raut, S. (2015) 'Microbial degradation of low density polyethylene (LDPE): A review', *Journal of Environmental Chemical*

Engineering, 3(1), pp. 462–473. doi: 10.1016/j.jece.2015.01.003.

Lacey, H. J. and Rutledge, P. J. (2022) 'Recently Discovered Secondary Metabolites from Streptomyces Species', *Molecules*, 27(3), p. 887. doi: 10.3390/molecules27030887.

Land, M. *et al.* (2015) 'Insights from 20 years of bacterial genome sequencing', *Functional & Integrative Genomics*, 15(2), pp. 141–161. doi: 10.1007/s10142-015-0433-4.

Lear, G. *et al.* (2021) 'Plastics and the microbiome: impacts and solutions', *Environmental Microbiome*, 16(1), p. 2. doi: 10.1186/s40793-020-00371-w.

Lear, G. *et al.* (2022) 'Microbial abilities to degrade global environmental plastic polymer waste are overstated', *Environmental Research Letters*, 17(4), p. 043002. doi: 10.1088/1748-9326/ac59a7.

Leblond, P. and Decaris, B. (1994) 'New insights into the genetic instability of streptomyces.', *FEMS microbiology letters*, 123(3), pp. 225–32. doi: 10.1111/j.1574-6968.1994.tb07229.x.

Lee, B. *et al.* (1991) 'Biodegradation of Degradable Plastic Polyethylene by Phanerochaete and Streptomyces Species', *Applied and Environmental Microbiology*, 57(3), pp. 678–685. doi: 10.1128/aem.57.3.678-685.1991.

Lee, N. *et al.* (2020) 'Thirty complete Streptomyces genome sequences for mining novel secondary metabolite biosynthetic gene clusters', *Scientific Data*, 7(1), p. 55. doi: 10.1038/s41597-020-0395-9.

Leslie, H. A. *et al.* (2022) 'Discovery and quantification of plastic particle pollution in human blood', *Environment International*, 163(December 2021), p. 107199. doi: 10.1016/j.envint.2022.107199.

Li, L. *et al.* (2008) 'Crystal Structure of Long-Chain Alkane Monooxygenase (LadA) in Complex with Coenzyme FMN: Unveiling the Long-Chain Alkane Hydroxylase', *Journal of Molecular Biology*, 376(2), pp. 453–465. doi: 10.1016/j.jmb.2007.11.069.

Li, P. *et al.* (2021) 'Characteristics of Plastic Pollution in the Environment: A

Review', *Bulletin of Environmental Contamination and Toxicology*, 107(4), pp. 577–584. doi: 10.1007/s00128-020-02820-1.

Li, W. *et al.* (2019) 'Laboratory evolution reveals the metabolic and regulatory basis of ethylene glycol metabolism by Pseudomonas putida KT2440', *Environmental Microbiology*, 21(10), pp. 3669–3682. doi: 10.1111/1462-2920.14703.

de Lima Procópio, R. E. *et al.* (2012) 'Antibiotics produced by Streptomyces', *The Brazilian Journal of Infectious Diseases*, 16(5), pp. 466–471. doi: 10.1016/j.bjid.2012.08.014.

Longo, N., Frigeni, M. and Pasquali, M. (2016) 'Carnitine transport and fatty acid oxidation', *Biochimica et Biophysica Acta (BBA) - Molecular Cell Research*, 1863(10), pp. 2422–2435. doi: 10.1016/j.bbamcr.2016.01.023.

Lu, H. *et al.* (2022) 'Machine learning-aided engineering of hydrolases for PET depolymerization', *Nature*, 604(7907), pp. 662–667. doi: 10.1038/s41586-022-04599-z.

Lu, Y. *et al.* (2016) 'Uptake and Accumulation of Polystyrene Microplastics in Zebrafish (Danio rerio) and Toxic Effects in Liver', *Environmental Science & Technology*, 50(7), pp. 4054–4060. doi: 10.1021/acs.est.6b00183.

Lucas, N. *et al.* (2008) 'Polymer biodegradation: Mechanisms and estimation techniques – A review', *Chemosphere*, 73(4), pp. 429–442. doi: 10.1016/j.chemosphere.2008.06.064.

Ma, Y. *et al.* (2018) 'Enhanced Poly(ethylene terephthalate) Hydrolase Activity by Protein Engineering', *Engineering*, 4(6), pp. 888–893. doi: 10.1016/j.eng.2018.09.007.

De Maio, N. *et al.* (2019) 'Comparison of long-read sequencing technologies in the hybrid assembly of complex bacterial genomes', *Microbial Genomics*, 5(9). doi: 10.1099/mgen.0.000294.

Margulies, M. *et al.* (2005) 'Genome sequencing in microfabricated high-density picolitre reactors', *Nature*, 437(7057), pp. 376–380. doi:

10.1038/nature03959.

MASAI, E. *et al.* (2007) ‘Characterization of ligV Essential for Catabolism of Vanillin by Sphingomonas paucimobilis SYK-6’, *Bioscience, Biotechnology, and Biochemistry*, 71(10), pp. 2487–2492. doi: 10.1271/bbb.70267.

McDonald, B. R. and Currie, C. R. (2017) ‘Lateral Gene Transfer Dynamics in the Ancient Bacterial Genus Streptomyces’, *mBio*. Edited by P. Keim, 8(3), pp. 1–12. doi: 10.1128/mBio.00644-17.

Meadows, J. A. and Wargo, M. J. (2013) ‘Characterization of Pseudomonas aeruginosa Growth on O -Acylcarnitines and Identification of a Short-Chain Acylcarnitine Hydrolase’, *Applied and Environmental Microbiology*, 79(11), pp. 3355–3363. doi: 10.1128/AEM.03943-12.

Menendez-Bravo, S. *et al.* (2017) ‘Identification of FadAB Complexes Involved in Fatty Acid β-Oxidation in Streptomyces coelicolor and Construction of a Triacylglycerol Overproducing strain’, *Frontiers in Microbiology*, 8. doi: 10.3389/fmicb.2017.01428.

Meng, X. *et al.* (2021) ‘Protein engineering of stable IsPETase for PET plastic degradation by Premuse’, *International Journal of Biological Macromolecules*, 180(March), pp. 667–676. doi: 10.1016/j.ijbiomac.2021.03.058.

Miller, J. R., Koren, S. and Sutton, G. (2011) ‘Assembly Algorithms for Next-Generation Sequencing Data Jason’, 95(6), pp. 315–327. doi: 10.1016/j.ygeno.2010.03.001.Assembly.

Mohanan, N. *et al.* (2020) ‘Microbial and Enzymatic Degradation of Synthetic Plastics’, *Frontiers in Microbiology*, 11(November). doi: 10.3389/fmicb.2020.580709.

Montazer, Z., Habibi Najafi, M. B. and Levin, D. B. (2019) ‘Microbial degradation of low-density polyethylene and synthesis of polyhydroxyalkanoate polymers’, *Canadian Journal of Microbiology*, 65(3), pp. 224–234. doi: 10.1139/cjm-2018-0335.

Montazer, Z., Habibi Najafi, M. B. and Levin, D. B. (2020) ‘Challenges with

Verifying Microbial Degradation of Polyethylene', *Polymers*, 12(1), p. 123. doi: 10.3390/polym12010123.

Morales, D. K., Ocampo, W. and Zambrano, M. M. (2007) 'Efficient removal of hexavalent chromium by a tolerant Streptomyces sp. affected by the toxic effect of metal exposure', *Journal of Applied Microbiology*, 103(6), pp. 2704–2712. doi: 10.1111/j.1365-2672.2007.03510.x.

Mückschel, B. *et al.* (2012) 'Ethylene Glycol Metabolism by Pseudomonas putida', *Applied and Environmental Microbiology*, 78(24), pp. 8531–8539. doi: 10.1128/AEM.02062-12.

Müller, R.-J. *et al.* (2005) 'Enzymatic Degradation of Poly(ethylene terephthalate): Rapid Hydrolyse using a Hydrolase fromT. fusca', *Macromolecular Rapid Communications*, 26(17), pp. 1400–1405. doi: 10.1002/marc.200500410.

Myronovskyi, M. *et al.* (2013) 'Complete genome sequence of Streptomyces fulvissimus', *Journal of Biotechnology*, 168(1), pp. 117–118. doi: 10.1016/j.jbiotec.2013.08.013.

Nandiyanto, A. B. D., Oktiani, R. and Ragadhita, R. (2019) 'How to Read and Interpret FTIR Spectroscope of Organic Material', *Indonesian Journal of Science and Technology*, 4(1), p. 97. doi: 10.17509/ijost.v4i1.15806.

Neira-Velázquez, M. G. *et al.* (2013) 'Polymer Molecular Weight Measurement', in Vivaldo-Lima, E. S.́ıvar-G. and E. (ed.) *Handbook of Polymer Synthesis, Characterization, and Processing*. First Edit. Hoboken, NJ, USA: John Wiley & Sons, Inc., pp. 355–366. doi: 10.1002/9781118480793.ch17.

Newsome, T. *et al.* (2004) 'Presence of Bacterial Phage-Like DNA Sequences in Commercial Taq DNA Polymerase Reagents', *Journal of Clinical Microbiology*, 42(5), pp. 2264–2267. doi: 10.1128/JCM.42.5.2264-2267.2004.

Ng, E.-L. *et al.* (2018) 'An overview of microplastic and nanoplastic pollution in agroecosystems', *Science of The Total Environment*, 627, pp. 1377–1388.

doi: 10.1016/j.scitotenv.2018.01.341.

Nikodinovic, J., Barrow, K. D. and Chuck, J.-A. (2003) ‘High yield preparation of genomic DNA from Streptomyces’, *BioTechniques*, 35(5), pp. 932–936. doi: 10.2144/03355bm05.

Nishimura, M., Kawakami, S. and Otsuka, H. (2018) ‘Molecular cloning and characterization of vanillin dehydrogenase from Streptomyces sp. NL15-2K’, *BMC Microbiology*, 18(1), p. 154. doi: 10.1186/s12866-018-1309-2.

Nivina, A. *et al.* (2019) ‘Evolution and Diversity of Assembly-Line Polyketide Synthases’, *Chemical Reviews*, 119(24), pp. 12524–12547. doi: 10.1021/acs.chemrev.9b00525.

Nowak, B. *et al.* (2011) ‘Microorganisms participating in the biodegradation of modified polyethylene films in different soils under laboratory conditions’, *International Biodeterioration & Biodegradation*, 65(6), pp. 757–767. doi: 10.1016/j.ibiod.2011.04.007.

Opperdoes, F. R. and Lemey, P. (2009) ‘Phylogenetic analysis using protein sequences’, in Lemey, P., Salemi, M., and Vandamme, A.-M. (eds) *The Phylogenetic Handbook*. Cambridge: Cambridge University Press, pp. 313–342. doi: 10.1017/CBO9780511819049.011.

El Othmany, R. *et al.* (2021) ‘Current Understanding on Adhesion and Biofilm Development in Actinobacteria’, *International Journal of Microbiology*. Edited by J. Falkinham, 2021, pp. 1–11. doi: 10.1155/2021/6637438.

Pandit, A. V., Harrison, E. and Mahadevan, R. (2021) ‘Engineering Escherichia coli for the utilization of ethylene glycol’, *Microbial Cell Factories*, 20(1), p. 22. doi: 10.1186/s12934-021-01509-2.

Pérez, V. *et al.* (2021) ‘Ectoine Production from Biogas in Waste Treatment Facilities: A Techno-Economic and Sensitivity Analysis’, *ACS Sustainable Chemistry & Engineering*, 9(51), pp. 17371–17380. doi: 10.1021/acssuschemeng.1c06772.

Petković, H., Lukežič, T. and Šušković, J. (2017) ‘Biosynthesis of

Oxytetracycline by Streptomyces rimosus: Past, Present and Future Directions in the Development of Tetracycline Antibiotics', *Food Technology and Biotechnology*, 55(1), pp. 3–13. doi: 10.17113/ftb.55.01.17.4617.

Pirillo, V., Pollegioni, L. and Molla, G. (2021) 'Analytical methods for the investigation of enzyme-catalyzed degradation of polyethylene terephthalate', *The FEBS Journal*, 288(16), pp. 4730–4745. doi: 10.1111/febs.15850.

Plénat, T., Yoshizawa, S. and Fourmy, D. (2017) 'DNA-Guided Delivery of Single Molecules into Zero-Mode Waveguides', *ACS Applied Materials & Interfaces*, 9(36), pp. 30561–30566. doi: 10.1021/acsami.7b11953.

Pometto, A. L., Lee, B. T. and Johnson, K. E. (1992) 'Production of an extracellular polyethylene-degrading enzyme(s) by Streptomyces species', *Applied and Environmental Microbiology*, 58(2), pp. 731–733. doi: 10.1128/aem.58.2.731-733.1992.

Qureshi, M. S. *et al.* (2020) 'Pyrolysis of plastic waste: Opportunities and challenges', *Journal of Analytical and Applied Pyrolysis*, 152(October 2019), p. 104804. doi: 10.1016/j.jaap.2020.104804.

Rasmussen, S. C. (2021) 'From Parkesine to Celluloid: The Birth of Organic Plastics', *Angewandte Chemie*, 133(15), pp. 8090–8094. doi: 10.1002/ange.202015095.

Rehman, A. and McFadden, B. A. (1997) 'Lysine 194 Is Functional in Isocitrate Lyase from Escherichia coli', *Current Microbiology*, 35(1), pp. 14–17. doi: 10.1007/s002849900203.

Ren, L. *et al.* (2019) 'Biodegradation of Polyethylene by Enterobacter sp. D1 from the Guts of Wax Moth Galleria mellonella', *International Journal of Environmental Research and Public Health*, 16(11). doi: 10.3390/IJERPH16111941.

Repka, L. M. *et al.* (2017) 'Mechanistic Understanding of Lanthipeptide Biosynthetic Enzymes', *Chemical Reviews*, 117(8), pp. 5457–5520. doi: 10.1021/acs.chemrev.6b00591.

Restrepo-Flórez, J.-M., Bassi, A. and Thompson, M. R. (2014) 'Microbial degradation and deterioration of polyethylene – A review', *International Biodeterioration & Biodegradation*, 88, pp. 83–90. doi: 10.1016/j.ibiod.2013.12.014.

Rhoads, A. and Au, K. F. (2015) 'PacBio Sequencing and Its Applications', *Genomics, Proteomics & Bioinformatics*, 13(5), pp. 278–289. doi: 10.1016/j.gpb.2015.08.002.

Ribitsch, D. *et al.* (2011) 'Hydrolysis of polyethyleneterephthalate by p-nitrobenzylesterase from Bacillus subtilis', *Biotechnology Progress*, 27(4), pp. 951–960. doi: 10.1002/btpr.610.

Rintala, H. *et al.* (2001) 'PCR primers targeting the 16S rRNA gene for the specific detection of streptomycetes', *Molecular and Cellular Probes*, 15(6), pp. 337–347. doi: 10.1006/mcpr.2001.0379.

Rist, S. *et al.* (2018) 'A critical perspective on early communications concerning human health aspects of microplastics', *Science of The Total Environment*, 626, pp. 720–726. doi: 10.1016/j.scitotenv.2018.01.092.

Riyadi, F. A. *et al.* (2020) 'Enzymatic and genetic characterization of lignin depolymerization by Streptomyces sp. S6 isolated from a tropical environment', *Scientific Reports*, 10(1), p. 7813. doi: 10.1038/s41598-020-64817-4.

Rodríguez-Fonseca, M. F. *et al.* (2021) 'Streptomyces as Potential Synthetic Polymer Degraders: A Systematic Review', *Bioengineering*, 8(11), p. 154. doi: 10.3390/bioengineering8110154.

Romano, A. H. and Nickerson, W. J. (1956) 'THE BIOCHEMISTRY OF THE ACTINOMYCETALES. STUDIES ON THE CELL WALL OF STREPTOMYCES FRADIAE', *Journal of Bacteriology*, 72(4), pp. 478–482. doi: 10.1128/jb.72.4.478-482.1956.

Ronkvist, Å. M., Xie, W., Lu, W. and Gross, Richard A (2009) 'Cutinase-Catalyzed Hydrolysis of Poly(ethylene terephthalate)', *Macromolecules*, 42(14), pp. 5128–5138. doi: 10.1021/ma9005318.

Ronkvist, Å. M., Xie, W., Lu, W. and Gross, Richard A. (2009) ‘Cutinase-Catalyzed Hydrolysis of Poly(ethylene terephthalate)’, *Macromolecules*, 42(14), pp. 5128–5138. doi: 10.1021/ma9005318.

Rosenboom, J.-G., Langer, R. and Traverso, G. (2022) ‘Bioplastics for a circular economy’, *Nature Reviews Materials*, 7(2), pp. 117–137. doi: 10.1038/s41578-021-00407-8.

Rost, B. (1999) ‘Twilight zone of protein sequence alignments’, *Protein Engineering, Design and Selection*, 12(2), pp. 85–94. doi: 10.1093/protein/12.2.85.

Ru, J., Huo, Y. and Yang, Y. (2020) ‘Microbial Degradation and Valorization of Plastic Wastes’, *Frontiers in Microbiology*, 11(April). doi: 10.3389/fmicb.2020.00442.

Rüthi, J. *et al.* (2020) ‘The “Plastisphere” of Biodegradable Plastics Is Characterized by Specific Microbial Taxa of Alpine and Arctic Soils’, *Frontiers in Environmental Science*, 8(September), pp. 1–23. doi: 10.3389/fenvs.2020.562263.

Saadoun, I. *et al.* (2008) ‘Growth of Streptomyces spp. from hydrocarbon-polluted soil on diesel and their analysis for the presence of alkane hydroxylase gene (alkB) by PCR’, *World Journal of Microbiology and Biotechnology*, 24(10), pp. 2191–2198. doi: 10.1007/s11274-008-9729-z.

Sagong, H. *et al.* (2020) ‘Decomposition of the PET Film by MHETase Using Exo-PETase Function’, *ACS Catalysis*, 10(8), pp. 4805–4812. doi: 10.1021/acscatal.9b05604.

Sajwan, M., Aggarwal, S. and Singh, R. B. (2008) ‘Forensic characterization of HDPE pipes by DSC’, *Forensic Science International*, 175(2–3), pp. 130–133. doi: 10.1016/j.forsciint.2007.05.020.

Sam, S. T. *et al.* (2014) ‘Recent Advances in Polyolefins/Natural Polymer Blends Used for Packaging Application’, *Polymer-Plastics Technology and Engineering*, 53(6), pp. 631–644. doi: 10.1080/03602559.2013.866247.

Sander, M., Kohler, H.-P. E. and McNeill, K. (2019) ‘Assessing the environmental transformation of nanoplastic through 13C-labelled polymers’, *Nature Nanotechnology*, 14(4), pp. 301–303. doi: 10.1038/s41565-019-0420-3.

Santo, M., Weitsman, R. and Sivan, A. (2013) ‘The role of the copper-binding enzyme – laccase – in the biodegradation of polyethylene by the actinomycete Rhodococcus ruber’, *International Biodeterioration & Biodegradation*, 84, pp. 204–210. doi: 10.1016/j.ibiod.2012.03.001.

Sasoh, M. *et al.* (2006) ‘Characterization of the Terephthalate Degradation Genes of Comamonas sp. Strain E6’, *Applied and Environmental Microbiology*, 72(3), pp. 1825–1832. doi: 10.1128/AEM.72.3.1825-1832.2006.

Schuster, J. M., Schvezov, C. E. and Rosenberger, M. R. (2015) ‘Influence of Experimental Variables on the Measure of Contact Angle in Metals Using the Sessile Drop Method’, *Procedia Materials Science*, 8(2009), pp. 742–751. doi: 10.1016/j.mspro.2015.04.131.

Seger, C. (2012) ‘Usage and limitations of liquid chromatography-tandem mass spectrometry (LC–MS/MS) in clinical routine laboratories’, *Wiener Medizinische Wochenschrift*, 162(21–22), pp. 499–504. doi: 10.1007/s10354-012-0147-3.

SEJINY, M. (1991) ‘Growth Phases of Some Antibiotics Producing Streptomyces and their Identification’, *Journal of King Abdulaziz University-Science*, 3(1), pp. 21–29. doi: 10.4197/Sci.3-1.2.

Shahnawaz, M., Sangale, M. K. and Ade, A. B. (2016) ‘Rhizosphere of Avicennia marina (Forsk .) Vierh . as a landmark for polythene degrading bacteria’, *Environmental Science and Pollution Research*, pp. 14621–14635. doi: 10.1007/s11356-016-6542-3.

Shao, H. *et al.* (2019) ‘Complete Genome Sequence and Characterization of a Polyethylene Biodegradation Strain, Streptomyces Albogriseolus LBX-2’, *Microorganisms*, 7(10), p. 379. doi: 10.3390/microorganisms7100379.

Sievers, F. *et al.* (2011) ‘Fast, scalable generation of high-quality protein multiple sequence alignments using Clustal Omega’, *Molecular Systems Biology*, 7(1), p. 539. doi: 10.1038/msb.2011.75.

Singh, A. *et al.* (2021) ‘Techno-economic, life-cycle, and socioeconomic impact analysis of enzymatic recycling of poly(ethylene terephthalate)’, *Joule*, 5(9), pp. 2479–2503. doi: 10.1016/j.joule.2021.06.015.

Son, H. F. *et al.* (2019) ‘Rational Protein Engineering of Thermo-Stable PETase from Ideonella sakaiensis for Highly Efficient PET Degradation’, *ACS Catalysis*, 9(4), pp. 3519–3526. doi: 10.1021/acscatal.9b00568.

Son, H. F. *et al.* (2020) ‘Enzyme and Microbial Technology Structural bioinformatics-based protein engineering of thermo-stable PETase from Ideonella sakaiensis’, *Enzyme and Microbial Technology*, 141(May), p. 109656. doi: 10.1016/j.enzmictec.2020.109656.

Sudhakar, M. *et al.* (2008) ‘Marine microbe-mediated biodegradation of low- and high-density polyethylenes’, *International Biodeterioration & Biodegradation*, 61(3), pp. 203–213. doi: 10.1016/j.ibiod.2007.07.011.

Sulaiman, S. *et al.* (2012) ‘Isolation of a Novel Cutinase Homolog with Polyethylene Terephthalate-Degrading Activity from Leaf-Branch Compost by Using a Metagenomic Approach’, *Applied and Environmental Microbiology*, 78(5), pp. 1556–1562. doi: 10.1128/AEM.06725-11.

Sundt, P., Schulze, P.-E. and Syversen, F. (2014) *Sources of microplastic-pollution to the marine environment Project report*. Available at: https://d3n8a8pro7vhmx.cloudfront.net/boomerangalliance/pages/507/attachments/original/1481155578/Norway_Sources_of_Microplastic_Pollution.pdf?1481155578.

de Swart, H. E. and Zimmerman, J. T. F. (2009) ‘Morphodynamics of Tidal Inlet Systems’, *Annual Review of Fluid Mechanics*, 41(1), pp. 203–229. doi: 10.1146/annurev.fluid.010908.165159.

Szklarczyk, D. *et al.* (2019) ‘STRING v11: protein–protein association networks with increased coverage, supporting functional discovery in

genome-wide experimental datasets', *Nucleic Acids Research*, 47(D1), pp. D607–D613. doi: 10.1093/nar/gky1131.

Tan, F. *et al.* (2022) 'Genomics analysis and degradation characteristics of lignin by Streptomyces thermocarboxydus strain DF3-3', *Biotechnology for Biofuels and Bioproducts*, 15(1), p. 78. doi: 10.1186/s13068-022-02175-1.

Teng, J. L. L. *et al.* (2017) 'PacBio But Not Illumina Technology Can Achieve Fast, Accurate and Complete Closure of the High GC, Complex Burkholderia pseudomallei Two-Chromosome Genome', *Frontiers in Microbiology*, 8(August), pp. 1–15. doi: 10.3389/fmicb.2017.01448.

Then, J. *et al.* (2015a) 'Ca 2+ and Mg 2+ binding site engineering increases the degradation of polyethylene terephthalate films by polyester hydrolases from Thermobifida fusca', *Biotechnology Journal*, 10(4), pp. 592–598. doi: 10.1002/biot.201400620.

Then, J. *et al.* (2015b) 'Ca 2+ and Mg 2+ binding site engineering increases the degradation of polyethylene terephthalate films by polyester hydrolases from Thermobifida fusca', *Biotechnology Journal*, 10(4), pp. 592–598. doi: 10.1002/biot.201400620.

Thomas, R. T. and Sandhyarani, N. (2013) 'Enhancement in the photocatalytic degradation of low density polyethylene–TiO2 nanocomposite films under solar irradiation', *RSC Advances*, 3(33), p. 14080. doi: 10.1039/c3ra42226g.

Thompson, R. C. *et al.* (2004) 'Lost at Sea: Where Is All the Plastic?', *Science*, 304(5672), pp. 838–838. doi: 10.1126/science.1094559.

Tournier, V. *et al.* (2020) 'An engineered PET depolymerase to break down and recycle plastic bottles', *Nature*, 580(7802), pp. 216–219. doi: 10.1038/s41586-020-2149-4.

Tsirigotaki, A. *et al.* (2017) 'Protein export through the bacterial Sec pathway', *Nature Reviews Microbiology*, 15(1), pp. 21–36. doi: 10.1038/nrmicro.2016.161.

Tweeddale, H., Notley-McRobb, L. and Ferenci, T. (1998) ‘Effect of Slow Growth on Metabolism of Escherichia coli , as Revealed by Global Metabolite Pool (“Metabolome”) Analysis’, *Journal of Bacteriology*, 180(19), pp. 5109–5116. doi: 10.1128/JB.180.19.5109-5116.1998.

Untrau-Taghian, S. *et al.* (1995) ‘Influence of growth rate and precursor availability on spiramycin production in Streptomyces ambofaciens’, *Canadian Journal of Microbiology*, 41(2), pp. 157–162. doi: 10.1139/m95-021.

Vamsee-Krishna, C. and Phale, P. S. (2008) ‘Bacterial degradation of phthalate isomers and their esters’, *Indian Journal of Microbiology*, 48(1), pp. 19–34. doi: 10.1007/s12088-008-0003-8.

Vinaixa, M. *et al.* (2016) ‘Mass spectral databases for LC/MS- and GC/MS-based metabolomics: State of the field and future prospects’, *TrAC Trends in Analytical Chemistry*, 78, pp. 23–35. doi: 10.1016/j.trac.2015.09.005.

Volff, J.-N. and Altenbuchner, J. (1998) ‘Genetic instability of the Streptomyces chromosome’, *Molecular Microbiology*, 27(2), pp. 239–246. doi: 10.1046/j.1365-2958.1998.00652.x.

Volke-Sepúlveda, T. *et al.* (2002) ‘Thermally treated low density polyethylene biodegradation by Penicillium pinophilum and Aspergillus niger’, *Journal of Applied Polymer Science*, 83(2), pp. 305–314. doi: 10.1002/app.2245.

Waldman, W. R. and Rillig, M. C. (2020) ‘Microplastic Research Should Embrace the Complexity of Secondary Particles’, *Environmental Science & Technology*, 54(13), pp. 7751–7753. doi: 10.1021/acs.est.0c02194.

Wang, W. and Shao, Z. (2013) ‘Enzymes and genes involved in aerobic alkane degradation’, *Frontiers in Microbiology*, 4(May), pp. 1–7. doi: 10.3389/fmicb.2013.00116.

Wang, X. *et al.* (2008) ‘Preparation of a PET-Hydrolyzing Lipase from Aspergillus oryzae by the Addition of Bis(2-hydroxyethyl) Terephthalate to the Culture Medium and Enzymatic Modification of PET Fabrics’, *Engineering in Life Sciences*, 8(3), pp. 268–276. doi: 10.1002/elsc.200700058.

Wargo, M. J. and Meadows, J. A. (2015) ‘Carnitine in bacterial physiology and metabolism’, *Microbiology*, 161(6), pp. 1161–1174. doi: 10.1099/mic.0.000080.

Waterhouse, A. *et al.* (2018) ‘SWISS-MODEL: homology modelling of protein structures and complexes’, *Nucleic Acids Research*, 46(W1), pp. W296–W303. doi: 10.1093/nar/gky427.

Weber, C., Pusch, S. and Opatz, T. (2017) ‘Polyethylene bio-degradation by caterpillars?’, *Current Biology*, 27(15), pp. R744–R745. doi: 10.1016/j.cub.2017.07.004.

Wei, R. and Zimmermann, W. (2017) ‘Microbial enzymes for the recycling of recalcitrant petroleum-based plastics: how far are we?’, *Microbial Biotechnology*, 10(6), pp. 1308–1322. doi: 10.1111/1751-7915.12710.

Wen, Z. *et al.* (2021) ‘China’s plastic import ban increases prospects of environmental impact mitigation of plastic waste trade flow worldwide’, *Nature Communications*, 12(1), p. 425. doi: 10.1038/s41467-020-20741-9.

Whitt, M. *et al.* (2013) ‘Survey of heavy metal contamination in recycled polyethylene terephthalate used for food packaging’, *Journal of Plastic Film & Sheeting*, 29(2), pp. 163–173. doi: 10.1177/8756087912467028.

Winn, M. *et al.* (2014) ‘Characteristics of Streptomyces griseus biofilms in continuous flow tubular reactors’, *FEMS Microbiology Letters*, 352(2), pp. 157–164. doi: 10.1111/1574-6968.12378.

World Economic Forum (2016) *The new plastics economy: Rethinking the future of plastics*, *Ellen MacArthur Foundation*. Available at: http://www3.weforum.org/docs/WEF_The_New_Plastics_Economy.pdf.

Worley, B. and Powers, R. (2012) ‘Multivariate Analysis in Metabolomics’, *Current Metabolomics*, 1(1), pp. 92–107. doi: 10.2174/2213235X11301010092.

Xiao, X. (2008) ‘Dynamic tensile testing of plastic materials’, *Polymer Testing*, 27(2), pp. 164–178. doi: 10.1016/j.polymertesting.2007.09.010.

Xu, Z. *et al.* (2022) ‘Metabolic engineering of Streptomyces to enhance the synthesis of valuable natural products’, *Engineering Microbiology*, 2(2), p. 100022. doi: 10.1016/j.engmic.2022.100022.

Yagüe, P. *et al.* (2013) ‘Pre-sporulation stages of Streptomyces differentiation: state-of-the-art and future perspectives’, *FEMS Microbiology Letters*, 342(2), pp. 79–88. doi: 10.1111/1574-6968.12128.

Yang, J., Yang, Y., Wu, W., *et al.* (2014) ‘Evidence of Polyethylene Biodegradation by Bacterial Strains from the Guts of Plastic-Eating Waxworms’, *Environmental Science & Technology*, 48(23), pp. 13776–13784. doi: 10.1021/es504038a.

Yang, J., Yang, Y., Wu, W.-M., *et al.* (2014) ‘Evidence of Polyethylene Biodegradation by Bacterial Strains from the Guts of Plastic-Eating Waxworms’, *Environmental Science & Technology*, 48(23), pp. 13776–13784. doi: 10.1021/es504038a.

Yoshida, S. *et al.* (2016) ‘A bacterium that degrades and assimilates poly(ethylene terephthalate)’, *Science*, 351(6278), pp. 1196–1199. doi: 10.1126/science.aad6359.

Yoshida, S. *et al.* (2021) ‘Ideonella sakaiensis, PETase, and MHETase: From identification of microbial PET degradation to enzyme characterization’, in *Enzymatic Plastic Degradation*. 1st edn. Elsevier Inc., pp. 187–205. doi: 10.1016/bs.mie.2020.12.007.

Zampolli, J. *et al.* (2021) ‘Transcriptomic analysis of Rhodococcus opacus R7 grown on polyethylene by RNA-seq’, *Scientific Reports*, 11(1), p. 21311. doi: 10.1038/s41598-021-00525-x.

Zettler, E. R., Mincer, T. J. and Amaral-Zettler, L. A. (2013) ‘Life in the “Plastisphere”: Microbial Communities on Plastic Marine Debris’, *Environmental Science & Technology*, 47(13), pp. 7137–7146. doi: 10.1021/es401288x.

Zhang, J. *et al.* (2020) ‘Biodegradation of polyethylene microplastic particles by the fungus Aspergillus flavus from the guts of wax moth Galleria

mellonella', *Science of The Total Environment*, 704, p. 135931. doi: 10.1016/j.scitotenv.2019.135931.

Zhang, Y.-M. *et al.* (2013) 'Degradation of terephthalic acid by a newly isolated strain of Arthrobacter sp . 0574', *South African Journal of Science*, 109(7–8), pp. 1–4. Available at: http://www.scielo.org.za/scielo.php?script=sci_arttext&pid=S0038-23532013000400020&lng=en&tlng=en. .

Zhang, Z. *et al.* (2020) 'Antibiotic production in Streptomyces is organized by a division of labor through terminal genomic differentiation', *Science Advances*, 6(3), pp. 1–10. doi: 10.1126/sciadv.aay5781.

Zhao, Q. *et al.* (2019) 'High ectoine production by an engineered Halomonas hydrothermalis Y2 in a reduced salinity medium', *Microbial Cell Factories*, 18(1), p. 184. doi: 10.1186/s12934-019-1230-x.

Zheng, Y., Yanful, E. K. and Bassi, A. S. (2005) 'A Review of Plastic Waste Biodegradation', *Critical Reviews in Biotechnology*, 25(4), pp. 243–250. doi: 10.1080/07388550500346359.